



National Library
of Canada

Acquisitions and
Bibliographic Services Branch

395 Wellington Street
Ottawa, Ontario
K1A 0N4

Bibliothèque nationale
du Canada

Direction des acquisitions et
des services bibliographiques

395, rue Wellington
Ottawa (Ontario)
K1A 0N4

Your file *Votre référence*

Our file *Notre référence*

NOTICE

The quality of this microform is heavily dependent upon the quality of the original thesis submitted for microfilming. Every effort has been made to ensure the highest quality of reproduction possible.

If pages are missing, contact the university which granted the degree.

Some pages may have indistinct print especially if the original pages were typed with a poor typewriter ribbon or if the university sent us an inferior photocopy.

Reproduction in full or in part of this microform is governed by the Canadian Copyright Act, R.S.C. 1970, c. C-30, and subsequent amendments.

AVIS

La qualité de cette microforme dépend grandement de la qualité de la thèse soumise au microfilmage. Nous avons tout fait pour assurer une qualité supérieure de reproduction.

S'il manque des pages, veuillez communiquer avec l'université qui a conféré le grade.

La qualité d'impression de certaines pages peut laisser à désirer, surtout si les pages originales ont été dactylographiées à l'aide d'un ruban usé ou si l'université nous a fait parvenir une photocopie de qualité inférieure.

La reproduction, même partielle, de cette microforme est soumise à la Loi canadienne sur le droit d'auteur, SRC 1970, c. C-30, et ses amendements subséquents.

Canada

**Characterization of Eleven Monoclonal Antibodies to Human
Mammary Carcinoma Associated Antigens and Evaluation of
Their Diagnostic and Therapeutic Potential**

by

Ashim Kumar Guha

**Submitted in partial fulfillment of the requirements
for the degree of Doctor of Philosophy**

at

Dalhousie University

Halifax, Nova Scotia

March, 1994

© COPYRIGHT BY ASHIM KUMAR GUHA, 1994



National Library
of Canada

Bibliothèque nationale
du Canada

Acquisitions and
Bibliographic Services Branch

Direction des acquisitions et
des services bibliographiques

395 Wellington Street
Ottawa, Ontario
K1A 0N4

395, rue Wellington
Ottawa (Ontario)
K1A 0N4

Your file *Voire référence*

Our file *Notre référence*

The author has granted an irrevocable non-exclusive licence allowing the National Library of Canada to reproduce, loan, distribute or sell copies of his/her thesis by any means and in any form or format, making this thesis available to interested persons.

L'auteur a accordé une licence irrévocable et non exclusive permettant à la Bibliothèque nationale du Canada de reproduire, prêter, distribuer ou vendre des copies de sa thèse de quelque manière et sous quelque forme que ce soit pour mettre des exemplaires de cette thèse à la disposition des personnes intéressées.

The author retains ownership of the copyright in his/her thesis. Neither the thesis nor substantial extracts from it may be printed or otherwise reproduced without his/her permission.

L'auteur conserve la propriété du droit d'auteur qui protège sa thèse. Ni la thèse ni des extraits substantiels de celle-ci ne doivent être imprimés ou autrement reproduits sans son autorisation.

ISBN 0-315-93815-3

Canada

Name **ASHIM KUMAR GUHA**

Dissertation Abstracts International is arranged by broad, general subject categories. Please select the one subject which most nearly describes the content of your dissertation. Enter the corresponding four digit code in the spaces provided.

IMMUNOLOGY

SUBJECT TERM

0 9 8 2 U-M-I

SUBJECT CODE

Subject Categories

THE HUMANITIES AND SOCIAL SCIENCES

COMMUNICATIONS AND THE ARTS

Architecture 0729
 Art History 0177
 Cinema 0900
 Dance 0378
 Fine Arts 0357
 Information Science 0723
 Journalism 0391
 Library Science 0399
 Mass Communications 0708
 Music 0413
 Speech Communication 0459
 Theater 0465

EDUCATION

General 0515
 Administration 0514
 Adult and Continuing 0516
 Agricultural 0517
 Art 0273
 Bilingual and Multicultural 0282
 Business 0688
 Community College 0275
 Curriculum and Instruction 0727
 Early Childhood 0518
 Elementary 0524
 Finance 0277
 Guidance and Counseling 0519
 Health 0680
 Higher 0745
 History of 0520
 Home Economics 0278
 Industrial 0521
 Language and Literature 0279
 Mathematics 0280
 Music 0522
 Philosophy of 0998
 Physical 0523

Psychology 0525
 Reading 0535
 Religious 0527
 Sciences 0714
 Secondary 0533
 Social Sciences 0534
 Sociology of 0340
 Special 0529
 Teacher Training 0530
 Technology 0710
 Tests and Measurements 0288
 Vocational 0747

LANGUAGE, LITERATURE AND LINGUISTICS

Language
 General 0679
 Ancient 0289
 Linguistics 0290
 Modern 0291
 Literature
 General 0401
 Classical 0294
 Comparative 0295
 Medieval 0297
 Modern 0298
 African 0316
 American 0591
 Asian 0305
 Canadian (English) 0352
 Canadian (French) 0355
 English 0593
 Germanic 0311
 Latin American 0312
 Middle Eastern 0315
 Romance 0313
 Slavic and East European 0314

PHILOSOPHY, RELIGION AND THEOLOGY

Philosophy 0422
 Religion
 General 0318
 Biblical Studies 0321
 Clergy 0319
 History of 0320
 Philosophy of 0322
 Theology 0469

SOCIAL SCIENCES

American Studies 0323
 Anthropology
 Archaeology 0324
 Cultural 0326
 Physical 0327
 Business Administration
 General 0310
 Accounting 0272
 Banking 0770
 Management 0454
 Marketing 0338
 Canadian Studies 0385
 Economics
 General 0501
 Agricultural 0503
 Commerce Business 0505
 Finance 0508
 History 0509
 Labor 0510
 Theory 0511
 Folklore 0358
 Geography 0366
 Gerontology 0351
 History
 General 0578

Ancient 0579
 Medieval 0581
 Modern 0582
 Black 0328
 African 0331
 Asia, Australia and Oceania 0332
 Canadian 0334
 European 0335
 Latin American 0336
 Middle Eastern 0333
 United States 0337
 History of Science 0585
 Law 0398
 Political Science
 General 0615
 International Law and Relations 0616
 Public Administration 0617
 Recreation 0814
 Social Work 0152
 Sociology
 General 0626
 Criminology and Penology 0627
 Demography 0938
 Ethnic and Racial Studies
 Individual and Family Studies 0628
 Industrial and Labor Relations 0629
 Public and Social Welfare
 Social Structure and Development 0700
 Theory and Methods 0344
 Transportation 0709
 Urban and Regional Planning 0999
 Women's Studies 0453

THE SCIENCES AND ENGINEERING

BIOLOGICAL SCIENCES

Agriculture
 General 0473
 Agronomy 0285
 Animal Culture and Nutrition 0475
 Animal Pathology 0476
 Food Science and Technology 0359
 Forestry and Wildlife 0478
 Plant Culture 0479
 Plant Pathology 0480
 Plant Physiology 0817
 Range Management 0777
 Wood Technology 0746
 Biology
 General 0306
 Anatomy 0287
 Biostatistics 0308
 Botany 0309
 Cell 0370
 Ecology 0329
 Entomology 0353
 Genetics 0369
 Immunology 0793
 Microbiology 0410
 Molecular 0307
 Neuroscience 0317
 Oceanography 0416
 Physiology 0433
 Radiation 0821
 Veterinary Science 0778
 Zoology 0472
 Biophysics
 General 0786
 Medical 0760

Geodesy 0370
 Geology 0372
 Geophysics 0373
 Hydrology 0388
 Mineralogy 0411
 Paleobotany 0345
 Paleocology 0426
 Paleontology 0418
 Paleozoology 0985
 Palynology 0427
 Physical Geography 0368
 Physical Oceanography 0415

HEALTH AND ENVIRONMENTAL SCIENCES

Environmental Sciences 0768
 Health Sciences
 General 0566
 Audiology 0300
 Chemotherapy 0992
 Dentistry 0567
 Education 0350
 Hospital Management 0769
 Human Development 0758
 Immunology 0982
 Medicine and Surgery 0564
 Mental Health 0347
 Nursing 0569
 Nutrition 0570
 Obstetrics and Gynecology 0380
 Occupational Health and Therapy 0354
 Ophthalmology 0381
 Pathology 0571
 Pharmacology 0419
 Pharmacy 0572
 Physical Therapy 0382
 Public Health 0573
 Radiology 0574
 Recreation 0575

Speech Pathology 0460
 Toxicology 0383
 Home Economics 0386

PHYSICAL SCIENCES

Pure Sciences
 Chemistry
 General 0485
 Agricultural 0749
 Analytical 0486
 Biochemistry 0487
 Inorganic 0488
 Nuclear 0738
 Organic 0490
 Pharmaceutical 0491
 Physical 0494
 Polymer 0495
 Radiation 0754
 Mathematics 0405
 Physics
 General 0605
 Acoustics 0986
 Astronomy and Astrophysics 0606
 Atmospheric Science 0608
 Atomic 0748
 Electronics and Electricity 0607
 Elementary Particles and High Energy 0798
 Fluid and Plasma 0759
 Molecular 0609
 Nuclear 0610
 Optics 0752
 Radiation 0756
 Solid State 0611
 Statistics 0463
Applied Sciences
 Applied Mechanics 0346
 Computer Science 0984

Engineering
 General 0537
 Aerospace 0538
 Agricultural 0539
 Automotive 0540
 Biomedical 0541
 Chemical 0542
 Civil 0543
 Electronics and Electrical 0544
 Heat and Thermodynamics 0348
 Hydraulic 0545
 Industrial 0546
 Marine 0547
 Materials Science 0794
 Mechanical 0548
 Metallurgy 0743
 Mining 0551
 Nuclear 0552
 Packaging 0549
 Petroleum 0765
 Sanitary and Municipal System Science 0700
 Geotechnology 0428
 Operations Research 0796
 Plastics Technology 0795
 Textile Technology 0994

PSYCHOLOGY

General 0621
 Behavioral 0384
 Clinical 0622
 Developmental 0620
 Experimental 0623
 Industrial 0624
 Personality 0625
 Physiological 0989
 Psychological 0349
 Psychometrics 0632
 Social 0451



DEDICATION

I dedicate this thesis to the memory of my father

Dr. Phani Bhusan Guha

Table of Contents

Table of Contents	v
Abstract	vii
Abbreviations	viii
Acknowledgements	xii
Introduction	1
Organization of Thesis	1
Summary of the Studies	3
Objectives of the Studies	5
Review of Literature	7
Materials	28
Methods	50
Results	82
Part 1: Characterization of MABs and Distribution of Their Target Antigens	
Part 2: Characterization of the Target Antigen(s) for the MABs	102
Part 3: Determination of the IRF and Binding Parameters of the MABs, and Mapping of the Determinants Recognized by 2 MABs	117

Part 4: Immuno-gold Studies	130
Part 5: Direct Cytotoxicity and Effect of MABs on Tumor Cell Proliferation	146
Part 6: Effect of Anti-Cancer Drugs and MAB-Drug Conjugates on Tumor Cell Proliferation <u>in vitro</u>	160
Part 7: Preparation of F(ab)₂ Fragments From Anti-HMC MABs	164
Part 8: Localization of Radiolabeled Anti- HMC MABs and Their F(ab)₂ Fragments in Tumor Xenografts	172
Summary of Results	262
Discussion	264
Addendum	311a
References	312

ABSTRACT

Eleven IgG murine monoclonal antibodies (MABs) to human mammary carcinoma (HMC), DAL-BR1 to DAL-BR11, have been characterized. Six of the 11 MABs belong to the IgG₁ subclass, one each to the IgG_{2a} and IgG_{2b} subclasses, and three to the IgG₃ subclass and all but 2 MABs, DAL-BR5 and 11, bear Kappa light chains. These MABs had a very restricted or no reactivity to normal human tissues and strong reactivity to 5 HMC, 1 renal carcinoma, 1 colonic carcinoma, and 3 melanoma cell lines but no reactivity to lymphoma, nephroblastoma, or prostatic carcinoma cell lines. An immunofluorescence assay using unfixed, frozen tissue sections showed that each MAB reacted with a variable number of 13 surgically excised HMC specimens and with a variable number of tumor cells in these specimens. Immunoperoxidase stained sections of formalin fixed, paraffin embedded tissues showed only DAL-BR7 staining most HMC as well as benign breast lesions and with the exception of DAL-BR6, which stained a small proportion of tumor cells in 3/5 melanoma cases, none of the MABs stained non-HMC tumors. DAL-BR6 and 7 immunoprecipitated an identical 47 Kd protein from surface radiolabeled target cell extract: and radiolabeled preparations of these 2 MABs showed partial competitive binding to this antigen. DAL-BR6 and 7 were also able to induce caps on HMC cells and were endocytosed after binding to their antigen. Four MABs (DAL-BR2, 3, 9 and 11) immunoprecipitated a protein from surface radiolabeled target cell extracts that ran as a 73 Kd band under reducing conditions but which was not iodinated. The target antigens of the MABs were sensitive to trypsin but not to neuraminidase and the MABs did not react with CEA, human milk fat globules, lactalbumin, lactoferrin, bovine kappa casein, and except for DAL-BR8, human casein. There was reduction in the reactivity of only DAL-BR6 and 7 to heat treated cells. None of the MABs were cytotoxic to HMC cells but DAL-BR2, 3,4,5,8,10 and 11 did inhibit the proliferation of these cells after a 6 hour pulse exposure. Methotrexate and Adriamycin conjugates of a few MABs also inhibited cell proliferation but at higher concentrations than observed with native drug. When injected into nude mice, radiolabeled DAL-BR5,6,7,9, and 11 as well as the F(ab)₂ fragments of DAL-BR6 and 7 selectively localized in HMC xenografts.

ABBREVIATIONS

ADM	Adriamycin
ADM-CAA	Adriamycin linked with cis-aconityl-anhydride spacer at the amino-sugar moiety of the drug
ADM-C13	Adriamycin linked with hydrazone spacer at the C13 position of the drug
BS	Binding Sites
BSA	Bovine Serum Albumin
CAA	Cis-Aconityl-Anhydride Spacer
CEA	Carcinoembryonic Antigen
CLL	Chronic Lymphocytic Leukemia
cm	Centimeter
cpm	Counts per Minute
DHFR	Dihydrofolate Reductase
dpm	Disintegrations per Minute
DPBS	Dulbecco's Phosphate-Buffered Saline
EBV	Epstein Barr Virus
EDTA	Ethylene-Diamine-Tetra-Acetate
ELISA	Enzyme-Linked Immunosorbent Assay
F(ab) ₂	F(ab) ₂ Fragment of Immunoglobulin
FITC	Fluorescein Isothiocyanate

g	Gram
x g	Acceleration of Gravity
HAMA	Human Anti-Mouse Antibody
HMC	Human Mammary Carcinoma
HPDP	3-(2-pyridylidithio)-Propionic Acid
hr	Hour
I	Iodine
IC₅₀	Concentration that Inhibits Growth by 50%
IgG	Immunoglobulin G
IRF	Immuno-Reactive Fraction
ITES	Insulin-Transferrin-Ethanolamine- Selenium Containing Serum Free Tissue Culture Medium
i.p.	Intraperitoneal
i.v.	Intravenous
K_A	Association or Affinity Constant
L	Liter
M	Molar
MAB	Monoclonal Antibody
mCi	Millicurie (1 mCi = 3.7 x10⁷ Becquerels where 1 Becquerel = 1 nuclear transfor- mation per second)

mg	Milligram
mm	Millimeter
mM	Millimolar
min	Minute
ml	Milliliter
ug	Microgram
ul	Microliter
uCi	Microcurie (1 uCi = 3.7×10^4 Becquerels where 1 Becquerel = 1 nuclear transformation per second)
MTX	Methotrexate
NET	Nonidet P40 - EDTA-Tris-HCl Buffer, pH 7.1, Containing 1% Ovalbumin
ng	Nanogram
NMG	Normal Mouse IgG
OPD	Ortho-Phenyldiamine
PBS	Phosphate-Buffered Saline (0.01 M sodium phosphate, pH 7.1, containing 0.15 M sodium chloride)
RCC	Renal Cell Carcinoma
RPMI	Roswell Park Memorial Institute Medium 1640

s.c.	Subcutaneous
SDS PAGE	Sodium Dodecyl Sulfate - Polyacrylamide Gel Electrophoresis
SPDP	N-succinimidyl-3-(2-pyridyldithio)-propionate
TBS	1% BSA-Tris buffer, pH 8.2
Tris-HCl	Tris (hydroxymethyl) aminomethane - Hydrochloride Buffer

ACKNOWLEDGEMENTS

I would like to thank Dr. Tarun Ghose for being my mentor during the past several years. I am very grateful for his encouragement and dedication during my Ph.D. program. I would also like to thank the members of UALMA as well as its Executive and Awards Committees for their support of a fellowship that enabled me to complete a Ph.D. program. I especially thank Dr. M.A. MacAulay, former Head Dept. of Pathology, and Dr. I. Zayid, Director of Anatomic Pathology at the V.G.H., for their support of my Ph.D. program. I express thanks to the Dept. of Microbiology for accepting me in their Ph.D. program, to Drs. R. Carr, S. Lee, A.H. Blair, and L. Fernandez for being on my Ph.D. committee, and to Dr. R. Mandeville for being the external thesis examiner.

I would like to acknowledge the assistance of Drs. S. Luner, G. Faulkner, R. Rajaraman, S. Boudreau, M. Givner, S. Norvell, S. Iles, J. Aquino and J. Kralovek during the course of the research. I also acknowledge Mrs. M. Mammen, H. Nolido-Cruz, M. Moore, J. Howell and the staff of the Immunopathology lab for their expert technical assistance. I give special thanks to Mrs. Shirley Engbers for her help and support in the preparation of this thesis.

Finally, I would like to express my appreciation for the love, support and patience of my family during these years. My wife Pauline, daughter Shona, son Ravi, mother Mrs. Nilima Guha, sister Maya, brother Ranjan, and brother in-law Bart Selman should all be acknowledged for giving me their sound advice and encouragement.

INTRODUCTION

MABs are increasingly being used to diagnose and treat human malignancies. This thesis presents the characteristics of 11 MABs to breast cancer-associated antigens and the evaluation of their diagnostic and therapeutic potential. A complete summary of all the studies performed as well as the objectives of these studies will be stated. Following this, several important topics will be introduced to illustrate the current state of knowledge of breast cancer including the epidemiology, the molecular biology, and the accepted protocols for the management of patients. A review will then describe the use of MABs to diagnose and treat malignancy. Issues will be raised to address the potential hazards of using MABs in humans for these purposes and a few strategies to overcome these problems will be highlighted. To conclude the introduction, a summary of reported anti-HMC MABs and their target antigens will be presented to show the increasing value of breast cancer immunology in diagnosing, prognosticating, and treating this disease.

The organization of subsequent sections of this thesis is now described. The Materials section lists all chemicals, drugs, equipment, animals, tissues, tumor cell lines, and antibodies used. It also details the composition of all buffers, reagents, and solutions. The Methods section then follows to describe all the experimental protocols under the appropriate headings.

The results of the experiments are presented in 8 parts. Each part consolidates the results from several experiments that address similar issues. Part 1 presents the results that characterize the 11 anti-HMC MABs and demonstrate the distribution of

their target antigen(s) in normal human tissues, cancer cell lines, and human tumors. Part 2 then presents the results that characterize the target antigen(s) of these MABs. This section includes a few results that were obtained by Dr. S. Luner with his consent. These are identified and detailed explicitly below and also in the text of Part 2. In the next section, Part 3, there are results of experiments that investigated the interaction of radiolabeled MABs with HMC cells in vitro to determine important parameters of the MABs. Part 4 then presents the results of experiments that studied the fate of gold-labeled MABs after binding to target cells. This section includes the ultrastructural identification of cell-associated gold particles by Dr. G. Faulkner, the details of which are clearly identified below and also in the text of Part 4. The results of experiments that investigated the direct cytotoxic effect of MABs are presented in Part 5. Part 6 then presents the results of experiments that determined the in vitro growth inhibition of cells by 2 anti-cancer drugs and MAB-drug conjugates. Part 7 then describes the conditions necessary to digest MABs of different subclass with pepsin to produce F(ab)₂ fragments. The final section, Part 8, presents the results of several in vivo tumor localization studies that used radiolabeled MABs or their F(ab)₂ fragments.

Following a brief summary of all the results, a discussion of the relevant issues arising from the results will be made. The sequence of topics discussed will generally be the same as that presented in the Results section. The thesis ends by alphabetically listing the references cited in all sections.

1. Summary of Studies Conducted

This thesis describes the characteristics of 11 anti-HMC MABs that were produced in Dr. Ghose's laboratory, the distribution and nature of their target antigens, the ability of these MABs to inhibit the proliferation of target cells in vitro either alone or when conjugated to anti-cancer drugs, the production of immunoreactive F(ab)₂ fragments from 4 of these MABs, and the in vivo tumor localization of these MABs or their F(ab)₂ fragments using xenograft models. To characterize these 11 anti-HMC MABs, the isotype, subclass, and light chain type were determined. Methods to isolate, purify and evaluate the reactivity of each MAB were also determined. In addition, the in vitro parameters of interaction between these MABs and target cells were compared. The parameters investigated were the number of cell-associated binding sites available for each MAB, the association constant of binding to these sites, and the immunoreactive fraction of radiolabeled MAB preparations.

The distribution of the target antigens in normal human tissues, cancer cell lines, and fresh, frozen or formalin fixed, paraffin embedded human tumors was determined. The target antigen of 6 of the panel of 11 MABs was immunochemically characterized and the determinants recognized by two of the MABs specific for a cell-surface antigen were investigated. Also studied were the sensitivity of the target antigen(s) of each MAB to neuraminidase and the reactivity of the MABs with known human or bovine milk proteins as well as with a known breast cancer marker, CEA. To assist the reader in appreciating the nature of these target antigen(s) more fully in

this thesis, Dr. S. Luner has kindly given permission to report the results of some experiments he performed. These results are the reactivity of the MABs to trypsin and heat treated target cells as well as to human milk fat globules.

In addition, kinetic studies were conducted to determine the fate of MABs bound to the cell surface of viable target cells over time. Each MAB used in these experiments was dual-labeled with ^{125}I and gold to determine both the amount and ultrastructural location of cell-associated MAB. After fixing the cell aliquots from these experiments with glutaraldehyde, the ^{125}I activity in each aliquot was determined using a gamma emission counter. All these cell aliquots were then delivered to Dr. G. Faulkner's laboratory where each was processed and sectioned for transmission electron microscopic examination. Dr. G. Faulkner examined these sections with the electron microscope to determine the number and ultrastructural location of gold particles in the various aliquots from the experiments and took electron photomicrographs to illustrate the observations he made. After reviewing all the photomicrographs obtained from these studies and consulting with Dr. Faulkner, the ultrastructural observations made by Dr. Faulkner were tabulated and appropriate photomicrographs were selected to demonstrate the findings.

The cytotoxic and growth inhibitory effects of each MAB, anti-cancer drugs MTX and ADM, and MAB-drug conjugates (the latter prepared by Dr. J. Kralovek in Dr. Ghose's laboratory) on target and non-target cells were evaluated in vitro. From these studies, the IC_{50} concentration of each agent used was determined. The optimal enzyme digestion conditions to produce and recover the F(ab)_2 fragments of

a selected panel of MABs which belong to different murine IgG subclasses were also determined. Finally, a series of in vivo tumor localization studies were conducted using selected radiolabeled MABs or their F(ab)₂ fragments in tumor-xenografted nude mice. From these studies, a clear summary will be presented describing the biological half-life of intravenously injected radiolabeled MABs, their potential use as radioimmunoimaging agents of solid tumors, their capability to localize in solid tumors in sufficient amounts to allow possible targeting of drugs or radionuclides for therapy of these tumors, the effect of using MABs that are directed to cell-surface targets and to cytosol or extracellular targets, and the potential of injecting mixtures of different MABs to increase the amount of MAB that can localize to target tumors in vivo.

2. Objectives of the Studies

The first two objectives were to characterize the 11 anti-HMC MABs and evaluate methods of MAB purification so that (1) characteristic markers of each MAB be identified to categorize these MABs and to select conditions (like the pH and type of buffers) for the purification and F(ab)₂ production from different subclasses of IgG MABs; and (2) the in vitro parameters of interaction between these MABs and target cells be defined to guide the selection of appropriate MABs from the panel of 11 MABs for in vivo tumor radioimmunoimaging and for preparation of anti-cancer drug conjugates. To achieve these objectives, it was necessary to evaluate the reactivity of the MABs with fresh target cells and those exposed to different fixatives so that (1) an appropriate antigen-containing substrate be identified and used in experiments to

determine and compare the reactivity of different MABs and to compare the titers of a single MAB isolated by different methods or by the same method at different times; and (2) information be obtained to help select the state of human tissues (either fresh or appropriately fixed) required for screening the reactivity of MABs.

The third objective was to define the target antigen(s) of each MAB in terms of (1) the distribution in normal and neoplastic cell lines and human tissues; (2) the immunochemical characteristics; (3) the epitopes recognized; (4) the likeness to known normal and neoplastic breast tissue proteins or markers; and (5) the specific cellular location. For those MABs that were shown to react with cell-surface antigens, experiments were conducted to assess the fate of cell-surface bound MAB over time. The characterization of the target antigens constitutes a major part of this thesis since the compilation of many characteristics is necessary to adequately compare this panel of 11 anti-HMC MABs with others reported in the literature. The results from screening panels of normal and neoplastic human tissues for their reactivity with the MABs will help identify the appropriate MABs with a potential for use in diagnostic immunohistology or immunocytology.

The fourth objective was to assess the ability of the MABs or MAB-anticancer-drug conjugates to inhibit the proliferation of tumor cells *in vitro*. The purpose was to evaluate the potential use of these MABs as therapeutic agents in breast cancer.

The fifth objective was to study the *in vivo* tumor localization of appropriate anti-HMC MABs. These studies also constitute another major part of the thesis and the results will identify those MABs with potential for radioimmunoimaging and

radioimmunotherapy as well as for targeting drugs or toxins to tumors in cancer patients. Since $F(ab)_2$ fragments may be even more useful than their intact parent MABs to target radionuclides or drugs in vivo, it was also necessary to determine the best method to produce these immunoreactive fragments from selected MABs for use in these studies.

3. Current State of Knowledge of Breast Cancer

a) Epidemiological Considerations

The current epidemiology of human breast cancer will now be elaborated to illustrate the magnitude of the problem and the need for continued research in this field. Of the estimated 54,800 new cases of all female cancers to be diagnosed in Canada in 1992 (1900 new cases in Nova Scotia), 28% will be HMC (Gaudette and Makomaski Illing, 1992), making breast cancer the most common cancer in women. Of the total estimated 26,200 cancer deaths among Canadian women in 1992 (1050 female cancer deaths in Nova Scotia), 20% will be due to HMC making it the leading cause of cancer deaths in women. One in ten Canadian women will develop HMC sometime in their life and 4% of Canadian women will die from HMC. The mortality rate from HMC (0.028% in Canada and 0.027% in the USA) has remained virtually unchanged for the past 50 years despite advances in surgery, radiotherapy and chemotherapy. Recent attention has therefore been focused on early disease detection when tumors are still localized to the breast and when chances of cure are maximal (Henson and Ries, 1990; and Scanlon, 1990). Indeed, the emphasis on early detection of breast cancer has been singled out as a possible cause of the recently recognized

trend of increasing breast cancer incidence among North American women (Garfinkel, 1993; and Miller et al., 1993). However, the problem remains that current treatment modalities have not been able in many cases to eradicate all malignant cells since some tumor cells have spread beyond the primary lesion by the time cancer is diagnosed. These metastatic tumor cells will eventually cause recurrences and ultimately result in the death of many breast cancer patients. It is not surprising that increasing numbers of anti-HMC MABs are being produced for the early detection of primary and metastatic breast cancer lesions and for better immunohistological diagnosis and treatment of the disease (Garcia et al., 1985; Iacobelli et al., 1986; Edwards et al., 1986; Gendler et al., 1987; Czuppon, 1987; Dairkee and Hackett, 1988; Shaw et al., 1988; Bieglmayer et al., 1989; Pancino et al., 1989; Ishida et al., 1989; Kjeldsen et al., 1989; Skilton et al., 1990; Williams et al., 1990; Layton et al., 1990; Garcia et al., 1990; Duda et al., 1991; Pancino et al., twice in 1991; Bieglmayer et al., 1991; Pastan et al., 1991; Ceriani et al., 1992; Hanna et al., 1992; Goodman et al., 1993; and reviewed by Tjandra and McKenzie, 1988; and twice by Price, 1988).

b) Molecular Biology of Breast Cancer

The molecular biology and the mutations observed in human breast cancer have been described (Van de Vijver and Nusse, 1991; and Callahan and Campbell, 1989) and transgenic mice have been used as a breast cancer model system to directly study the effects of oncogene expression (Muller, 1991). Since some genetic changes observed in breast tumors have been shown to be prognostically significant, several

investigators have used MABs to detect abnormal gene products in tumor cells. Eight mutations in human breast cancer have been identified and include amplification of c-myc, c-erbB2, and int-2 (Henry et al., 1993; Fantl et al., 1990; and Tavassoli et al., 1989) as well as loss of heterozygosity on five chromosomes (1q, 3p, 11p, 13q, and 17p) which is felt to unmask recessive mutations of tumor-suppressor genes. One of the tumor suppressor genes which is located on 17p and which codes for a nuclear phosphoprotein, p53, has particularly been investigated. Although immunohistological studies in breast cancer specimens have shown overexpression of p53 in 25% to 50% of cases (Barbareschi et al., 1992; Walker et al., 1991; and Bartek et al., 1990), there appears to be no clear association between p53 DNA abnormalities and p53 expression (Thompson et al., 1992; and Lohmann et al., 1993). Nevertheless, further studies are needed to correlate p53 gene mutations and/or the presence of p53 with tumor behaviour. Currently, it appears that detecting p53 by immunohistology may offer more information on the functional status of the p53 control pathway in a malignant cell than the mere detection of p53 gene mutations (Wynford-Thomas, 1992). In addition to immunohistological detection of oncogene or tumor suppressor gene products in breast cancer specimens, recent studies have also demonstrated that HMC xenografts in nude mice that overexpress c-erbB2 protein can be successfully imaged with ¹²⁴I-labeled MAB to this protein using positron emission tomography (Bakir et al., 1992). The implication is that similar studies may also be useful in detecting breast cancer in patients. Furthermore, in order to study the characteristics and behaviour of malignant cells with aberrant oncogene expression, the MCF-7 human

breast cancer cell line which requires estrogen for optimal growth has been transfected with c-erbB2 (Benz et al., 1992) and c-ras^H (Gelmann et al., 1992; and Sommers et al., 1990). The MCF-7/c-erbB2 cells expressed the p185^{c-erbB2} surface receptor and were resistant to cisplatin and no longer sensitive to the antiestrogen, tamoxifen, in vitro unlike their parental cells. In addition, like MCF-7 cells, these transfected cells needed estradiol supplements to produce tumors in nude mice but MCF-7/c-erbB2 xenografts grew more quicker than MCF-7 xenografts. Tamoxifen injections promptly stopped the growth of MCF-7 tumors but had no effect on the accelerated growth of MCF-7/c-erbB2 tumors. These studies suggest that p185^{c-erbB2} overexpression in human breast cancers may be associated with therapeutic resistance to tamoxifen and cisplatin. With regards to MCF-7/c-ras^H cells, studies have shown an increased in vitro growth and invasive capacity of these cells compared to their parental MCF-7 cells. However, there was no effect of c-ras^H transtfection of MCF-7 cells on metastasis formation in vivo when these cells were orthotopically inoculated in nude mice (i.e. inoculated into the mammary fat pads). Interestingly, other xenograft models of human cancer (such as colon and lung carcinoma) in nude mice have been used in radioimmunosciintigraphy studies where MABs specific for the ras p21 in tumor cells successfully localized to in vivo tumors (Katoh et al., 1990).

c) Current Status of Breast Cancer Management

The current accepted protocols for diagnosing, treating, and prognosticating breast cancer as well as the common problems encountered with these activities will now be elaborated. It is quite evident that the role of the surgeon, though paramount

in the overall management of breast cancer patients, must be in conjunction with a multidisciplinary team that includes medical and radiation oncologists, radiologists, pathologists, and cytologists in order to provide the best care for the patient (Forrest, 1988). The fact remains, breast cancer is an excellent example of how central dogmas, especially of treatment options, have been ingrained into practitioners over the years and enforced by an "Inquisition" in medicine (Hellman, 1993) despite ample evidence contrary to dogmatic beliefs. While mutilation treatment has thankfully diminished in recent times, the question still remains "What is the best treatment of the various clinical presentations of breast cancer?". The literature is replete with reviews, studies, and editorials on this subject too numerous to assimilate but a few recent papers will be highlighted. The American Cancer Society has published its guidelines for diagnosing and treating various clinico-pathological breast cancer scenarios in a supplement issue of the journal *Cancer* (Scanlon and Hutter, 1990). The main exercise is to ascertain grade and stage of disease (tumor size and type including hormone receptor as well as lymph node status) in a given patient all in an effort to estimate prognosis and then to offer available types of therapy including surgery, radiotherapy or chemotherapy (cytotoxic drugs or hormones) or a combination of treatments to manage the disease. But should surgery be the initial treatment of operable breast cancer (Kurtz, 1991) and does axillary lymph node metastasis represent aggressiveness or duration of disease (Mitra and MacRae, 1991)? Are there prognostic factors in axillary lymph node negative patients which identify a subgroup in this population that will do poorly (Aaltomaa et al., 1991)? What are

the minimal criteria to be considered when evaluating a new prognostic factor in breast cancer (McGuire, 1991) and will preferred treatment options change even after the results of large clinical trials evaluating these factors are known given the fact that dogmatic beliefs are still held by many physicians (Belanger et al., 1991)? Should node negative patients be given adjuvant or neoadjuvant chemotherapy (Scholl et al., 1991; Bonadonna et al., 1991; and Hartmann et al., 1991) and what are the mechanisms of drug resistance in breast cancer (Dalton, 1990; and Clarke et al., 1993)? What is the role of radiotherapy in all forms of breast cancer (Mansfield et al., 1991) and what is the management of locally recurrent breast cancer (Kennedy and Abeloff, 1992)? The answers to all these questions are not fixed and should definitely not be dogmatic if we as a medical and scientific community have learned from the history of this disorder. Nevertheless, as far as progress in cancer is concerned, great strides have been made in the early diagnosis and treatment of breast cancer primarily due to mammography (Leffall, 1991). However, according to a report from the General Accounting Office of the USA which documented that despite the National Cancer Institute spending more than \$1 billion on breast cancer in the last 2 decades, there is a "stalemate in the war against breast cancer" (Marshall, 1991).

d) Chemotherapy of Breast Cancer

With regards to the chemotherapy of breast cancer, an overview of numerous clinical trials has demonstrated that polychemotherapy can improve the survival of 26% of premenopausal patients with Stage II (lymph node positive) disease and of a much smaller % of postmenopausal patients with estrogen-receptor negative tumors

(Carbone, 1990). Tamoxifen treatment of postmenopausal patients with estrogen-receptor positive tumors is now well established but its role in premenopausal patients is less clear (Henderson, 1990). The most common chemotherapy protocols used in various clinical trials were: (1) CMF - Cytosin, Methotrexate, and 5-Fluorouracil; (2) CMFP - (1) plus Prednisone; and (3) CMFPT - (2) plus Tamoxifen. Adriamycin combined with other drugs has also been investigated and current ongoing studies are addressing the role of Adriamycin in adjuvant therapy. The use of adjuvant chemotherapy in patients with node negative disease has not yet been clearly defined (Henderson et al., 1990) since the risks from chemotherapy may outweigh the benefits achieved. With all the promise of chemotherapy in breast cancer, the fact remains that treatment with cytotoxic drugs often does not eliminate all cancer cells and considerable side effects are experienced by patients receiving treatment due to the action of these drugs on normal proliferating cells. As such, immunological approaches to the treatment of breast cancer, particularly immunochemotherapy using drug-MAB conjugates, are very appealing (Ghose et al., 1987).

Two of the drugs used in the treatment of breast cancer, MTX and ADM, have been used in experiments described in this thesis. MTX has benefitted many patients over the last 40 years and its history, present status, and future have been recently discussed (Bertino, 1993). MTX is an antimetabolite that is a powerful inhibitor of dihydrofolate reductase and which requires intracellular polyglutamylation for retention and cytotoxic activity. Furthermore, active carrier transport systems for MTX that are present in normal and neoplastic cells are also used by reduced folates.

By linking MTX chemically to MABs, it is possible to bypass these cellular transport systems for MTX and get MTX into the cell by an antibody-receptor complex-mediated process instead. Dr. Ghose and Dr. Blair developed an active ester method to link MTX to antibodies and showed more effective target tumor growth inhibition in vivo using a conjugate of MTX and tumor specific antibody prepared by this method compared to using free MTX or MTX conjugated to non-tumor specific IgG (Kulkarni et al., 1981). This active ester method of linkage was used to prepare conjugates of MTX and anti HMC MABs in this thesis. The synthesis and testing of a variety of antibody-antifolate conjugates have also been reviewed (Ghose et al., 1988). ADM (also called doxorubicin) is an anthracycline antitumor antibiotic which is the C-14 hydroxy derivative of daunomycin (also called daunorubicin). The development of these two drugs, their use in the treatment of a variety of malignancies including breast cancer, and their toxicity have been elaborated (Muggia and Green, 1991). The primary target of antitumor anthracyclines is perceived to be DNA topoisomerase II (Zunino and Capranico, 1991; Cummings et al., 1991) but cell surface actions of these drugs are also evident (Tritton, 1991; Thompson and Hickman, 1991; Diociaiuti et al., 1991). The major drawback of ADM has been its cardiotoxicity but when administered with cardioprotective agents such as Cardioxane, the toxicity has been reduced (Koning et al., 1991). Methods for conjugating ADM to antibodies have also been developed in an effort to target this drug specifically to tumor cells where either the surface effects of ADM or antibody-receptor complex-mediated cellular uptake of drug will kill tumor cells. Two types ADM-MAB

conjugates were studied in this thesis. Preparation of the first conjugate utilized a cis-aconityl anhydride spacer to link MAB to the amino sugar moiety of ADM (Shen and Ryser, 1981). Preparation of the second conjugate utilized a hydrazone spacer to link the C-13 moiety of ADM to a carbohydrate residue on the MAB (Greenfield et al., 1990). The design of different cytotoxic-agent-antibody conjugates for cancer therapy has also been reviewed (Ghose and Blair, 1987).

4. Immunodiagnostic and Immunotherapeutic Applications of MABs

The use of MABs for cancer detection and therapy has recently been reviewed (Goldenberg, 1993; Old, 1992; and Epenetos, 1988) and described by us previously (Guha et al., 1988). Numerous new cancer-associated antigens defined by MABs have been described (Reisfeld et al., 1987) but there really is no MAB that is exclusively specific for cancer and no antigen that is exclusively found on cancer cells. Nevertheless, MAB-defined cancer-associated antigens are highly expressed in many cancers compared to normal tissues and because of this, MAB-based cancer diagnostic procedures and treatment protocols have been investigated and in certain instances are in clinical use (Dillman, 1989; Schlom, 1987; Riethmuller and Johnson, 1992).

The MAB-based diagnostic procedures include laboratory methods like immunohistology and immunoassays that assist pathologists, clinical chemists and hematologists in making or confirming a diagnosis of cancer in appropriate specimens. In addition, there is widespread clinical use of MABs to screen selected patients for cancer or to monitor cancer patients for evidence of recurrences by detecting cancer

markers such as CEA, beta-human chorionic gonadotropin and alpha-fetoprotein in the circulation or in body fluids such as urine. The other MAB-based diagnostic procedure is radioimmunosintigraphy and it is being used increasingly as a clinical tool to evaluate pre- and post-surgical extent of disease (either to confirm the presence of or to discover previously undetected lesions) and to evaluate the ability of MABs to localize in tumors in preparation for planned radioimmunotherapy (as reviewed by Serafini, 1993; Collier and Foley, 1993; Galandiuk, 1993; Krag, 1993; Texter and Neal, 1993; Wagner Jr. et al., 1991; Mach et al., 1991; Larson, twice in 1991; and Goldenberg, 1988).

MAB-based therapeutic modalities include the use of (1) MABs alone as cytotoxic agents (complement or antibody-dependent-cellular-cytotoxicity mediated); (2) MABs alone to bind growth-factor receptors; (3) MABs conjugated to anti-cancer drugs (either directly or conjugated to carrier structures such liposomes that have been loaded with anti-cancer drugs), toxins, or radioisotopes; (4) MABs to purge primary or metastatic tumor cells from harvested bone marrow (or *ex vivo* purging); (5) anti-idiotypic MABs as tumor vaccines; and (6) bispecific MABs which have one arm specific for tumor antigen and the other arm that may be specific for any desired target (e.g. cytotoxic lymphocyte or chelated hapten bearing an isotope). These immunotherapeutic applications of MABs have been described or reviewed in recent years (Tjandra et al., 1988; Mariani et al., 1990; Ballow et al., 1990; Begent and Pedley, 1990; Nolan and O'Kennedy, 1990; Liliemark, 1991; Bergh, 1991; Schlom et al., 1991; Scheinberg, 1991; Sjogren, 1991; Fanger et al., 1992; and Goldenberg,

1993).

5. Safety Considerations for the Use of MABs in Humans

The injection of murine MABs into the blood stream of humans either for radioimmunotherapy or for radioimmunoscinigraphy may pose problems that could hinder the objective of the procedure. The first problem that may arise is the binding of the injected MAB to circulating target antigen either in the free form or on blood cells. The formation of circulating immune complexes which could then deposit in capillary beds and sites such as the kidneys, may also have deleterious effects on patients. The second effect of immune complex formation may be the decreased amount of injected MAB that localizes in tumor. However, studies where MABs or IgG to CEA or alpha-fetoprotein were injected i.v. into patients with high circulating levels of these proteins have shown that immune complexes do form but that these complexes do not interfere with tumor localization. Furthermore, these reports state that serious complications did not occur in these patients (Primm and Goldenberg, 1980; Mach et al., 1981; Bergmann et al., 1987; Goldenberg, 1987; Kramer et al., 1988; and Goldenberg, 1988). Similar findings have been described with MABs specific for other tumor associated antigens such as the OC-125 defined antigen in ovarian cancer (Hnatowich et al., 1987). However, in other studies that used tumor-bearing mice, intravenously injected MAB did form circulating immune complexes in sufficient amounts to decrease tumor localization of the MABs (Nakamura et al., 1990). This illustrates some of the difficulties in making direct inferences or predicting outcomes of studies in humans only from experimental results obtained in

mice.

A more serious problem that may arise after repeated injections of murine MABs is the development of human anti-mouse antibodies (or HAMA) in the "immunized" individual. HAMA can be responsible for the onset of serum sickness or anaphylaxis and can also significantly hamper localization of the injected MABs in tumors. Strategies to decrease HAMA include the use of (1) F(ab)₂ or F(ab) fragments or the even smaller recombinant single-chain Fv antibodies, all of which do not have the highly immunogenic Fc portion; and (2) "humanized" MABs, either a mouse-human chimera where the human constant region through genetic engineering has replaced the mouse constant region of the MAB, or a "reshaped" MAB where only the complementarity-determining regions of the mouse MAB is grafted onto the framework of an otherwise human antibody. The theory, methods of production, properties and potential uses of genetically engineered antibodies produced have recently been thoroughly reviewed by a number authors in an issue of the monograph series *Immunological Reviews* (Moller, 1992) and in an issue of *Critical Reviews in Immunology* (Wright et al., 1992). The risk of developing HAMA can also be decreased by using intralesional or intracavitary administration of MABs instead of intravenous injection without seriously compromising the imaging or therapy of tumors at these localized or enclosed sites.

A final consideration before injecting murine proteins into humans for cancer diagnosis or treatment is the general safety of the injectable agent. It is now essential to repeatedly test all MAB preparations intended for human use to assure sterility and

absence of pyrogens or murine viruses. Contamination, if present, may have originated in the MAB-producing hybridomas or may have occurred during the purification or other physico-chemical processes the MABs underwent. There are now guidelines for the parenteral clinical use of monoclonal and engineered antibodies that have been set by the Food and Drug Administration of the USA (Manohar and Hoffman, 1992; and Hoffman et al., 1985).

6. Summary of Reported Anti-HMC MABs and their Target Antigens that are Useful for Tumor Diagnosis and Therapy

With regards to breast cancer, several reports have described the use of MABs as clinical laboratory reagents in a variety of assays to aid the diagnosis and to estimate the prognosis of disease. In addition, a number of reports have described the diagnostic and therapeutic uses of anti-HMC MABs in both mice and women. As reviewed below, these MABs are directed to a variety of targets that are expressed, shed or secreted by malignant breast cells and that are either specific for HMC or specific for a number of carcinomas including HMC.

a) Protein Markers of HMC

Immunocytochemical detection of casein and alpha-lactalbumin as markers of primary and metastatic breast cancer has been described for over 15 years (Hebert et al., 1978; and Lee et al., 1984) but in many cases, the breast cancer is not differentiated enough to express these proteins. Other proteins such alpha-2-Zn-glycoprotein, alpha-1-antichymotrypsin, and alpha-lipoprotein which are present in serum and synthesized as an acute response to inflammation, have been shown to be

elevated in breast cancer patients (Pettingale and Tee, 1977). Recently, these proteins were immunohistologically detected and found to be expressed in the majority of surgically excised breast carcinoma specimens (Hurlimann and van Melle, 1991). These patients were followed for more than 6 years and the expression of these proteins in their resected tumors did correlate with the clinical outcome of the disease. The immunohistological detection of these proteins in surgically excised breast cancer tissue may therefore be useful in predicting the prognosis of patients. Also, gross cystic disease fluid protein-15, which is one of the four major component proteins of cyst fluid, has been shown to be marker for HMC and apocrine metaplastic cells (Mazoujian et al., 1989).

b) Breast Cancer-Associated Antigens

In addition to these protein markers of breast cancer, there have been numerous reports of other breast cancer-associated antigens that are defined by MABs and which are also described as markers of breast cancer. These antigens may be segregated into 3 broad groups. The first group consists of mucin or mucin-like molecules (glycoproteins of high molecular weight) produced and often secreted by breast cancer cells. This group includes components of human milk fat globule membranes that are high molecular weight glycoproteins 400,000 daltons or greater and low molecular weight glycoproteins, in particular the 46,000 dalton glycoprotein (Tjandra and McKenzie, 1988; and Larocca et al., 1991). This group also includes proteins which are currently described by the term polymorphic epithelial mucin. This term is now applied because there is considerable evidence for genetic

polymorphism detectable at the protein or DNA levels (Swallow et al., 1987) and most MABs against this mucin have been shown to react with a hydrophilic sequence of the tandem repeat composed of 20 amino acids starting with PDTRPAP (Peterson et al., 1991; Layton et al., 1990; and Gendler et al., 1988). The gene coding for this mucin molecule has been designated MUC1 and its structure and biology have been reviewed (Gendler et al., 1991). There are other anti-HMC MABs that react with carbohydrate epitopes on this MUC1 mucin (Devine et al., 1991; Pancino et al., 1991). Furthermore, a total of 73 MABs, many of which are anti-HMC MABs and directed to MUC1 mucins, were evaluated in an international workshop on carcinoma-associated mucins (Taylor-Papadimitriou, 1991).

The second group consists of surface-associated proteins found on breast cancer cells and includes a 43,000 dalton antigen (Edwards et al., 1986) and Tumor-Associated Glycoprotein-72 (Johnson et al., 1986; and Sheer et al., 1988). The third group consists of a number of antigens that are present in but not usually associated primarily with breast cancer. These are the general epithelial cell markers, oncogene products, abnormal tumor suppressor gene products and tumor-associated antigens that are expressed mainly in adenocarcinomas arising from sites other than the breast and which may or may not have been well characterized.

MABs that react with components of human milk fat globule membranes or polymorphic epithelial mucin epitopes have been used in immunohistological studies to detect occult lymph node breast cancer metastases (Galea et al., 1991; and McGuckin et al., 1990). These MABs were also used to determine the presence of

antigen expression in suspected primary breast carcinomas and high levels of antigen expression in these specimens correlated with both the diagnosis of cancer and the poor clinical course of patients (Ceriani et al., 1992; and Werner et al., 1991). However, there are reports of immunohistological studies which show no useful diagnostic potential of the MAB investigated. One such MAB is BC4E549 which reacts with one of the human milk fat globule membrane antigens, CA-549 (Hoagland et al., 1992). There also have been immunoelectron microscopy studies using these MABs to show altered localization of target antigens in breast cancer cells (Hanna et al., 1992; Corcoran et al., 1991; and Corcoran and Walker, 1990). In addition, these MABs have been used in a variety of immunoassays to detect circulating target antigens that were either shed or secreted into the blood stream of breast cancer patients (Gion et al., 1991; Bieglmayer et al., 1991; Garcia et al., 1990; Price et al., 1990; Bieglmayer et al., 1989; Ashorn et al., 1988; Iacobelli, 1986; and Hilkens et al., 1986). One breast tumor associated antigen, CA15.3 (which has similarity to other members of the polymorphic mucin-like glycoproteins such as MCA, CAM26 and CAM29, and which is defined by MABs DF3 and 115D8), has been shown to be a marker of tumor burden as well as an indicator for tumor invasiveness in cases of primary breast cancer (Gion et al., 1991). Ex vivo purging of bone marrow with MABs alone or with immunotoxins to eliminate clonogenic breast cancer cells also promises to be useful (O'Briant et al., 1991; and Yu et al., 1990). Using magnetic microspheres coated with sheep anti-mouse IgG, one could immunoseparate normal hematopoietic cells from cancer cells to which MABs are bound.

MAB 323/A3 which recognizes the surface 43,000 dalton antigen on breast cancer cells has been shown to have a positive predictive value of 100% in diagnosing the presence of carcinoma in biopsies when there was strong cytoplasmic immunostaining (Courtney et al., 1991). MABs B72.3, CC49, and 83D4 which recognize the Tumor-Associated Glycoprotein-72 antigen have also been used to immunostain breast carcinomas and up to 80% of specimens were positive (Soomro and Shousha, 1992; Prey et al., 1991; and Pancino et al., 1991). Since the target antigen of B72.3 and the other 2 MABs is also expressed in other cancers, the clinical applications of these MABs both in vitro and in vivo are diverse (Colcher et al., 1991). The specificity of B72.3 and CC49 along with 3 other different MABs has been shown to be based on their reactivity with sialyl-Tn (Taylor-Papadimitriou, 1991) which is strongly expressed on human carcinoma cells and is an independent predictor of poor prognosis (Itzkowitz et al., 1990; and Kobayashi et al., 1992). The interest in this tumor antigen in recent years has led a group in Alberta, Canada, to conduct a pilot study in 12 breast cancer patients with metastatic disease to investigate the toxicity and humoral immunogenicity of a synthetic sialyl-Tn glycoconjugate administered with a Detox adjuvant (MacLean et al., 1993). While the assessment of the clinical relevance of such a small pilot study is difficult, the results were encouraging enough to prompt this group to institute Phase II studies to assess this immunization procedure as a treatment for minimal metastatic breast cancer.

c) In Vivo Studies Using Anti-HMC MABs

There have also been several in vivo studies (in laboratory animals and in

women) which have utilized MABs already described above that react with antigens like human milk fat globule membranes. In nude mice, breast cancer xenografts were effectively radioimmunoimaged with MABs (Yemul et al., 1993; Khaw et al., 1988; and Colcher et al., 1983) and effectively treated either with radioimmunotherapy (Ceriani and Blank, 1988) or with immunotoxin therapy (Ozello et al., 1989). Radioimmunoscinigraphy of breast cancer patients using MABs have also been described as successful (Major et al., 1990; Kalofonos et al., 1989; and Griffin et al., 1989) and a phase 1 clinical study was conducted of an anti-HMC MAB, 260F9, which was conjugated to the A chain of the toxin, ricin (Weiner et al., 1989). In preparation for the radioimmunotherapy of breast cancer patients, radiation doses and distribution of radiolabel have been studied in female baboons using ^{99m}Tc-labeled MABs to the human milk fat globule (Calitz et al., 1993). Additionally, a human reshaped antibody with HMFG1 specificity has been produced and compared with the parent murine MAB (Verhoeyen et al., 1993). This represents only the tenth reshaped human antibody that has been described (6 of 10 having specificities for targets on lymphoid cells). Human IgM MABs derived from lymph nodes of breast cancer patients that react with HMC have also been produced (Baba et al., 1992). Furthermore, it has been shown in a rodent model that immunization with human MUC1 synthetic peptides which are related to the core peptide sequence can generate cell-mediated immunity and inhibit MUC1-transfected tumor cell growth to prolong the survival of tumor-bearing mice (Ding et al., 1993). The use of MABs to MUC1 gene products or of anti-idiotypic MABs may therefore have prophylactic and

therapeutic potential in breast cancer and further studies are needed to explore these possibilities.

7. MABs to Non-specific HMC Antigens

Other MABs directed to targets not exclusively specific for HMC that are nevertheless very useful clinically will now be described. These targets include cell membrane and cytoskeletal proteins, receptors for extracellular matrix molecules, degradative enzymes produced by cells, tumor-associated antigens, oncogene or altered tumor suppressor gene products, cell proliferation markers, and the multidrug resistance gene product, p-glycoprotein. Bone marrow micrometastases in primary breast cancer have been detected with antibodies to epithelial membrane antigen (Mansi et al., 1991), epithelial surface glycoproteins and cytokeratin intermediate filaments (Cote et al., 1991) and the presence of micrometastases did correlate with early recurrence and decreased survival. Internal antigens in breast cancer cells such as keratin may also be accessible for tumor targeting with MABs due to the presence of cells permeable to macromolecules (Dairkee and Hackett, 1988). Receptors for laminin have been shown to be expressed by breast cancer cell lines such as MCF-7 (Terranova et al., 1983) as well as by breast carcinoma tissues (Barsky et al., 1984). MABs to the laminin receptor may be used to target anti-cancer drugs to breast cancer cells and *in vitro* experiments have had promising results (Rahman et al., 1989). Cathepsin D, an estrogen-induced lysosomal protease that can digest extracellular-matrix proteins, has been shown to be an independent predictor of poor breast cancer prognosis (Tandon et al., 1990) and it has been detected by immunochemical methods

in breast cancer (Brouillet et al., 1990) as well as in breast cyst fluid (Scambia et al., 1991). Besides the role of Cathepsin D as a possible marker for mammary carcinogenesis and poor prognosis in breast cancer, it may also serve as an alternate target antigen for radioimmunoscinigraphy. In addition, MABs like Ki-67 to a nuclear antigen present in cycling cells have been used in the grading of breast cancers (Bacus et al., 1989).

There are several reports of MABs to tumor-associated antigens expressed by many kinds of carcinoma and that have been used as immunohistological reagents to diagnose breast cancer. CEA, for example, is a tumor marker primarily associated with colon cancer but is also often expressed and can be immunohistologically detected in breast cancer. However, there are other MABs that are potentially just as useful as immunohistological reagents. Two of these MABs are 44-3A6, which detects a 40 kilodalton cell surface protein on adenocarcinomas (Duda et al., 1991), and A-80, which detects a high molecular weight mucin present in colon, prostate, lung, breast and other cancers (Eriksson et al., 1992). Another successful application of MABs to CEA has been to radioimmunoimage and diagnose breast cancer in patients with suspected primary, recurrent or metastatic disease (Lind et al., 1991). Furthermore, phase I clinical trials of a murine MAB L6 (Goodman et al., 1990) and a chimeric (human-mouse) MAB L6 (Goodman et al., 1993), both of which react with a 24 kilodalton protein present on the surface of breast, lung and colon cancer cells, have shown favourable in vivo tumor binding characteristics and in the case of the chimeric MAB, also low immunogenicity in humans. These L6 MABs have potential

for targeting anti-cancer drugs in breast cancer patients.

This introduction has given an overview of the organization of this thesis and summarized the current state of knowledge of breast cancer. It then focused primarily on the practical and potential use of MABs to diagnose and treat this disease. The experimental results presented in this thesis will contribute to the expanding body of information on breast cancer and will facilitate the early clinical use of these anti-HMC MABs for the diagnosis and therapy of breast cancer.

MATERIALS

1. Chemicals and Drugs:

Materials provided by Adria Laboratories Inc., Columbus, Ohio-

Adriamycin

Materials purchased from BDH Chemicals, Toronto, Ontario -

Folin Phenol Reagent

Acetic Acid

Absolute Methanol

Materials purchased from Becton Dickinson Canada Inc., Mississauga, Ontario -

Mouse Anti-Human Kappa Light Chain IgG

Mouse Anti-Human Lambda Light Chain IgG

Materials purchased from BIO-RAD, Richmond, California -

Enzymobeads™

Acrylamide

N,N'-Methylenebisacrylamide

Protein A along with Binding and Elution Buffers

Mouse Sub-isotyping Kit

Materials purchased from CALBIOCHEM, La Jolla, California-

Human CEA

Materials purchased from Canlab, American Hospital Supply Canada Inc.,
Mississauga, Ontario -

Sulfuric Acid

Glacial Acetic Acid

Materials purchased from Cappel, Cochranville, Pennsylvania -

FITC-conjugated Goat antimouse IgG

Sheep antimouse IgG, Affinity purified

Materials purchased from Eastman Organic Chemicals, Distillation Products
Industries, Rochester 3, New York -

B-mercaptoethanol

Materials purchased from Fisher Scientific Company, Fair Lawn, New Jersey -

Dichloromethane

Ammonium Sulfate

Sodium Azide

Ether

Chloroform

Potassium Iodide

Iodine

Materials purchased from Flow Laboratories Inc., Mississauga, Ontario -

Fetal Calf Serum

Materials purchased from Harleco, Philadelphia, Pennsylvania -

Nessler's Reagent

Materials purchased from ICN Immunobiologicals, Lisle, Illinois-

FITC-labeled rabbit IgG antibodies specific for mouse IgG

subclasses and mouse Kappa and Lambda light chains

Materials purchased from Meloy Laboratories Inc., Springfield, Virginia -

Mouse Anti-Human IgG

Mouse Anti-Human IgM

Mouse Anti-Human IgA

Materials purchased from Millipore Corporation, Bedford, Massachusetts -

Millipore Filters

Materials purchased from Pharmacia Chemicals, Pharmacia Inc., Dorval, Quebec -

Prepacked Sephadex G-25M PD-10 Columns

Sephacryl S200

Materials purchased from SARSTEDT 83.1835, Newton, USA -

96-well Microtiter plates

Materials Purchased from Sigma Chemical Company, St. Louis, Missouri -

BSA (88-90% pure)

Methotrexate

MW-SDS-200 (Standard Molecular Weight Marker

Proteins for SDS-PAGE)

Lactoperoxidase

Glucose Oxidase

Antimouse IgG Agarose Beads

Antihuman Polyvalent Immunoglobulins

Coomassie Brilliant Blue

Chloramine-T

Sodium Metabisulfite

Sodium Iodide

Sodium Dodecyl Sulfate

Ammonium Persulfate

TEMED (N,N,N',N'-Tetramethylethylenediamine)

Trizma Base

Nonidet P40

Phenylmethylsulfonyl Fluoride

3-Amino-9-ethylcarbazole (AEC)

N,N-dimethylformamide (DMF)

Caprylic Acid

Pepsin

Ovalbumin

Insulin (Bovine)

Transferrin (Human)

Ethanolamine

Selenium

Auric chloride (HAuCl₄-4H₂O)

Pristane (2,6,10,14-tetramethyl pentadecane)

Freund's incomplete Adjuvant

Gold-labeled Goat antimouse IgG

Human Lactoferrin

Human alpha-Lactalbumin

Human Casein

Bovine Kappa Casein

Trypsin, type XII (TPCK treated; 12,000 BAEE units/mg)

Neuraminidase, type V (containing a total of 2.5 NAN Lactose units)

Dulbecco's Cell Culture Medium

RPMI (Roswell Park Memorial Institute) - 1640 Cell

Culture Medium

McCoy's 5A (Modified) Cell Culture Medium DME F-12

(Dulbecco's Modified Eagle's Medium and

Ham's Nutrient Mixture F-12) Cell Culture

Medium

MEM-NEAA (Minimal Essential Medium with Non-essential amino acids)

Materials obtained from The Animal Care Center, Tupper Building, Dalhousie University, Halifax, Nova Scotia -

Somnatal

Materials obtained from individuals -

Vitronectin, Fibronectin and Laminin as well as polyclonal antibodies to the vitronectin receptor were provided by Dr. R. Rajaraman, Dept. of Microbiology

2. Equipment:

Equipment purchased from Baker Company Inc., Sanford, Maine -
BioGard Hood

Equipment purchased from BIOSOFT, Milltown, New Jersey
Ligand Curve Fitting IBM PC Program

Equipment purchased from BIO-RAD, Richmond, California -
Mini-gel SDS-PAGE and Mini-Transblot Apparatus

Equipment purchased from Brinkman Instruments Inc., Westbury, New York -
Eppendorf[®] Pipettes
Eppendorf[®] Polypropylene Tubes (0.4 ml and 1.5 ml)

Equipment purchased from LKB, Bromma, Sweden -
LKB 700 UltraRac[®] Fraction Collector
LKB-Productor AB

Equipment purchased from Beckman Instruments Inc., Fullerton, California -
Beckman Liquid Scintillation Counter, Model LS 3133T
Beckman 152 Microfuge
UV Spectrophotometer, Model 24

Equipment purchased from Carl Zeiss, Oberkochen, West
Germany -

Universal Spectrophotometer, Model PMQ11

Standard Universal Microscope

Equipment purchased from Coulter Electronic Inc., Hialeah, Florida -

Coulter Counter[®], Model Z_r

Equipment purchased from Dynatech Laboratories Inc., Alexandria, Virginia -

MicroELISA Plate Reader, Model MR580

Equipment purchased from International Equipment Company (IEC), Needham
Heights, Massachusetts -

International Preparative Centrifuge, Model B-35

Refrigerated Centrifuge, Model PR-6

Equipment purchased from Hoeffler Scientific Instruments, San Francisco,
California -

PS-1200 DC Power Supply (for SDS-PAGE)

Equipment purchased from Nuclear Chicago Corporation, DesPlaines, Illinois -

Gamma Emission Counter, Model 1085

Equipment purchased from Olympus, Tokyo, Japan -

Olympus Inverted Microscope

Equipment used with the consent, supervision, and kindness of Departments and Individuals -

Computer - Linked General Electric Maxicam Gamma Camera (for scanning tumor-bearing nude mice injected with ^{131}I -labeled antibodies or fragments - Nuclear Medicine Departments of the, Halifax Infirmary and Victoria General Hospitals, Halifax, Nova Scotia; Drs. J. Aquino and S. Iles, Directors)

SDS-PAGE Chamber (locally manufactured to use 83 x 100 x 0.5 mm minigel polyacrylamide slabs)

Transmission Electron Microscope for Ultrastructural Analysis (courtesy of Dr. G. Faulkner, Dept. of Microbiology)

Radioimmunoassay for CEA was kindly performed by the Endocrinology Laboratory at the Victoria General Hospital, Halifax, N.S. (courtesy of Dr. M. Givner)

3. Radiochemicals:

Materials purchased from Amersham, Arlington, Illinois -

Na^{125}I with specific activity ranges of 15-18 mCi / ug iodine

Na^{131}I of specific activity ranges of 10-30 mCi / ug iodine

³⁵S-methionine of specific activity 1000 Ci / mMol

Amplify^R to enhance autoradiographs

Materials purchased from New England Nuclear, Boston, Massachusetts -

[3,5,7-³H]-Methotrexate sodium salt (³H-MTX) of

specific activity 200 mCi / mMole

4. Animals:

The inbred female BALB/c mice (retired breeders) were purchased from Charles River Canada Inc., LaSalle, St. Constant, Quebec. Female athymic nude mice nu/nu of BALB/c strain (6 week old) were obtained from Harlan Sprague Dawley Inc., Indianapolis, Indiana and maintained under aseptic conditions in a restricted environment under positive pressure and 28°C. These animals were kept in sterile cages with filter tops in groups of 5 and provided with sterile bedding, and autoclaved Purina Laboratory Chow 5510 (Ralston Purina of Canada Ltd., Woodstock, Ontario) and tap water ad libitum.

5. Tissue Specimens

Specimens of normal human tissues and human tumors were obtained at surgery or at autopsy. Tissue blocks 1 cm³ were snap frozen in liquid nitrogen and stored in tightly wrapped aluminum foil at -70°C until sections were made. Specimens

of normal tissue from at least 3 different individuals were evaluated for reactivity with all eleven anti-HMC MABs.

6. Tumor Cell Lines:

Human cancer cell lines including the mammary carcinoma lines BT20 (HTB-19), MCF-7 (HTB-22), BT474 (HTB-20), T47D (HTB-133), the two non-tumorigenic human breast epithelium lines HBL-100 (HTB-124) and Hs578Bst (HTB-125), the human renal carcinoma lines Caki-1, Caki-2, A-498 and A-704 were obtained from the American Type Culture Collection (Bethesda, Maryland) and grown in MEM-NEAA medium containing 10% fetal calf serum and maintained at 37°C in a humidified atmosphere with 5% CO₂. The EBV-CLL-1 cell line and its D10-1 clonal subline were derived from an Epstein-Barr virus transformed human chronic lymphocytic B cell leukemia line that was developed in Dr. Ghose's laboratory, Dept. of Pathology, Dalhousie University, Halifax, Nova Scotia and maintained in RPMI cell culture medium supplemented with 10% fetal calf serum and incubated at 37°C in a humidified 5% CO₂ atmosphere (Lee et al., 1986). The M-1 and M-21 melanoma lines were obtained as gifts respectively from Dr. P.B. Dent (Dept. of Pediatrics, McMaster University, Hamilton, Ontario) and Dr. Soldano Ferrone (Dept. of Microbiology, New York Medical College, Valhalla, New York). The Zwicker melanoma line was established in Dr. Ghose's laboratory from a primary cutaneous melanoma in a caucasian patient.

7. Antibodies:

a) MABs to HMC, RCC, and B-cell CLL

The eleven anti-HMC MABs (DAL-BR1 to DAL-BR11) were produced in Dr. Ghose's laboratory by immunizing BALB/c mice s.c. with HTB-19, HTB-20, or HTB-133 cells mixed with complete Freund's adjuvant followed by a final i.v. booster injection of tumor cells only. The methods used for the fusion of immune splenic cells with the SP2 myeloma line P3X63Ag8 using polyethelene glycol, selection of heterokaryons, and screening of hybridoma produced immunoglobulins by ELISA and immunofluorescence have been described previously for the production of three anti-renal carcinoma MABs (DAL-K20, DAL-K29, and DAL-K45) and of two anti-B-cell leukemia MABs (DAL-B01 and DAL-B02) that were also produced in Dr. Ghose's laboratory (Luner et al., 1986 and Guha et al., 1990). The generation, sensitivity, and specificity of MABs DAL-K20, DAL-K29, DAL-K45, DAL-B01, and DAL-B02 as well as the characterization of their target cell surface antigens have also been described (Luner et al., 1986 and Guha et al., 1990). All eleven anti-HMC MAB secreting hybridomas were selected from screening 3415 hybridomas that resulted after eleven fusions and were maintained in Dulbecco's medium containing 10% horse serum and incubated in a humidified 5% CO₂ atmosphere. The three anti-RCC hybridoma clones each secrete an IgG₁ subclass MAB and were maintained in ITES serum free cell culture medium. One of the two anti-B-cell leukemia

hybridomas secretes an IgG₁ subclass MAB (DAL-B02) while the other secretes an IgG_{2a} subclass MAB (DAL-B01) and both were maintained in Dulbecco's medium containing 10% fetal calf serum.

To produce MAB containing ascites fluid, 1.5×10^7 hybridoma cells were injected into the peritoneal cavity of Pristane primed BALB/c mice. For this, female BALB/c mice were initially injected i.p. with 0.5 ml of Pristane followed after one week with an i.p. injection of hybridoma cells which resulted in the development of ascites generally one week later for most MABs. In addition to this protocol, a few anti-HMC MAB-producing hybridomas were also injected i.p. into mice one week following 2 previous i.p. Pristane injections that were given 3 weeks apart sequentially with volumes of 0.3 ml and 0.5 ml. Furthermore, a few of these hybridomas were also injected i.p. into mice one week after an i.p. injection of 0.3 ml of Freund's incomplete adjuvant. Double Pristane and Freund's incomplete adjuvant primed mice also produced ascites approximately one week after hybridoma cell inoculation. Ascites fluid was harvested by repeated i.p. taps from these mice and inactivated at 56°C for 30 min before storage at -20°C until MABs were isolated and purified.

b) Other MABs

The normal mouse IgG₁ and IgG_{2a} MAB secreting myeloma clones, derived respectively from mouse myeloma lines P3X63Ag8 (originating from MOPC21) and RPC5.4, as well as the rat MAB 187.1 secreting clone specific for mouse Kappa chain were obtained from The American Type Culture Collection and maintained in ITES

medium. To generate ascites fluid containing IgG₁, 1.5×10^7 cells were injected into Pristane primed BALB/c mice. After inactivation at 56°C, the IgG fraction was isolated from the ascites by precipitation with 33% saturated ammonium sulfate. Normal mouse IgG was obtained from the sera of normal mice similarly with ammonium sulfate.

8. Composition of Buffers, Reagents and Solutions Used:

a) Acetate Buffer, pH 5.0

1 M acetic acid	84 ml
anhydrous sodium acetate	17.2 g
distilled water	4 L

b) 10% Acetic Acid (Acrylamide Gel Destaining Solution)

glacial acetic acid	100 ml
distilled water q.s.	1 L

c) 0.1 M Acetate Buffer, 0.15 M NaCl, pH 4.5

glacial acetic acid	5.72 ml
1 N NaOH q.s.	pH 4.5
NaCl	8.5 g
distilled water q.s.	1 L

d) 0.1 M Sodium Phosphate Buffer, 0.15 M NaCl, pH 7.4

Na_2HPO_4	10.7 g
NaH_2PO_4	21.4
NaCl	170 g
distilled water q.s.	2 L

e) 0.01 M Phosphate Buffered Saline, pH 7.4 (PBS)

$\text{NaH}_2\text{PO}_4\text{H}_2\text{O}$	6.9 g
Na_2HPO_4	21.4 g
NaCl	170 g
distilled water	2 L

f) EDTA Solution for Harvesting Cells in Tissue Culture

EDTA (sodium salt)	0.2 g
KCl	0.4 g
NaCl	8.0 g
NaHCO_3	0.35 g
glucose	1.0 g
phenol red	0.005 g
distilled water q.s.	1 L

g) Alkaline Water

sodium citrate	2 g
NaHCO_3	2 g
tap water q.s.	1 L

h) Dulbecco's PBS (DPBS) 20 x concentrated

NaCl	160 g
KCl	410 g
Na ₂ HPO ₄	23 g
KH ₂ PO ₄	4 g
distilled water q.s.	1 L

(dilute 1:20 with distilled water prior to use)

i) Lugol's Iodine

KI	1.95 g
distilled water q.s.	3 ml

j) NET Immunoprecipitation Buffer

Nonidet P40 0.5%	0.5 ml
50 mM Tris-HCl buffer, pH 7.4	0.6 g
0.15 M NaCl	0.85 g
5 mM EDTA	5 ml of 0.1M solution
1 mg/ml ovalbumin	100 mg
distilled water q.s.	100 ml

k) 50% Glycerol - Tris Buffer (For Mounting Sections or

Cell Suspensions for Immunofluorescence Microscopy)

glycerol	5 ml
0.1 M Tris Buffer, pH 8.5	5 ml

l) Reagents for Protein Estimation by Lowry's Method

(i) Alkaline copper reagent -

- Stock solutions:
1. 2% sodium carbonate in 0.1N NaOH
 2. 1% cupric sulfate in H₂O
 3. 2% potassium tartrate in H₂O

Mix equal volumes of (2) and (3) and add 1 ml to 50 ml of (1).

(ii) Folin Ciocalteu Reagent -

Dilute 1 volume of this with 2 volumes H₂O.

m) Cell Culture Media

1. ITES Serum Free Cell Culture Medium

Insulin dissolved in 50 mM HCl	5 mg
Transferrin	33 mg
ethanolamine	1.2 mg
selenium (Na ₂ SeO ₃ -5H ₂ O)	6.6 ug
NaHCO ₃	1.2 g
DE-F12 Cell Culture Medium	For 1 L

Powder

distilled water (and 0.1 N NaOH or

0.1 N HCl to pH 7.0) q.s. 1 L

Filter the solution with a Millipore filter, and

add 4 ml Penicillin / Streptomycin stock solution

per liter of medium and store at 4°C.

2. McCoy's, MEM-NEAA, Dulbecco's and RPMI Sterilized prepared media were supplemented with and 10% fetal calf or horse serum as required along with Penicillin / Streptomycin solution and Glutamine.

n) Substrate Buffer for ELISA

0.1 M citric acid	2.4 ml
0.2 M Phosphate	2.6 ml
distilled water q.s.	10 ml
OPD (ortho-phenyldiamine)	4 mg in 0.2 ml ethanol
30% H ₂ O ₂	5 ul

o) SDS-Buffer for Lysing Cells

0.01 M Tris-HCl buffer, pH 7.4, containing
0.1 M NaCl
0.001 M EDTA
0.5% SDS (sodium dodecyl sulfate)

p) Crystal Violet Solution

Crystal violet	1 g
0.2 M Sodium acetate Buffer, pH 5.5	1 L

q) TBS (1% BSA-Tris Buffer)

1% BSA solution, pH 8.2 containing

20 mM Tris

150 mM NaCl

20 mM NaN₃

r) Amino-ethylcarbizole (AEC) Stock Solution

AEC 0.1 g

N,N-dimethylformamide 25 ml

Store in dark bottle at 4°C

s) AEC Working solution

0.02 M sodium acetate buffer, pH 5.2 9.5 ml

AEC stock solution 0.5 ml

Mix and filter before adding 100 ul of 0.3% H₂O₂

t) Polyvinyl Alcohol Mountant

Polyvinyl alcohol 20 g

PBS 80 ml

Mix with heating but do not boil

Add Glycerol 50 ml

Mix well, filter and store in aliquots at 4°C

Heat mountant to liquefy before use

9. SDS-PAGE Reagents and Buffers:**a) Separation Gel Buffer (1.5 M Tris-HCl, pH 8.8)**

HCl	48 ml
Tris	363 g
distilled water q.s.	100 ml

b) Stacking Gel Buffer (0.5 M Tris-HCl, pH 6.8)

Tris	5.98 g
1 N HCl q.s.	pH 6.8
distilled water q.s.	100 ml

c) Electrode Buffer (10 x concentrated Tris-Glycine, pH 8.3)

Tris	6 g
Glycine	28.8 g
1 N HCl or 1 N NaOH q.s.	pH 8.3
distilled water	1 L

d) Sample Buffer (2 x concentrated) with reducing agent

20% glycerol	2 ml
0.2% B-mercaptoethanol	20 ul
0.004% bromophenol blue dye	40 ul
2% sodium dodecyl sulfate	2 ml
Stacking gel buffer	2.5 ml
distilled water q.s.	10 ml

To make a sample buffer with no reducing agent do not add any B-mercaptoethanol.

e) 7.5% Separation Acrylamide Gel

distilled water	12-14 ml
30% acrylamide	7.5 ml
separation gel buffer	7.5 ml
ammonium persulfate 100 mg/ml	0.15 ml
10% sodium dodecyl sulfate	0.3 ml

Deaerate under vacuum suction

TEMED	15 ul
-------	-------

Pour solution in between 83 x 100 x 0.5 mm glass plates to fill up to 75% of total volume and wait 20-30 min for solution to gel

f) 3.75% Stacking Acrylamide Gel

distilled water	6.7 ml
30% acrylamide	1.88 ml
Stacking buffer	3.75 ml
10% sodium dodecyl sulfate	0.15 ml
ammonium persulfate 100 mg/ml	75 ul

Deaerate under vacuum suction

TEMED	7 ul
-------	------

Pour solution onto the top of separation gel to fill the remaining 25% volume of the glass plates and then place plastic fingers into the top of the gel slabs to make sample lanes.

g) Protein Staining Solution

Coomassie Brilliant Blue	100 mg
methanol	40 ml
10% acetic acid	60 ml

Destain gels with 10% acetic acid until background is clear.

10. Western Blotting Reagents and Buffers:

a) Transfer Buffer

25 mM Tris	3.03 g/L
192 mM Glycine	14.4 g/L
20% v/v Methanol	200 ml/L
pH 8.1-8.4	

b) Blocking and Washing Buffer (0.05% PBS-Tween)

NaCl	9 g/L
Na ₂ HPO ₄	0.61 g/L
KH ₂ PO ₄	0.2 g/L
Tween 20	0.5 ml/L
pH 7-7.4	

c) Detection Substrate for Immunoassay

Chloronaphthol (4-Chloro-1-naphthol)	0.21 g
Dissolved in methanol	60 ml
Added to PBS	240 ml
H ₂ O ₂ to start reaction	300 ul

d) Reagents for Transblotting and Immunoassay

Nitrocellulose paper

Coomassie Blue protein stain

Acetic acid / methanol destaining solution

Goat antimouse IgG horseradish peroxidase 1:3000 in PBS-Tween

METHODS

1. Isolation and Purification of MABs from Ascites Fluid

Small volumes (1-2 ml) of hybridoma DAL-BR1 to DAL-BR11 derived ascites fluid were evaluated for their IgG content using 2 methods of IgG isolation (1) Caprylic acid method (McKinney and Parkinson, 1987; Habeeb and Francis, 1984) and affinity purification with Protein A. The caprylic acid method involves diluting the ascites fluid first with 4 volumes of acetate buffer, pH 4.0, and adjusting the pH to 4.5 with 0.1N NaOH. Next, caprylic acid is added slowly and dropwise with thorough mixing at a ratio of 25 ul caprylic acid : 1 ml of diluted ascites fluid. After 30 minutes of stirring, the precipitate is removed by centrifuging at 10,000 x g for 30 min. The supernatant is then passed through a Millipore filter to remove fine particulate debris. The resultant fluid is mixed with 10 x concentrated PBS (10 parts supernatant : 1 part concentrated PBS) and the pH adjusted to 7.4 with 1N NaOH. The solution is cooled to 4°C and fractionated with ammonium sulfate (0.277 g/ml to yield 45% saturation). After stirring in the cold for 30 min, the protein precipitate is harvested by centrifuging at 5000 x g for 15 min. The pellet is dissolved with PBS in a volume usually 1/10th the original volume of the ascites fluid. After adequate dialysis against PBS to remove the contaminating ammonium sulfate as confirmed by using Nessler's reagent, the protein solution is passed through a Millipore filter before storing. Protein A affinity purification of IgG from ascites fluid was accomplished by strictly following instructions from BIO-RAD. Briefly, ascites fluid was diluted 1:1 with binding buffer and then passed through a Protein A column followed by

repeated washes with binding buffer alone. The bound IgG was then eluted from the column with elution buffer and the pH of the eluent was immediately neutralized with 1 M Tris-buffer, pH 9. The Protein A column was cleaned by washing repeatedly with regeneration buffer and was stored in PBS containing 0.05% sodium azide.

Protein estimations on all the samples were done using the Folin phenol reagent (Lowry et al., 1951).

2. Immunofluorescence Staining

Frozen sections of tissues or cell smears were covered with MAB solutions obtained from culture supernatants as well as from purified ascites for 2-4 hours before repeated washing with PBS and followed by application of 1:10 diluted FITC-conjugated goat antimouse IgG for 30 min. They were again repeatedly washed with PBS and then mounted in 50% glycerol-Tris buffer for examination under a fluorescence microscope. Appropriate dilutions of murine IgG₁, IgG_{2a}, and NMG were used as negative controls in these assays. For membrane staining, 100 ul of MAB solution was added to 5×10^5 viable target cells suspended in 100 ul of serum free media and the mixture was incubated for 1 hr at 4°C before washing 3 times with 0.1% BSA in PBS. The cells were resuspended in 20 ul of FITC-conjugated anti-mouse IgG for 0.5 hr at 4°C and again washed 3 times. To assess MAB reactivity with 0.5% glutaraldehyde or acetone fixed target cells, multiwell slides were plated with 2500 cells in MEM-NEAA media per well containing 10% fetal calf serum and then incubated at 37°C in a humidified 5% CO₂ atmosphere for 4 days before removing the media from the wells and exposing the cells to the appropriate fixative

for 1 min followed by 3 washes with PBS. MAB solutions were then applied to the wells for 1 hr at room temperature in a humidified container before washing the wells three times with PBS. FITC-conjugated goat anti-mouse IgG was applied to the wells for 30 min at room temperature followed by 3 washes with PBS and examination under a fluorescence microscope. The titer of antibody was defined as the concentration of MAB giving positive staining of 50% of target cells.

3. Immunoperoxidase Staining

Frozen or formalin fixed, paraffin embedded tissue sections from the surgical pathology archives of the Victoria General Hospital, Halifax, N.S., that were rehydrated and blocked with H₂O₂ and 1% goat serum in PBS were incubated overnight at 4°C with appropriate MABs at a concentration of 100 ug/ml (or 50 times the concentration required to achieve 100% staining of cultured target cells). After washing the slides with PBS, goat antimouse IgG peroxidase conjugate diluted 1:2000 was added and the sections incubated for 45 min followed by washing with PBS. The sections were then covered with 400 ul of freshly filtered 3-amino-9-ethylcarbazole for 10 min before washing with tap water and counter staining with Mayer's hematoxylin for 2 min. The slides were dipped in ammonia water for 0.5 min, rinsed in distilled water, and mounted with polyvinyl alcohol mountant.

4. Studies on Capping of Antibodies on Target Cells

For 1 hour, 25 ug of MABs DAL-BR1 to DAL-BR11 was incubated at 4°C with viable (trypan blue impermeable) 10⁶ HTB-19 or MCF-7 cells. A "0 hour" sample was taken and then the cells were washed thrice in PBS containing 0.1% BSA

at 4°C. The cells were put into serum free medium at 37°C and aliquots were taken at 2, 4, 6, and 8 hours. These aliquots were washed 3 times with 0.1% BSA in PBS containing 0.1% sodium azide. The cells were placed in a 1:8 diluted solution of FITC-conjugated goat antimouse IgG for 30 min and then washed 3 times with 0.1% BSA in PBS containing 0.1% sodium azide. Cell suspensions were mounted with 50% glycerol-Tris buffer for examination under a fluorescence microscope. Controls for these experiments included the use as appropriate of nonspecific IgG₁, IgG_{2a} or NMG in place of MAB and using FITC-conjugated anti-mouse IgG alone. The viability of cells was evaluated by the trypan blue permeability assay (Paul, 1975). For this test, all cell suspensions were routinely diluted in a 0.25% solution of trypan blue in PBS and put in a Neubauer hemacytometer chamber. After settling, the percentage of viable cells (cells that excluded the dye) was counted. All capping experiments were done in triplicate and the number of caps observed per each 100 viable cells counted for each time interval were tabulated.

5. Determination of MAB subclass

MCF-7 cells grown on multiwell slides and fixed with 0.5% glutaraldehyde in PBS were coated with the eleven anti-HMC MABs for 1 hr at room temperature before washing with PBS 3 times and adding FITC-conjugated rabbit IgG antibodies specific for murine IgG subclasses or Kappa and Lambda light chains. After 30 min incubation at room temperature, the wells were washed 3 times with PBS and examined under a fluorescence microscope. Negative and positive controls used in these experiments respectively were (1) nonspecific IgG₁ or IgG_{2a} instead of the anti-

HMC MABs on MCF-7 cells and (2) K29 and DAL-B01 on their respective target Caki-1 and EBV-CLL-1 cells. The results were verified by using a BIO-RAD mouse sub-isotyping ELISA kit and the rat MAB 187.1 against mouse Kappa chain.

6. ELISA assays

For ELISA assays on cells to determine MAB reactivity, 5000 target cells in MEM-NEAA medium containing 10% fetal calf serum were added to the wells of a SARSTEDT polystyrene 96 flat bottom well microtiter plate in a volume to fill each well. After overnight incubation at 37°C in a humidified 5% CO₂ atmosphere to allow cell attachment, the culture medium from the wells was discarded. The plates were then either used immediately or fixed with 0.5% glutaraldehyde in PBS for 1 min followed by repeated PBS washes. The glutaraldehyde fixed plates were then used immediately or frozen at -20°C until used. For ELISA assays on suspended, enzyme treated live cells, 96 V-well plates were used instead. For ELISA assays to determine MAB reactivity to specific antigens such as lactoferrin, alpha-lactalbumin, casein, and CEA, as well as 1% Nonidet-P40 cellular extracts of target and nontarget cells, 96 flat bottom well plates were coated overnight at 4°C with 100 ul/well of antigen solution at a concentration of 1, 5 and 10 ug protein diluted in 0.05% carbonate coating buffer, pH 9.6. The wells were then blocked with 1% BSA in PBS for 1 hr at room temperature. ELISA assays that determined MAB titer on target cells used an initial MAB concentration of 100 ug MAB/well that was diluted to 33 ug/ml and then to 11 ug/ml and so on serially. Duplicate samples of each dilution were added sequentially to successive wells containing target cells and the ELISA procedure described below

was followed to determine the lowest concentration of MAB that bound to tumor cells defined as three times the background absorbance. The titer established the minimum concentration of a MAB that had to be used in an ELISA assay to obtain a positive reaction. This knowledge was crucial when a constant concentration of any MAB was selected to be used in a number of ELISA assays. Examples of such assays included those that determined the reactivity of a MAB with enzyme treated target cells, with target cells in the presence of equivalent to excess amounts of other MABs or polyclonal antibodies, and with antigens coated in the wells. In all these types of ELISA assays, a subclass matched nonspecific murine IgG was always tested along with the MAB under investigation to estimate background activity. The concentration of the nonspecific IgG used in these assays was always the same as that of the MAB.

The volume of MAB solution used per well in all ELISA assays was 100 μ l. The wells were incubated at room temperature (or 4°C when live cells were used) for 90 min followed by 4 washes with PBS containing 0.05% Tween 20 (or 0.2% BSA in PBS when live cells were used). Finally, 100 μ l of a 1:3000 diluted solution of goat antimouse IgG peroxidase conjugate was added to the wells. After standing at room temperature (or 4°C when live cells were used) for 90 min, the wells were again washed 3 times with PBS containing 0.05% Tween 20 and once with PBS alone (or 4 times with 0.2% BSA in PBS when live cells were used). For experiments using V-well plates, between washes the plates were centrifuged in carriers followed by resuspension of cells using a Dynatech Microshaker. To each well 70 μ l of the substrate buffer, containing OPD, was then added and the color reaction was allowed

to proceed for 2-15 minutes, depending on the MAB concentrations used in the experiment, after which the reaction was terminated by the addition of 70 μ l of 0.05 M sulfuric acid. The absorbances in the wells were measured at 492 nm wavelength of light using a Dynatech microELISA plate reader.

7. Methods of Radioiodination, Cell Surface and Metabolic Labeling, and Immunoprecipitation

a) Chloramine-T Method:

The reaction conditions were modifications of previously reported methods (Hunter and Greenwood, 1962; Greenwood et al., 1963; Parratt et al., 1982) and have been described by us (Guha et al. 1991). Briefly, to a 0.5 M PBS (pH 7.0) solution of a known quantity of antibody, was added an appropriate quantity of ^{125}I or ^{131}I to achieve the desired level of radioiodination (e.g. From pilot studies, it was observed that to attain a radioiodination level of 1 atom of iodine per 2000 molecules of IgG under our experimental conditions, it was necessary to use 5 mg of IgG and 250 μCi ^{125}I ; and to attain a radioiodination level of 1 atom of iodine per 2 molecules of IgG, it was necessary to use 180 μg IgG and 4 mCi ^{125}I). The factors that determine the extent of radioiodination include the amount of chloramine-T, ^{125}I , and protein in the reaction mixture, the duration of reaction time, and the pH of the reaction mixture. For our radioidination procedures, it was determined that 0.5 mg of chloramine-T and a reaction time of 3 minutes with gentle stirring of the reaction mixture at room temperature were adequate to achieve the desired level of iodination. The oxidation reaction was terminated with 0.5 mg sodium metabisulfite and then 0.5 mg of NaI was

added. The reason for adding NaI was that it served as a carrier salt for the very small quantity of ^{125}I in the reaction mixture during the separation procedure as described now. The final reaction volume of 2.5 ml was transferred onto a PD-10 Sephadex G-25 column which was previously coated with BSA and repeatedly washed with PBS. The radioiodination products were eluted from the column using PBS and 1 ml fractions were collected. The peak radiolabeled protein fractions of the eluent were determined from the radioactive counts of each fraction and the elution profile of the column for separating macromolecules such as IgG from salts such as NaI. These peak radiolabeled protein fractions devoid of free radioactive iodine, which typically were the second and third 1 ml fractions after the void volume of the column, were combined. For counting, 5 μl samples of each 1 ml fraction were mixed with 1 ml PBS containing 1% BSA. The test tubes were capped and counted individually in a gamma emission counter along with appropriate standards consisting of 0.025 μCi of either ^{125}I or ^{131}I as needed. The specific activity and molar ratio of iodine incorporation in radiolabeled preparations were determined from the radioactive iodine counts of pooled protein fractions, determination of the amount of protein in the pooled protein fractions, counts obtained at any given time from standards of radioactive iodine preparations, and specific activity of the radioactive iodine used. Illustrative calculations are given on the following page to show how levels of radioiodination were determined for the labeled products. Radiolabeled MAB preparations were assessed for purity and confirmation of protein-bound radioactivity by SDS-PAGE and gel autoradiography as described later.

ILLUSTRATIVE CALCULATIONS TO DETERMINE
LEVELS OF RADIOIODINATION

Information required:

- Specific activity of Radioactive Iodine (obtained from the distributing company)
- Standard Iodine cpm per known uCi (typically 0.025 uCi of ¹²⁵I or ¹³¹I used to determine cpm)
- Specific activity of radioiodinated IgG (calculated from sample cpm, sample protein concentration and Standard Iodine cpm as stated above)

1. Determine uCi / atom of I

$$\frac{\text{sp. activity I (uCi / ug I)}}{6.02 \times 10^{23} \text{ atoms/mole}} \times \frac{\text{atomic wt. of I (g/mole)}}{10^{-6} \text{ g / ug}}$$

2. Determine specific activity of radiolabeled IgG

uCi / ug IgG =

$$\frac{\frac{\text{pooled protein fraction cpm}}{\text{volume of sample counted (ml)}}}{\text{cpm std. I / 0.025 uCi}} \times \frac{1}{\text{sample protein conc. (ug / ml)}}$$

3. Determine uCi / molecule of IgG

$$\frac{\text{sp. activity IgG (uCi/ug)}}{6.02 \times 10^{23} \text{ molecules/mole}} \times \frac{\text{molecular wt. IgG (g/mole)}}{10^{-6} \text{ g / ug}}$$

4. Determine level of radioiodination (atoms I/molecule IgG)

$$\text{ratio of \#3 to \#1} = \frac{\text{uCi / molecule IgG}}{\text{uCi / atom Iodine}}$$

b) Para-iodobenzoyl (PIB) Based Method for the Radioiodination of IgG:

The method used was an adaptation of methods described previously (Badger et al., 1990, Murray et al., 1991, and Wilbur et al, 1991). To summarize, in a stoppered reaction vial 50 ul of a solution containing 12.5 ug of N-succinimidyl m-(tri-n-butylstannyl)benzoate in 5% acetic acid in methanol, 10 ul of a solution containing 10 ug of N-chlorosuccinimide in methanol, and 10 ul of PBS were added. To this mixture, 2.0 mCi of ^{131}I in 2 ul of a 0.1 N NaOH solution was added and the reaction proceeded at room temperature for 5 min before quenching was achieved with 10 ul of a H_2O solution containing 0.72 mg/ml $\text{Na}_2\text{S}_2\text{O}_5$. The methanol was evaporated under a stream of N_2 gas in a fume hood. To the dried radiolabeled PIB product was added 200 ul of 1 mg/ml of the MAB solution in PBS along with 150 ul of 1.0 M solution of Na_2CO_3 , pH 9.25. Conjugation was allowed to proceed for 5 min at room temperature before passing the reaction mixture through a Sephadex G-25 PD-10 column using PBS as an eluent buffer. The radioactive protein fractions were collected and pooled as described for the Chloramine-T method.

c) Cell surface Radioiodination:

Iodination of surface antigens on D10-1 cells and subsequent preparation of a Nonidet P-40 extract of labeled cells were done using a modification of previously described methods (Hubbard and Cohn, 1972; Peltz et al., 1987; Liao et al., 1987) and reported by us previously (Guha et al 1990). Briefly, to 1.5×10^7 D10-1 cells in 5 ml Dulbecco's PBS was added 0.1 ml of 0.75 M glucose, 0.5 ml of 1M N-tris(hydroxymethyl)methylglycine (pH 7.5), 0.01 ml of a 1 mg/ml solution of

lactoperoxidase, and 0.5 mCi ^{125}I . To start the reaction, 0.01 ml of a 1 mg/ml solution of glucose oxidase was then added. The cell suspension was gently rocked for 40 min before centrifuging at 250 x g for 5 min. After 4 washes and centrifugation at 250 x g for 5 min, the cell pellet was brought to a volume of 0.5 ml with Dulbecco's PBS. For surface-labeling confluent monolayers of HTB-19, MCF-7, and M21 cells, exactly the same procedure was used with the exception that centrifugations were not required and the cells were washed by addition, manual shaking and discarding of Dulbecco's PBS. After the last wash, the cells were detached from the incubation plates by using EDTA, centrifuged and the cell pellet brought up to a final volume of 0.5 ml with Dulbecco's PBS. To the 0.5 ml cell pellets from both cell suspension and monolayer preparations, an equal volume of 2% Nonidet P-40 containing 0.1 mM phenylmethylsulfonyl fluoride was added. The mixture was rotated for 30 min at 4°C and then the coarse particulate cell debris was removed by centrifugation at 250 x g for 10 min followed by centrifuging the supernatant for 30 min at 48,000 x g to remove the fine particulate matter. The resultant supernatant consisting of surface radiolabeled cell debris was stored in aliquots at -70°C for subsequent use in immunoprecipitation.

d) Metabolic Labeling:

The method for metabolic labeling is an adaptation of the previously reported method (Liao et al., 1982). Confluent monolayers of HTB-19 and MCF-7 cells grown in methionine deficient medium were incubated with ^{35}S -methionine for 24 hr at 37°C in a humidified 5% CO_2 atmosphere. The cells were detached from the incubation

plates using EDTA, washed once with Dulbecco's PBS, and the resultant cell pellet brought up to a 0.5 ml volume with Dulbecco's PBS. Using procedures similar to those described for the isolation of cell surface-labeled antigens, these metabolically-labeled cells were lysed by adding an equal volume of 2% Nonidet P-40 and the soluble labeled antigens present in the supernatants of centrifuged cell lysates were stored in aliquots at -70°C for subsequent use in immunoprecipitation.

e) Immunoprecipitation:

The method used for immunoprecipitation has been described by us (Guha et al., 1990) and is based on methods previously reported ((Hubbard and Cohn, 1972; Peltz et al., 1987; and Liao et al., 1987). Briefly, 20 ml of cell culture supernatants of hybridomas as well as NMG, DAL-B02 (each 100 ug/ml) and PBS alone were mixed with 0.25 ml of packed goat antimouse IgG agarose beads (Sigma, St. Louis, Mo.) on a rotator overnight at 4°C. After washing the beads 3 times with cold PBS and twice with NET, 0.2 ml of radiolabeled Nonidet-P40 extract of given cell line was added and the volume brought up to 1 ml with NET. The mixture was rotated at 4°C for 4 hours. After washing the beads 3 times with NET, twice with PBS, and twice with 50 mM Tris-HCl buffer, pH 6.8, the beads were boiled in SDS-PAGE sample buffer with and without 0.2% B-mercaptoethanol. The samples were centrifuged and the supernatants were electrophoresed on a 7.5% resolving polyacrylamide gel. After staining, destaining and drying, the gels were sandwiched between a Kodak XRP film and a Dupont Cronex intensifying screen for 2-5 days at -70°C for autoradiography. The gels obtained from experiments using metabolically labeled antigens were first

soaked in Amplify[®] prior to drying and autoradiography. The molecular weights of immunoprecipitated antigens were identified by comparing with the electrophoretic migration of molecular weight standards.

8. SDS-PAGE

A mixture consisting of 20 ul of sample protein and 20 ul of sample buffer (with or without the reducing agent, B-mercaptoethanol, as desired) was boiled for 3 minutes. Using a Hamilton syringe, 5-15 ul volumes of test samples and standard molecular weight protein markers were placed into sample wells lying above the sample lanes on the polyacrylamide gels. The electrophoresis chambers were filled with electrode buffer and the current was set at 20 milliamps from the power source.

The samples were allowed to migrate till the tracer bromophenol dye present in the sample buffer reached the bottom of the gel. The gels were removed from the glass plates and put into a 100 mg% Coomassie Blue staining solution for 1 hour. After destaining with 10% acetic acid (requiring several changes of destaining fluid), the gels were mounted on Whatman chromatography paper and dried under suction and heat.

9. Western Blotting

Antigen extracts of HTB-19, MCF-7, Caki-2, and foreskin fibroblast cells using 1% Nonidet-P40 with protein concentrations of 1 mg/ml were mixed with an equal volume of SDS-PAGE reducing and non-reducing sample buffer. The samples were then electrophoresed in a Mini-gel SDS-PAGE system. After the run, the stacking gel was discarded and the resolving gel was soaked in cold transfer buffer

for 20 min to remove salt and SDS. Transfer buffer soaked nitrocellulose paper was then applied to the gel and both were sandwiched between filter paper and fiber pads in a cassette. The cassette was placed in the Transblot apparatus equipped with cooling units and a magnetic stirrer. Transblotting proceeded for 1 hr at 100 volts and 250 mAmps. The nitrocellulose paper was then carefully removed and soaked in PBS-Tween buffer for 2 hr while the gel was stained with Coomassie blue to confirm complete protein transfer. The nitrocellulose paper was cut in 1/4 inch strips corresponding to the sample lanes and one strip was stained with Amido black to confirm the presence and location of protein bands. The nitrocellulose strips were then probed with the anti-HMC MABs and nonspecific murine IgG₁. For this, the nitrocellulose strips were incubated by inversion for 2 hr with 100 ug/ml of MABs in a plastic test tube containing 15 ml of blocking buffer followed by 6 washes with the same buffer. The strips were then incubated by inversion with 15 ml of a 1:3000 diluted solution of goat antimouse IgG peroxidase conjugate for 2 hr. After a further 6 washes, Chloronaphthol substrate solution was added to the tubes and color was allowed to develop for 10 min or longer as required. Substrate solution was then removed and replaced with water to save the preparations.

10. Preparation of F(ab)₂ Fragments from Purified MABs

Standardized methods for generating F(ab)₂ fragments from purified preparations of MABs were utilized to obtain F(ab)₂ fragments of several anti-HMC MABs. Pilot experiments for each MAB were initially performed to determine the optimal pepsin digestion time and pepsin to protein ratio which results in maximal

F(ab)₂ fragment yield. Pepsin digestion was carried out at 37°C on the intact IgG molecules in 0.1M acetate or citrate buffer, at pH 3.5, 4.0, and 4.2, with pepsin : protein ratios of 1:40, 1:80 and 1:120. The digestion was allowed to proceed for various durations (times 0 hr, 0.5 hr, 1 hr, 2 hr, 4 hr, 8 hr, 16 hr and 24 hr) before being terminated by immersing the reaction vial in crushed ice for 10 min followed by centrifugation at 5000 x g for 10 min at 4°C. An aliquot of each digested MAB reaction mixture was subjected to SDS-PAGE under non-reducing conditions to assess the completeness of IgG digestion and the purity as well as the quantity of F(ab)₂ fragment present. Based on these results, the optimal digestion time and pepsin to protein ratio were used to prepare the F(ab)₂ fragments in a larger scale. After pepsin digestion and centrifugation, the supernatants were passed through a pre-equilibrated S200 column and fractions collected with an UltraRac fraction collector (LKB, Bromma, Sweden). The fractions corresponding to the first and second protein peaks corresponded to whole undigested IgG and F(ab)₂ respectively. The preparations were precipitated with ammonium sulfate (50% saturation), dissolved in PBS, dialysed against PBS, and passed through a Millipore filter before storage.

11. Determination of the Number of Binding Sites, Immunoreactive Fraction, and Association Constant of Binding for the anti-HMC MABs on HTB-19 and MCF-7 Cells

The principles underlying the determination of these parameters are shown in on the following page and given in more detail elsewhere (Lindmo and Bunn, 1986).

PRINCIPLES OF AN IDEAL ANTIBODY - ANTIGEN
REACTION AND FORMULATION OF EQUATIONS TO
DETERMINE THE IMMUNOREACTIVE FRACTION

EQUILIBRIUM OF BOUND ANTIBODY TO ANTIGEN IN AN
 IDEAL REACTION

$$\text{EQ.1 :} \quad [B] = K_A [F] [T - B]$$

WHERE

K_A = ASSOCIATION CONSTANT
 $[B]$ = CONCENTRATION OF BOUND ANTIBODY
 $[F]$ = CONCENTRATION OF FREE ANTIGEN
 $[T-B]$ = CONCENTRATION OF UNBOUND
 ANTIBODY (i.e. TOTAL - BOUND)

IF NOT ALL BUT A FRACTION (r) OF THE TOTAL AMOUNT OF
 ANTIBODY IS IMMUNOLOGICALLY REACTIVE , THEN EQ. 1 BECOMES

$$\text{EQ.2 :} \quad [B] = K_A [F] [rT - B]$$

WHICH CAN BE TRANSFORMED TO

$$\text{EQ.3 :} \quad \frac{[T]}{[B]} = \frac{1}{r} + \frac{1}{r K_A [F]}$$

THUS A PLOT OF $[T] / [B]$ VS. $1 / [F]$ YIELDS A STRAIGHT LINE WITH Y -
 INTERCEPT $1 / r$ (INVERSE OF THE IMMUNOREACTIVE FRACTION)

a) Procedures for MABs that React with Cell Surface-Associated Antigen(s)

For the determination of the immunoreactive fraction, known fixed amounts of radiolabeled MAB, typically 1 ug, which corresponds to approximately 1 / 100-200 of the saturation concentrations (that were already established from the determination of binding sites experiments described below), were incubated with decreasing numbers of live target cells, typically from 10^7 to 10^5 , in a 100 ul of medium. For the determination of the number of binding sites and K_A , a known fixed number of live target cells (usually $1-2 \times 10^5$) was incubated for 2 hr with increasing concentrations of radiolabeled preparations of MABs (0.03-3.0 mg) in a reaction volume of 0.1 ml. The reaction occurred in 0.4 ml plastic Eppendorf tubes precoated with 1% BSA in PBS and the mixtures were gently rocked at 4°C. After centrifuging at 250 x g for 3 min, the cell pellets were washed with 1% BSA in PBS containing 0.02% sodium azide and recentrifuged thrice. The cell pellets were then counted for radioactivity in a gamma emission counter. Blank tubes containing reaction mixtures but no cells showed negligible radioactive counts after the washing procedures. Nonspecific binding to the cell lines was estimated using radiolabeled normal mouse IgG preparations of the same subclass or cells labeled with specific antibody plus an excess of unlabeled MAB, both of which typically showed less than 5% binding even at the highest levels of MABs in the incubation mixtures. Appropriate corrections for IRF and nonspecific binding were introduced during the analysis of binding data using the LIGAND^R program of Munson and Rodbard as adapted for an IBM PC (McPherson 1985).

b) Procedures for MABs that React with Intracellular and Extracellular Antigen(s)

An estimate of the number of binding sites per a given number of cells and K_A of binding of these MABs was made using constant numbers of 0.5% glutaraldehyde fixed HTB-19 cells (either 86,500 or 87,400 cells in the different experiments) in 96 well flat bottom plates. This fixation method is identical to the fixation method used in both immunofluorescence and ELISA assays which confirmed the preservation of immunoreactivity of the MAB-defined antigens. To the wells, increasing amounts of a radioiodine-labeled MAB or radioiodine-labeled nonspecific IgG were added (typically 0.3-3.0 ug). After incubation at room temperature for 90 min, the wells were digested with 50% sulfuric acid overnight at 37°C. Measured volumes of cell digests were then counted for radioactivity in a gamma counter. The results were analyzed by the LIGAND^R program as above to determine the binding parameters.

Alternatively, an assay based on the competitive inhibition of binding of a radiolabeled MAB by the unlabeled MAB was also used to determine these parameters. For this, a labeled MAB (typically 3 ug) was diluted with varying amounts of the unlabeled MAB (typically 0-18 ug). The mixtures of the labeled and unlabeled MAB were then added to 96 flat bottom well plates containing 20,000 glutaraldehyde fixed HTB-19 or MCF-7 cells. After incubation at room temperature for 90 min, the cells in each well were digested in 200 ul of 50% sulfuric acid and a fixed cell digest volume (typically 150 ul) was counted for radioactivity as before. For the estimation of the binding parameters, the total radioactivity in each well was calculated and the results were analyzed using the LIGAND^R program.

In prior pilot studies, glutaraldehyde fixed cells were digested with 1% Nonidet-P40, 1% SDS, various mixtures of Nonidet-P40 and SDS, Protosol^R, 40% NaOH, concentrated and 50% sulfuric acid at different temperatures and for different durations. After treatment, wells were examined microscopically for evidence of any remaining intact cells or cellular debris and the visual interpretation was verified by a crystal violet assay which is described later. These studies showed that 50% sulfuric acid was an adequate agent for digesting glutaraldehyde fixed cells overnight at 37°C.

12. Competitive Binding Experiments

To assess the spatial relationship between the determinants recognized by 2 anti-HMC MABs that reacted with a cell surface antigen, a constant amount of a given radiolabeled MAB (typically 1-4 ug/ml) was mixed with increasing amounts of the same unlabeled MAB or of a different unlabeled MAB (typically 0-120 ug/ml) and the mixtures reacted with a constant number of live HMC cells. The procedure followed in these experiments was very similar to the procedures for determining IRF and binding parameters as described in item 11a (page 66). Briefly, the mixtures of labeled and unlabeled MABs were incubated for 2 hr at 4°C and after washing, the live cell-associated radioactivity was directly determined. Reaction mixtures consisting of target cells and only labeled MAB were used to determine the maximum amount of MAB that could bind under the reaction conditions. To produce data for plotting % binding inhibition curves, the radioactivity counts obtained from assaying a given mixture was divided by the radioactivity counts obtained from assaying the

mixture which determined maximum MAB binding. Each of these ratios was then multiplied by 100% and the percentages were plotted against the concentration of unlabeled MAB in each mixture. The principle and results of similar types of competitive binding experiments to determine the spatial relationships among the determinants of other anti-HMC MABs have been previously described (Price, 1988).

13. Determination of the Sensitivity of Antigens to Neuraminidase:

To assess whether anti-HMC MABs react with sialic acid determinants on the target antigens, 10^7 EDTA harvested HTB-19 and MCF-7 cells were incubated in 5 ml of Hank's balanced salt solution or 0.06 M acetate buffer with or without 1.5 mg of neuraminidase with a total of 2.5 NAN lactose units for 30 min at 37°C. After the enzyme treatment, the cells were washed three times with cold 0.5% BSA in PBS and then aliquoted into 96 V well plates to evaluate the reactivity of these cells with each anti-HMC MAB or with a nonspecific murine IgG using the ELISA technique as described earlier in item 6 (pages 54-56). The ELISA assay concurrently assessed the reactivity of each MAB with cultured HMC cells that were detached with EDTA but not treated and with HMC cells that were treated identically as the test cells except for the addition of neuraminidase. The ELISA-based reactivity of each MAB with neuraminidase treated cells was compared to the reactivity of each MAB with cells not treated with the enzyme. The reactivity of each MAB with these target cells was confirmed by treating additional aliquots of cells from each assay with FITC-conjugated goat antimouse IgG and then processing for examination under a fluorescence microscope as described earlier in item 2 (pages 51-52).

14. Complement-dependent Cytotoxicity Assay

Cytotoxicity of the anti-HMC MABs was assessed by a previously described vital dye (trypan blue) exclusion method from this laboratory (Ghose et al., 1977) using a minimum of 250 ug/ml of all MABs and up to 1000 ug/ml for most MABs and fresh human AB serum as a source of complement. The complement activity of this freshly obtained human AB serum, however, was not confirmed. The same serum, which was heated at 56°C for 30 min to inactivate complement, was used as a control in these experiments. Observations of incubated cells at 37°C occurred every 30 min for the first 4 hr and then at 8 hr, 16 hr and 24 hr.

15. Tumor Cell Proliferation Assay

The effect of HMC-specific and nonspecific MABs by themselves, the two anti-cancer chemotherapeutic drugs ADM and MTX, and different HMC-specific and nonspecific MAB-drug conjugates on the proliferation of HTB-19, MCF-7, and Caki-2 cells was evaluated with a crystal violet assay (Kueng et al., 1989). For this assay, 2500 cells in MEM-NEAA containing 10% fetal calf serum were pipetted into SARSTEDT 96 well culture plates and incubated for 30 hr at 37°C in a humidified 5% CO₂ atmosphere to allow attachment of cells. Serum dialysed against PBS was used in all experiments involving MTX as reported by this laboratory previously (Uadia et al., 1983; Singh et al., 1989) since it is known that inhibitors of uptake of MTX by cells such as PO₄⁻³, CL⁻, HCO₃⁻, Ca⁺², and Na⁺ (Henderson and Zevely, 1980) as well as compounds structurally related to MTX and extracellular tetrahydrofolate cofactors (Goldman, 1971 and 1981; Goldman et al., 1968) are present in serum. Appropriate

MABs, drugs or MAB-drug conjugates in a volume of MEM equal to that present in the wells was then added to appropriate wells in triplicate. Two different procedures were used to evaluate the effect of a 6 hr pulse or continuous exposure to these agents on test cells. After incubation of cells with a test agent for 6 hr at 37°C for pulse exposure studies, the wells were washed with Dulbecco's PBS 3 times and fresh medium was added. This washing step was omitted in the continuous exposure studies and after 7 days of incubation at 37°C in a humidified 5% CO₂ atmosphere, the medium was discarded from the wells followed by fixation of cells with 1.0% glutaraldehyde in PBS for 20 min at room temperature before extensive washing with distilled water and air drying. Crystal violet solution (100 ul/well) was then added and the plates shaken on a Dynatech shaker for 15 min prior to further washing with distilled water and air drying. The color was eluted from the wells with 100 ul of 10% acetic acid and the absorbance at 570 nm was determined with a Dynatech plate reader. In these assays, free MAB concentrations ranged from 0-1000 ug MAB/ml per well, free MTX and MAB-linked MTX concentrations ranged from 0-20 ug MTX/ml per well, and lastly free ADM and MAB-linked ADM concentrations ranged respectively from 0-0.8 ug ADM/ml and 0-25 ug ADM/ml per well.

MAB-drug conjugates used were prepared by Dr. J. Kralovec. MTX was linked to MAEs by the active ester intermediate method developed by Drs. A.H. Blair and T. Ghose (Ghose et al., 1983). Briefly, 0.76 mg of MTX, 0.21 mg of N-hydroxysuccinimide, and 0.38 mg of dicyclohexylcarbodiimide were dissolved in 0.2 ml of dimethylformamide at 4°C and stirred at room temperature for 18 hr after which

any precipitate was removed. The mixture was then added dropwise to 10 mg of MAB in 2 ml PBS with 0.2 ml dimethylformamide and then stirred for 2 hr. Precipitates from the reaction mixture were then removed by centrifugation and the supernatant was dialysed for 3 days against PBS. The soluble conjugate product again cleared from precipitates was then sterilized by millipore filtration. Molar incorporation ranged from 4-6 MTX per IgG.

ADM was linked to MABs either by a hydrazone spacer at the C13 drug position using a modification of a previously reported method (Greenfield et al., 1990) or by a CAA spacer at the drug's amino sugar moiety (Shen and Ryser, 1981). Briefly, the hydrazone linkage method consisted of mixing 2 drops of trifluoromethane sulfonic acid with 5.45 mg of ADM and 2.3 mg of HPDP in 0.5 ml methanol at room temperature overnight before adjusting the pH to 7.0 and evaporating the methanol. The residue was chromatographed on a C-18 RP silica gel column using 3% HCO_2NH_4 in aqueous 50% methanol and the isolated ADM-hydrazone was lyophilized. Next, 5.0 mg of MAB in 1 ml PBS was reacted with a 20 fold excess of SPDP in 100 ul of dimethylformamide before desalting in an Econo-pac P6 column (BIO-RAD, Richmond, CA). The average content of spacer per IgG in the product was 4 (mole/mole). To this was added 100 ul of a 15% dithiothreitol solution and the mixture was incubated at room temperature for 30 min before passing it through a pre-equilibrated column with phosphate buffer, pH 7.2, containing 1 mM EDTA. The modified MAB was then reacted with a 50 fold molar excess of ADM-hydrazone reconstituted in 100 ul of dimethylformamide. After incubation at 4°C overnight,

precipitate was removed by centrifugation and the mixture was passed through an Econo-pac P6 column using 0.1 M phosphate buffer. The concentration of ADM was determined by absorbance of the pooled protein fractions at 480 nm utilizing the extinction coefficient of ADM at this wavelength. After protein concentration of the product was determined (Lowry, 1951), the various ADM-C13 conjugates prepared were shown to contain 1.5-7 moles of ADM per mole IgG.

The CAA linkage method consisted of mixing overnight at 4°C a solution formed by the dropwise addition of 10 mg CAA in 1.0 ml of dioxane to 7.9 mg of ADM in 300 ul pyridine. This mixture was purified by distributing it between chloroform and 5% NaHCO₃ followed by the removal of chloroform after 2 extractions. The pH of the aqueous phase was lowered to 2.5 and the ADM was extracted by ethyl acetate. The organic phase was washed with brine, dried with Na₂SO₄ and the solvent evaporated to yield ADM-CAA. Next, 10 mg of MAB in 0.2 M phosphate buffer, pH 8.0, was added a mixture consisting of 3 mg ADM-CAA in 100 ul dimethylformamide and 13 mg of 1-(3-dimethylaminopropyl)-3-ethylcarbodiimide in 200 ul of 0.01 M acetate buffer, pH 5, that was standing for 10 min at room temperature. After stirring overnight at 4°C, the product was passed through an Econo-pac P6 column. Molar incorporation of ADM in the various conjugates was 3-9.

All MTX and ADM conjugated anti-HMC MABs were evaluated for retention of antibody activity by ELISA on glutaraldehyde fixed target cells and by immunofluorescence assay before use in cell proliferation assays.

16. Immuno-Gold Studies

The methods for preparing gold sol and adsorption of MABs to gold particles are described in detail (DeMey, 1986) and reviewed elsewhere (Beesley, 1989, Baschong and Wrigley, 1990, and Stirling, 1990). To prepare 15 nm citrate gold sol, 2.5 ml of a 1% HAuCl_4 was added to 240 ml of boiling distilled water. To this was quickly added 7.5 ml of a 1% trisodium citrate solution and the mixture was boiled for an additional 30 min. The gold sol solution was evaluated for the mean size of gold particles with electron microscopy (courtesy of Dr. G. Faulkner) and then stored in the dark at 4°C. The minimal amount of MAB at either pH 7.0 (in PBS) or pH 9.0 (in sodium borate buffer) needed to stabilize the 15 nm size gold particles was determined by constructing a concentration variable isotherm for each MAB. For this, a series of test tubes containing 10 μl to 100 μl of a 1 mg/ml MAB solution diluted with 90 μl to 0 μl of either PBS or borate buffer was prepared. To these tubes, 1 ml of pH-adjusted gold sol was added and the tubes immediately vortexed. After 2 min, 1 ml of a 10% NaCl solution was added followed again by vortexing. After an additional 5 min, the absorbance at 580 nm of each tube was taken using 1 ml gold sol containing 100 μl of protein solvent and 100 μl of distilled water as a blank. The results were plotted for each MAB with the absorbance at 580 nm as the ordinate and the amount of added protein expressed in $\mu\text{g/ml}$ gold sol as the abscissa.

For adsorption of radiolabeled MABs on to gold particles, an appropriate amount of ^{125}I -labeled MAB (DAL-BR6, DAL-BR7, DAL-K29, DAL-K45, and DAL-B01) was added to sufficient gold sol as determined by the above procedure and the

gold-IgG complex was isolated by repeated washes and centrifugations using Tris-buffered BSA solution, pH 8.2 as described (DeMey, 1986). The isolated dual labeled (^{125}I and gold) MABs were millipore filtered and kept at 4°C in the dark until used.

For binding and uptake assays, dual labeled MABs were incubated with suspensions of target and nontarget cell lines (HTB-19, MCF-7, Caki-1, and Caki-2 cells) for 2 hr at 4°C before 3 washes with 0.1% BSA in PBS. A 0 hr aliquot was taken and the cells were resuspended in medium for incubation at 37°C . Further aliquots were taken at 1 hr, 2 hr, 4 hr, and 6 hr. The cells were pelleted by centrifugation and fixed overnight with 2.5% EM grade glutaraldehyde in PBS. The ^{125}I activity of the cell pellets was determined using a gamma emission counter. The cell pellets were then delivered to Dr. G. Faulkner who processed the specimens for thin sectioning and who examined the sections with a transmission electron microscopic.

17. Binding of HTB-19 and MCF-7 Cells to Vitronectin, Fibronectin and Laminin Coated Plates and Assessment of Inhibition of Binding of the MABs to HTB-19 Cells by Polyclonal anti-Vitronectin Receptor Antibodies

These studies involved coating appropriate wells of a 96 well culture plate with 200 μl of either a 10 $\mu\text{g}/\text{ml}$ solution of fibronectin containing 0.1% BSA or of 5 $\mu\text{g}/\text{ml}$ solutions of laminin or vitronectin also containing 0.1% BSA. Uncoated and BSA coated wells served as controls. HTB-19 and MCF-7 cells in 200 μl of MEM-NEAA medium without serum were put into these wells and observed for attachment over a

period of 16-48 hr. A competitive binding assay was used to assess whether polyclonal anti-vitronectin receptor antibodies could inhibit the binding of radiolabeled anti-HMC MABs to HTB-19 cells. To the wells of 96 well plates containing 5000 glutaraldehyde fixed HTB-19 cells per well was added a mixture consisting of polyclonal anti-vitronectin receptor antibody at concentrations ranging from 0.03 ug/ml to 200 ug/ml and a given concentration (1-4 ug/ml) of a radiolabeled anti-HMC MABs. The mixture was allowed to react with HTB-19 cells for 2 hr followed by 3 washes with 1% BSA in PBS and the amount of cell associated MAB was assessed by the method using 50% sulfuric acid to digest the cells as described earlier in item 11b (pages 67-68).

18. Comparison of anti-HMC MAB Reactivity to Melanoma and Caki-1 Cells Grown in vitro and to Cells Grown as Xenografts in vivo

Fresh, unfixed 5 micron thick frozen sections of melanoma or Caki-1 xenografts were incubated with MABs and evaluated by immunofluorescence assay. Also, tumor cells from melanoma and Caki-1 xenografts as well as from surgically excised cutaneous melanoma tissues from three patients which failed to react with the anti-HMC MABs were grown in vitro in 96 well culture plates. After 1-18 days of culture, the cells were fixed in 0.5% glutaraldehyde in PBS and MAB reactivity was evaluated by an ELISA assay.

19. Tumor Localization and Biodistribution of Radiolabeled anti-HMC MABs in Nude Mice Xenografted with HTB-19 Cells

Inoculation of 2×10^6 HTB-19 cells s.c. in 6-10 week-old female nude mice resulted in progressive tumors in most mice. A photograph of a mouse bearing a typical tumor is presented in Figure 1 (pages 78-79). Similar inoculations of Caki-1 or M21 cells produced progressive tumors in all mice. Two days prior to radiolabeled MAB or $F(ab)_2$ injections, the tumor bearing nude mice were given sterilized tap water supplemented with Lugol's iodine solution to load the thyroid gland of the animals with iodine. ^{131}I -labeled preparations of MAB or its $F(ab)_2$ fragment were made using the chloramine-T method and in one experiment with DAL-BR6, using the PIB method. Similarly, ^{125}I -labeled preparations of tumor nonspecific murine IgG or $F(ab)_2$ fragment of matching subclass were prepared for different experiments. A mixture of the two radiolabeled preparations was then made consisting ideally of 40-50 uCi ^{131}I -labeled preparation and 2-10 uCi ^{125}I -labeled preparation. This mixture was injected i.v. into the tail veins of each mouse for most experiments that evaluated the tumor localization and biodistribution of individual anti-HMC MABs in the HTB-19 xenograft model.

FIGURE 1:

**PHOTOGRAPH OF A NUDE MOUSE WITH A HTB-19 HUMAN MAMMARY
CARCINOMA SUBCUTANEOUS XENOGRAFT**



FIGURE 1

The amount of protein injected per mouse for most experiments ranged from 5-20 ug and equal amounts of the HMC-specific and HMC-nonspecific MAB were injected in all experiments. In the experiment evaluating the PIB method, more of the ^{125}I preparation was used (40 uCi per mouse) than the ^{131}I preparation (10 uCi per mouse) and an equal amount of protein was injected (72 ug of each radiolabeled preparation per mouse).

For two experiments using a combination of 2 tumor specific MABs, equal amounts of each MAB (28 or 52 ug in the respective studies) were used, one MAB of the pair was labeled with ^{131}I and the other with ^{125}I . In these two experiments, the mice were given between 40-50 uCi ^{131}I and 2-10 uCi of ^{125}I .

Tumor-bearing mice in groups of three were used in virtually all experiments to evaluate the tumor localization of anti-HMC MABs or their F(ab)₂ fragments. The animals under Somnatol^R anaesthesia (35 mg/kg/i.p.) were scanned daily with a gamma camera equipped with either a wide field of view or pin-hole collimator (General Electric Maxicam, Nuclear Medicine Departments, Halifax Infirmary or Victoria General Hospitals). The total body radioactivity was measured using a Mediac Dose Calibrator at 8 hr intervals initially and then daily. Depending on the experiment, animals were sacrificed at specified times (24, 48, 72, 96 or 144 hr). Blood was collected by intracardiac puncture of anaesthetized animals and after severing the axillary and iliac vessels, their organs flushed with PBS via the inferior vena cava, and right and left ventricles of the heart. The organs and tumors were then removed, blotted dry, and weighed. The ^{131}I and ^{125}I activities in aliquots of

tissue were determined along with ^{131}I and ^{125}I standards using a gamma emission counter and appropriate windows to distinguish between ^{131}I and ^{125}I activities. To confirm the findings, specimens were counted again for ^{125}I activity after allowing the ^{131}I to decay for 6 half lives. Counts were converted to uCi and then divided by tissue weights for generation of appropriate plots to analyze the data.

21. Autoradiography

Autoradiography on 5 um thick formalin-vapor fixed cryostat sections of tumor tissue obtained after radio-immunolocalization studies was carried out using Eastman Kodak NTB 3 emulsion to cover the slides as described by us before (Ghose et al., 1988). After 2-4 days at 4°C in the dark, the slides were developed with Dektol^R (diluted 1:2 with water) and fixed with Kodak photographic fixing solution prior to Hematoxylin-Eosin staining.

RESULTS

PART 1

CHARACTERIZATION OF MABS AND THE DISTRIBUTION OF THEIR TARGET ANTIGENS

1. Purification of MABs from Ascites Fluid

The amount and titer of each MAB recovered from MAB-containing ascites fluid using Protein A or caprylic acid purification methods are presented in Table 1 (page 83). For all MABs, except DAL-BR3, Protein A affinity purification yielded a higher recovery per ml of ascites fluid than that obtained with the caprylic acid method. SDS-PAGE of purified MABs showed that the Protein A method yielded a more pure IgG preparation. Figure 2 (pages 84-85) presents the SDS-PAGE of several MABs to illustrate the purity of the preparations isolated by the 2 methods.

2. Isotype, Subclass and Immunoglobulin Light Chain of the MABs

Table 1 also presents the isotype, subclass and the immunoglobulin light chain of the MABs. All the 11 anti-HMC MABs are murine IgG. Six of the 11 anti-HMC MABs belong to the murine IgG₁ subclass, one each to the IgG_{2a} and IgG_{2b} subclasses, and three to the IgG₃ subclass thereby encompassing all murine IgG subclasses in this panel of 11 MABs. All but two of the 11 MABs are Kappa light chain-bearing, the exceptions being DAL-BR5 and DAL-BR10 which bear Lambda light chains.

TABLE 1: RESULTS OF MAB SUB-ISOTYPING AND
ASCITES PURIFICATION METHODS

MAB	Subclass	Isolation Method	Recovery (mg/ml ascites)	Titer (ug/ml)
Br1	IgG ₃ K	Protein A	1.34	0.039
		Caprylic	0.26	3.125
Br2	IgG ₁ K	Protein A	0.98	1.56
		Caprylic	0.04	2.5
Br3	IgG ₁ K	Protein A	0.25	50
		Caprylic	1.17	0.156
Br4	IgG ₁ K	Protein A	2.92	0.005
		Caprylic	2.8	0.0049
Br5	IgG ₁ L	Protein A	3.75	0.005
		Caprylic	2.62	0.0025
Br6	IgG ₁ K	Protein A	3.4	0.022
		Caprylic	1.71	0.09
Br7	IgG _{2b} K	Protein A	2.16	0.005
		Caprylic	1.2	0.0049
Br8	IgG ₁ K	Protein A	5.45	0.005
		Caprylic	0.15	0.39
Br9	IgG ₃ K	Protein A	0.715	0.0098
		Caprylic	0.18	0.19
Br10	IgG ₃ L	Protein A	1.82	0.005
		Caprylic	1.05	0.09
Br11	IgG _{2a} K	Protein A	1.24	1.56
		Caprylic	0.08	0.78

FIGURE 2:

SDS-PAGE OF ANTI-HMC MABS, K29, K45, AND IgG₁.

EACH MAB WAS PURIFIED EITHER BY THE PROTEIN A OR

CAPRYLIC ACID METHOD. THE GELS WERE RUN UNDER

NON-REDUCING CONDITIONS AND STAINED WITH COOMASSIE BLUE.

LANE 1: DAL-BR6 PROTEIN A PURIFIED

LANE 2: DAL-BR7 PROTEIN A PURIFIED

LANE 3: K45 PROTEIN A PURIFIED

LANE 4: DAL-BR8 PROTEIN A PURIFIED

LANE 5: DAL-BR5 PROTEIN A PURIFIED

LANE 6: DAL-BR4 PROTEIN A PURIFIED

LANE 7: K29 CAPRYLIC ACID PURIFIED

LANE 8: IgG₁ CAPRYLIC ACID PURIFIED

LANE 9: DAL-BR11 CAPRYLIC ACID PURIFIED

LANE 10: DAL-BR9 CAPRYLIC ACID PURIFIED

LANE 11: DAL-BR8 CAPRYLIC ACID PURIFIED

LANE 12: DAL-BR7 CAPRYLIC ACID PURIFIED

LANE 13: DAL-BR6 CAPRYLIC ACID PURIFIED

LANE 14: DAL-BR1 CAPRYLIC ACID PURIFIED

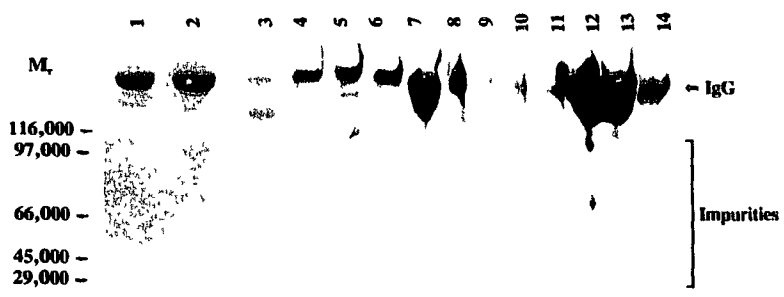


FIGURE 2

3. MAB Reactivity with Human Normal Tissues and Cancer Cell Lines

Tables 2 and 3 (pages 87 and 88) respectively present the reactivity of MABs based on immunofluorescence assay with a panel of 28 normal tissues and several human cancer cell lines. MABs DAL-BR3, 4, 9, 10, and 11 did not react with any normal human tissue while the remaining MABs showed a very restricted reactivity with isolated tissues. Each of the 11 MABs reacted with varying intensity with all the 5 HMC cell lines including the HTB-124 line that forms colonies in soft agar but is not tumorigenic in nude mice. However, none of the MABs reacted with the "normal" breast epithelium line HTB-125. Using an ELISA assay, MABs that were purified by either the Protein A or caprylic acid method reacted with these HMC lines at comparable titers. Table 3 also shows that these anti-HMC MABs reacted with equal intensity with all 3 melanoma, one of 4 renal cell cancer lines, and the single colon carcinoma cell line tested. None reacted with the lymphoma, nephroblastoma or prostatic adenocarcinoma cell lines tested.

TABLE 2: IMMUNOFLUORESCENCE REACTIVITY OF ANTI-HMC MABS WITH NORMAL HUMAN TISSUES

TISSUES	BR1	BR2	BR3	BR4	BR5	BR6	BR7	BR8	BR9	BR10	BR11
Nerve	-	-	-	-	-	-	-	-	-	-	-
Testes	-	-	-	-	-	-	-	-	-	-	-
Heart	-	-	-	-	-	-	-	-	-	-	-
Tonsil	+ ¹	-	-	-	-	-	-	-	-	-	-
Lymph Node	+ ²	-	-	-	-	-	-	-	-	-	-
Placenta	-	-	-	-	-	-	-	-	-	-	-
Spleen	-	-	-	-	-	-	-	-	-	-	-
Cerebrum	-	-	-	-	-	-	-	-	-	-	-
Liver	-	-	-	-	-	-	-	-	-	-	-
Kidney	-	-	-	-	-	-	-	-	-	-	-
Thymus	-	+ ³	-	-	-	-	-	-	-	-	-
Breast	-	-	-	-	-	-	-	-	-	-	-
Uterus	-	-	-	-	-	-	-	+ ⁴	-	-	-
Tube	-	-	-	-	-	+ ⁵	+ ⁶	-	-	-	-
Ovary	-	-	-	-	-	-	-	-	-	-	-
Thyroid	-	-	-	-	+ ⁷	-	-	-	-	-	-
Parotid	-	-	-	-	+ ⁸	-	-	-	-	-	-
Muscle	-	-	-	-	-	-	-	-	-	-	-
Pancreas	-	-	-	-	-	-	-	-	-	-	-
Adrenal	-	-	-	-	-	-	-	-	-	-	-
Stomach	-	-	-	-	-	-	-	-	-	-	-
Colon	-	-	-	-	-	-	-	-	-	-	-
Bladder	-	-	-	-	-	-	-	-	-	-	-
Prostate	-	-	-	-	-	-	-	-	-	-	-
Skin	-	-	-	-	-	-	-	-	-	-	-
Sm. Bowel	+ ⁹	-	-	-	-	-	-	-	-	-	-
F. Skin	-	-	-	-	-	-	-	-	-	-	-
F. Kidney	-	-	-	-	-	-	-	-	-	-	-

* Fetal

- 1 Weak staining of germinal center cells
- 2 Scattered positive cortical lymphocytes
- 3 Scattered positive dendritic cells
- 4 Strongly positive staining of endometrial epithelial cells
- 5 Epithelial cells mildly positive
- 6 Epithelial cells moderately positive
- 7 Weakly positive epithelial cells
- 8 Weakly positive epithelial cells
- 9 Faintly positive epithelial cells

4. Membrane Staining, Staining of Fixed Cells, and Capping Studies

DAL-BR6 showed membrane staining of viable HMC cell suspensions (Figure 3, pages 90-91) as did DAL-BR7 (data not shown). All the other anti-HMC MABs showed staining of small cytoplasmic globules in acetone fixed cells. In multowell slides containing 0.5% glutaraldehyde fixed cells, these globules were also seen irregularly distributed on cell surfaces and immediately outside cells. A representative experiment is shown in Figure 4 (pages 90-91). Of the 11 anti-HMC MABs, only DAL-BR6 and DAL-BR7 were able to induce caps on HTB-19 and MCF-7 target cells. The experiments revealed 8-10% of exposed cells that had caps after 4-6 hr of incubation at 37°C.

FIGURES 3 AND 4:

IMMUNOFLUORESCENCE PHOTOMICROGRAPHS SHOWING MEMBRANE STAINING OF HTB-19 CELLS BY DAL-BR6 (FIGURE 3) AND STAINING OF EXTRACELLULAR MATERIAL FROM HTB-19 CELLS BY DAL-BR1 (FIGURE 4).

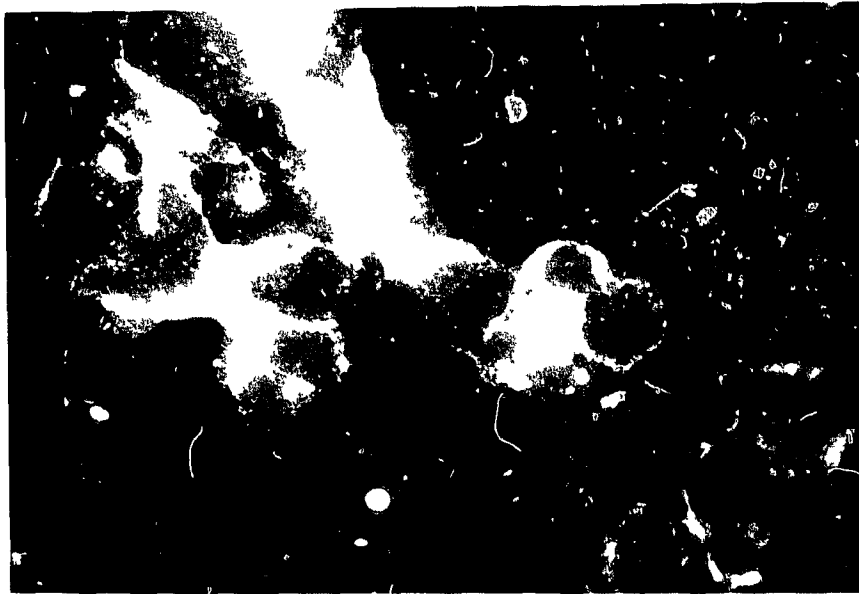


FIGURE 3

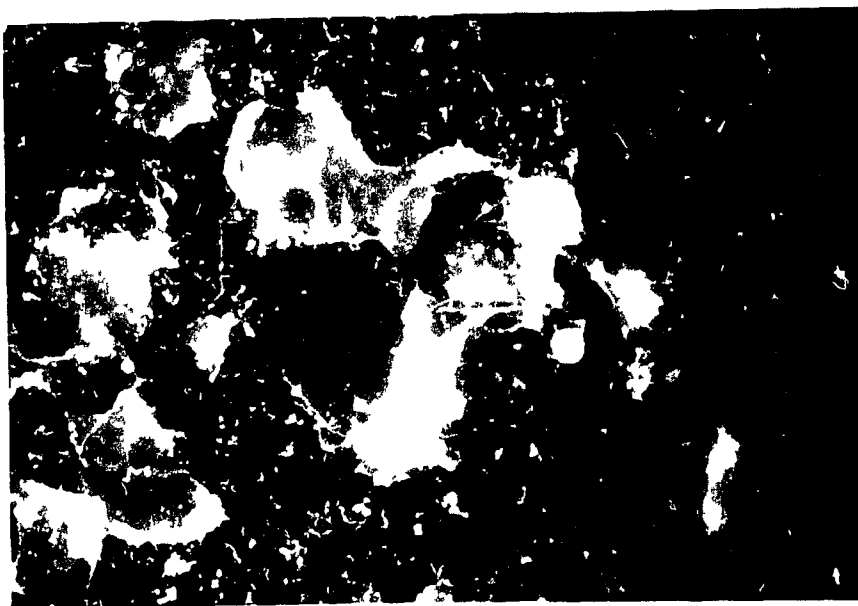


FIGURE 4

5. MAB Reactivity with Human Fresh Frozen or Formalin Fixed, Paraffin Embedded Tumors

Table 4 (page 93) presents the reactivity of the anti-HMC MABs with fresh frozen sections of surgically resected infiltrating mammary duct carcinomas from 13 patients using an immunofluorescence assay. DAL-BR6 stained tumor cells in all specimens examined while DAL-BR7 stained tumor cells in 11/13 specimens. With all the 11 MABs, the intensity of staining of tumor cells varied within a given specimen as well as from specimen to specimen. DAL-BR5 stained 100% of tumor cells in 9/13 specimens whereas DAL-BR7 stained 100% of tumor cells in 9/11 specimens. Tumor cells in specimen #12 stained only with DAL-BR6 and tumor cells in specimen #13 stained only with DAL-BR6 and DAL-BR11. Three tumors, specimens #8, #9, and #10, stained with all the 11 anti-HMC MABs. In specimen #10, 100% of tumor cells reacted with all the MABs. DAL-BR5,6 and 7 demonstrated the most consistent staining pattern in these frozen section specimens in terms of either cell surface or diffuse cytoplasmic reactivity. Representative patterns of staining exhibited by 2 of the 11 MABs are shown in Figures 5 and 6 (pages 94-95).

TABLE 4: REACTIVITY OF ANTI-HMC MABS WITH UNFIXED FROZEN SECTIONS OF HUMAN BREAST CARCINOMA SPECIMENS

SPECIMEN #	BR1	BR2	BR3	BR4	BR5	BR6	BR7	BR8	BR9	BR10	BR11
1.	+A	+A	-	-	-	++A	++C	-	-	-	-
2.	+A	+A	+A	+A	+A	++A	++C	+A	-	-	-
3.	+B	+B	-	+B	++C	+A	+A	+B	+B	+B	-
4.	-	-	+C	-	+A	++C	++C	-	-	-	-
5.	-	+B	++B	+A	++B	+C	+C	-	+B	+B	-
6.	+A	-	++C	++C	+C	+C	+C	-	+A	-	+A
7.	++C	-	-	-	+C	+C	+C	-	+C	++B	++B
8.	+A	+B	+B	+B	+C	+C	+C	+C	+C	+C	+C
9.	++B	++C	+B	-	+B	+C	+C	++C	+B	+B	+C
10.	+C	++C	++C	+C							
11.	-	-	-	-	-	+A	+A	-	-	+A	+A
12.	-	-	-	-	-	+C	-	-	-	-	-
13.	-	-	-	-	-	+C	-	-	-	-	+C

LEGEND:

- NEGATIVE REACTIVITY
- + MILD TO MODERATE REACTIVITY
- ++ STRONG REACTIVITY
- A < 25% OF MALIGNANT CELLS POSITIVE
- B 25% TO 75% OF MALIGNANT CELLS POSITIVE
- C > 75% TO 100% OF MALIGNANT CELLS POSITIVE

CONCENTRATION OF MAB USED: 100 ug/ml

CONTROLS USED:

1. GAMG-FITC CONJUGATE ALONE
2. NMG INSTEAD OF MAB
3. MAB DAL-B02 (IgG₁) INSTEAD OF MAB

SPECIMENS WERE ALL INFILTRATING DUCTAL CARCINOMAS WITH OR WITHOUT AN INTRADUCTAL CARCINOMA COMPONENT

FIGURES 5 AND 6:

**REACTIVITY OF ANTI-HMC MABS WITH UNFIXED FROZEN SECTIONS OF
EXCISED INFILTRATING MAMMARY DUCT CARCINOMA SPECIMENS
WITH OR WITHOUT AN INTRADUCTAL CARCINOMA COMPONENT**

**FIGURE 5: INTRADUCTAL CARCINOMA STAINED WITH DAL-BR5
(NOTE CYTOPLASMIC STAINING OF TUMOR CELLS)**

**FIGURE 6: INFILTRATING DUCT CARCINOMA STAINED WITH DAL-BR7
(NOTE MEMBRANE STAINING OF TUMOR CELLS)**

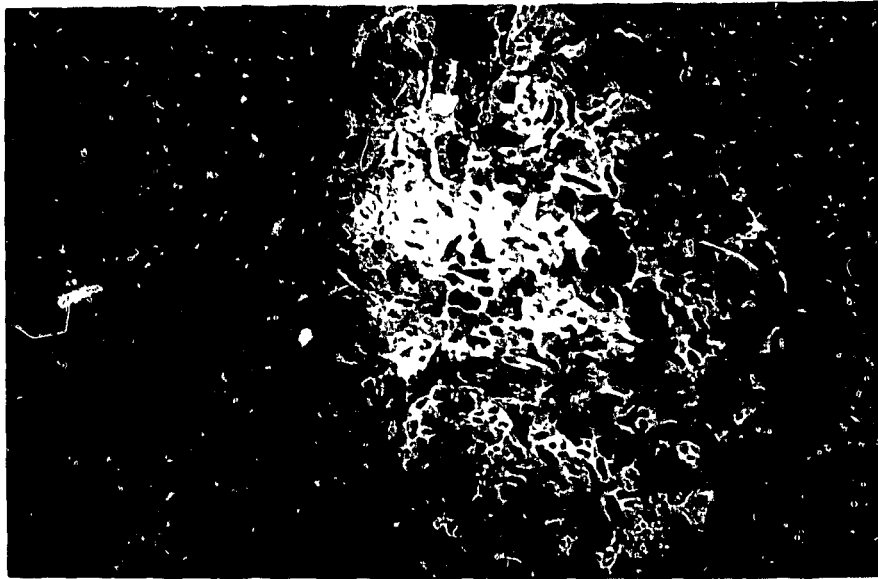


FIGURE 5

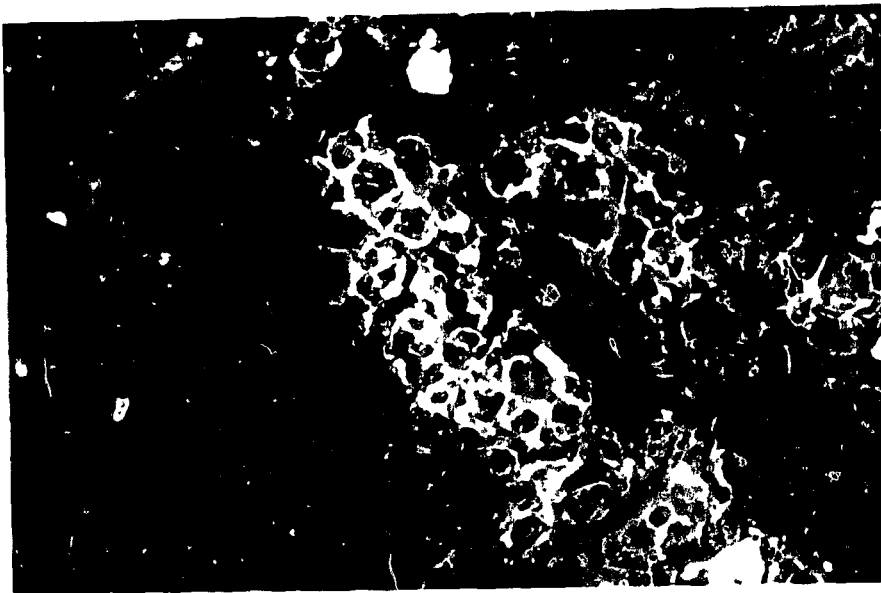


FIGURE 6

Table 5 (page 97) illustrates the results of immunofluorescence assay of MABs with fresh frozen sections of freshly excised specimens of malignant melanoma from 3 patients and RCC from 7 patients. Melanoma cells in one of the three specimens did not react with any of the 11 anti-HMC MABs and in another did not react with DAL-BR1,2,3,4 and 5. However, a small proportion of cells in two of these melanoma specimens did react with DAL-BR6,7,8,9,10 and 11. With the exception of DAL-BR1 and DAL-BR2, the other 9 MABs reacted with various proportions of tumor cells in one or more of the 7 RCC specimens.

Table 6 (page 98) presents the reactivity of all the 11 anti-HMC MABs with sections of formalin-fixed, paraffin-embedded tissues from various histological types of HMC, benign human breast lesions, and several other human malignant lesions. DAL-BR4, DAL-BR5, and DAL-BR10 failed to react with sections of all the tumors tested. Only MAB DAL-BR6 reacted with small proportion of cells in a non-mammary tumor (3/5 melanomas). Only MAB DAL-BR3 appeared to have specificity for paraffin embedded HMC tissues indicated by its reactivity with 2/5 intraductal carcinomas and 1/5 infiltrating carcinomas but not with any benign breast lesion. However, its sensitivity appears to be very low since it reacted with only 3/18 paraffin embedded HMC. DAL-BR1, 2, 6, 7, 8, 9 and 11 reacted with both benign and malignant epithelial lesions of the breast. DAL-BR6 reacted with a total of 10/18 malignant lesions and 3/9 benign lesions whereas DAL-BR7 reacted with 16/18 malignant lesions and 8/9 benign lesions indicating a loss of specificity with the increased sensitivity of DAL-BR7 for HMC.

TABLE 5: IMMUNOFLUORESCENCE ASSAY OF MAB REACTIVITY TO UNFIXED FROZEN SECTIONS OF HUMAN RCC AND MELANOMA

MAB	RENAL CELL CARCINOMA	MALIGNANT MELANOMA
DAL-BR1	0/7*	0/3
DAL-BR2	0/7	0/3
DAL-BR3	4/7	0/3
DAL-BR4	1/7	0/3
DAL-BR5	1/7	0/3
DAL-BR6	5/7	2/3
DAL-BR7	5/7	1/3
DAL-BR8	1/7	2/3
DAL-BR9	3/7	2/3
DAL-BR10	1/7	2/3
DAL-BR11	1/7	2/3

* # of specimens with MAB reactive tumor cells / Total # of specimens examined

TABLE 6: IMMUNOPEROXIDASE BASED ASSAY OF MAB REACTIVITY WITH FORMALIN FIXED, PARAFFIN EMBEDDED HUMAN TUMORS

	B R 1	B R 2	B R 3	B R 4	B R 5	B R 6	B R 7	B R 8	B R 9	B R 10	B R 11
BREAST CARCINOMAS:											
Intraductal (n=5)	3	3	2	0	0	2	4	3	2	0	2
Infiltrating Ductal (n=5)	5	2	1	0	0	2	5	5	1	0	4
In situ Lobular (n=1)	1	0	0	0	0	1	1	1	1	0	1
Infiltrating Lobular (n=3)	1	0	0	0	0	1	2	3	1	0	2
Medullary (n=2)	1	0	0	0	0	1	2	2	0	0	1
Mucinous (n=1)	0	0	0	0	0	0	1	0	0	0	0
Papillary (n=1)	0	0	0	0	0	0	1	0	0	0	0
BENIGN BREAST LESIONS:											
Fibrocystic Change (n=5)	3	1	0	0	0	2	5	1	3	0	1
Fibroadenoma (n=3)	2	0	0	0	0	1	2	0	0	0	1
Tubular Adenoma (n=1)	0	0	0	0	0	0	1	1	0	0	0
OTHER MALIGNANT TUMORS:											
Osteosarcoma (n=3)	0	0	0	0	0	0	0	0	0	0	0
Diffuse Lymphoma (n=3)	0	0	0	0	0	0	0	0	0	0	0
Hodgkin's Lymphoma (n=4)	0	0	0	0	0	0	0	0	0	0	0
Large Bowel Carcinoma (n=4)	0	0	0	0	0	0	0	0	0	0	0
Malignant Melanoma (n=5)	0	0	0	0	0	3	0	0	0	0	0

Representative patterns of staining exhibited by DAL-BR7 using an immunoperoxidase-based assay on sections from formalin fixed, paraffin embedded benign and malignant breast tissue are shown in Figures 7 and 8 (pages 100-101).

6. Reactivity of MABs with Melanoma Xenografts in Nude Mice and Cultured Melanoma Cells

There was no reactivity of the anti-HMC MABs with M21 melanoma cell xenografts in nude mice when fresh frozen sections of these tumors were assessed by immunofluorescence. However, when melanoma cells from these xenografts or from biopsies of 3 patients that did not react with the anti-HMC MABs were cultured in vitro, 100% of the melanoma cells reacted with all 11 anti-HMC MABs after 7-9 days in culture. The titer of reactivity of each MAB to these melanoma cells was similar to the titer observed when routinely cultured M21 or other melanoma cells were assayed.

7. Reactivity of MABs with Caki-1 Xenografts in Nude Mice and Cultured Caki-1 Cells

All 11 anti-HMC MABs reacted with fresh frozen sections of Caki-1 cell xenografts by immunofluorescence assay. These MABs also reacted with Caki-1 cells that were obtained from the xenografts and grown in culture for at least 24 hr. The titer of reactivity of each MAB to these cultured cells was similar to the titer observed when routinely cultured Caki-1 cells were assayed.

FIGURES 7 AND 8:

**PHOTOMICROGRAPHS OF FORMALIN FIXED, PARAFFIN EMBEDDED
TISSUE SECTIONS OF BENIGN AND MALIGNANT BREAST LESIONS
STAINED WITH DAL-BR7 USING AN IMMUNOPEROXIDASE-BASED ASSAY**

FIGURE 7: FIBROCYSTIC CHANGE OF BREAST -

**NOTE STAINING OF HYPERPLASTIC EPITHELIAL CELLS THAT
LINE SOME DUCTS AND ABSENCE OF STAINING OF
EPITHELIAL CELLS THAT LINE SIMPLE, CYSTIC DUCTS.**

FIGURE 8: INTRADUCTAL CARCINOMA -

NOTE CYTOPLASMIC STAINING OF TUMOR CELLS.

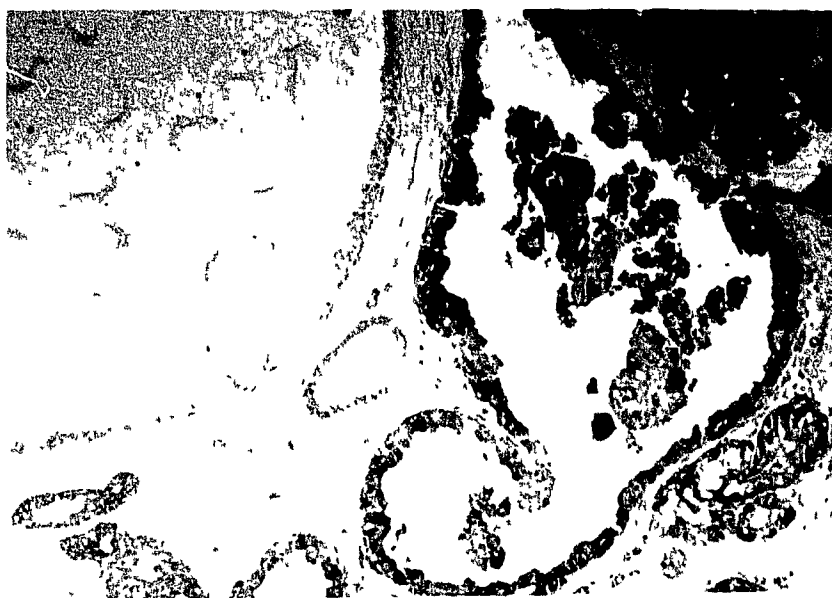


FIGURE 7

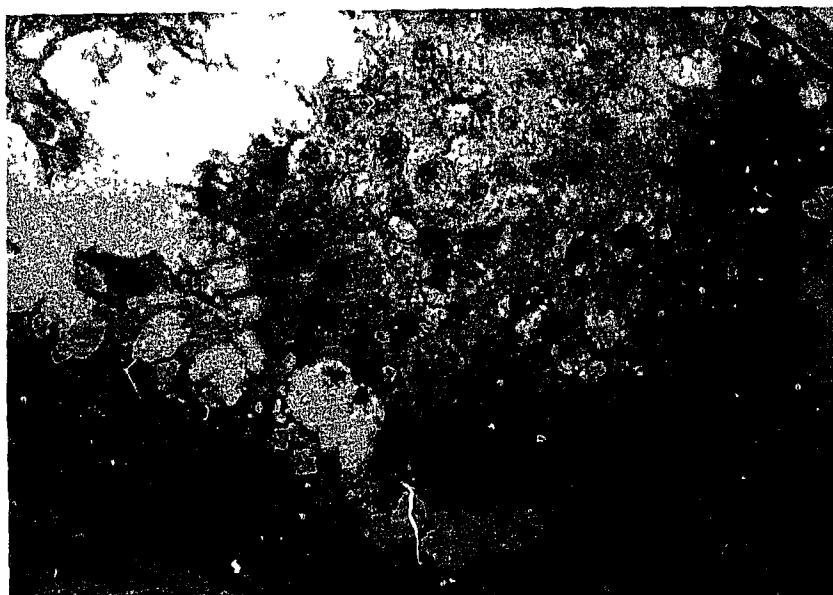


FIGURE 8

PART 2

CHARACTERIZATION OF THE TARGET ANTIGEN(S) FOR THE MABS

1. Immunoprecipitation

Only MABs DAL-BR6 and DAL-BR7 could immunoprecipitate an identical 47 kilodalton band under both reducing and non-reducing conditions from membrane extracts of radioiodinated HTB-19, MCF-7, and M21 cells. Figure 9 (pages 103-104) shows this band in an autoradiograph from an experiment that used radiolabeled membrane extracts of HTB-19 cells. No such band could be seen after SDS-PAGE of ¹²⁵I-labeled HTB-19, MCF-7, or M21 cell surface proteins treated with the other 9 anti-HMC MABs, DAL-B02 (that does not react with HMC), normal mouse IgG or the anti-mouse IgG antibody-coated agarose beads alone. Visual examination of Coomassie blue stained gels following SDS-PAGE, under non-reducing conditions, of the immunoprecipitates obtained with the extracts from HTB-19 and MCF-7 cells revealed a high molecular weight protein band in the stacking gel lanes of DAL-BR2, DAL-BR3, DAL-BR9 and DAL-BR11 that failed to migrate into the resolving gel. Figure 10 (pages 105-106) shows this band in the stacking gel lanes of these 4 MABs from an experiment that used radiolabeled membrane extracts of MCF-7 cells. This band was not present in lanes corresponding to the other MABs and no unique bands were observed in the resolving gel. Under reducing conditions, SDS-PAGE of the same samples showed a distinct 73 kilodalton band in the lanes corresponding to the immunoprecipitates of the same 4 anti-HMC MABs and disappearance of the bands in the stacking gel (Figure 11, pages 105, 107).

FIGURE 9:

AUTORADIOGRAPH OF SDS-PAGE UNDER REDUCING CONDITIONS OF IMMUNOPRECIPITATES OF DAL-BR6, DAL-BR7 AND NORMAL MOUSE IgG AFTER INCUBATING WITH NONIDET P40 EXTRACTS OF CELL SURFACE-RADIOLABELED HTB-19 CELLS

Mr = MOLECULAR WEIGHT

LANE A = DAL-BR6

LANE B = NORMAL MOUSE IgG

LANE C = DAL-BR7

NOTE DISTINCT BAND WITH Mr 47,000 IN THE LANES CORRESPONDING TO DAL-BR6 AND DAL-BR7 AS WELL AS THE ABSENCE OF BANDS IN THE LANE CORRESPONDING TO NORMAL MOUSE IgG.

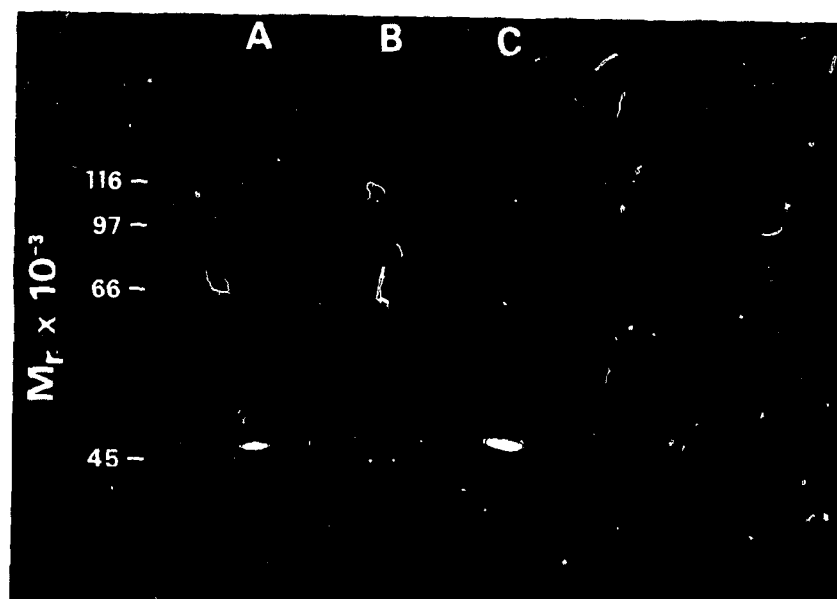


FIGURE 9

FIGURES 10 AND 11:

SDS-PAGE OF IMMUNOPRECIPITATES OF 11 ANTI-HMC MABS, DAL-B02 AND NORMAL MOUSE IgG (MOPC21 IN THE FIGURES) AFTER INCUBATING WITH NONIDET-P40 EXTRACTS OF CELL SURFACE-RADIOLABELED MCF-7 CELLS. THE EXPERIMENT WAS PERFORMED UNDER NON-REDUCING CONDITIONS (FIGURE 10) AND UNDER REDUCING CONDITIONS (FIGURE 11), AND THE GELS WERE STAINED WITH COOMASSIE BLUE

FIGURE 10: NOTE A PROTEIN BAND IN EACH OF THE STACKING GEL LANES OF DAL-BR2, DAL-BR3, DAL-BR9 AND DAL-BR11 JUST BELOW THE ORIGIN OF THE STACKING GEL LANES (ARROW). THE BANDS IN THE RESOLVING GEL CORRESPOND TO IgG FROM THE ANTI-MOUSE IgG AGAROSE BEADS (ARROW IgG) AND ALSO SMALL AMOUNTS OF BREAKDOWN PRODUCTS OF IgG (HEAVY AND LIGHT CHAINS OF IgG) IN SOME LANES.

FIGURE 11: NOTE THE DISTINCT Mr 73,000 BAND IN THE RESOVING GEL LANES OF THE SAME 4 ANTI-HMC MABS (POSITION INDICATED BY AN ARROW). THE STACKING GEL DID NOT SHOW ANY BANDS AND IS NOT PRESENTED.

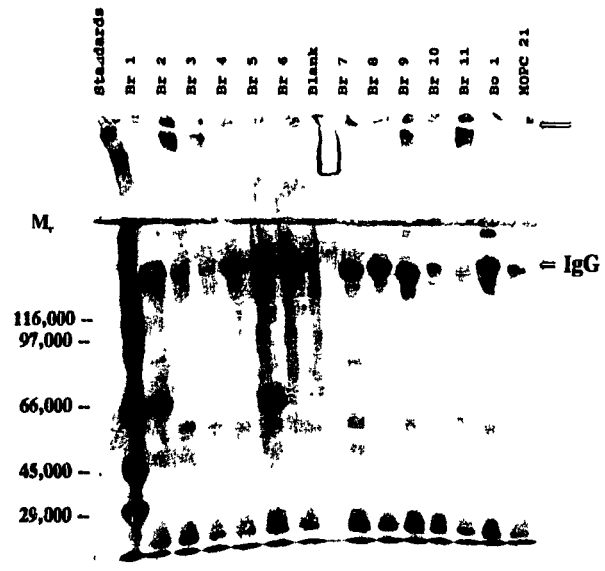


FIGURE 10

Br 1
Br 2
Br 3
Br 4
Br 5
Br 6
Standards
Br 7
Br 8
Br 9
Br10
Br11
BO 1
WOPC 21

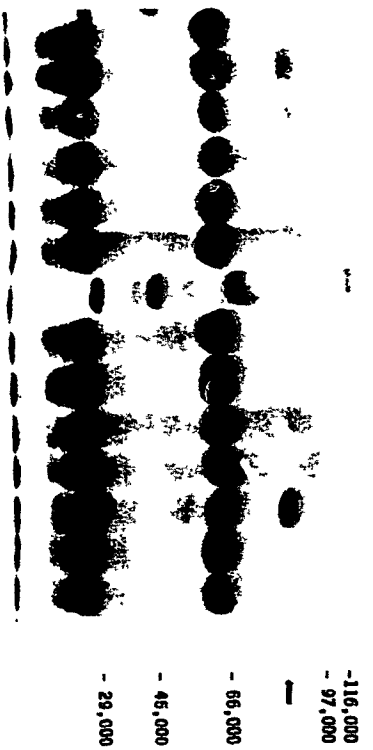


FIGURE 11

Autoradiography of gels following SDS-PAGE (under both reducing and non-reducing conditions) of the immunoprecipitates obtained with the extracts from HTB-19 and MCF-7 cells that were grown in ^{35}S -methionine supplemented medium produced numerous bands but none of the bands appeared to be associated with the reactivity of any of the anti-HMC MABs. To decrease the number of background radioactive bands that were present in the lanes of both the anti-HMC and control MABs, the Nonidet-P extracts were first cleared with anti-mouse IgG-coated C^{H} arose beads before immunoprecipitating with the MABs. While there was a considerable reduction in the number of bands in the autoradiograph with this procedure, no distinct band that was unique to any of the MABs studied, was seen. Also, to enhance the sensitivity of the x-ray film in the autoradiographic process, the gels were first soaked in AMPLIFY[®], but this procedure did not yield a distinct band with any MAB either. Furthermore, additional experiments demonstrated that none of the anti-HMC MABs could immunoprecipitate any labeled cell surface protein from extracts of the non-target cell lines D10-1 or Caki-2.

2. Reactivity of the MABs with Neuraminidase Treated HMC Cells, Milk Proteins, CEA, Antigen Extracts of HMC Cells, and Spent HMC Culture Medium

Treating HMC cells with neuraminidase had no effect on the reactivity of any MAB suggesting that sialic acid is not part of the epitope. None of the MABs reacted with lactoferrin, alpha-lactalbumin, bovine Kappa casein, or CEA. Only one of the 11 MABs, DAL-BR8, showed some reactivity with human casein. The ELISA assay

used to determine the reactivity of each MAB with the milk proteins and CEA did have a positive control to assess the reaction conditions of the assay. This positive control consisted of glutaraldehyde fixed HMC cells which did react with each MAB in the assay. Furthermore, the immunoreactivity of the CEA used was confirmed by radioimmunoassay in Dr. M. Givner's endocrinology laboratory at the Victoria General Hospital, Halifax, Nova Scotia. However, it should be noted that antibodies which react specifically with each of these proteins were neither obtained or used in these assays as positive control antibodies. A non-specific murine IgG was used as a negative control antibody in these assays and this did not show reactivity with any protein.

Using the same ELISA assay just related, all 11 MABs were shown to react with 1% Nonidet-P40 extracts of HTB-19 and MCF-7 cells when 96 well plates were coated with these extracts at a protein concentration of 1 ug/ml per well. To briefly describe the nature of these extracts, HMC cells were first grown to confluence in MEM-NEAA media containing 10% fetal calf serum. The cells were detached with EDTA solution, washed and pelleted. Nonidet-P40 was then added to the cell pellets to yield a 1% solution and the mixture was rotated for 30 min at 4°C. The mixture was centrifuged and the protein content of the supernatant was determined. Using sodium carbonate buffer to dilute the extract, wells were coated at a protein concentration of 1 ug/ml as stated above. None of the MABs reacted with identically prepared extracts of Caki-2 or cultured human foreskin fibroblast cells at the same protein concentration per well. Spent culture medium from the same 2 HMC cell

lines that were grown to confluence in MEM-NEAA medium with and without 10% fetal calf serum was also used to coat individual wells. The spent medium was first centrifuged and the supernatants then diluted with sodium carbonate buffer to protein concentrations ranging from 1 ug/ml per well to 100 ug/ml per well. Using ELISA, none of these spent media coated wells reacted with any anti-HMC MAB.

Since 1% Nonidet-P40 HMC cellular extracts were shown to react with the MABs in an ELISA assay, SDS-PAGE under reducing and non-reducing conditions followed by Western blotting was performed on these extracts along with extracts from Caki-2 and foreskin fibroblasts in an attempt to elucidate the molecular weight of the target antigen for the 9 anti-HMC MABs which did not react with cell surface associated antigens. None of the MABs demonstrated any unique band under reducing or non-reducing conditions indicating an inability of the MABs to react with SDS or B-mercaptoethanol denatured antigen.

3. Results of Experiments Performed by Dr. S. Luner

A brief description of each experiment performed by Dr. S. Luner and the results obtained are presented with the full consent of Dr. S. Luner to provide the reader additional information about the known characteristics of the antigen(s).

a) Sensitivity of the Target Antigen(s) to Trypsin and Heat Treatment

Dr. S. Luner treated HTB-19 cells with trypsin and evaluated the reactivity of each anti-HMC MAB and DAL-B02 (which does not react with HMC) to these trypsinized cells by an ELISA assay. The ELISA reactivity of each MAB to

trypsinized cells was then compared with their reactivity to untreated cells as shown in Table 7 (page 112, reproduced with the permission of Dr. S. Luner). The target antigen(s) for all the 11 anti-HMC MABs seem to be trypsin-sensitive. These results suggest that the antigen for each MAB could be protein in composition.

Dr. S. Luner also evaluated the reactivity of each MAB to heat treated HTB-19 cells. The cells in this experiment were heated over 2 min to 100°C and maintained at that temperature for 5 min before cooling in an ice bath and washing with culture medium. Aliquots of treated and untreated cells were incubated with each MAB, then washed and reacted with ¹²⁵I-labeled sheep anti-mouse IgG. The cell-associated radioactivity in each aliquot was determined using a gamma emission counter. Heat denaturation of target antigens decreased the reactivity of only DAL-BR6 and DAL-BR7 indicating that the target antigen for these 2 MABs is likely to be glycoprotein or lipoprotein in nature.

b) Reactivity of the MABs with Human Milk Fat Globules

Human milk fat globules were prepared from lactating mother's breast milk by Dr. S. Luner and then coated onto multiwell slides. After washing and drying these coated wells, the reactivity of each anti-HMC MAB to this protein was determined by an immunofluorescence assay. Positive and negative control antibodies were used in the assay and respectively consisted of a human fibroblast reactive MAB and a nonspecific IgG. None of the MABs reacted with this human milk fat globule preparation.

TABLE 7: REACTIVITY OF MABS WITH TRYPSIN TREATED
HTB-19 CELLS USING AN ELISA ASSAY

MAB	UNTREATED CELLS	TRYPSINIZED CELLS
DAL-BR1	0.956 \pm .143*	0.117 \pm .033
DAL-BR2	0.491 \pm .068	0.175 \pm .010
DAL-BR3	0.457 \pm .069	0.166 \pm .058
DAL-BR4	1.310 \pm .029	0.093 \pm .003
DAL-BR5	1.204 \pm .217	0.090 \pm .020
DAL-BR6	0.654 \pm .015	0.039 \pm .024
DAL-BR7	1.070 \pm .173	0.198 \pm .077
DAL-BR8	1.143 \pm .165	0.121 \pm .015
DAL-BR9	0.779 \pm .103	0.030 \pm .010
DAL-BR10	0.499 \pm .076	0.103 \pm .012
DAL-BR11	0.494 \pm .087	0.078 \pm .011
DAL-B02	0.204 \pm .073	0.001 \pm .002

* Absorbance at 490 nm \pm standard deviation of quadruplicates

(PRESENTED WITH THE PERMISSION OF DR. S. LUNER)

4. Binding of HMC Cells to Vitronectin, Fibronectin and Laminin Coated Plates and Binding Inhibition of MABs to HTB-19 Cells with Polyclonal Anti-Vitronectin Receptor Antibodies

A high proportion of both HTB-19 and MCF-7 cells that were put into wells coated with vitronectin was able to effectively bind to and spread out on the coated well bottom. Figure 12 (pages 114-115) shows an experiment using HTB-19 cells. Using laminin coated wells, a lower proportion of HTB-19 and MCF-7 cells was able to bind and spread out on the coated well bottom. In contrast, all HMC cells failed to bind and spread out on uncoated wells or wells coated with BSA or fibronectin. The HMC cells in these wells remained suspended in the medium. Figure 13 (pages 114- 115) shows an experiment using BSA coated wells and HTB-19 cells. Based on these results, it is likely that the 2 HMC lines possess receptors to vitronectin and also to laminin permitting the binding and subsequent spreading of the cells in wells coated with these agents. In another study, excess amounts of anti-vitronectin receptor polyclonal antibodies did not inhibit the binding of any radiolabeled preparation of the 11 anti-HMC MABs to HTB-19 cells. From these results, it appears that although the vitronectin receptor is likely present on HMC cells, the target antigen for the 11 anti-HMC MABs is not the vitronectin receptor.

A summary of the anti-HMC MAB subclasses, nature of the target antigens and immunizing HMC lines that produced the 11 hybridomas is shown in Table 8 (page 116).

FIGURES 12 AND 13:

BINDING OF HTB-19 CELLS TO WELLS COATED WITH VITRONECTIN (FIGURE 12) AND NON-BINDING OF HTB-19 CELLS TO WELLS COATED WITH BSA (FIGURE 13)

NOTE: OBSERVE THE SPREADING OUT OF CELLS IN THE WELL BOTTOM COATED WITH VITRONECTIN WHILE THE CELLS IN THE WELL COATED WITH BSA REMAIN SUSPENDED AS CIRCULAR BODIES IN THE MEDIUM INDICATING LACK OF BINDING AND ATTACHMENT TO THE BSA COATED SURFACE.



FIGURE 12

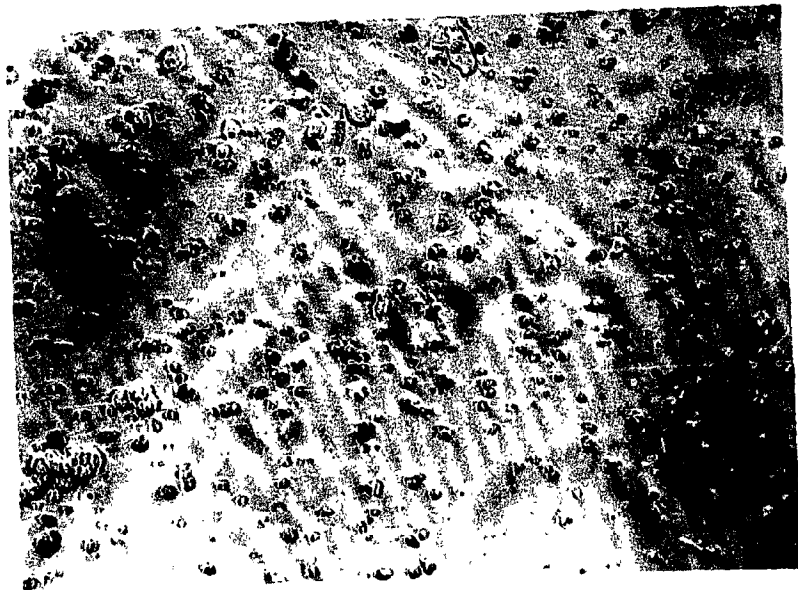


FIGURE 13

TABLE 8

Designation of MAB	Isotype	Target Antigen	Immunizing cells
DAL-BR1	IgG _{2bKappa}	Intracellular and extracellular; no distinctive band could be resolved in the immunoprecipitate	HTB-19* (BT20) Adenocarcinoma
DAL-BR2	IgG _{1Kappa}	Intracellular and extracellular; a Mr 73 KD moiety could be identified in the immunoprecipitates only under reducing conditions	HTB-20 (BT474) Invasive Duct Carcinoma (produces osmiophilic granules)
DAL-BR3	IgG _{1Kappa}	Intracellular and extracellular; a Mr 73 KD moiety could be identified as with DAL-BR2	HTB-133 (T47D) Pleural effusion cells from a duct carcinoma
DAL-BR4	IgG _{1Kappa}	Intracellular and extracellular; could not be immunoprecipitated	HTB-133
DAL-BR5	IgG _{1Lambdab}	Intracellular and extracellular; could not be immunoprecipitated	HTB-20
DAL-BR6	IgG _{1Kappa}	Cell surface-associated antigen Mr 47,000	HTB-133
DAL-BR7	IgG _{2bKappa}	Cell surface-associated antigen Mr 47,000; different epitope of the antigen defined by BR6	HTB-20
DAL-BR8	IgG _{1Kappa}	Intracellular and extracellular; could not be immunoprecipitated	HTB-133
DAL-BR9	IgG _{1Kappa}	Intracellular and extracellular; a Mr 73 KD moiety could be identified as with DAL-BR2	HTB-133
DAL-BR10	IgG _{1Lambdab}	Intracellular and extracellular; no distinctive band could be resolved	HTB-133
DAL-BR11	IgG _{2bKappa}	Intracellular and extracellular; a Mr 73 KD moiety could be identified as with DAL-BR2	HTB-20

* HTB numbering is as designated by ATCC; the code inside the parenthesis is from the original description of the cell lines.

PART 3

DETERMINATION OF THE IRF AND BINDING PARAMETERS OF THE MABS AND MAPPING OF THE DETERMINANTS RECOGNIZED BY 2 MABS

1. IRF and Binding Parameters of DAL-BR6 and DAL-BR7 Against HMC Cells

Since DAL-BR6 and DAL-BR7 were shown to react with a cell membrane associated antigen and react with viable target cells, experiments to determine IRF, number of BS and K_A used viable HMC cell suspensions. Analyses of binding data from a number of experiments to determine the IRF of different radiolabeled preparations of DAL-BR6 and DAL-BR7, with molar iodine incorporation of 3-5 ^{125}I atoms per 100 IgG molecules, against HTB-19 and MCF-7 cells are presented in Figures 14 to 25 (pages 118-122). The calculated IRF values of three radiolabeled preparations of DAL-BR6 against viable HTB-19 cells were be 54%, 64%, and 74% and against viable MCF-7 cells were 36%, 58%, and 68%. Similarly, for DAL-BR7, the comparable IRF values against HTB-19 cells were 51%, 55% and 97% and against MCF-7 cells were 25%, 84% and 90%. Therefore, the range of IRF values for DAL-BR6 against HMC lines was 36%-74% whereas for DAL-BR7 was 25%-97%.

FIGURES 14 TO 25:

PLOTS TO DETERMINE THE IRF OF ^{125}I -LABELED DAL-BR6 AND ^{125}I -LABELED DAL-BR7 WHEN TESTED AGAINST HTB-19 OR MCF-7 CELLS.

THE RATIO OF THE TOTAL AMOUNT OF RADIOLABELED MAB USED IN EACH EXPERIMENT TO THE AMOUNT OF MAB BOUND TO TUMOR CELLS (TOTAL / BOUND) IS PLOTTED AGAINST THE INVERSE OF THE CELL CONCENTRATIONS USED (ml / MILLION CELLS).

LINEAR REGRESSION OF THE DATA IN EACH EXPERIMENT TO DETERMINE THE Y-AXIS INTERCEPT OF EACH PLOT YIELDED A VALUE EQUAL TO THE INVERSE OF THE IRF.

THE IRF DETERMINED FROM EACH PLOT IS STATED IN THE TEXT OF PART 3 (PAGE 117).

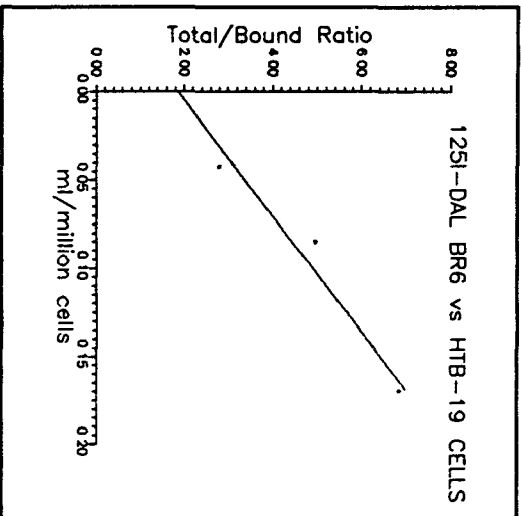


FIGURE 14

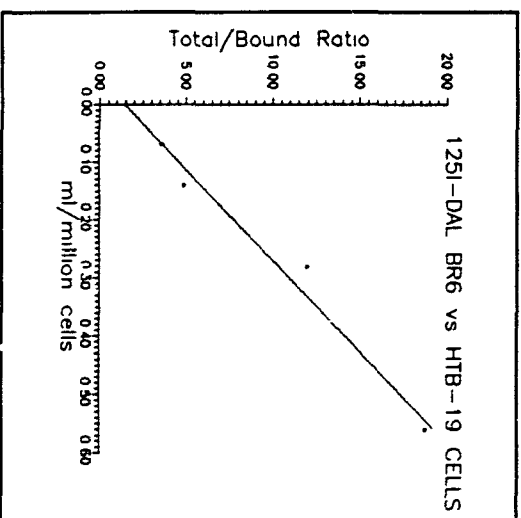


FIGURE 15

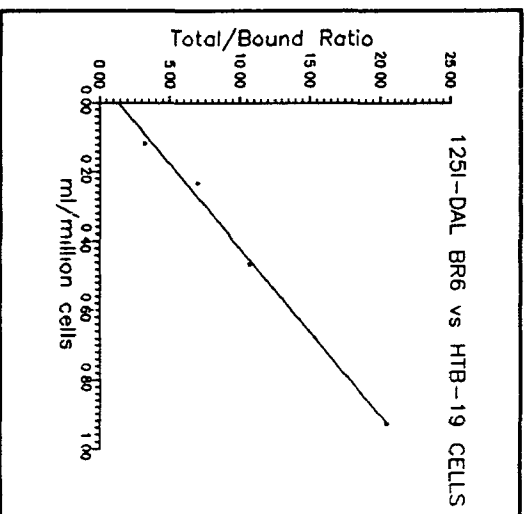


FIGURE 16

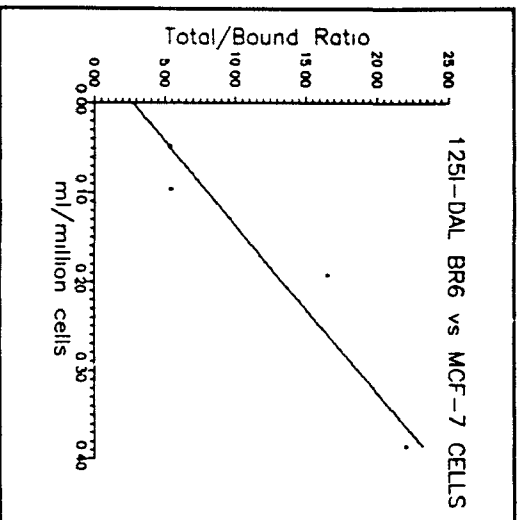


FIGURE 17

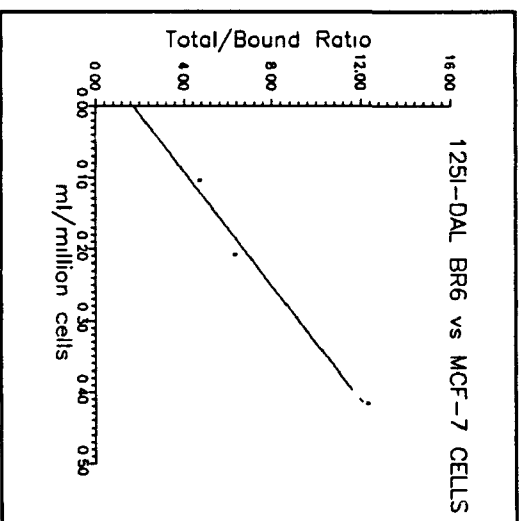


FIGURE 18

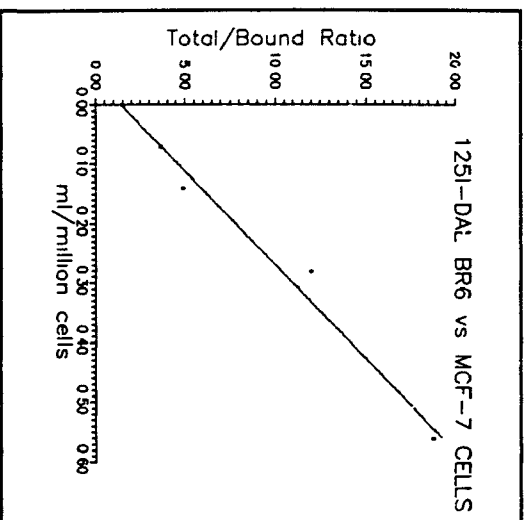


FIGURE 19

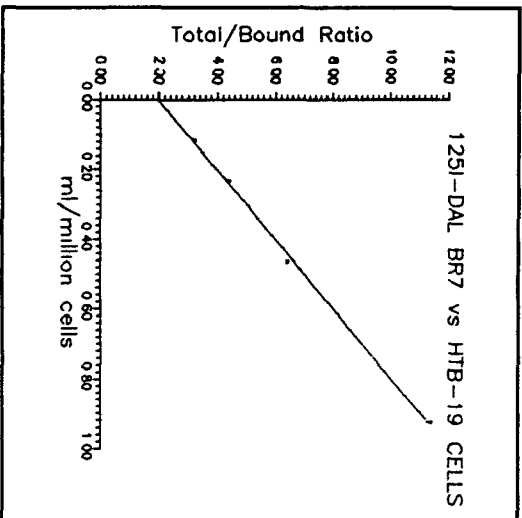


FIGURE 20

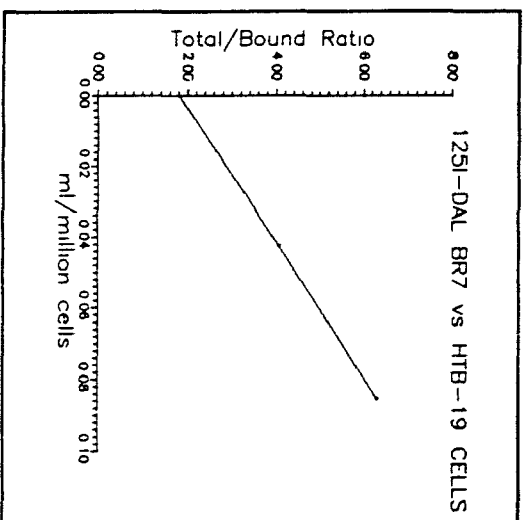


FIGURE 21

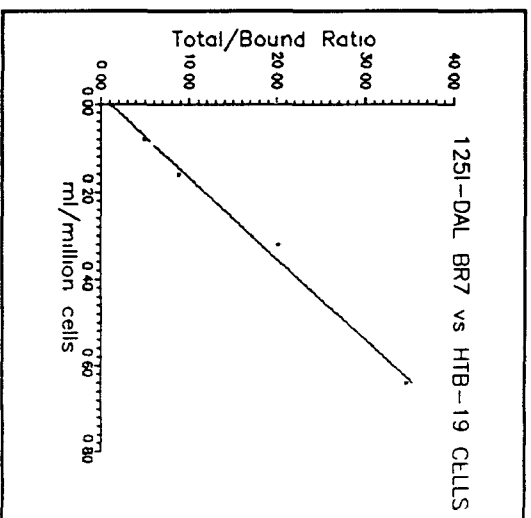


FIGURE 22

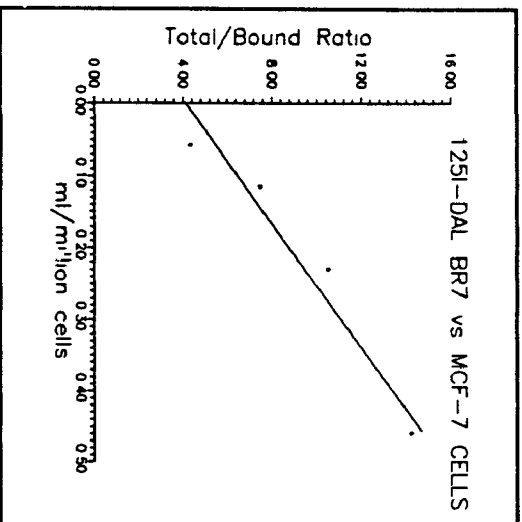


FIGURE 23

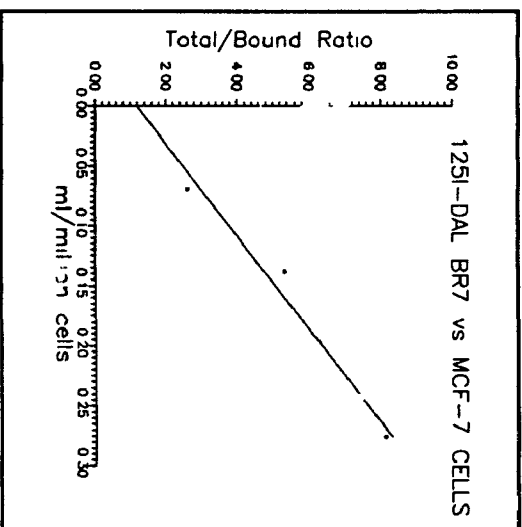


FIGURE 24

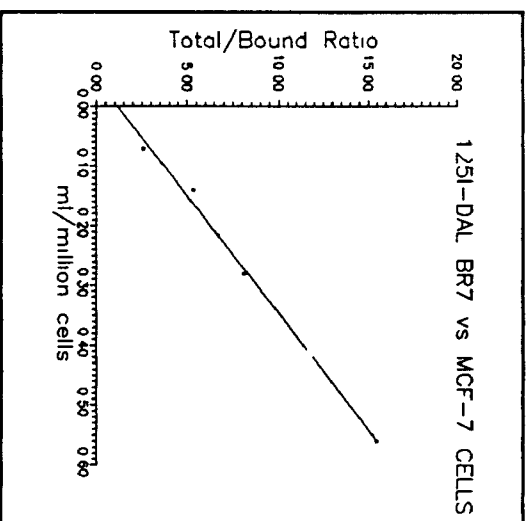


FIGURE 25

Table 9 (page 124) presents the results of binding experiments to determine the number of BS and K_A using 4 radiolabeled preparations of DAL-BR6 and DAL-BR7 against viable suspensions of HTB-19 and MCF-7 cells after analysis of the data from each experiment by LIGAND^R program. The LIGAND^R estimates of the number of BS for DAL-BR6 on viable HTB-19 and MCF-7 cells respectively ranged from 5.6×10^5 to 1.0×10^7 and 3.4×10^5 to 4.6×10^6 . The corresponding K_A values respectively ranged from 7.6×10^6 to $1.3 \times 10^8 \text{ M}^{-1}$ and 4.3×10^6 to $5.5 \times 10^7 \text{ M}^{-1}$. For DAL-BR7, the LIGAND^R estimates of the number of BS on viable HTB-19 and MCF-7 cells respectively ranged from 6.4×10^5 to 4.6×10^6 and 7.7×10^5 to 3.8×10^6 . The corresponding K_A values respectively ranged from 3.8×10^7 to $1.8 \times 10^8 \text{ M}^{-1}$ and from 8.7×10^6 to $2.0 \times 10^8 \text{ M}^{-1}$. From these results, DAL-BR7 had a K_A mean value that is significantly ($p < 0.05$ Student's T-Test) higher than that of DAL-BR6 for both HMC lines. However, these two MABs had approximately equal mean values for the number of available BS on the same two HMC lines.

TABLE 9: AFFINITY CONSTANTS AND NUMBER OF BINDING SITES
PER TARGET CELL FOR BR6 AND BR7

		CELL LINE			
		HTB-19		MCF-7	
MAB		$K_A (M^{-1})$	# BS/CELL	$K_A (M^{-1})$	# BS/CELL
		$\times 10^7$	$\times 10^6$	$\times 10^7$	$\times 10^6$
BR6	MEAN	4.37	3.55	2.45	2.96
	SEM	2.60	2.18	1.08	0.93
BR7	MEAN	9.89	2.32	9.24	2.11
	SEM	2.99	1.00	4.08	0.66

MEAN = MEAN OF THE RESULTS FROM LIGAND ANALYSIS OF
4 SEPARATE AND INDEPENDENT EXPERIMENTS

SEM = STANDARD ERROR OF THE MEAN

2. IRF and Binding Parameters of the Other 9 MABs Against Target HMC Cells

Similar binding experiments using viable HMC cell suspensions to determine the IRF (and later, the number of BS and K_A) initially with DAL-BR1 and DAL-BR2 (and subsequently with the remaining 7 anti-HMC MABs) resulted in binding data that varied widely. These binding data had no consistent pattern and were not proportional to the cell concentration in IRF studies and not proportional to MAB concentration in binding parameter studies. As a result, these data could not be properly interpreted either to determine IRF or to determine the number of BS and K_A of these MABs with the LIGAND^R program. To circumvent the problems encountered from using viable cells in these binding experiments with these 9 MABs, glutaraldehyde fixed HMC cells in 96 wells were used instead to determine the number of BS and K_A for these MABs. The rationale for using fixed cells in these experiments was related to the earlier observation that glutaraldehyde fixed cells reacted effectively with these 9 MABs in both immunofluorescence and ELISA assays. The results obtained from these experiments yielded data which the LIGAND^R program could estimate the binding parameters. These estimates of the number of BS on HTB-19 and MCF-7 cells for these 9 MABs ranged from 2×10^6 to 5.4×10^7 and 6×10^6 to 8.4×10^7 . The corresponding K_A values of the 9 MABs for both HTB-19 and MCF-7 cells were all approximately 10^7 M^{-1} . In these studies, DAL-BR5 had the highest K_A estimates for its epitope ($3.0\text{-}4.3 \times 10^7 \text{ M}^{-1}$) and along with DAL-BR2 had the lowest number of BS estimates ($2.5\text{-}9.8 \times 10^6$ for DAL-BR5 and $1.8\text{-}6.4 \times 10^6$ for DAL-BR2) compared to the other 8 MABs. Experiments that used increasing amounts of

radiolabeled MAB alone to determine the binding parameters generally yielded higher K_A estimates with LIGAND^R than experiments that used a fixed amount of radiolabeled MAB diluted with increasing amounts of unlabeled MAB. HTB-19 and MCF-7 cells had comparable LIGAND estimates of the number of BS and K_A of each of the 9 MABs.

The IRF of radiolabeled MAB preparations could not be adequately determined using fixed cells in 96 well plates since the number of cells that could attach as a monolayer in each well was limited and was not sufficient to properly follow the experimental protocol required for the determination of this parameter. Using plates with fewer but larger wells proved also to be inadequate to handle the large number of cells required to do the IRF procedure properly.

3. Epitope Mapping for DAL-BR6 and DAL-BR7

The results of several competitive binding experiments using ¹²⁵I-labeled preparations of DAL-BR6 and DAL-BR7 against viable HTB-19 and MCF-7 cell suspensions are shown in Figures 26 to 29 (pages 127-129). Unlabeled DAL-BR7 could inhibit the binding of ¹²⁵I-labeled DAL-BR6 to HMC cells just as effectively as unlabeled DAL-BR6. However, unlabeled DAL-BR6, even at a 40 fold molar excess, could inhibit the binding of ¹²⁵I-labeled DAL-BR7 by only 70% of what unlabeled DAL-BR7 could. Both DAL-BR6 and DAL-BR7 were shown to react with identical 47 KD HMC cell surface protein but based on these results, it appears that the epitope recognized by DAL-BR6 is part of a larger epitope that is recognized by DAL-BR7.

FIGURES 26 TO 29:

RESULTS OF INDIVIDUAL EXPERIMENTS FOR THE DETERMINATION OF COMPETITIVE BINDING INHIBITION BETWEEN UNLABELED (OR "COLD") DAL-BR6 AND DAL-BR7 AND RADIOLABELED DAL-BR6 AND DAL-BR7 USING VIABLE HTB-19 AND MCF-7 CELLS (PAGES 128-129).

THE PLOTS SHOW THE PERCENTAGE OF RADIOLABELED MAB BOUND TO HMC CELLS IN EACH EXPERIMENT AGAINST THE CONCENTRATION OF THE UNLABELED MAB USED TO INHIBIT THE BINDING OF A CONSTANT AMOUNT OF THE RADIOLABELED MAB STATED IN EACH FIGURE.

FIGURES 26 AND 27 SHOW INHIBITION OF RADIOLABELED MAB BINDING TO HMC CELLS BY THE UNLABELED COUNTERPART MAB.

FIGURE 28 SHOWS INHIBITION OF RADIOLABELED MAB BINDING TO HMC CELLS BY THE UNLABELED COUNTERPART MAB AS WELL AS UNLABELED DIFFERENT MAB.

FIGURE 29 SHOWS ANOTHER EXPERIMENT DEMONSTRATING THE BINDING INHIBITION OF RADIOLABELED DAL-BR7 HMC CELLS BY UNLABELED DAL-BR6.

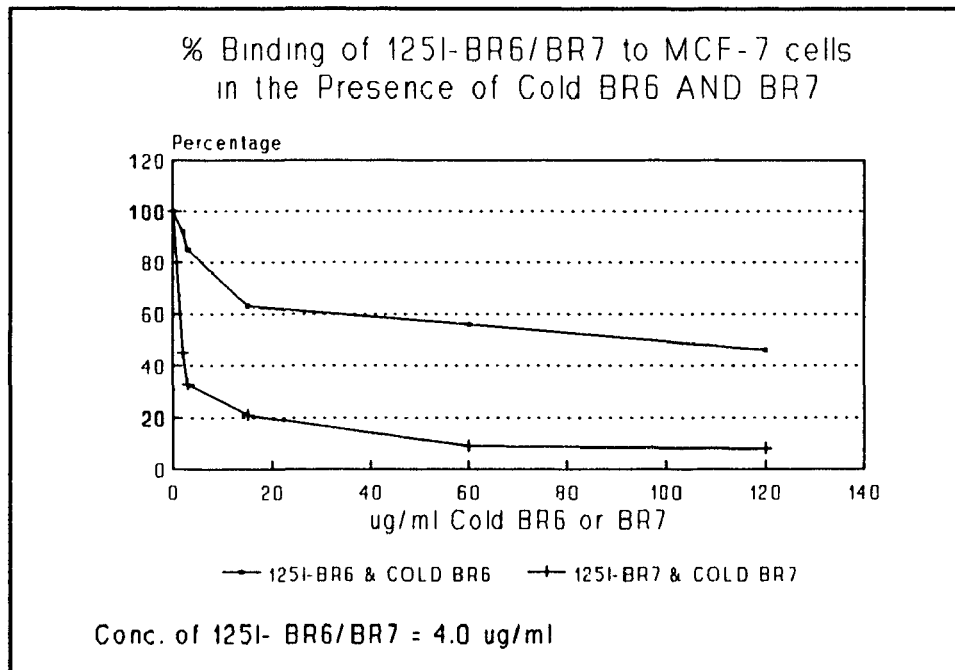


FIGURE 26

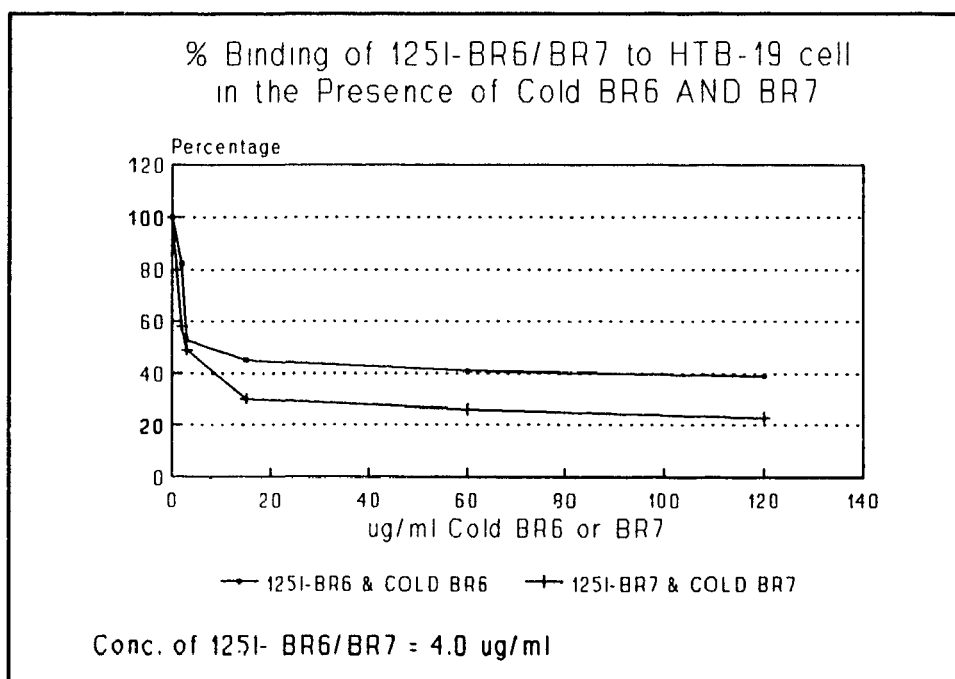


FIGURE 27

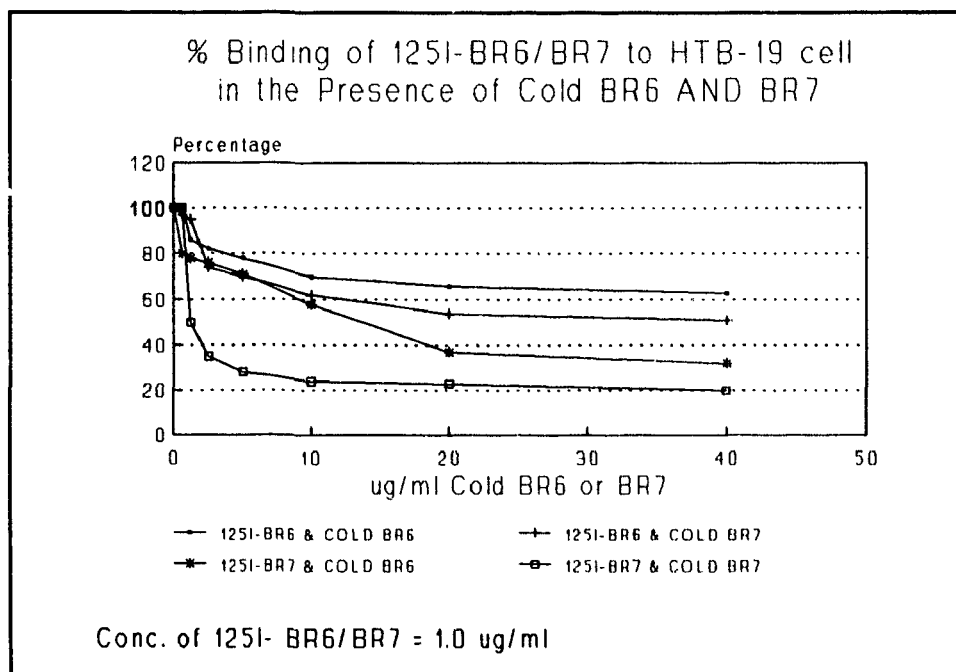


FIGURE 28

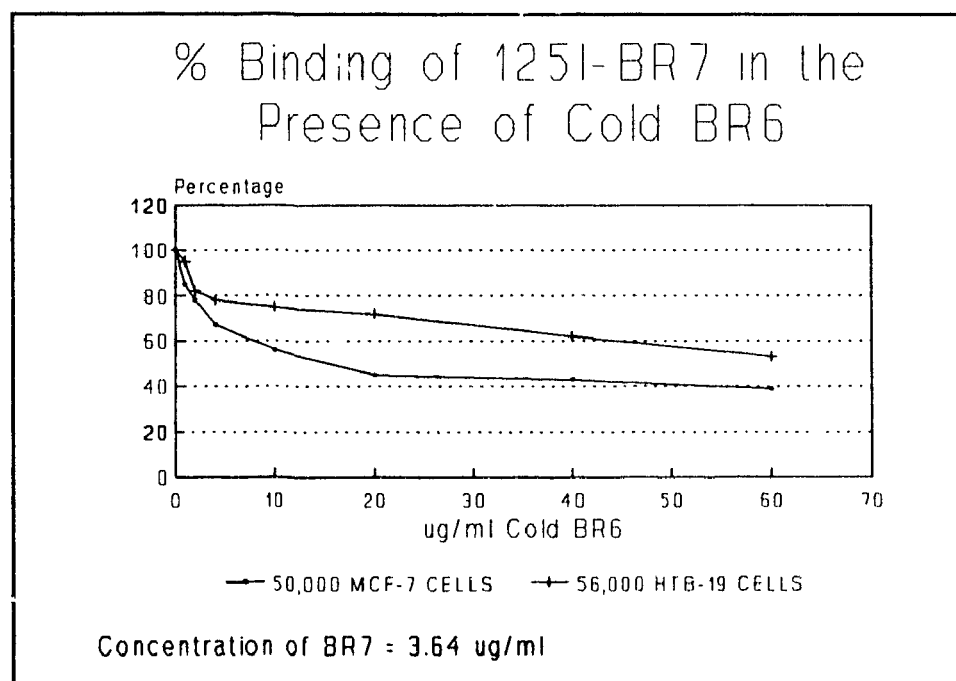


FIGURE 29

PART 4

IMMUNO-GOLD STUDIES

1. Concentration Variable Isotherms

The concentration variable isotherms for MABs DAL-BR6, DAL-BR7, K29, K45 and DAL-B02 at different pH conditions are presented in Figures 30 to 34 (pages 131-134). The minimal amounts of protein required to stabilize gold particles at pH 7.0 based on these concentration variable isotherms were 60 ug DAL-BR6, 50 ug DAL-BR7, 60 ug K29, and 40 ug K45 per ml of gold sol. At pH 9.0, the minimal amounts of protein to stabilize gold particles were 70 ug DAL-BR6, 90 ug DAL-BR7 and 50 ug DAL-B02 per ml gold sol. The concentration variable isotherms for K29 and K45 at pH 9.0 and for DAL-B02 at pH 7.0 did not show a significant decrease in the absorbance at 580 nm as the ratio amount of protein added to the gold sol increased. The minimal amount of protein needed to stabilize gold particles was determined from these graphs at the point where there was a significant decrease in absorbance at 580 nm. Since more DAL-BR6, DAL-BR7 and DAL-B02 could be adsorbed to gold particles at pH 9.0 and more K29 and K45 could be adsorbed to gold particles at pH 7.0, these pH conditions were selected for the adsorption of the respective MABs onto gold particles. The MABs used for adsorption were previously radiolabeled with ^{125}I and therefore after adsorption to gold the MABs were dual-labeled with ^{125}I and gold.

FIGURES 30 TO 34:

CONCENTRATION VARIABLE ISOTHERMS FOR DAL-BR6, DAL-BR7, K29, K45 AND DAL-B02 AT SPECIFIC pH EXPERIMENTAL CONDITIONS STATED IN EACH FIGURE.

THE ABSORBANCE (OR O.D.) AT 580 nm IS PLOTTED AGAINST THE AMOUNT OF MAB (ug) PER ml OF GOLD SOL.

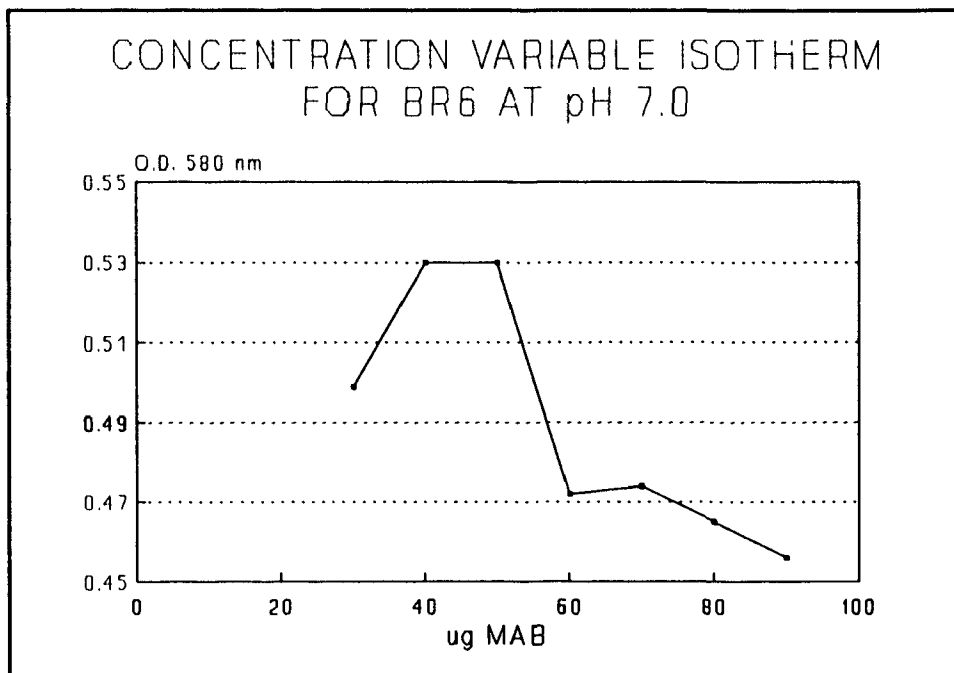


FIGURE 30

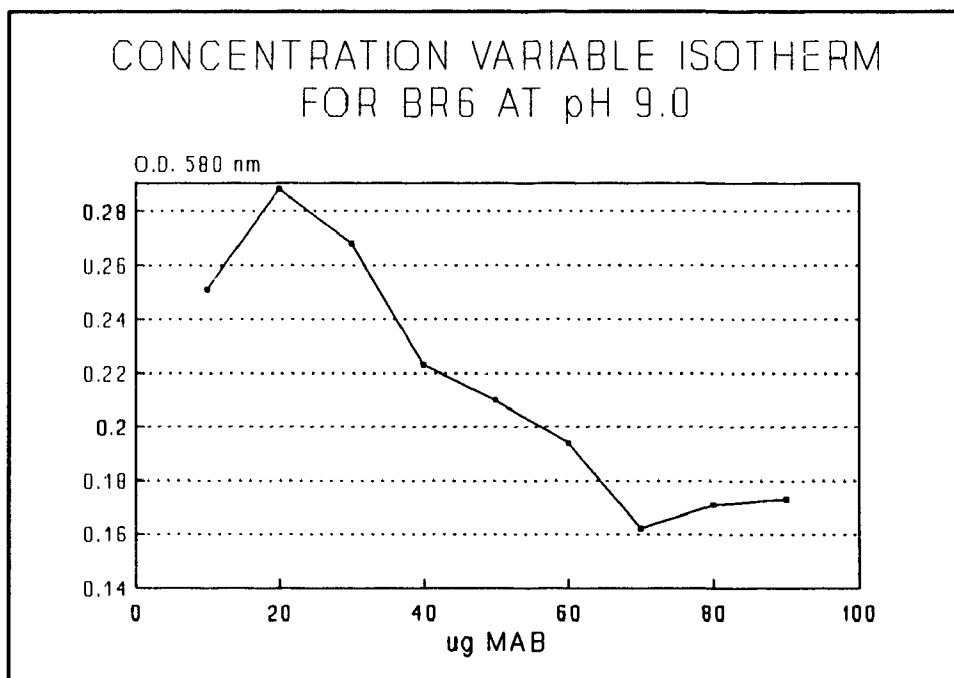


FIGURE 31

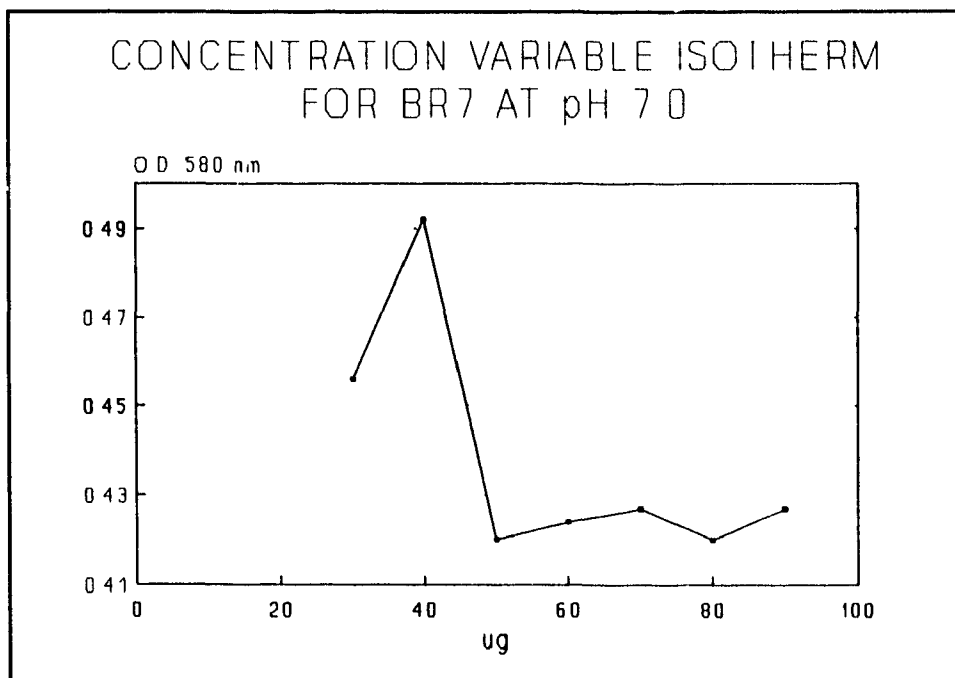


FIGURE 32

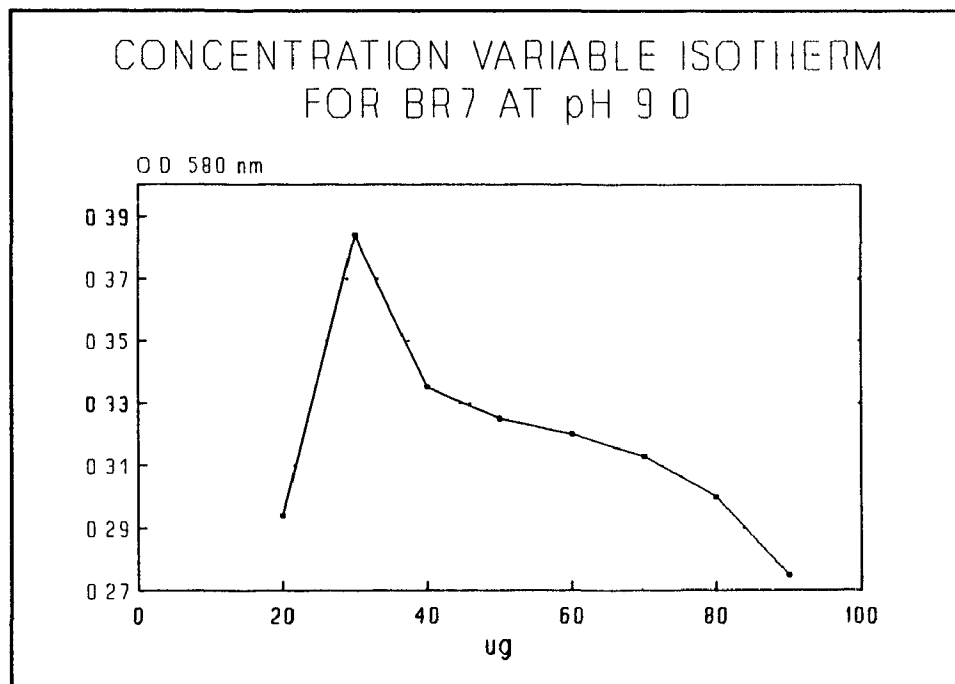


FIGURE 33

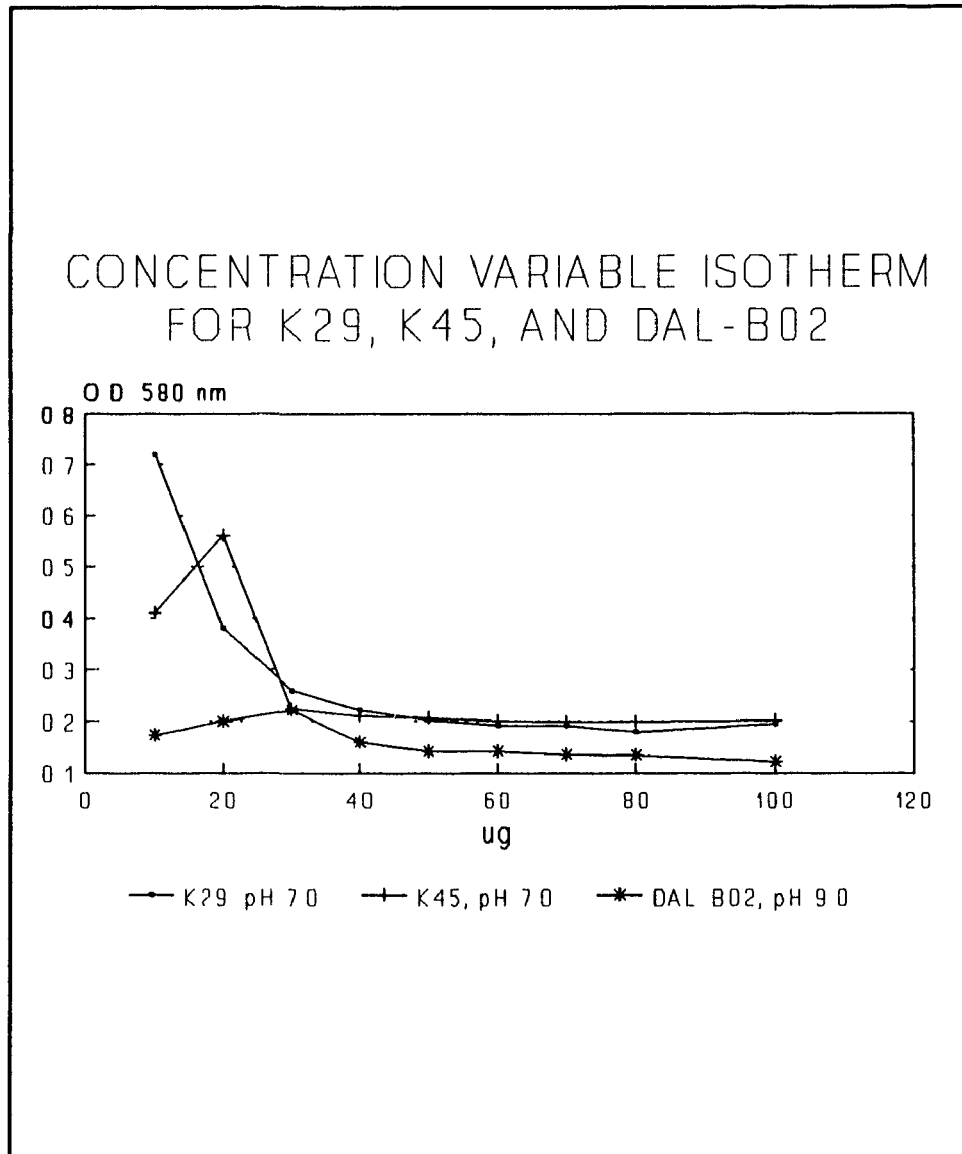


FIGURE 34

2. Adsorption of ¹²⁵I-labeled MABs onto Gold Particles and Binding of Dual-labeled MABs to Cell Lines

The specific activities of ¹²⁵I-labeled MABs used to adsorb onto gold particles were 0.362 uCi/ug DAL-BR6, 0.425 uCi/ug DAL-BR7, 0.397 uCi/ug K29, 0.698 uCi/ug K45 and 0.41 uCi/ug DAL-B02. After adsorption of MABs, the calculated values for the mean number of molecules of each MAB per gold particle were 15.5 DAL-BR6 molecules/gold particle, 23.6 DAL-BR7 molecules/gold particle, 140 K29 molecules/gold particle, 28 K45 molecules/gold particle and 95 DAL-B02 molecules/gold particle. The amount of each MAB that bound to cells after a 2 hr incubation at 4°C (expressed as cpm bound at time 0 hr on the graphs) and subsequent amount of cell-associated MAB after incubation at 37°C for specific times is presented in Figures 35 to 38 (pages 136-138). To properly understand these graphs and the subsequent electron microscopic results obtained by Dr. G. Faulkner on these same aliquots of cells to produce these graphs, a brief review of the reactivity of the MABs (based on ELISA and immunofluorescence assays results) with the cell lines used in these experiments is following. HTB-19 and MCF-7 cells react not only with DAL-BR6 and DAL-BR7 but also with K29. However, these two HMC lines do not react with either K45 or DAL-B02. Caki-1 and Caki-2 cells, on the other hand, react with both K29 and K45 but not with DAL-B02.

FIGURES 35 TO 38:

RESULTS OF EXPERIMENTS PERFORMED WITH CELLS THAT WERE FIRST INCUBATED AT 4°C WITH DUAL GOLD AND ¹²⁵I-LABELED MABS AND THEN INCUBATED AT 37°C.

THE PLOTS SHOW THE AMOUNT OF EACH DUAL GOLD AND ¹²⁵I-LABELED MAB THAT BOUND TO SPECIFIC CELL LINES AFTER A 2 HR INCUBATION AT 4°C (EXPRESSED AS CPM AT TIME 0 HR IN EACH FIGURE) AND THE AMOUNT OF CELL ASSOCIATED RADIOACTIVITY (ALSO EXPRESSED AS CPM) AFTER INCUBATION AT 37°C FOR SPECIFIC TIMES.

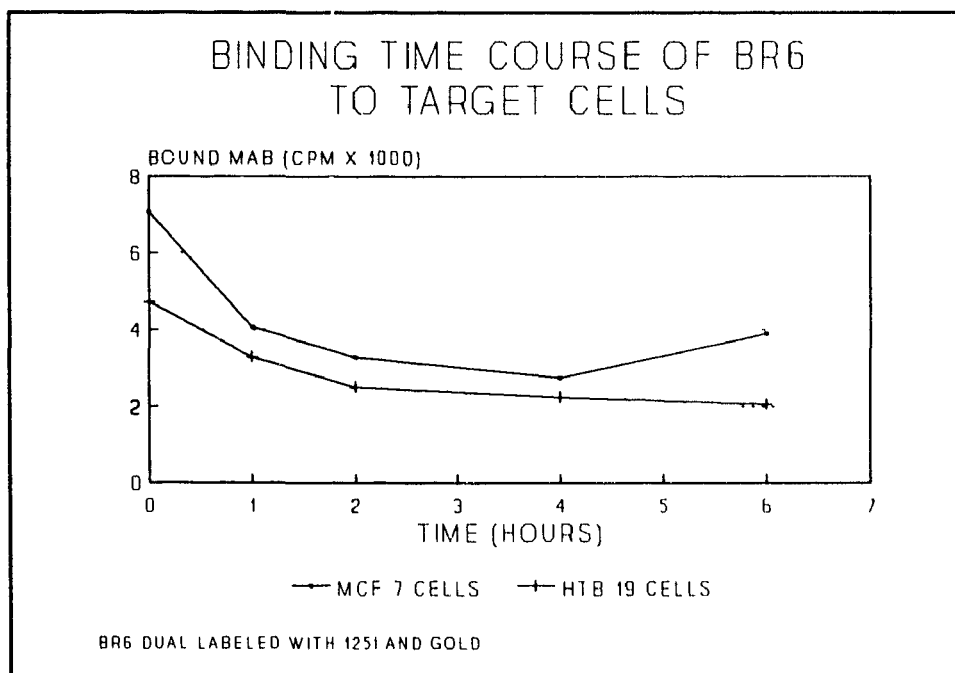


FIGURE 35

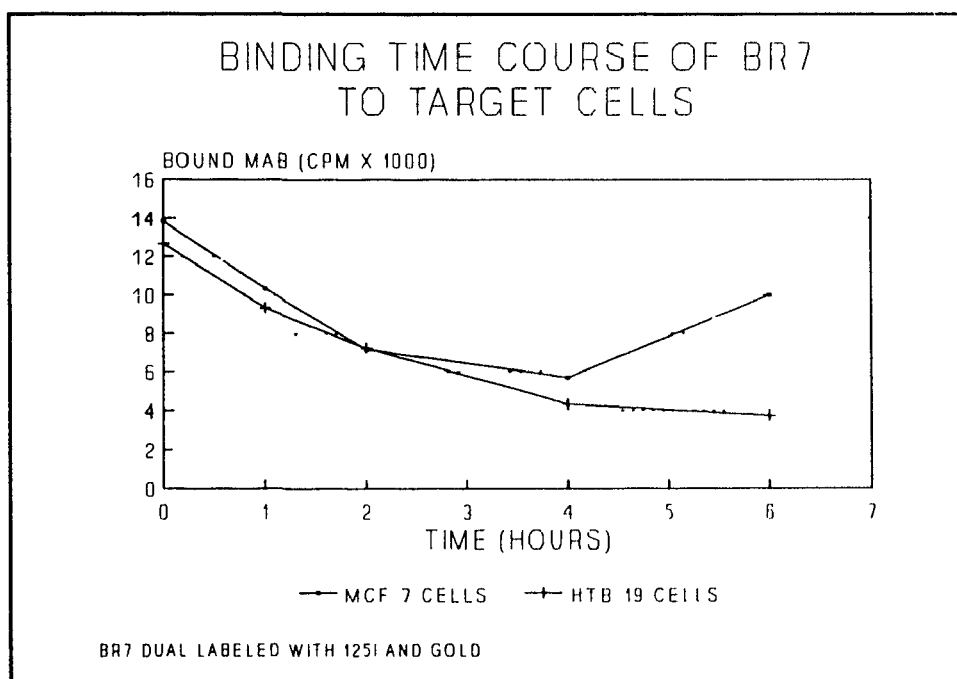


FIGURE 36

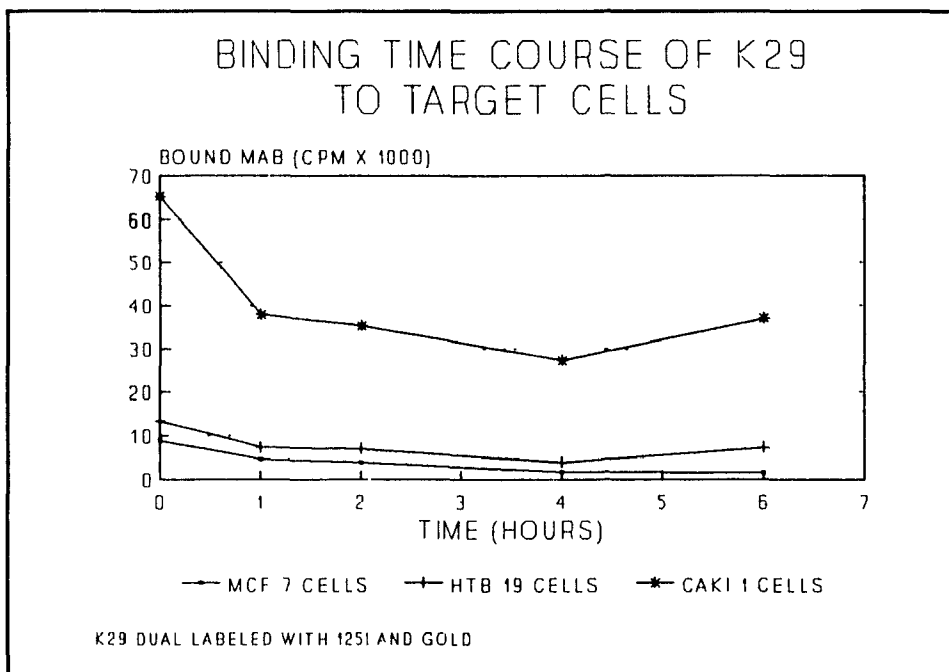


FIGURE 37

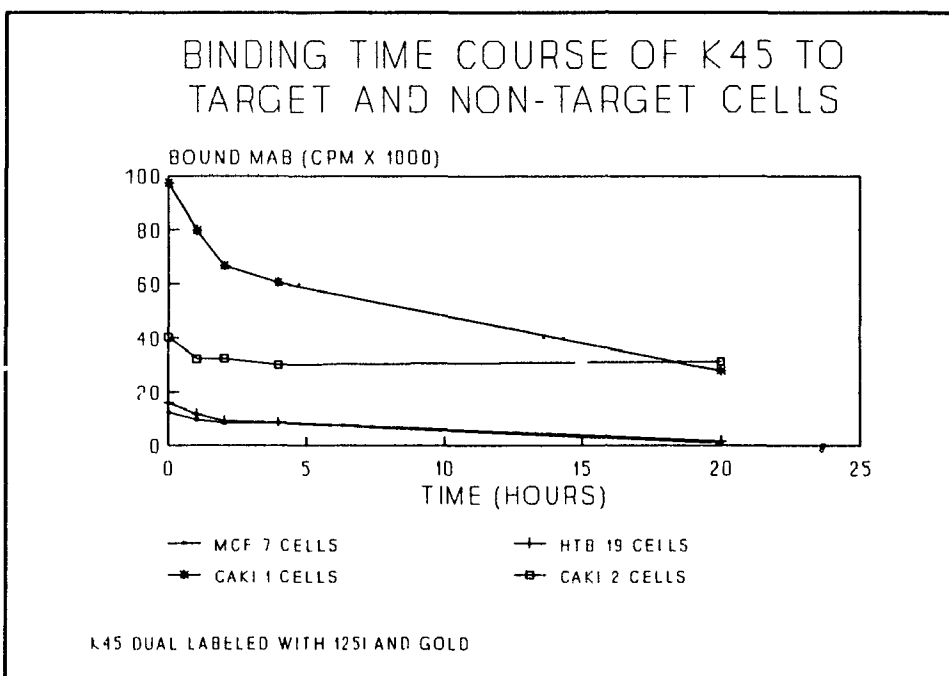


FIGURE 38

The experiments show that at 0 hrs, comparable amounts of DAL-BR6, DAL-BR7 or K29 bound to both HTB-19 and MCF-7 cells. In addition, there was a similar time dependent decrease in the amount of each MAB that was cell associated once the cells with bound MAB were incubated at 37°C. However, K29 bound significantly more to Caki-1 cells than to either of the HMC lines. Similarly, K45 also bound much more to both Caki-1 and Caki-2 cells than to HMC cells, and interestingly, bound more to Caki-1 cells than to Caki-2 cells. The HMC cell lines had a similar amount of bound K45 (expressed as cpm) and a similar amount of cell-associated K45 over time (also expressed as cpm) as did K29. However, the K45 radiolabeled preparation used in these experiments had almost double the specific activity of all the other radiolabeled MABs including K29. This implies that the actual amount of K45 that initially bound to HMC cells estimated by cpm was at least 50% less than the amount of K29 that bound to the same HMC cells. This negligible binding of K45 to HMC lines was confirmed by Dr. G. Faulkner who examined sections of the same sample aliquots with a transmission electron microscope as described below. Experiments using the B-cell CLL-specific MAB, DAL-B02, showed negligible initial binding and subsequent cell associated radioactivity with all these non-B cell CLL cell lines.

3. Ultrastructural Analysis of Cells Used in Binding Experiments with Dual-Labeled MABs by Dr. G. Faulkner

Each aliquot of cells from the experiment described above in item 2 (pages 135-139) that had its ^{125}I -activity determined was also processed and sectioned for transmission electron microscopy in Dr. G. Faulkner's laboratory. The ultrathin sections of cells in each aliquot were examined for the number and ultrastructural location of gold particles by Dr. G. Faulkner. The number of gold particles associated with several cells was determined by direct counting by Dr. G. Faulkner during the electron microscopic examination of each specimen and the results were expressed on a scale (- to +++) based on the relative number of gold particles observed in each specimen. A specimen which had no gold particles in the sections was assigned a (-) value while a specimen with an occasional, rare gold particle in the sections was assigned a (+) value. A specimen was assigned a (++) value when its sections contained more than a rare gold particle but fewer than that found in sections of other specimens. Finally, a (+++) value was assigned to a specimen with sections containing more gold particles than the sections of specimens described above but containing fewer gold particles than the sections of specimens which had the most gold particles observed in these experiments and which were assigned the maximum value of (+++). Table 10 (page 141) presents a summary of all these observations made by Dr. G. Faulkner on specimens taken at 0 hr and 4 hr in the experiments described in item 2 (pages 135-139).

TABLE 10: ULTRASTRUCTURAL QUANTITATION AND LOCALIZATION OF GOLD PARTICLES ASSOCIATED WITH CELL LINES (OBSERVATIONS MADE BY DR. G. FAULKNER)

SPECIMEN	HR	^a GOLD OVERALL	^b GOLD OUTSIDE	^c GOLD INSIDE
¹²⁵ I-DAL-BR6-GOLD + MCF-7	0	+++	+++	+
	4	+++	+	+++
¹²⁵ I-DAL-BR6-GOLD + HTB-19	0	+	+	-
	4	+++	+	+++
¹²⁵ I-DAL-BR7-GOLD + MCF-7	0	+	+	-
	4	+++	+	+++
¹²⁵ I-DAL-BR7-GOLD + HTB-19	0	++++	++++	-
	4	++	++	+
¹²⁵ I-K29-GOLD + MCF-7	0	+	+	-
	4	+++	++	+
¹²⁵ I-K29-GOLD + HTB-19	0	++	++	++
	4	++++	+	++++
¹²⁵ I-K29-GOLD + CAKI-1	0	++	+	+
	4	++++	+	++++
¹²⁵ I-K45-GOLD + CAKI-1	0	+++	+++	+
	4	+++	++	+++
¹²⁵ I-K45-GOLD + CAKI-2	0	++	++	+
	4	+++	+++	++
¹²⁵ I-K45-GOLD + MCF-7	0	+	+	-
	4	+	+	-
¹²⁵ I-K45-GOLD + HTB-19	0	+	+	-
	4	+	+	-

^aGold Overall = Total number of gold particles in the section

^bGold Outside = Number of gold particles associated with the cell membrane

^cGold Inside = Number of gold particles intracellularly

Most of the gold particles at 0 hr were observed decorating the cell membranes of all specimens except those of MCF-7 or HTB-19 cells incubated with K45 where very few gold particles were found. Three specimens, DAL-BR6 with MCF-7 cells at 0 and 4 hr and DAL-BR7 with HTB-19 cells at 0 hr had a substantial number of gold particles associated with cell membrane debris from disrupted cells in addition to particles associated with the surface of intact cells. Also at 0 hr, in specimens of both HTB-19 and Caki-1 cells incubated with K29, a higher proportion of gold particles were found intracellularly compared to all other specimens at this time indicating that this MAB was quickly endocytosed after binding to these cell lines. Other than the described binding of gold particles to cell membrane debris, there was no appreciable difference at 0 hr in the number of gold particles associated with MCF-7 and HTB-19 cells in specimens that were incubated with DAL-BR6, DAL-BR7 or K29. However at the same time, there were more cell associated gold particles in the specimen containing K29 with Caki-1 cells compared to specimens containing this MAB with either MCF-7 or HTB-19 cells. In addition at 0 hr, Caki-1 cells had more cell associated K45-gold particles than Caki-2 cells.

With the exception of K45 with MCF-7 and HTB-19 cells, all specimens at 4 hr showed more gold particles than at 0 hr and most of these particles were intracellular. There appeared to be very few gold particles free in the cytoplasm. Most of the gold particles were concentrated in cellular organelles identified as disrupted mitochondria, multivesicular bodies, and electron dense or electron translucent membrane-bound bodies. These latter two intracellular vacuoles are

identified as phagosomes or lysosomes or their fusion product. The disrupted gold-containing mitochondria were markedly altered structurally compared to intact nearby mitochondria not containing gold. Another intracellular site of gold particles was in saccules which appeared as short segments of endoplasmic reticulum. The two specimens containing K29 reacting with HTB-19 or Caki-1 cells had more gold particles located intracellularly than any other specimen at 4 hr. However, all specimens except K45 on MCF-7 or HTB-19 cells did have variable amounts of intracellular gold. Also identified at all time periods in all these specimens except for K45 with MCF-7 or HTB-19 cells was cell membrane-associated gold particles in the process of being phagocytosed or endocytosed by the respective cells at 4 hr. This process was more evident in all specimens examined ultrastructurally at 1 and 2 hr. Another finding was that in the specimen containing DAL-BR7 with HTB-19 cells, most gold particles bound to cell membrane debris. Furthermore, in this specimen there was less gold associated with surface membranes of intact cells or intracellularly over these time periods. Additional controls used in these experiments were dual gold and ^{125}I -labeled DAL-B02 as well as gold sol alone which were incubated with the cell lines and these specimens showed no gold particles associated with any cell either extracellularly or intracellularly at any time period.

Representative electron photomicrographs taken by Dr. G. Faulkner illustrating cell membrane-associated gold particles at 0 hr and intracellular gold particles at 4 hr from two experiments using dual-labeled DAL-BR6 and K29 with HTB-19 cells are shown in Figures 39 and 40 (pages 144-145).

FIGURES 39 AND 40:

TRANSMISSION ELECTRON PHOTOMICROGRAPHS TAKEN BY DR. G. FAULKNER TO ILLUSTRATE THE QUANTITY AND ULTRASTRUCTURAL LOCALIZATION OF DUAL GOLD AND ^{125}I -LABELED MABS AT 0 HR AND 4 HR IN AN EXPERIMENT USING HTB-19 CELLS.

FIGURE 39: HTB-19 CELLS INCUBATED WITH DAL-BR6 AT 0 HR

NOTE CELL MEMBRANE-ASSOCIATED GOLD PARTICLES

FIGURE 40: HTB-19 CELLS INCUBATED WITH K29 AT 4 HR

NOTE INTRACELLULAR GOLD PARTICLES IN VACUOLES

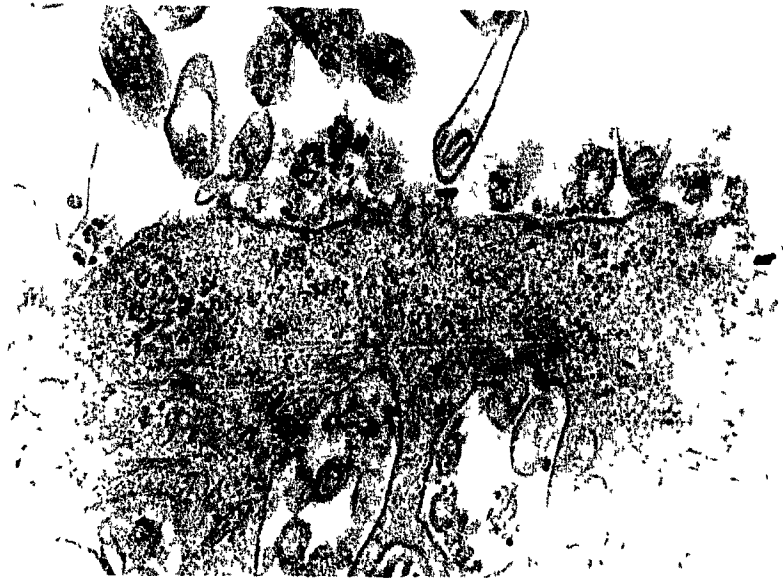


FIGURE 39

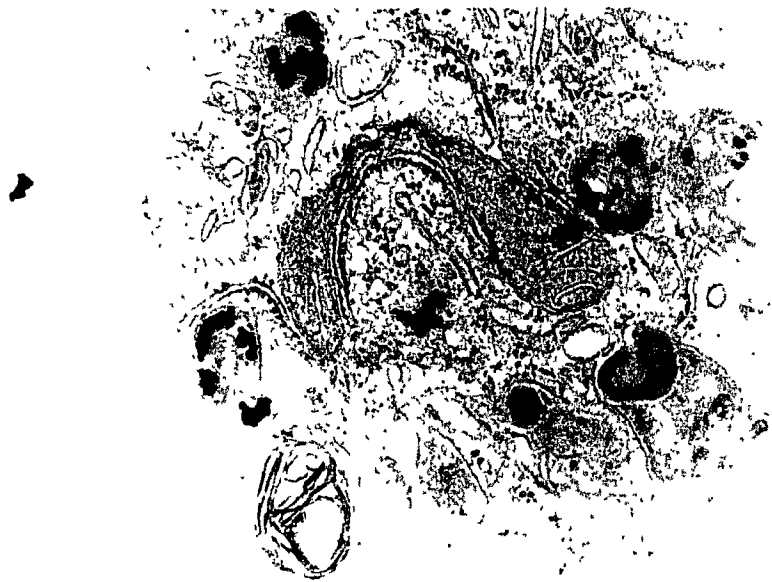


FIGURE 40

PART 5

DIRECT CYTOTOXICITY AND EFFECT OF MABS ON TUMOR CELL PROLIFERATION

1. Direct Cytotoxicity of the MABs

None of the anti-HMC MABs exhibited complement-mediated cytotoxicity towards MCF-7 or HTB-19 cells at concentrations of 250 ug/ml. For most MABs which were available in more concentrated solutions, concentrations greater than 250 ug/ml and up to 1000 ug/ml of MABs were also tested and these experiments again showed no complement-mediated cytotoxicity. These MABs included DAL-BR4 (530 ug/ml), DAL-BR5 (565 ug/ml), DAL-BR8 (500 ug/ml) and MABs DAL-BR1, DAL-BR3, DAL-BR6, DAL-BR7, DAL-BR9, and DAL-BR10 (all 1000 ug/ml). It must be reiterated that the freshly obtained human AB serum, which was used as the source of complement in these experiments, did not have its complement activity confirmed.

The target cells were agglutinated by each MAB at all these concentrations but the agglutinated cells remained viable over a 24 hr exposure to the MABs at 37°C. Control preparations included the same HMC cells incubated under the same conditions either with DAL-B02 at concentrations of 250 ug/ml and 1000 ug/ml or without added MAB. These experiments showed neither complement-mediated cytotoxicity nor agglutination of cells.

2. Direct Anti-Proliferative Effect of the MABs

A six hour pulse exposure of MCF-7, HTB-19 and Caki-2 cells to MABs DAL-BR1, DAL-BR6, DAL-BR7, DAL-BR9, or DAL-B02 (the latter MAB being a control since it does not react with HMC cells) followed by 7 days of cell culture at 37°C did not inhibit the proliferation of these cells at all MAB concentrations up to 1000 µg/ml. However, pulse exposure for 6 hours of the same HMC cells to each of the remaining 7 anti-HMC MABs inhibited the proliferation of these cells when MAB concentrations in excess of 100 µg/ml were used (Figures 41 to 54, pages 148-155). In fact, at the highest concentration of DAL-BR2, DAL-BR3, DAL-BR4, DAL-BR5, DAL-BR8, DAL-BR10 or DAL-BR11 (250 µg/ml up to a 1000 µg/ml depending on the MAB as shown respectively in Figures 41 to 54) there was complete growth inhibition as a result of cells in the wells becoming detached after the pulse exposure. Different maximum concentrations of some MABs were evaluated in this experiment as a consequence of these MABs being available only as dilute solutions due to poor isolation and recovery of these MABs from ascites fluid.

HTB-19 and MCF-7 cells were comparably inhibited to proliferate after the 6 hour pulse exposure to the MABs described above. Caki-2 cells (which do not react with any of the MABs tested) instead of HMC cells were used as an additional control preparation in these experiments. None of the anti-HMC MABs or DAL-B02 at concentrations identical to those used for each respective MAB described above inhibited the proliferation of these non-target tumor cells.

FIGURES 41 TO 54:

RESULTS OF EXPERIMENTS WHERE HMC CELLS WERE FIRST EXPOSED FOR 6 HOURS TO VARIOUS MABS AT DIFFERENT CONCENTRATIONS AND THEN CULTURED FOR 7 DAYS.

THE GROWTH OF THESE MAB-EXPOSED CELLS OVER 7 DAYS WAS COMPARED TO THE GROWTH OF CELLS NOT EXPOSED TO MABS USING A CRYSTAL VIOLET ASSAY. THE RESULTS ARE EXPRESSED IN PERCENTAGES (i.e. $\text{ABSORBANCE}_{570 \text{ NM}}$ OF WELLS CONTAINING MAB-EXPOSED CELLS DIVIDED BY $\text{ABSORBANCE}_{570 \text{ NM}}$ OF WELLS CONTAINING CELLS NOT EXPOSED TO MAB MULTIPLIED BY 100%). THESE PERCENTAGES ARE PLOTTED AGAINST THE CONCENTRATIONS OF MABS USED IN EACH EXPERIMENT ($\mu\text{g/ml}$) IN A LOGARITHMIC SCALE.

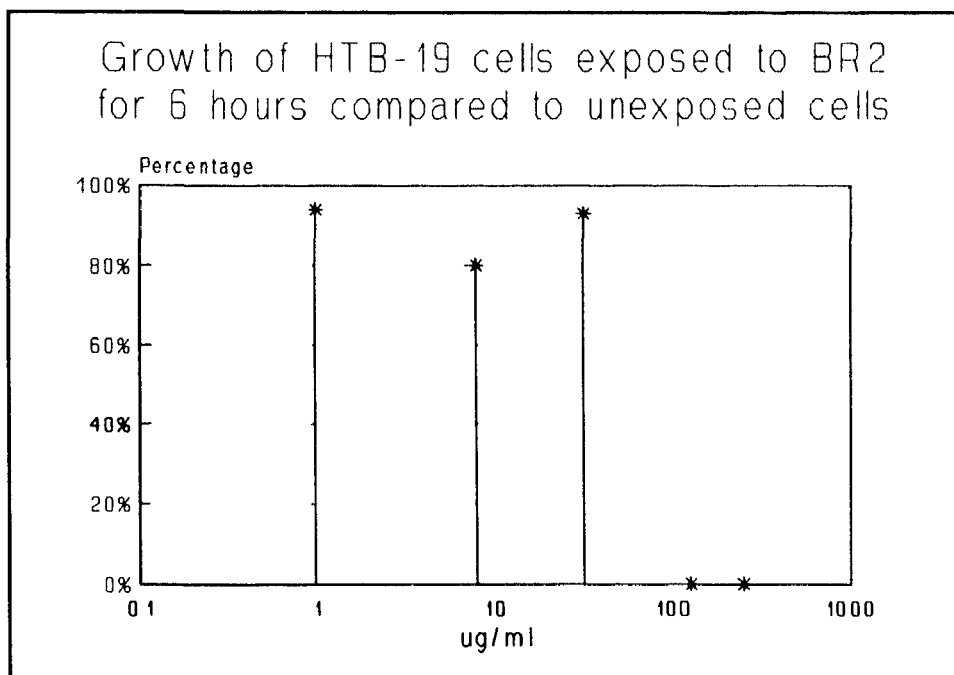


FIGURE 41

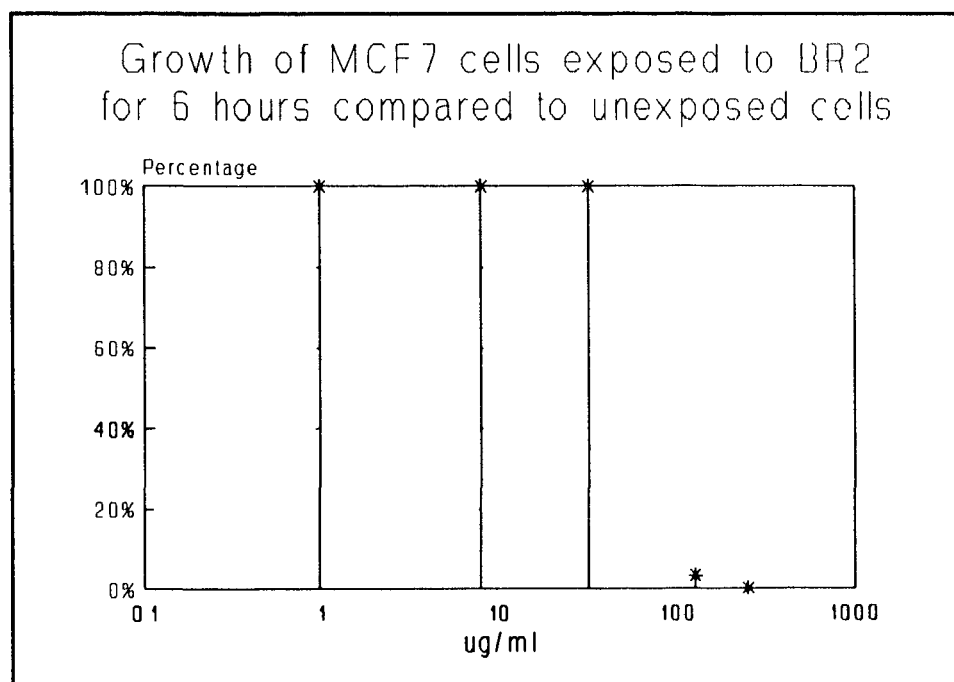


FIGURE 42

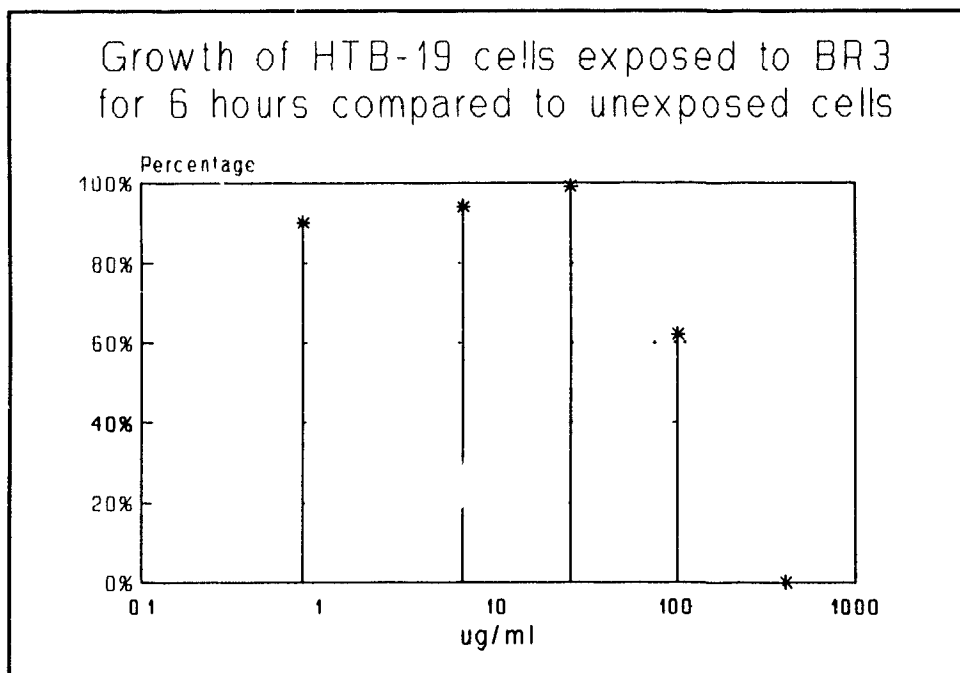


FIGURE 43

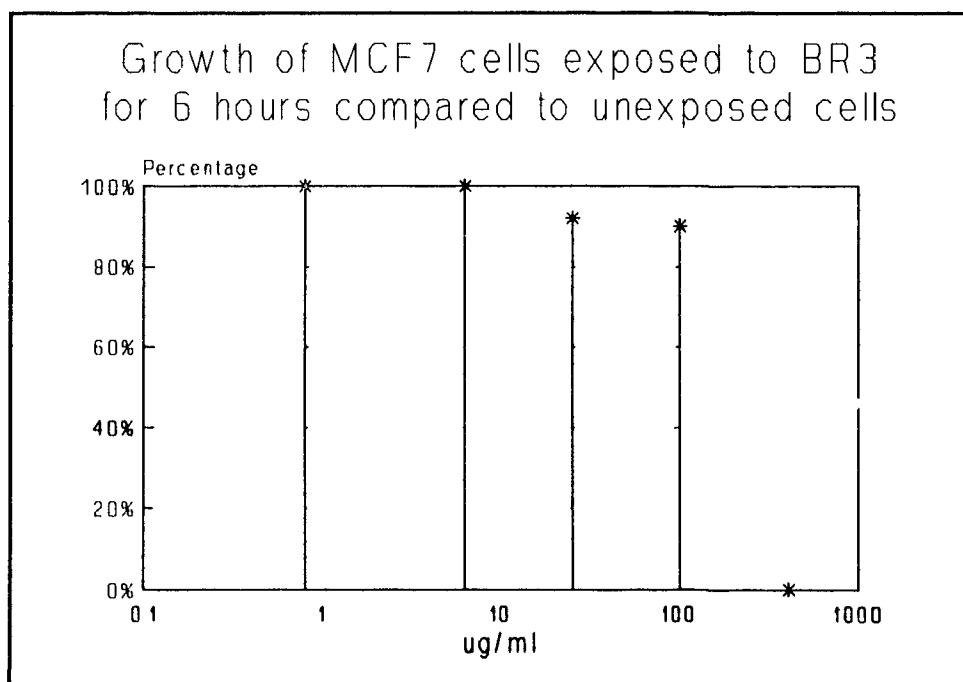


FIGURE 44

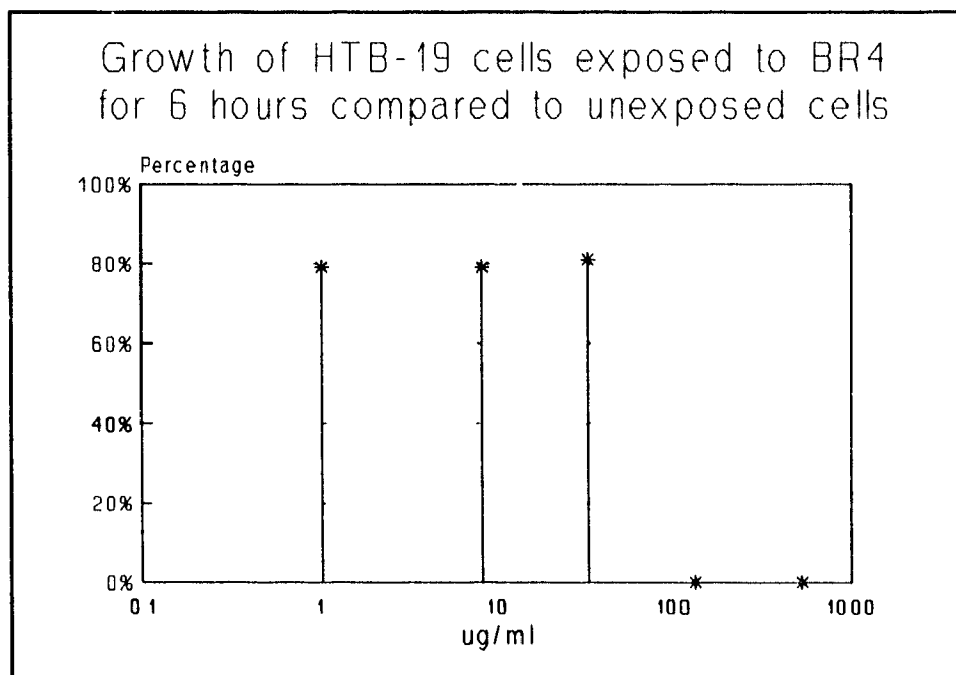


FIGURE 45

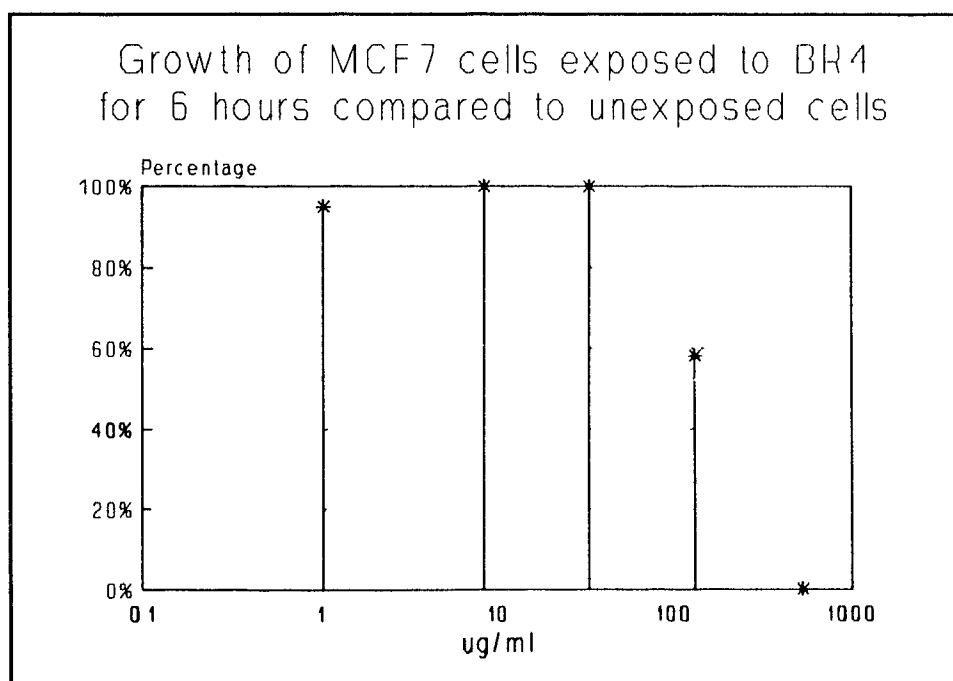


FIGURE 46

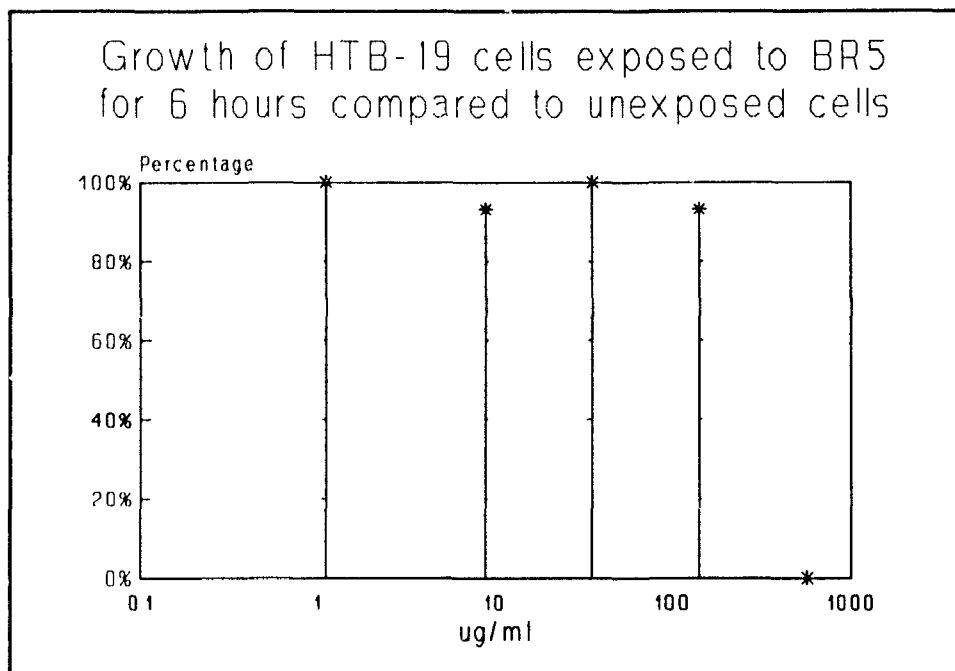


FIGURE 47

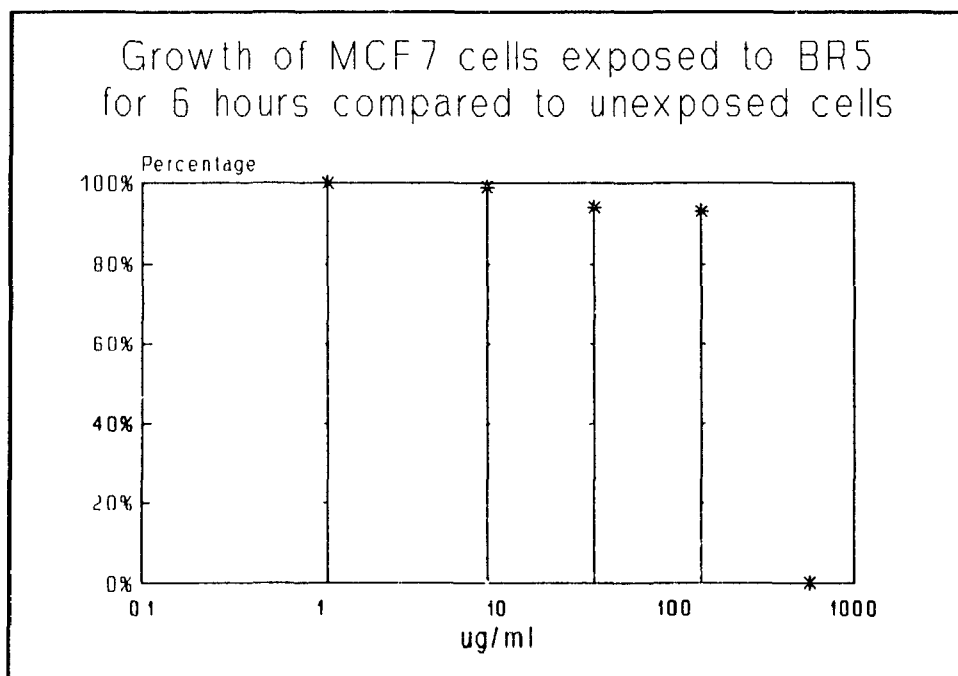


FIGURE 48

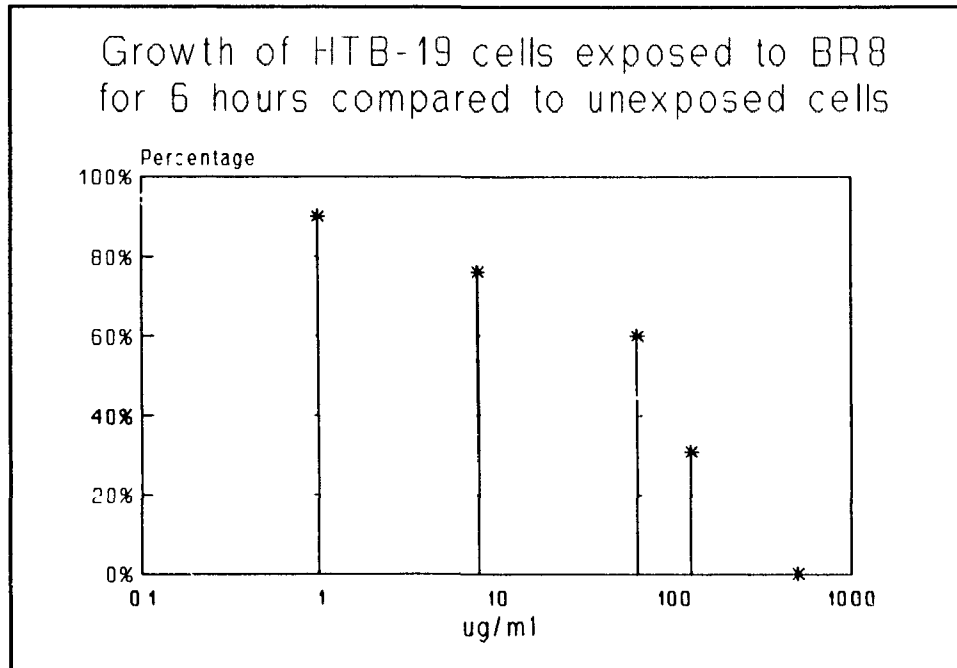


FIGURE 49

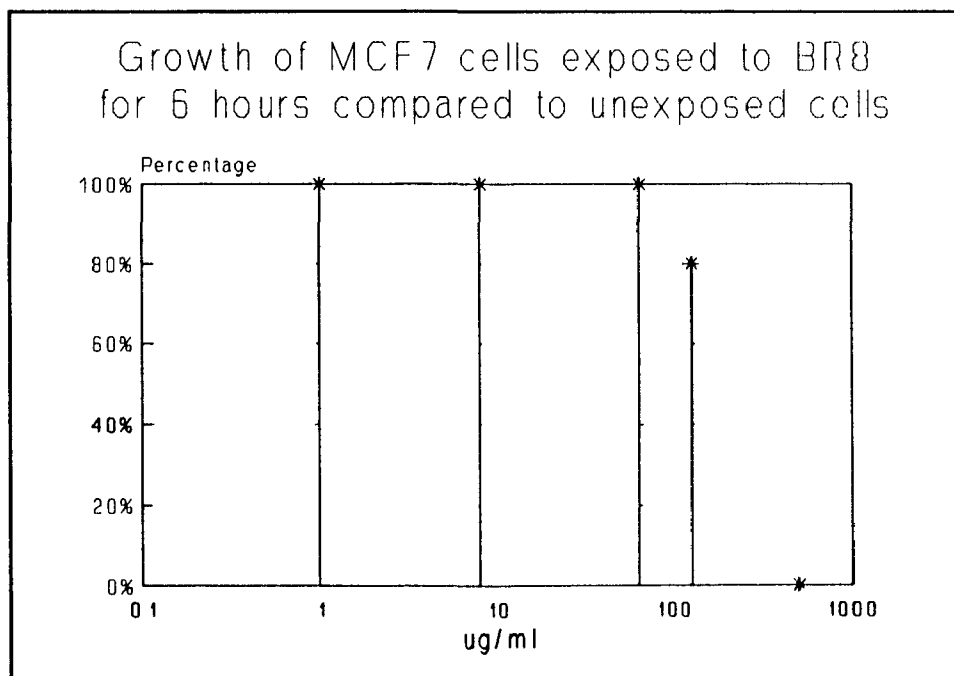


FIGURE 50

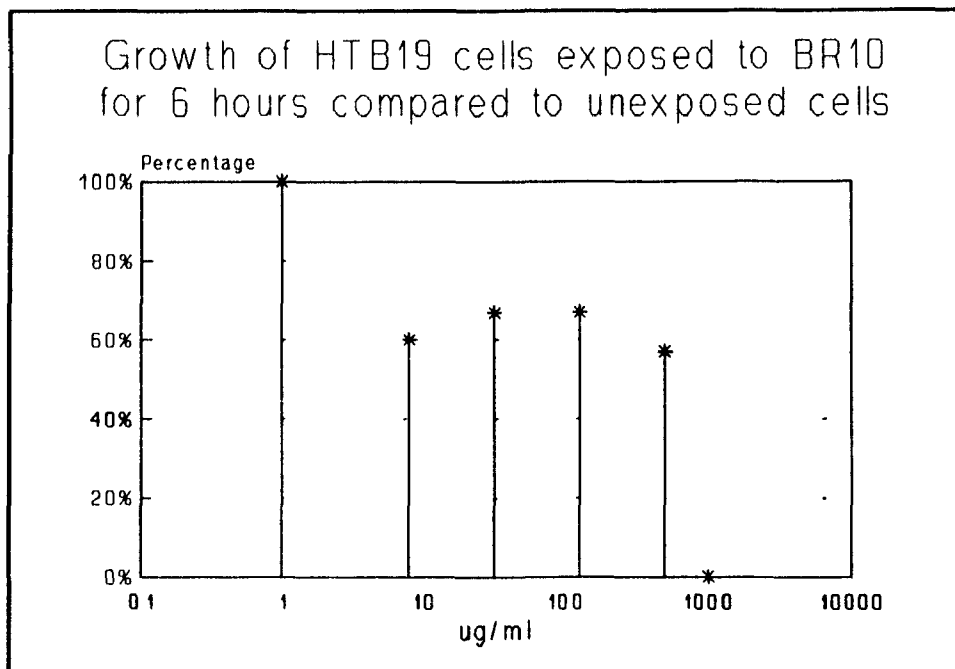


FIGURE 51

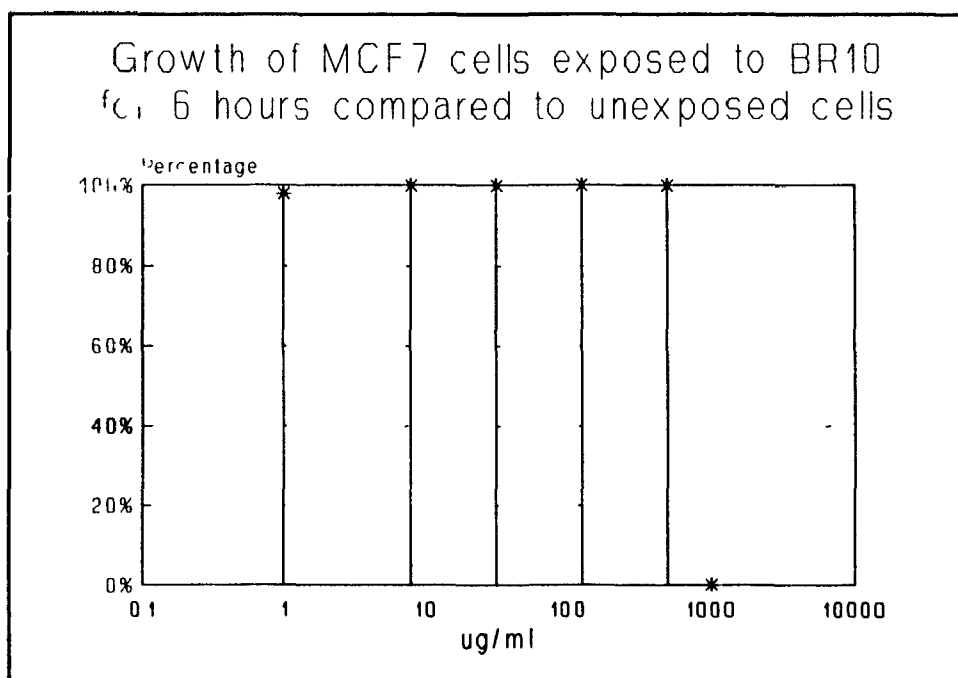


FIGURE 52

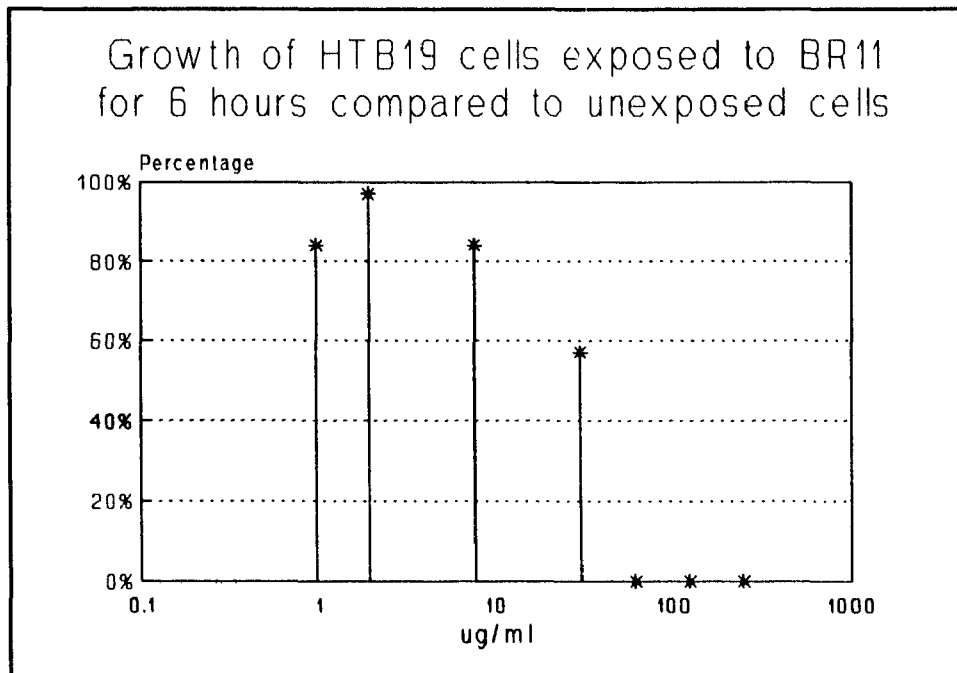


FIGURE 53

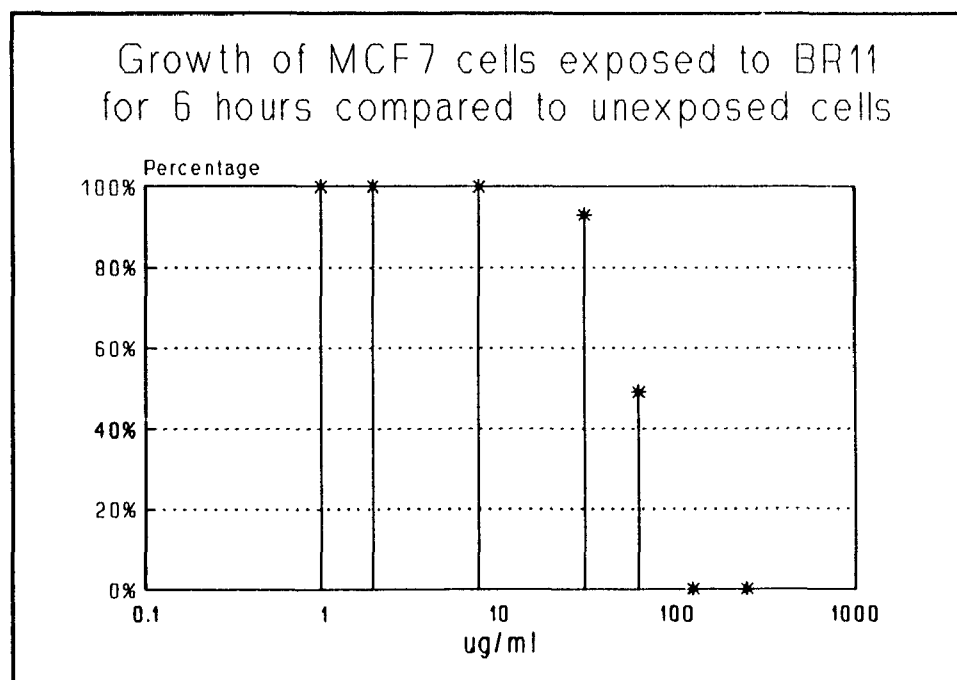


FIGURE 54

The results of experiments assessing the effect of a continuous 7 day exposure of cell lines to the MABs at a constant MAB concentration of 250 ug/ml are presented in Figure 55 (pages 157-158). In this set of experiments, all the MABs which inhibited the proliferation of target cells after a 6 hour pulse exposure also inhibited the proliferation of target cells after continuous exposure for 7 days except DAL-BR3 and DAL-BR4. MCF-7 cells were more sensitive to continuous MAB exposure in all cases and DAL-BR1, which did not inhibit the growth of HMC cells after a 6 hour pulse exposure, did inhibit HMC cell proliferation after a continuous 7 day exposure. None of the anti-HMC MABs or DAL-B02 had any growth inhibitory effect on the non-target Caki-1 or human foreskin fibroblast cells after continuous exposure at this 250 ug/ml concentration of MABs. Since DAL-BR3 and DAL-BR4 did not inhibit the proliferation of HMC cells in the above study, another experiment was conducted to verify these findings. The results of this repeat experiment in which HTB-19 cells were continuously exposed to DAL-BR3 or DAL-BR4 as well as to several other MABs at two or more concentrations for 7 days are presented in Figure 56 (pages 157, 159). As shown, both DAL-BR3 and DAL-BR4 as well as DAL-BR2 and DAL-BR11 did inhibit the proliferation of HTB-19 cells.

FIGURES 55 AND 56:

FIGURE 55: RESULTS OF EXPERIMENTS WHERE HMC CELLS WERE CONTINUOUSLY EXPOSED FOR 7 DAYS IN CELL CULTURE TO VARIOUS MABS AT A CONCENTRATION OF 250 ug/ml. THE GROWTH OF THESE MAB-EXPOSED CELLS OVER 7 DAYS WAS COMPARED TO THE GROWTH OF CELLS NOT EXPOSED TO MABS USING A CRYSTAL VIOLET ASSAY.

FIGURE 56: RESULTS OF EXPERIMENTS WHERE HTB-19 CELLS WERE CONTINUOUSLY EXPOSED FOR 7 DAYS IN CELL CULTURE TO VARIOUS MABS AT DIFFERENT CONCENTRATIONS. THE GROWTH OF THESE MAB-EXPOSED CELLS OVER 7 DAYS WAS COMPARED TO THE GROWTH OF CELLS NOT EXPOSED TO MABS USING A CRYSTAL VIOLET ASSAY.

THE RESULTS IN BOTH FIGURES ARE EXPRESSED IN PERCENTAGES (i.e. $\text{ABSORBANCE}_{570 \text{ NM}}$ OF WELLS CONTAINING MAB-EXPOSED CELLS DIVIDED BY $\text{ABSORBANCE}_{570 \text{ NM}}$ OF WELLS CONTAINING CELLS NOT EXPOSED TO MAB MULTIPLIED BY 100). THESE PERCENTAGES ARE PLOTTED AGAINST THE MAB CONCENTRATIONS OF 10, 100 AND 1000 AGAINST THE CONCENTRATIONS OF MAB ON A LOG₁₀ SCALE (IN FIGURE 56).

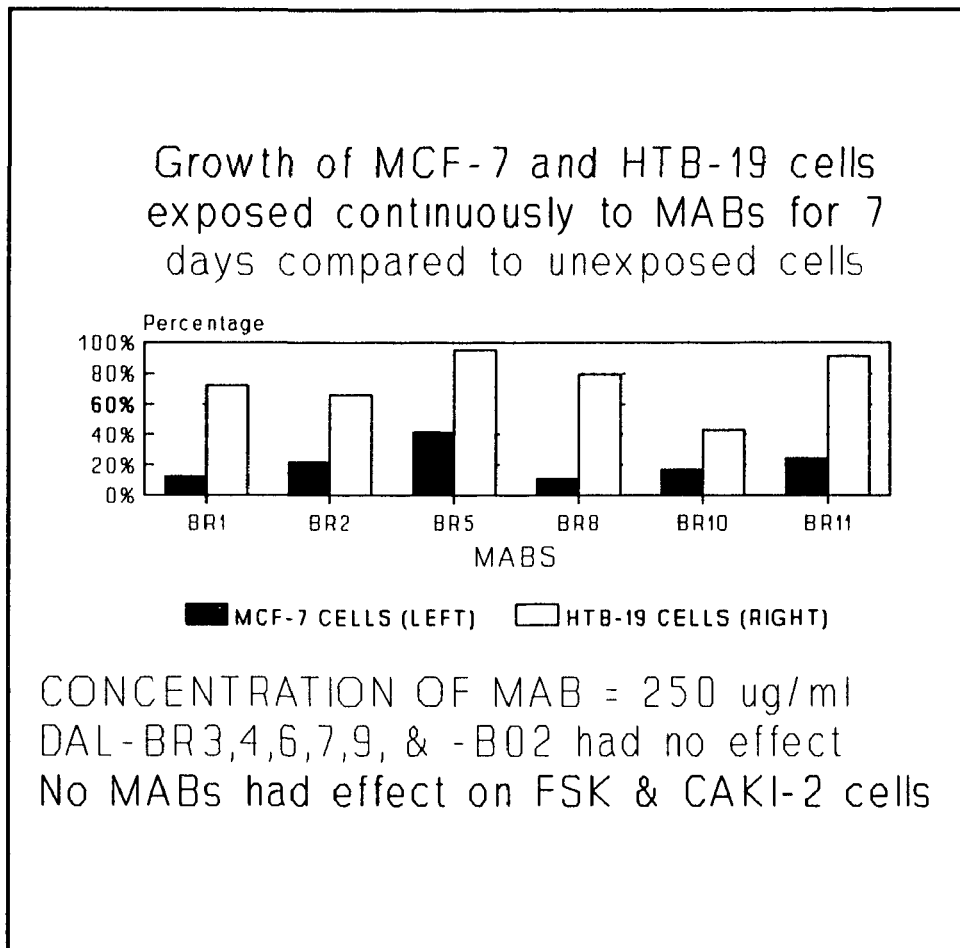


FIGURE 55

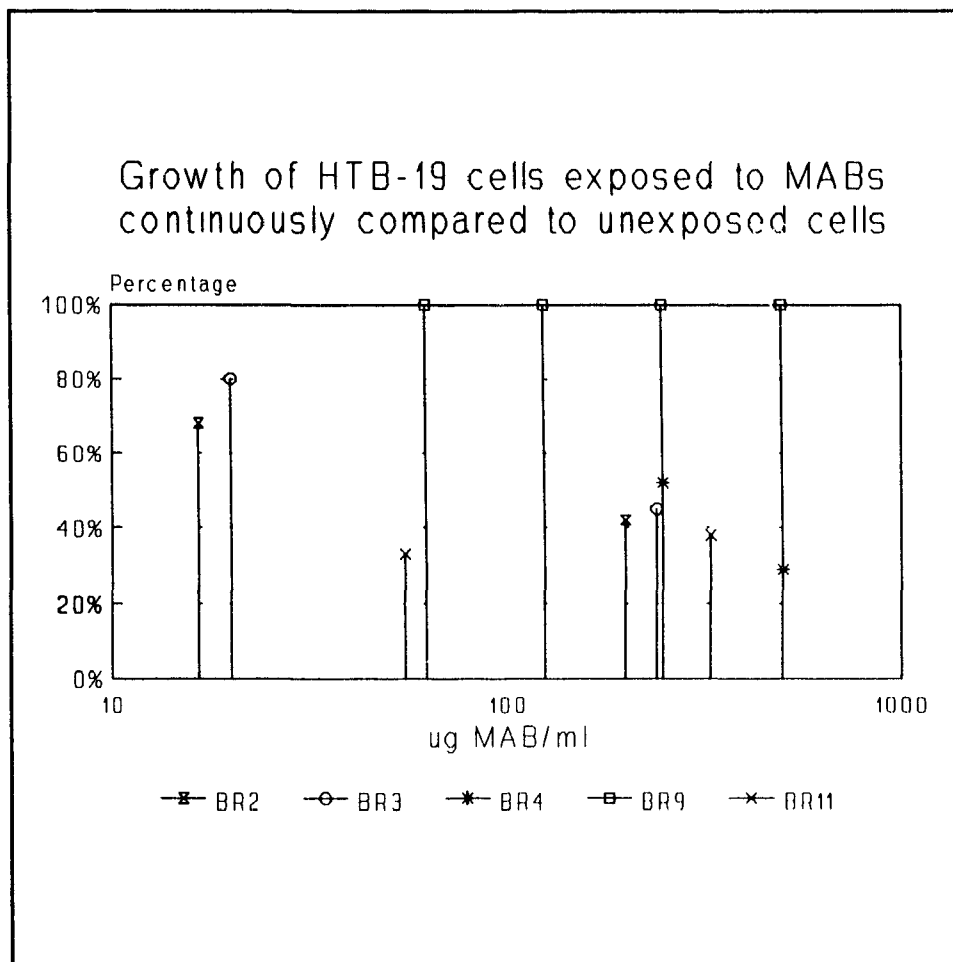


FIGURE 56

PART 6

EFFECT OF ANTI-CANCER DRUGS AND MAB-DRUG CONJUGATES ON TUMOR CELL PROLIFERATION IN VITRO

The growth inhibitory effect of MTX, ADM, and MAB-drug conjugates on the HMC cell lines, MCF-7 and HTB-19, was assessed by exposing these cells to each drug or conjugate for 6 hours and then incubating for 7 days. Following incubation, the crystal violet assay was used as described before in item 15 (pages 70-71). The results from these experiments are presented in Table 11 (page 161) which shows the IC_{50} concentrations, the sensitivity ratios, and the specificity ratios of each agent.

Native MTX and ADM did inhibit the proliferation of both HMC cell lines but ADM was the more potent drug. The active ester conjugate of MTX with DAL-BR6 had a slightly superior growth inhibitory effect on MCF-7 cells compared to that of the native drug. However, when this same conjugate was tested on HTB-19 cells, it was less potent than MTX. The sensitivity of both cell lines to MTX was approximately twice the sensitivity to the DAL-BR7-MTX conjugate.

Both cell lines were 80-200 times more sensitive to native ADM than to the CAA-ADM conjugate of DAL-BR6 or DAL-BR7. The C13-ADM conjugate of each MAB was a more potent growth inhibitor of both cell lines than either of the CAA-ADM conjugates. However, these C13-ADM conjugates were still 14-47 times less potent than native ADM. Except for DAL-BR9-C13-ADM on HTB-19 cells, all other MAB-C13-ADM conjugates inhibited the proliferation of HMC cells more effectively than DAL-B01-C13-ADM indicating carrier MAB-based potency of these conjugates.

TABLE 11: In VITRO IC₅₀ CONCENTRATIONS, SENSITIVITY RATIOS OR SER*, AND SPECIFICITY RATIOS OR (SPR)** OF MTX, ADM, AND THEIR RESPECTIVE MAB-CONJUGATES ON HMC CELLS AFTER A PULSE EXPOSURE FOR 6 HR

AGENT	MCF-7 CELLS		HTB-19 CELLS	
	IC ₅₀ (ug/ml)	SER (SPR)	IC ₅₀ (ug/ml)	SER (SPR)
MTX	2.00	1.00 (NA) ¹	2.50	1.00 (NA)
ADM	0.015	1.00 (NA)	0.015	1.00 (NA)
DAL-BR6-MTX	1.90	0.95 (ND) ²	6.00	2.40 (ND)
DAL-BR7-MTX	3.90	1.95 (ND)	6.00	2.40 (ND)
DAL-BR6-CAA-ADM	1.20	80 (ND)	2.90	193 (ND)
DAL-BR7-CAA-ADM	3.00	200 (ND)	1.20	80 (ND)
DAL-BR6-C13-ADM	0.30	20 (2.17)	0.21	14 (3.09)
DAL-BR7-C13-ADM	0.21	14 (3.09)	0.21	14 (3.09)
DAL-BR8-C13-ADM	0.38	25 (1.71)	0.15	10 (4.33)
DAL-BR9-C13-ADM	0.32	21 (2.03)	0.70	47 (0.93)
DAL-BR11-C13-ADM	0.30	20 (2.17)	0.30	20 (2.17)
DAL-B01-C13-ADM	0.65	43 (1.00)	0.65	43 (1.00)

* SENSITIVITY RATIO = $\frac{\text{IC}_{50} \text{ OF TEST AGENT}}{\text{IC}_{50} \text{ OF NATIVE DRUG}}$

** SPECIFICITY RATIO = $\frac{\text{IC}_{50} \text{ OF NONSPECIFIC MAB-CONJUGATE}}{\text{IC}_{50} \text{ OF MAB-CONJUGATE}}$

¹ NA = NOT APPLICABLE

² ND = EXPERIMENT NOT DONE

Also assessed was the growth inhibitory effect of the C13-ADM conjugates of DAL-BR8, DAL-BR9, DAL-BR11 and DAL-B01 on MCF-7, HTB-19 and Caki-2 cells. The cells in each experiment were exposed to each conjugate continuously for 7 days and then the crystal violet assay was used. In these experiments, the lowest concentration of ADM in the conjugates of each anti-HMC MAB that was tested, proved to be in excess of the IC_{50} drug concentrations for the two HMC cell lines. For this reason, the IC_{75} and IC_{90} concentrations were determined for each conjugate and the results of each experiment are summarized in Table 12 (page 163). This table also presents the specificity ratio and the selectivity ratio of each agent.

MCF-7 cells were consistently more sensitive to all these conjugates than HTB-19 cells. Furthermore, HMC cells were more sensitive to these agents than Caki-2 cells. Under these experimental conditions, some anti-HMC MAB conjugates had either a comparable or lower growth inhibitory effect as the nonspecific DAL-B02 conjugate on HMC cells indicating lack of specificity. However, MCF-7 cells were slightly more sensitive to the conjugates of DAL-BR8 and DAL-BR11 than to the conjugate of DAL-B01 while HTB-19 cells were likewise more sensitive to the DAL-BR8 conjugate. In contrast, Caki-2 cells were slightly less sensitive to the conjugate of each anti-HMC MAB than to the conjugate of DAL-B01. Although every agent that was tested demonstrated selective growth inhibition of HMC cells over Caki-2 cells, only the comparison with MCF-7 cells showed consistently high selectivity ratios of anti-HMC MABs which exceeded the ratios of DAL-B01. Therefore, the C13-ADM conjugates of anti-HMC MABS appear to be selective for MCF-7 cells.

TABLE 12: IN VITRO PERCENT GROWTH INHIBITORY CONCENTRATIONS (IC₇₅ AND IC₉₀), SPECIFICITY RATIOS (SPR)*, AND SELECTIVITY RATIOS (SLR)** OF MAB-C13-ADM CONJUGATES ON HMC AND CAKI-2 CELLS AFTER CONTINUOUS EXPOSURE FOR 7 DAYS

CONJUGATE	MCF-7 CELLS		HTB-19 CELLS		CAKI-2 CELLS		SLR	SLR
	ug/ml	(SPR)	ug/ml	(SPR)	ug/ml	(SPR)	1	2
<u>DAL-BR8-C13-ADM</u>								
IC ₇₅ ³	<0.2	(>0.8)	<0.2	(>1.2)	1.20	(0.70)	>6	>6
IC ₉₀	0.23	(1.73)	0.31	(1.94)	1.90	(0.78)	8.3	6.1
<u>DAL-BR9-C13-ADM</u>								
IC ₇₅	0.17	(1.00)	0.35	(0.71)	1.00	(0.80)	5.9	2.9
IC ₉₀	0.40	(1.00)	0.60	(1.00)	1.80	(0.83)	4.5	3.0
<u>DAL-BR11-C13-ADM</u>								
IC ₇₅	0.11	(1.55)	0.35	(0.71)	0.85	(0.94)	7.7	2.4
IC ₉₀	0.30	(1.33)	0.65	(0.92)	1.50	(1.00)	5.0	2.3
<u>DAL-B01-C13-ADM</u>								
IC ₇₅	0.17	(1.00)	0.25	(1.00)	0.80	(1.00)	4.7	3.2
IC ₉₀	0.40	(1.00)	0.60	(1.00)	1.50	(1.00)	3.8	2.5

* SPECIFICITY RATIO = $\frac{\text{IC}_{75 \text{ OR } 90} \text{ OF NONSPECIFIC MAB-CONJUGATE}}{\text{IC}_{75 \text{ OR } 90} \text{ OF MAB-CONJUGATE}}$

** SELECTIVITY RATIO = $\frac{\text{IC}_{75 \text{ OR } 90} \text{ OF MAB-CONJUGATE ON CAKI-2 CELLS}}{\text{IC}_{75 \text{ OR } 90} \text{ OF MAB-CONJUGATE ON HMC CELLS}}$

SLR 1 = SELECTIVITY RATIO USING MCF-7 AND CAKI-2 CELLS

SLR 2 = SELECTIVITY RATIO USING HTB-19 AND CAKI-2 CELLS

³ = EXACT VALUE COULD NOT BE DETERMINED FROM 2 EXPERIMENTS

PART 7

PREPARATION OF F(ab)₂ FRAGMENTS FROM ANTI-HMC MABS

Pilot experiments using 4 anti-HMC MABs (DAL-BR6, an IgG₁ MAB; DAL-BR7, an IgG_{2b} MAB; DAL-BR9, an IgG₃ MAB; and DAL-BR11, an IgG_{2a} MAB) determined the optimal digestion conditions for producing F(ab)₂ fragments. There was a 70% yield of the F(ab)₂ fragment of DAL-BR6 when this MAB was digested at pH 3.5 for 4 hr using a pepsin:MAB protein ratio of 1:80. As shown in Figure 57 (pages 166-167), there was complete digestion of the parent MAB to the F(ab)₂ fragment after 1 to 4 hours of digestion. Digestion products also included very minimal amounts of lower molecular weight proteins including light and heavy chains of the IgG molecules. Also illustrated in Figure 57, longer digestion times under these conditions decreased the yield of the F(ab)₂ fragment and increased the amounts of light and heavy chain products. At this pH, pepsin:MAB ratio digestion conditions and digestion times, there was complete protein digestion of the other 3 MABs to lower molecular weight proteins (especially light and heavy chains) and there was no F(ab)₂ fragment yield.

However, changing the pH to 4.2 and the pepsin:MAB protein ratio to 1:120 resulted in the near complete digestion of DAL-BR7 to its F(ab)₂ fragment by 4 hr as shown in Figure 58 (pages 166, 168). The yield of the F(ab)₂ fragment was only 25% since there was again significant breakdown to light and heavy chains (also shown in Figure 58). Longer incubations completely digested DAL-BR7 but decreased the yield of the F(ab)₂ fragment. A similar F(ab)₂ fragment yield of 25% was obtained with

DAL-BR11 using the same digestion conditions as DAL-BR7 except for a longer digestion time period of 8 hr. Though DAL-BR11 was completely digested to breakdown products very easily when higher pepsin:protein ratios and lower pH conditions were used, this MAB was more resistant than DAL-BR7 to pepsin digestion when these milder conditions were used. As illustrated in Figure 59 (pages 166,169), even after 6 hours of digestion, there still was a significant amount of IgG remaining in addition to the F(ab)₂ fragment product. By 24 hours of digestion, there was complete digestion of DAL-BR11 to its F(ab)₂ fragment (also shown in Figure 59) but the yield was very low. To compromise, an 8 hour digestion time was used to prepare the F(ab)₂ fragment of this MAB. An additional interesting finding from the digestion studies of DAL-BR11 was that its F(ab)₂ fragment had a higher apparent molecular weight than the F(ab)₂ fragments of the other anti-HMC MABs studied and the standard F(ab)₂ fragment run on the same polyacrylamide gel (see Figure 59).

In contrast, treating DAL-BR9 with pepsin for 6 hr at pH 4.2 and at a pepsin:MAB protein ratio of 1:120 resulted in the near complete digestion of this MAB to the F(ab)₂ fragment but the yield was less than 10% since there was again significant breakdown to light and heavy chains. Incubations longer than 6 hr further decreased the yield of F(ab)₂. At all digestion times, as illustrated in Figure 60 (pages 166, 170), there was persistent breakdown of the MAB to light and heavy chains.

A photograph of an SDS-PAGE gel performed with purified F(ab)₂ fragments obtained from digesting larger amounts of these MABs under non reducing conditions is shown in Figure 61 (pages 166, 171).

FIGURES 57 TO 61:

FIGURES 57 TO 60: PHOTOGRAPHS OF SDS-PAGE GELS (RUN UNDER NON-REDUCING CONDITIONS) OF SAMPLES FROM PEPSIN DIGESTION STUDIES OF DAL-BR6, DAL-BR7, DAL-BR11 AND DAL-BR9.

FIGURE 61: PHOTOGRAPH OF AN SDS-PAGE GEL (RUN UNDER NON-REDUCING CONDITIONS) OF PURIFIED F(ab)₂ FRAGMENTS OF DAL-BR6, DAL-BR7, AND DAL-BR9.

FIGURE 57: RESULTS OF DAL-BR6

LANE 1 - 24 HR DIGESTION
 LANE 2 - 8 HR DIGESTION
 LANE 3 - 6 HR DIGESTION
 LANE 4 - 4 HR DIGESTION
 LANE 5 - 2 HR DIGESTION
 LANE 6 - 1 HR DIGESTION
 LANE 7 - 0 HR SAMPLE
 LANE 8 - MOL. WT. STDS.

NOTE:

A - IgG
 B - F(ab)₂
 C - OTHER PRODUCTS

FIGURE 58: RESULTS OF DAL-BR7

LANE 1 - 0 HR DIGESTION
 LANE 2 - 1 HR DIGESTION
 LANE 3 - 2 HR DIGESTION
 LANE 4 - 4 HR DIGESTION
 LANE 5 - 6 HR DIGESTION
 LANE 6 - 8 HR DIGESTION
 LANE 7 - 24 HR DIGESTION
 LANE 8 - MOL. WT. STDS.
 LANE 9 - F(AB)₂ MARKER

NOTE:

A - IgG
 B - F(ab)₂
 C - OTHER PRODUCTS

FIGURE 59: RESULTS OF DAL-BR11

LANE 1 - F(ab)₂ MARKER
 LANE 2 - 24 HR DIGESTION
 LANE 3 - 6 HR DIGESTION
 LANE 4 - 4 HR DIGESTION
 LANE 5 - 2 HR DIGESTION
 LANE 6 - BR6 F(ab)₂
 LANE 7 - 0 HR DIGESTION

NOTE:

A - IgG
 B - F(ab)₂ FROM DAL-BR11
 C - F(ab)₂ FROM OTHER MABS
 D - OTHER PRODUCTS

FIGURE 60: RESULTS OF DAL-BR9

LANE 1 - MOL. WT. STDS.
 LANE 2 - 0 HR DIGESTION
 LANE 3 - 1 HR DIGESTION
 LANE 4 - 2 HR DIGESTION
 LANE 5 - 4 HR DIGESTION
 LANE 6 - 6 HR DIGESTION
 LANE 7 - 8 HR DIGESTION
 LANE 8 - 24 HR DIGESTION
 LANE 9 - F(ab)₂ MARKER
 LANE 10 - BSA MARKER
 LANE 11 - 0 HR DIGESTION

NOTE:

A - IgG
 B - F(ab)₂
 C - OTHER PRODUCTS

FIGURE 61: PURIFIED F(ab)₂ FRAGMENTS OF DAL-BR6, BR7, AND BR9

LANE 1 - DAL-BR6 F(ab)₂
 LANE 2 - DAL-BR7 F(ab)₂
 LANE 3 - DAL-BR9 F(ab)₂
 LANE 4 - BSA

LANE 5 - DAL-BR6
 LANE 6 - DAL-BR7
 LANE 7 - DAL-BR9

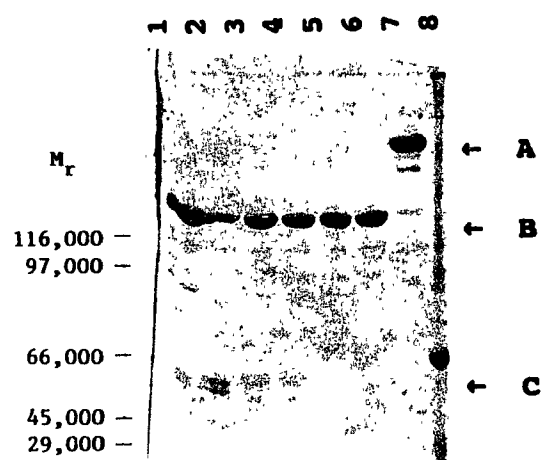


FIGURE 57

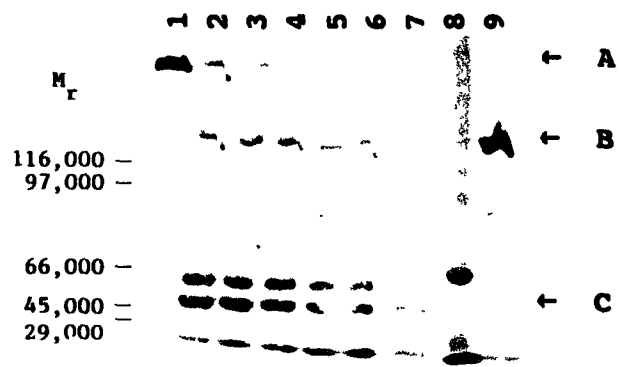


FIGURE 58

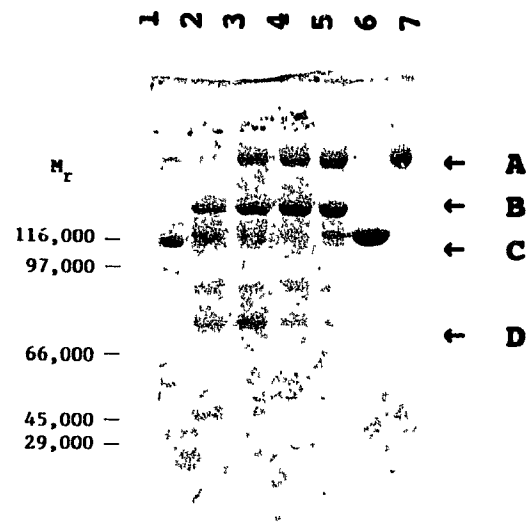


FIGURE 59

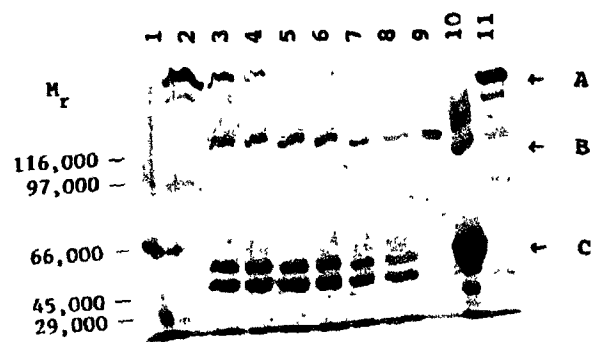


FIGURE 60

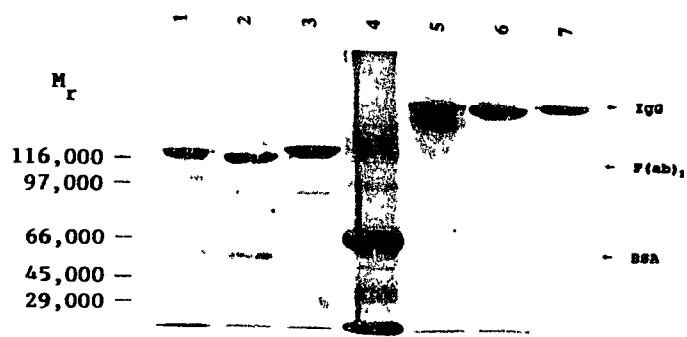


FIGURE 61

PART 8

LOCALIZATION OF RADIOLABELED ANTI-HMC MABS AND THEIR F(ab)₂ FRAGMENTS IN TUMOR XENOGRAFTS

A series of experiments was done to evaluate the biodistribution and tumor localization ability of several radiolabeled anti-HMC MABs or their F(ab)₂ fragments in tumor-xenografted nude mice. In one set of experiments, ¹³¹I-labeled MABs including DAL-BR5, DAL-BR6, DAL-BR7, DAL-BR9, and DAL-BR11 (produced with the chloramine-T method) as well as ¹³¹I-labeled F(ab)₂ fragments of DAL-BR6 and DAL-BR7 (also produced with the chloramine-T method) were evaluated in nude mice xenografted with the HMC cell line, HTB-19. The rationale for choosing these MABs from the panel of 11 available anti-HMC MABs was to evaluate a group of MABs that reacted well with HTB-19 cells (as determined by ELISA titer of MAB reactivity to HTB-19 cells). At the same time, it was reasonable to include MABs in this group which were directed to antigens located at different cellular or extracellular sites (i.e. cell surface and cytosol). In each of these experiments, a subclass-matched (whenever possible or class matched otherwise) non-tumor specific MAB labeled with ¹²⁵I was always used to determine the specificity index of localization (or SPIL) ratio of each MAB (as described below). Using the same HMC xenograft model, the effect of injecting a combination of two radiolabeled tumor-specific MABs (¹³¹I-labeled DAL-BR7 with either ¹²⁵I-labeled DAL-BR6 or DAL-BR9) was also evaluated to determine if one could achieve additive tumor localization in vivo of pairs of MABs

that react with same or different target antigens on tumor cells. In addition, the same nude mouse tumor model was used to evaluate the tumor localization ability of DAL-BR6 labeled with ^{131}I using the PIB method and with ^{125}I using the chloramine-T method.

In another experiment, nude mice xenografted with Caki-1 cells were used to evaluate the tumor localization ability of ^{131}I -labeled DAL-BR7 which was shown earlier to react with this RCC cell line by immunofluorescence. DAL-B01 radiolabeled with ^{125}I was used as the non-tumor specific MAB in this experiment. The purpose of this study was to determine if the anti-HMC MAB DAL-BR7 could localize in vivo to a solid renal cell tumor composed of cells which react in vitro with this MAB. Furthermore, the tumor localization ability of radiolabeled MABs DAL-BR7 and K45 (which is also specific for Caki-1 cells) used in combination was evaluated in this RCC tumor model to determine if one could achieve additive tumor localization in vivo of 2 MABs that react with different antigens on tumor cells. Still in other experiments, radiolabeled DAL-BR7 and DAL-BR6 were respectively used in experiments with nude mice xenografted with M21 melanoma cells to evaluate their respective tumor localization ability in this tumor model. Both these MABs were shown previously by immunofluorescence to react with cultured M21 cells. The purpose of this study was again to determine if these anti-HMC MABs could localize in vivo to a solid melanoma tumor composed of cells which react in vitro with these MABs.

The nude mice used for experiments involving MABs or F(ab)_2 fragments had

subcutaneous tumor xenografts in the left or right flank of the animals. The tumor sizes were 0.5 to 1.0 cm in diameter when the experiments were conducted. Groups of tumor-xenografted nude mice were scanned daily with a gamma camera and sacrificed at 1, 2, 3, or 6 days post-injection as indicated. The results from all the experiments described above will now be presented consecutively and will be illustrated in Figures 62 to 143 starting on page 177.

These figures show 5 types of plot obtained from analyzing radioactivity data from the experiments. The first type of plot is the total body radioactivity counts of mice (in uCi) taken daily post-injection which was then corrected for the natural decay of ^{131}I (half-life of 8 days) and plotted on the y-axis against time post-injection in days on the x-axis. Analysis of data from the appropriate experiments with curve fitting computer programs revealed the pattern of clearance of radioactivity from the animals over time approached a theoretical exponential decline starting from the given injected dose. These plots present the experimentally derived mean total body radioactivity counts obtained from six mice in each experiment (\pm the standard error of the mean) at indicated times. On the same plots, the best exponential decline curve fit based on the data is also shown. From these plots, the biological half-life of intravenously injected ^{131}I -labeled MABs or F(ab)_2 fragments can be determined.

The second type of plot is a bar graph whose y-axis shows the amount of radioactivity found in each organ or tissue and tumor (in uCi per gram tissue) obtained from groups of mice sacrificed at stated times post-injection and whose x-axis shows the tissues that were removed from the sacrificed mice, weighed and then counted in

a gamma counter. The x-axis shows abbreviations of the tissues which correspond to the following: HE=HEART; LU=LUNG; LI=LIVER; SP=SPLEEN; KI=KIDNEYS; MU=MUSCLE; BO=BONE; BR=BRAIN; BL=BLOOD; and TU=TUMOR. In the experiment comparing the PIB and chloramine-T methods of radiolabeling DAL-BR6, another tissue (NE=NECK) was also counted for radioactivity to assess the amount of iodine localized in the thyroid gland of these animals which did not receive Lugol's iodine prior to injection.

The third type of plot is the percentage of the injected radioactive dose of each MAB or F(ab)₂ fragment per gram tissue that localized at stated times post-injection (values on the y-axis) to each tissue indicated on the x-axis. The fourth type of plot is the tumor to normal tissue (or T/N) ratios obtained at stated times post-injection (values on the y-axis) of the tissues indicated on the x-axis. For all experiments except for the one comparing the PIB and chloramine-T methods, the T/N ratio for brain has been excluded from the plots since this ratio in each of these experiments far exceeded the presented y-axis scale in the T/N ratio plots. Inclusion of the T/N ratio for brain in these plots would have therefore obscured the more important ratios obtained for other tissues which had ratios that fell in a lower range of the y-axis scale. The fifth type of plot is the specificity index of localization (or SPIL) ratio of each MAB or F(ab)₂ fragment at stated times post-injection (values on the y-axis) of the tissues indicated on the x-axis. The SPIL ratio is a ratio of the T/N ratio for the distribution of the ¹³¹I-labeled tumor-specific MAB or F(ab)₂ fragment to the T/N ratio for the distribution of an irrelevant MAB or F(ab)₂ fragment labeled with ¹²⁵I.

1. In vivo Localization of DAL-BR5 in HTB-19 Xenografts

On average, 43 uCi (linked to 13.3 ug) of ¹³¹I-labeled DAL-BR5 along with 2 uCi (linked to 12.9 ug) of ¹²⁵I-labeled DAL-B02 were injected into each HTB-19 xenografted mouse. Figure 62 shows the clearance of injected DAL-BR5 from groups of mice over time. The biological half-life for radiolabeled DAL-BR5 based on these data is 1.8 days. Figures 63 and 64 respectively show the amount of DAL-BR5 that localized in each tissue and the corresponding percentage of the injected dose that localized in each tissue. Approximately 1% of the injected dose localized in the tumor at day 3 and this level persisted at day 6. Only the % of the injected dose that remained in the blood at day 3 and day 6 and localized in the lung at day 3 exceeded the % of the injected dose that localized in the tumor on these days. Figures 65 and 66 respectively show the T/N ratios and SPIL ratios for DAL-BR5. The T/N ratios were all >2 by day 6 for all tissues except blood which had a ratio <1 and lung which had a ratio >1.5. The T/N ratio of each tissue at day 6 was also approximately twice the ratio at day 3. The SPIL ratios at day 6 were >1 but <1.5 for most tissues. While a few tumors were visible with gamma camera imaging through variable amounts retained total body radioactivity at day 3 (Figure 67), very distinct tumor images were obtained at day 6 with virtually no background radioactivity (Figure 68).

FIGURES 62 TO 68:

DATA OBTAINED FROM INJECTING A MIXTURE OF ^{131}I -LABELED DAL-BR5 AND ^{125}I -LABELED DAL-B02 I.V. INTO NUDE MICE XENOGRAFTED WITH HTB-19 CELLS. FIGURES 67 AND 68 ARE GAMMA CAMERA IMAGES RESPECTIVELY AT 3 AND 6 DAYS POST-INJECTION.

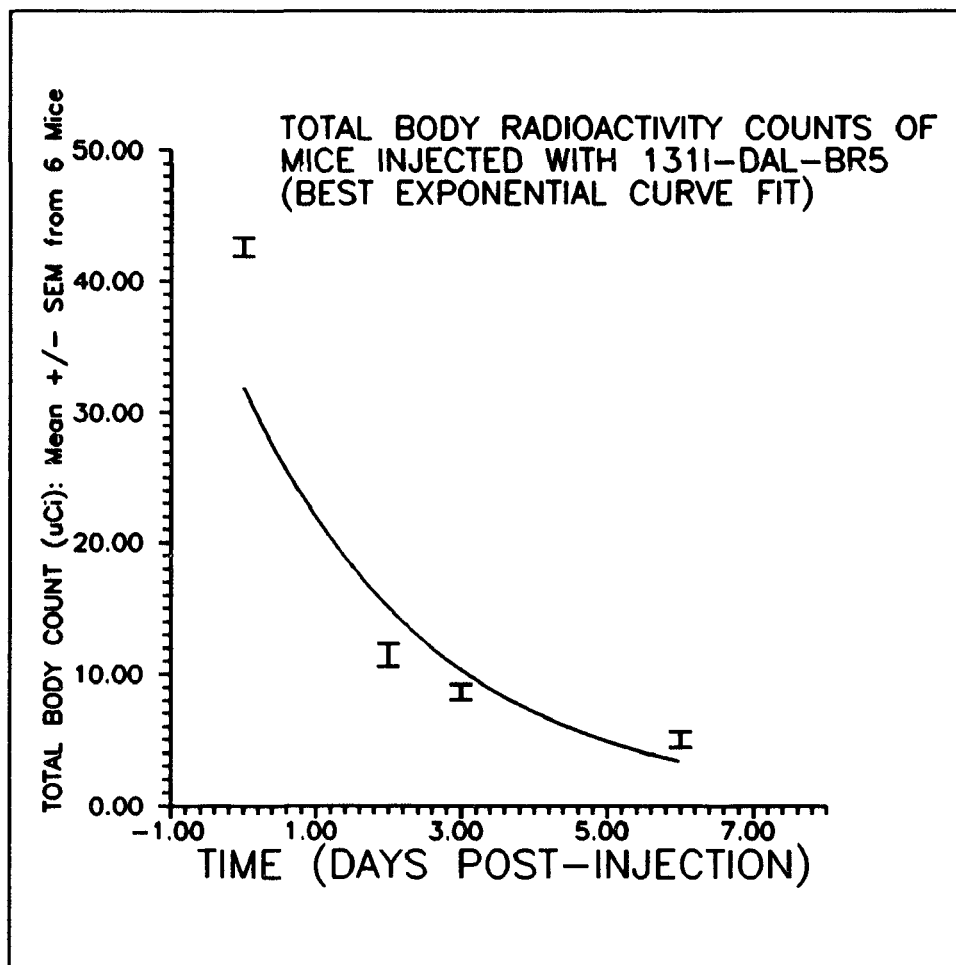


FIGURE 62

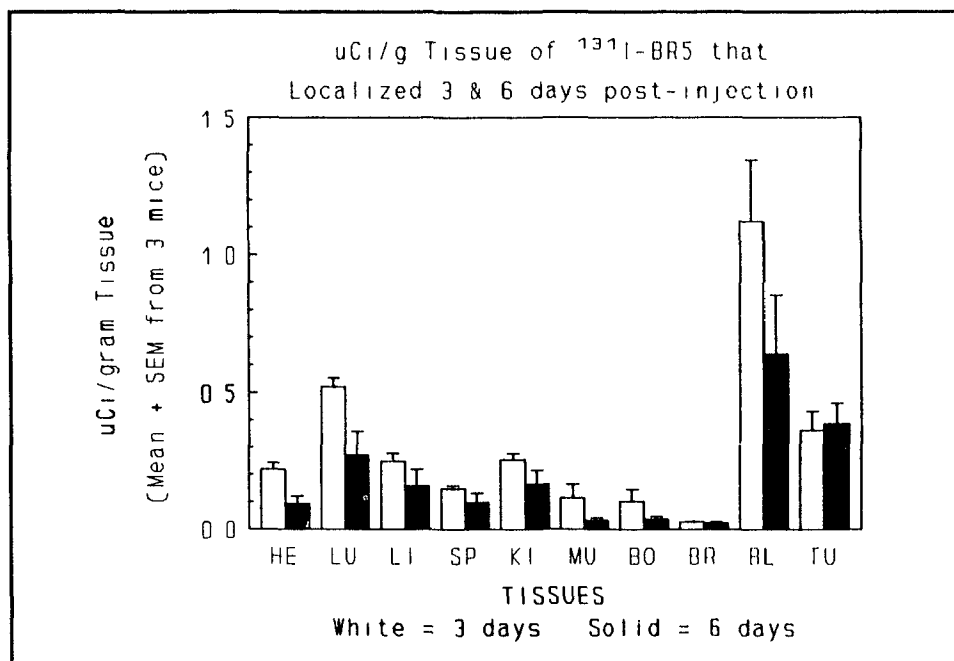


FIGURE 63

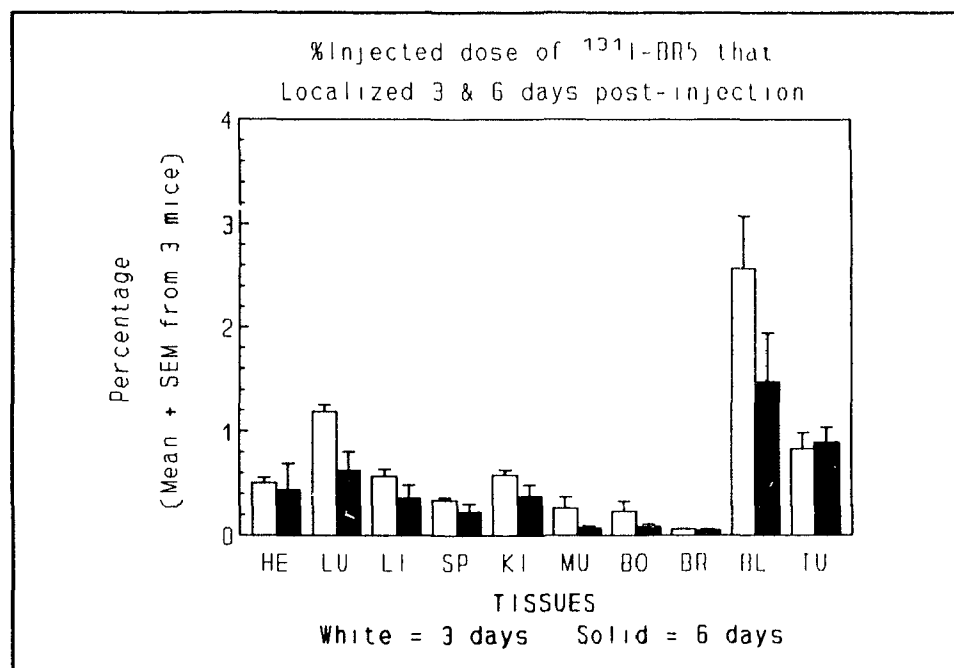
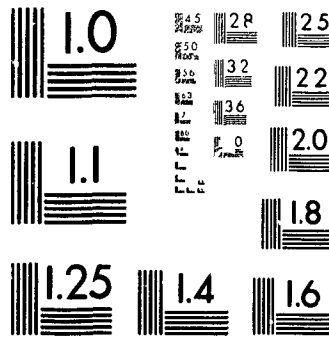


FIGURE 64

3

PM-1 3½"x4" PHOTOGRAPHIC MICROCOPY TARGET
NBS .010a ANSI/ISO #2 EQUIVALENT



PRECISIONSM RESOLUTION TARGETS

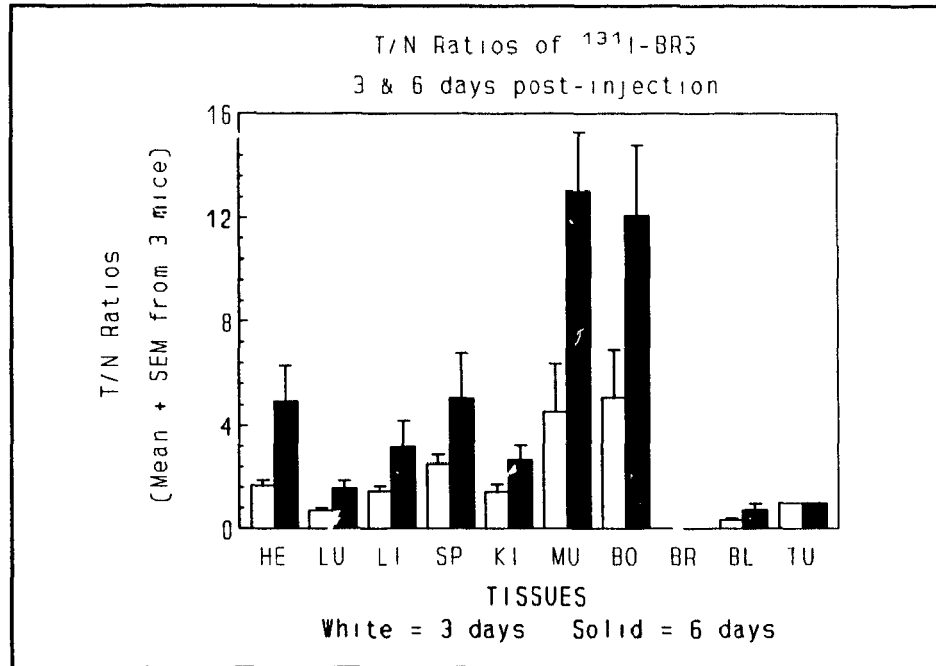


FIGURE 65

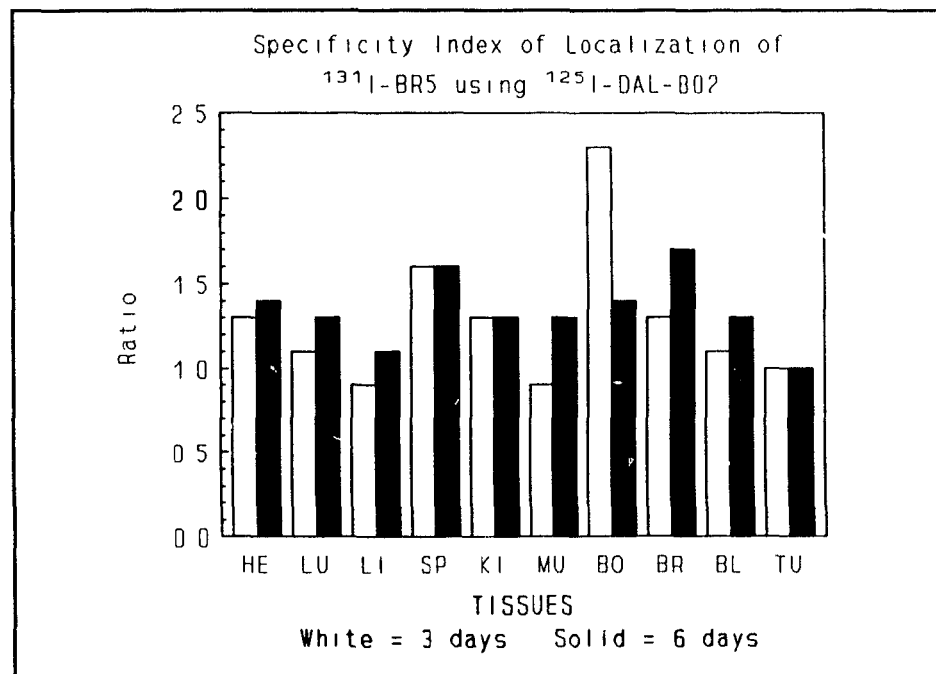


FIGURE 66

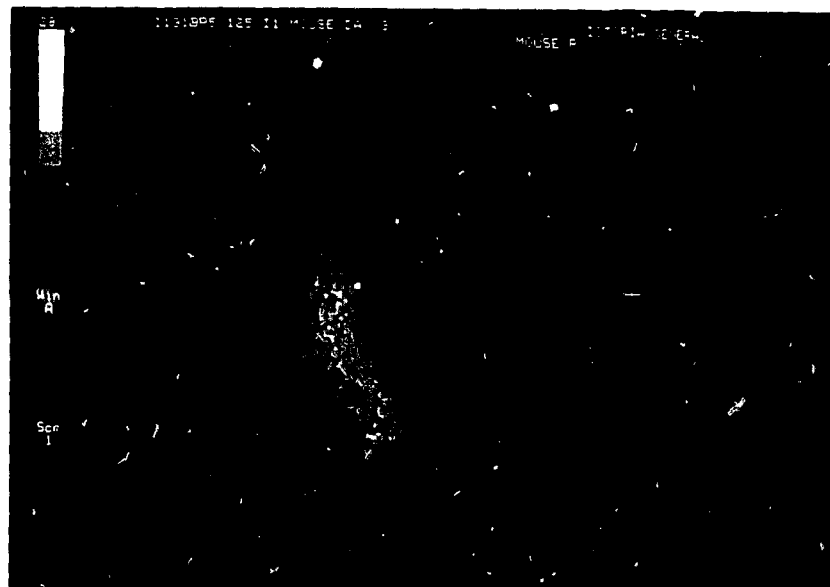


FIGURE 67

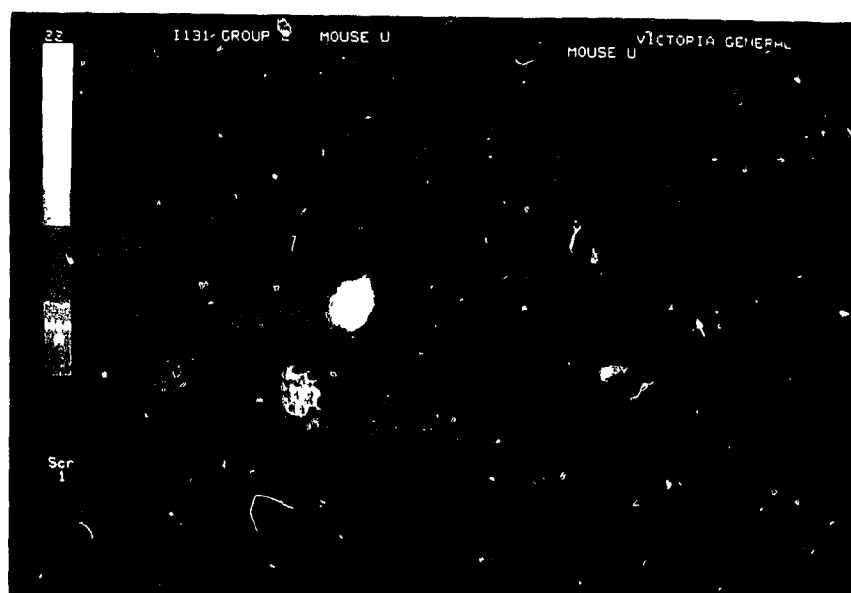


FIGURE 68

2. In vivo Localization of DAL-BR6 in HTB-19 Xenografts

Approximately 42 uCi (linked to 8 ug) of ^{131}I -labeled DAL-BR6 along with 2 uCi (linked to 7.7 ug) of ^{125}I -labeled DAL-B02 were injected into each mouse. Figure 69 shows the clearance of radiolabeled DAL-BR6 from groups of mice over time. The biological half-life of DAL-BR6 based on these data is 1.6 days. Figures 70 and 71 respectively present the amount of DAL-BR6 that localized in each tissue and the corresponding percentage of the injected dose that localized in the same tissues. Approximately 1.3% of the injected dose of DAL-BR6 localized in tumor at day 3 but this percentage decreased to 0.7% at day 6. On both these days however, the percentage of the injected dose of DAL-BR6 that localized in tumor was more than that localized in all other tissues except blood. Figure 72 shows that the T/N ratios of DAL-BR6 for all tissues except blood were near or > 3 on both day 3 and day 6. The SPIL ratios of DAL-BR6 were > 1 but < 2 for most tissues as shown in Figure 73. These mice were unfortunately scanned with a gamma camera equipped with a wide field of view collimator unlike the mice injected with DAL-BR5 (as described in the previous section) which were scanned with a gamma camera equipped with a pinhole collimator. The gamma camera images of mice injected with radiolabeled DAL-BR6 did not locate the tumor xenografts due to the extensive background whole body radioactivity that interfered with and overshadowed the image of the tumor even at day 6.

FIGURES 69 TO 73:

DATA OBTAINED FROM INJECTING A MIXTURE OF ^{131}I -LABELED DAL-BR6
AND ^{125}I -LABELED DAL-B02 I.V. INTO NUDE MICE XENOGRAFTED WITH
HTB-19 CELLS.

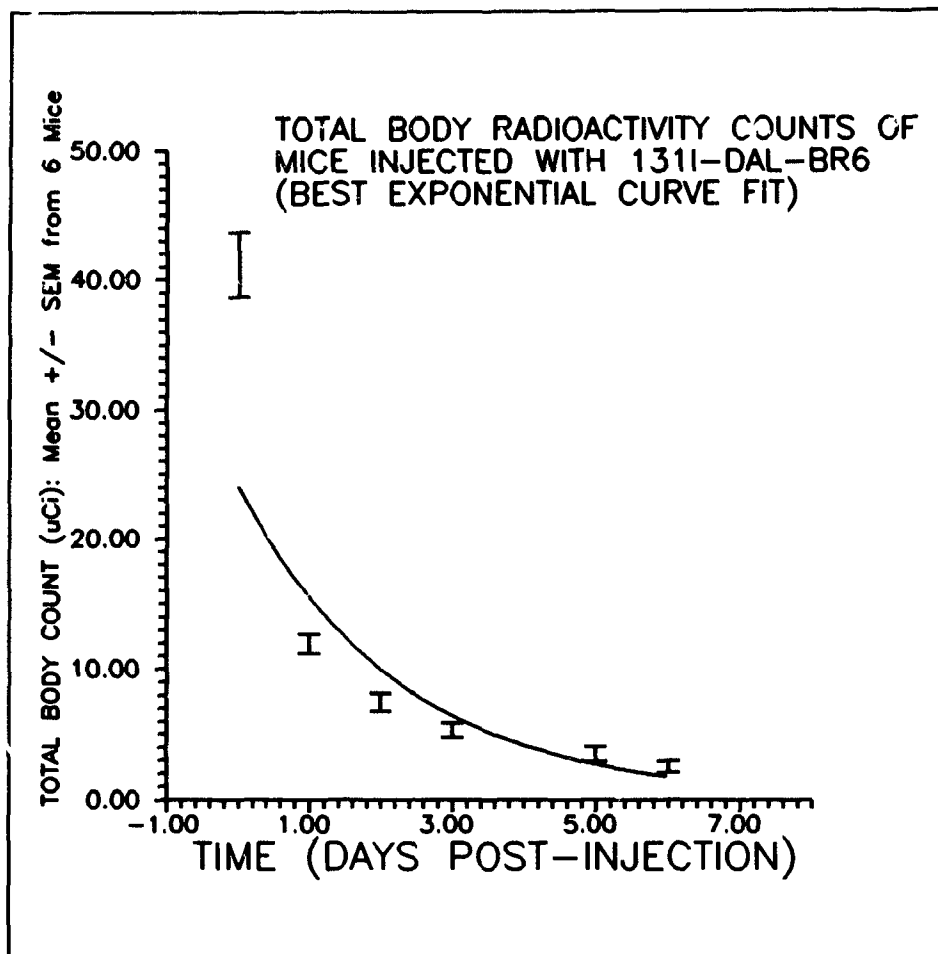


FIGURE 69

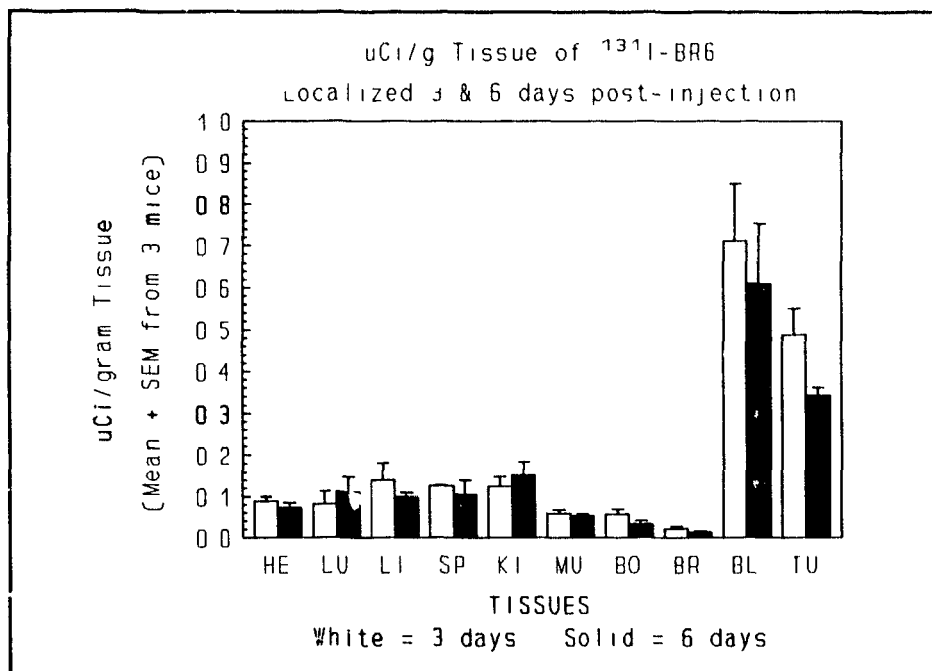


FIGURE 70

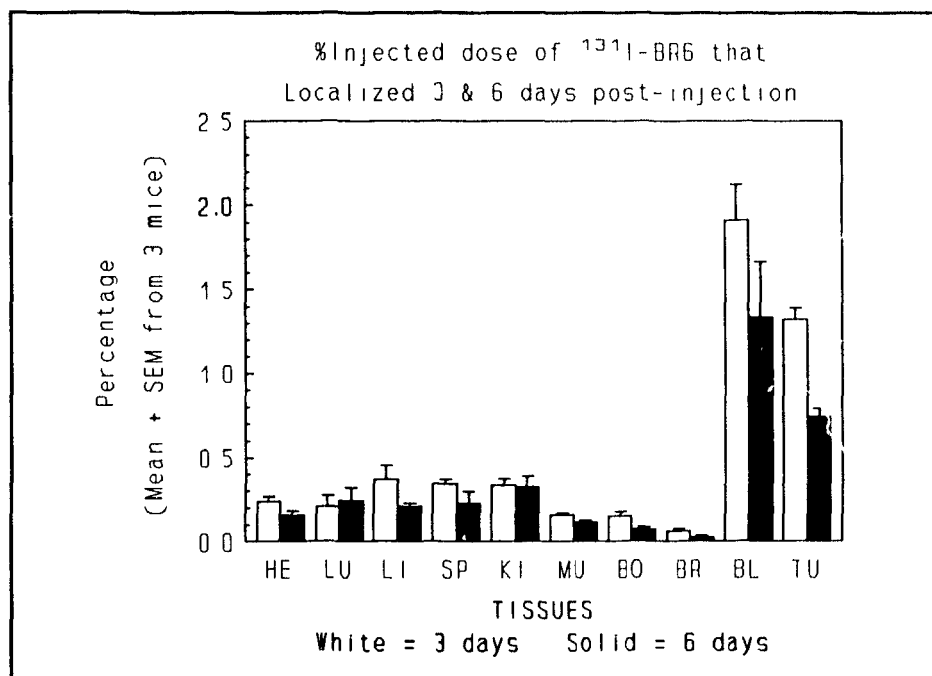


FIGURE 71

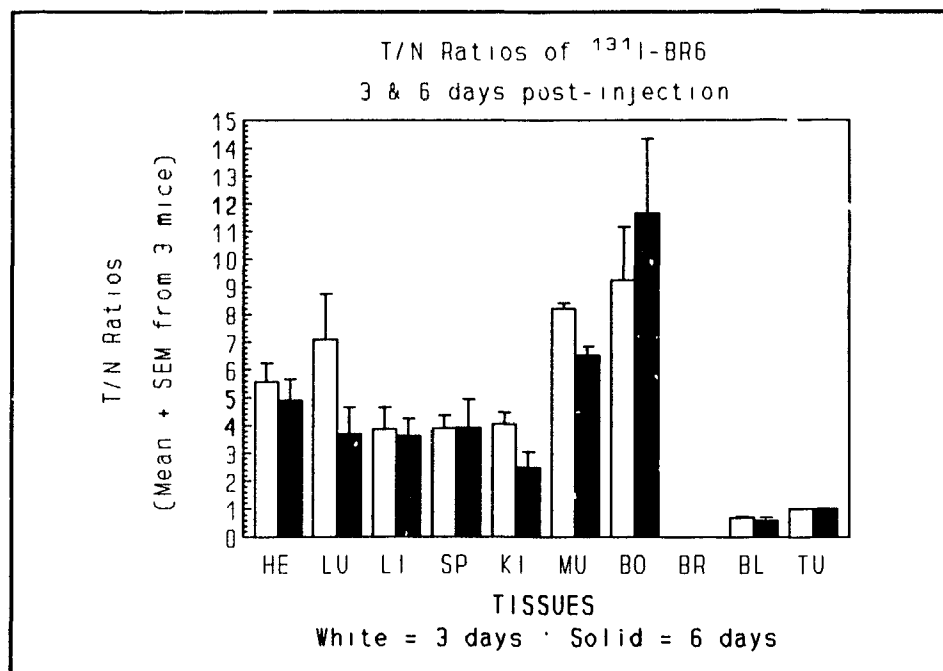


FIGURE 72

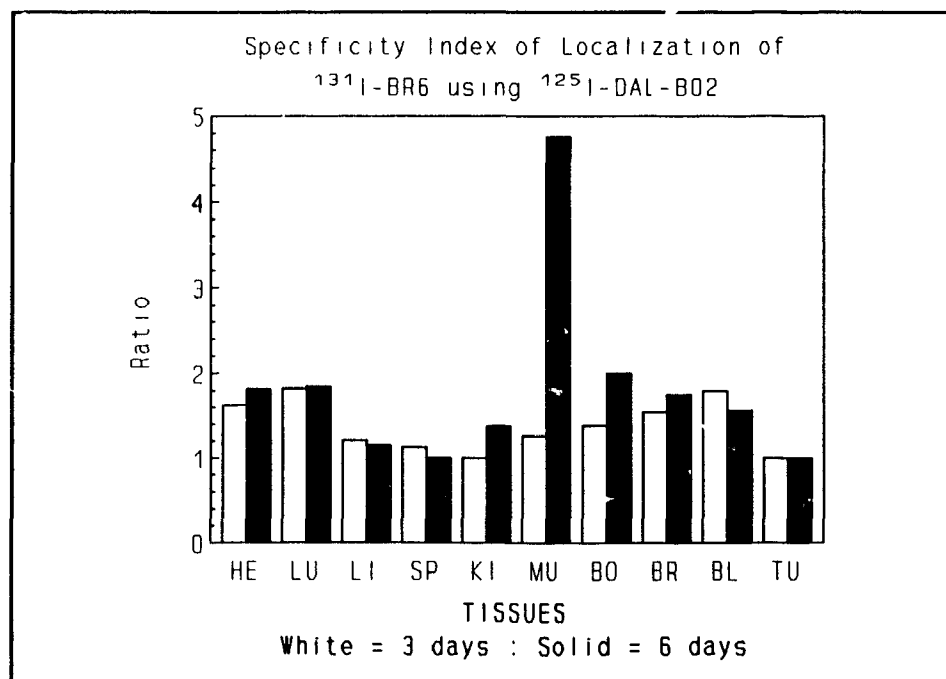


FIGURE 73

3. In vivo Localization of DAL-BR7 in HTB-19 Xenografts

Each tumor-xenografted mouse was injected with approximately 52 uCi of ¹³¹I-labeled DAL-BR7 and 2 uCi of ¹²⁵I-labeled DAL-B02 (each labeled MAB corresponding to 10 ug of protein). Figure 74 shows the clearance of radiolabeled DAL-BR7 from the injected mice over time. The biological half-life of i.v. injected DAL-BR7 based on these data is 2 days. Figures 75 and 76 respectively show the amount of DAL-BR7 that localized in each tissue and the corresponding percentage of the injected dose of DAL-BR7 that localized in the same tissues. There was 2.1% of the injected dose of DAL-BR7 that localized in tumor at day 3 but at day 6, the percentage of the injected dose that localized in tumor fell to 1.5%. Like DAL-BR6, a lower percentage of the injected dose of DAL-BR7 localized in all other tissues except blood at day 3 and day 6 than had localized in the tumor. Figures 77 and 78 respectively show the T/N ratios and SPIL ratios for the tissues. Like DAL-BR6, DAL-BR7 had T/N ratios near or >2 for all tissues except blood at day 3 and day 6 as well as SPIL ratios >1 but <1.5 for most tissues. At day 6, there was still a considerable amount of radioactivity remaining in the mice, 3-4 times the amount left in the mice injected with DAL-BR6 as described previously. Possible reasons for this high background radioactivity at day 6 were that each mouse received about 10 uCi more than the amount used in the experiment with DAL-BR6 and that i.v. injected DAL-BR7 had a longer biological half-life than DAL-BR6. The gamma camera images of tumors in these mice were obscured but still could be visualized. Better gamma camera images of tumors obtained with DAL-BR7 will be presented later.

FIGURES 74 TO 78:

DATA OBTAINED FROM INJECTING A MIXTURE OF ^{131}I -LABELED DAL-BR7
AND ^{125}I -LABELED DAL-B02 I.V. INTO NUDE MICE XENOGRAFTED WITH
HTB-19 CELLS.

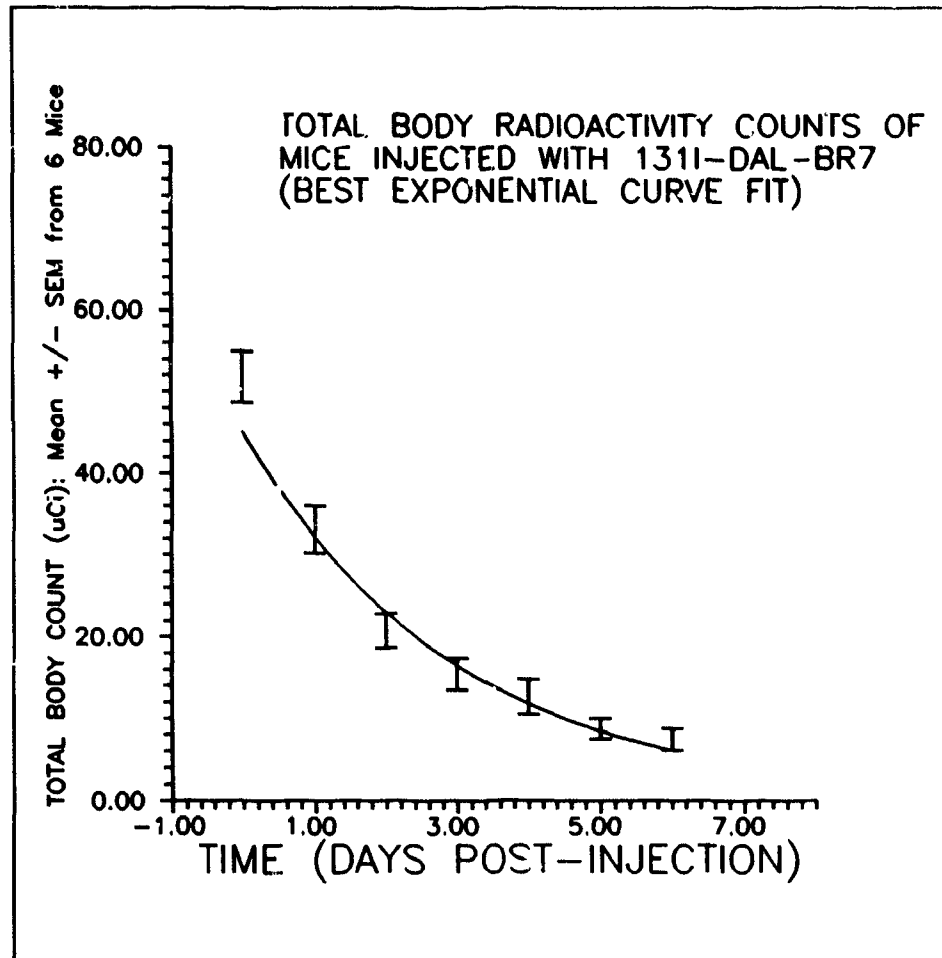


FIGURE 74

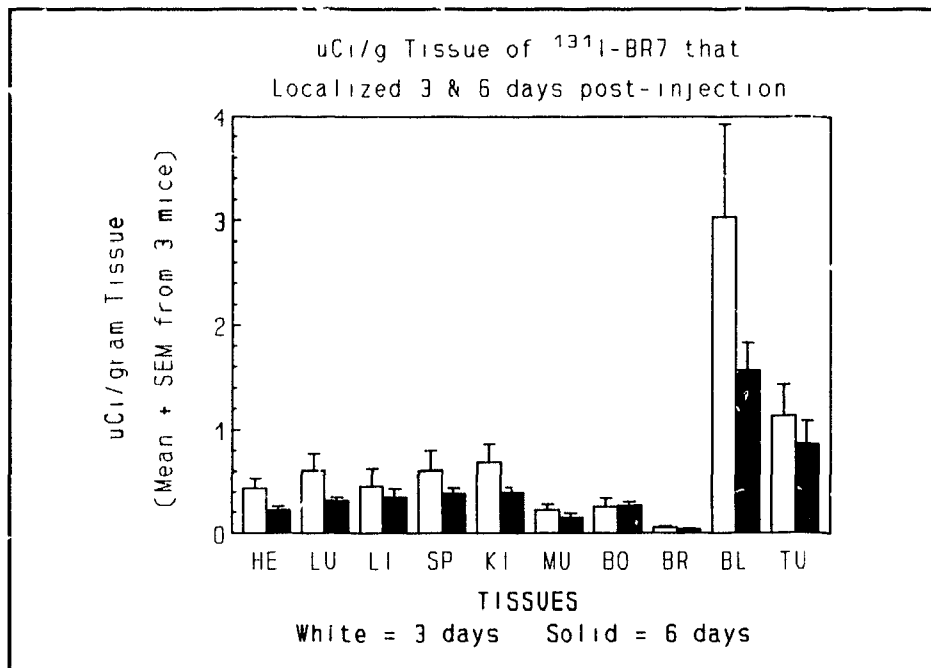


FIGURE 75

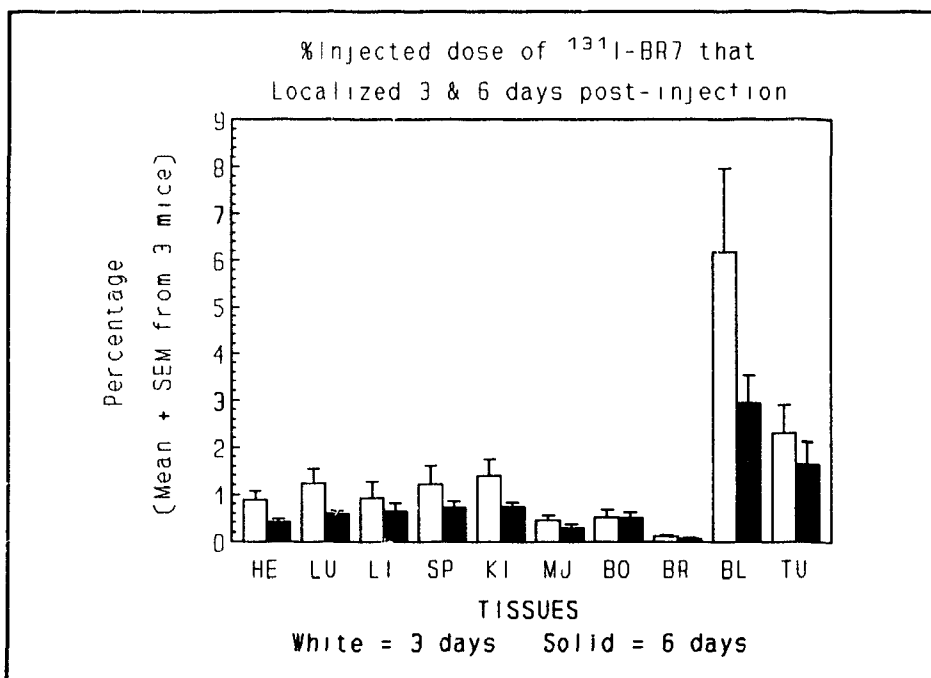


FIGURE 76

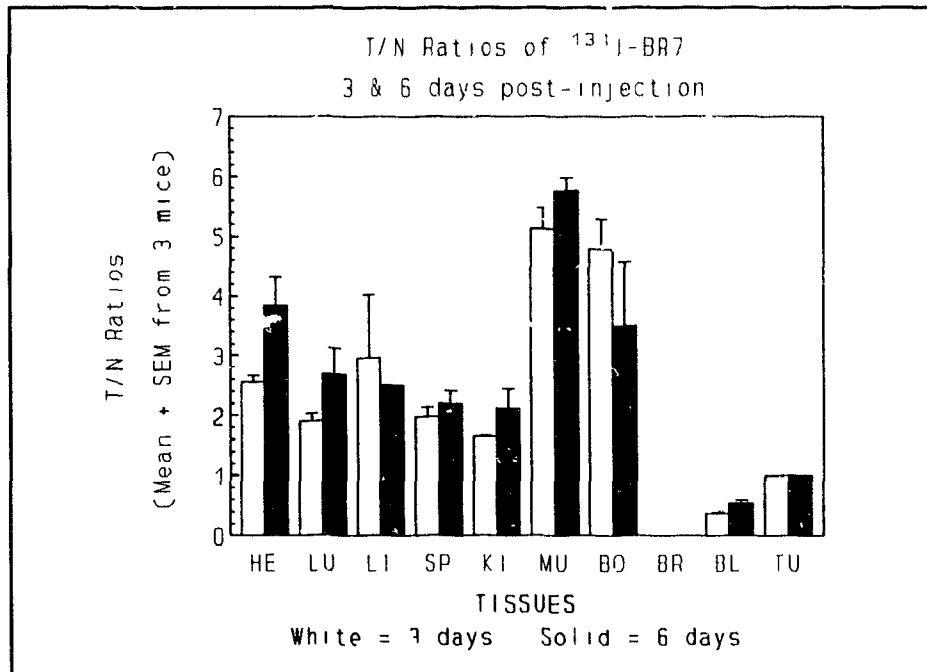


FIGURE 77

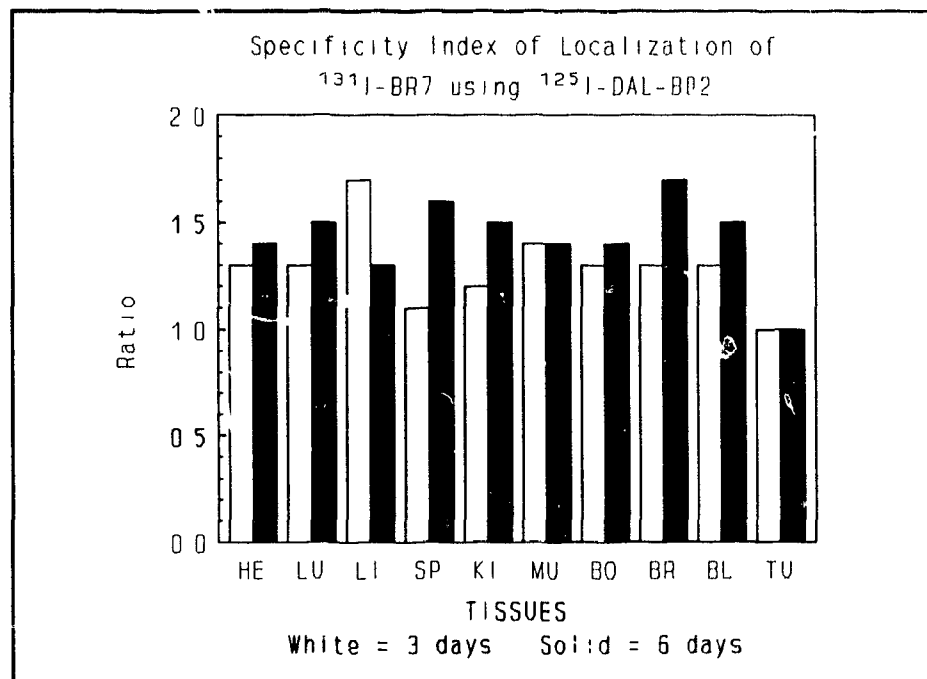


FIGURE 78

4. In vivo Localization of DAL-BR9 in HTB-19 Xenografts

On average, each mouse was injected i.v. with 30 uCi of ^{131}I linked to 16 ug of DAL-BR9 and with 2 uCi of ^{125}I linked to 15.4 ug of DAL-B02. The clearance of radioactivity from groups of mice is presented in Figure 79. The biological half-life of radiolabeled DAL-BR9 injected i.v. based on these data is 2.6 days. Figures 80 and 81 respectively show the amount of DAL-BR9 that localized in each tissue and the corresponding percentage of injected dose that localized in the same tissues. There was approximately 3-4% of the injected dose of DAL-BR9 that localized in tumor at day 3 and day 6. This percentage of injected dose that localized in tumor was the highest attained in all the experiments that investigated tumor localization with MABs. Figures 82 and 83 respectively show the T/N ratios and the SPIL ratios of DAL-BR9 for the tissues. The T/N ratios of DAL-BR9 were equal to or >2 for all tissues except blood both on day 3 and day 6. However, higher T/N ratios were observed on day 6. The SPIL ratios of DAL-BR9 were all >1 but <2 for all tissues. Gamma camera images obtained both at day 3 and day 6 revealed distinct tumor images but were much clearer on day 6 even though there was still some residual background body radioactivity (Figure 84).

FIGURES 79 TO 84:

DATA OBTAINED FROM INJECTING A MIXTURE OF ^{131}I -LABELED DAL-BR9 AND ^{125}I -LABELED DAL-B02 I.V. INTO NUDE MICE XENOGRAFTED WITH HTB-19 CELLS. FIGURE 84 IS A GAMMA CAMERA IMAGE AT 6 DAYS POST-INJECTION.

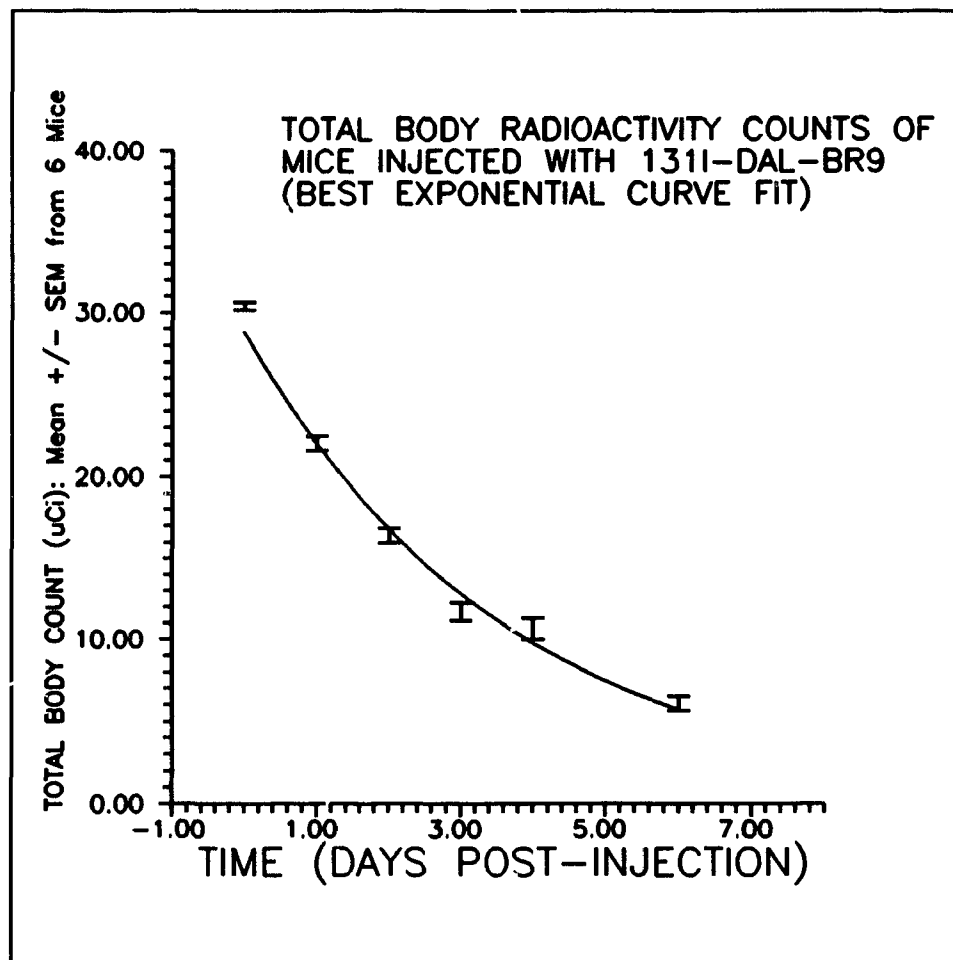


FIGURE 79

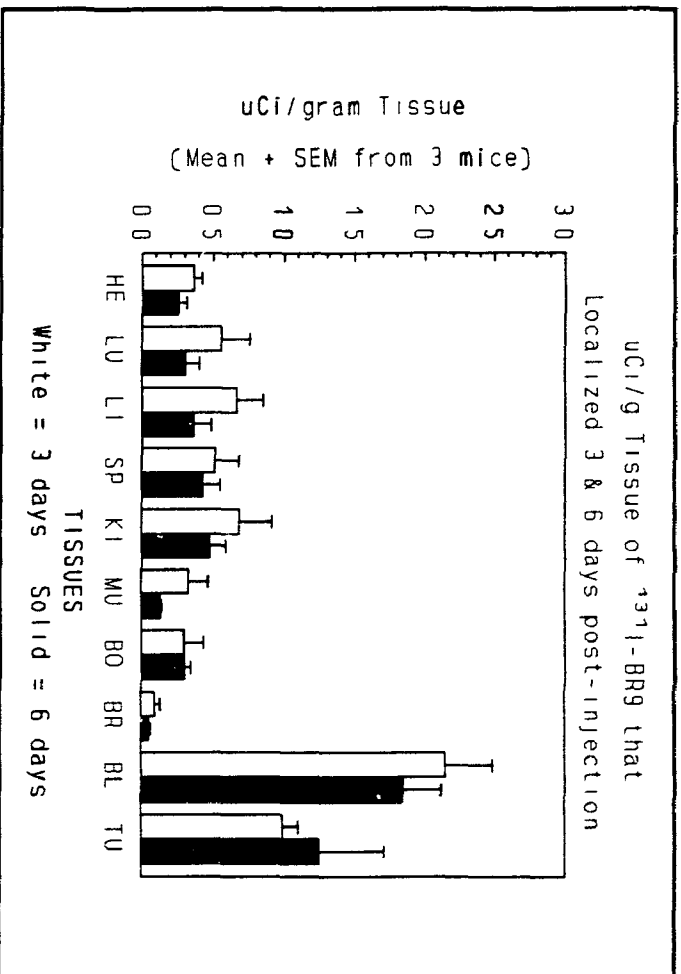


FIGURE 80

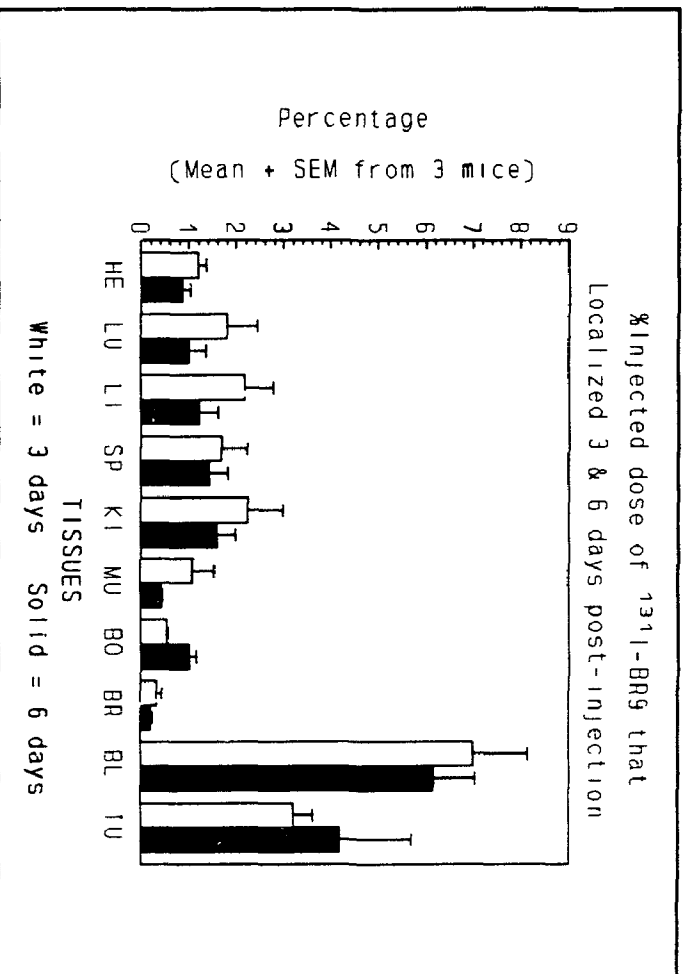


FIGURE 81

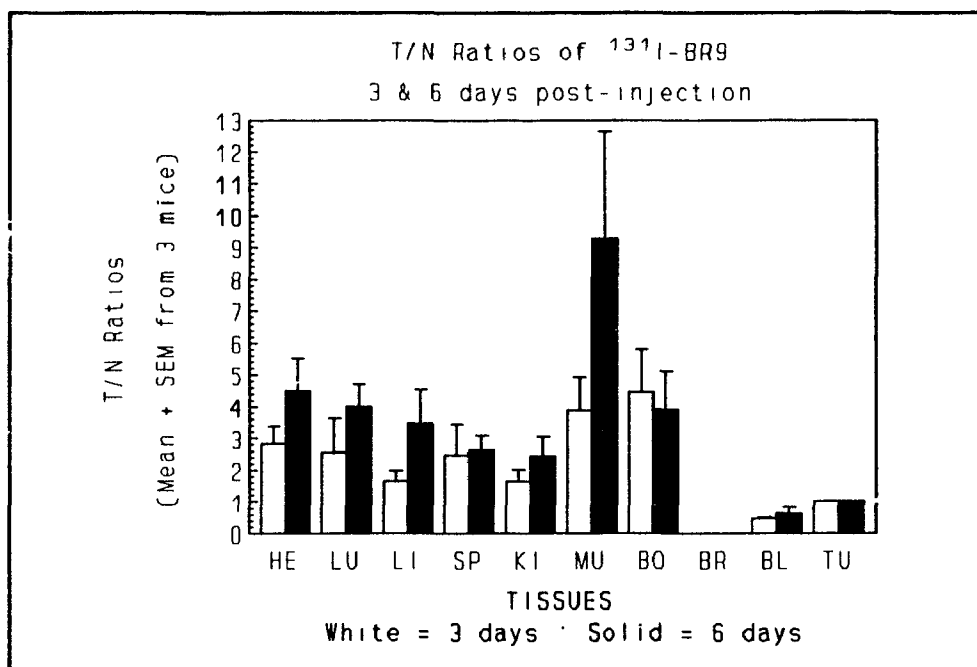


FIGURE 82

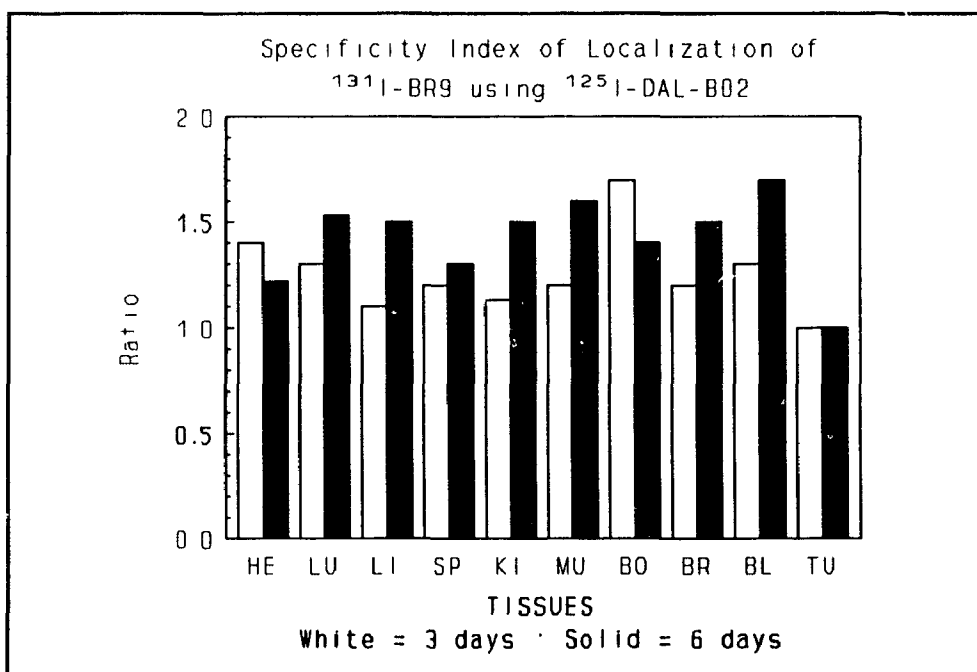


FIGURE 83



FIGURE 84

5. In vivo Localization of DAL-BR11 in HTB-19 Xenografts

Each mouse in this experiment was injected i.v. with approximately 58 uCi of ¹³¹I-labeled DAL-BR11 and 9 uCi of ¹²⁵I-labeled DAL-B01. The corresponding amount of protein of both MABs injected was 20 ug. Figure 85 shows the clearance of radioactivity from these animals over time. The biological half-life of i.v. injected radiolabeled DAL-BR11 based on these data was 1.8 days. The amount of DAL-BR11 that localized in tissues and the percentage of the injected dose of DAL-BR11 that localized in the same tissues are respectively presented in Figures 86 and 87. Like DAL-BR5, approximately 1% of the injected dose of DAL-BR11 localized in tumor at day 3 and day 6. Also like DAL-BR5, the amount of DAL-BR11 that localized in all tissues except blood and lung was much less than that localized to tumor at both day 3 and day 6. Figures 88 and 89 respectively present the T/N ratios and SPIL ratios of DAL-BR11 for the tissues. For all tissues except blood and lung, the T/N ratios of DAL-BR11 were all near 2 by day 6 which again was similar to the T/N ratios observed for DAL-BR5. However, unlike DAL-BR5 which had T/N ratios at day 6 greater than at day 3, the T/N ratios of DAL-BR11 at day 6 were only slightly higher than the ratios at day 3 for most tissues. The SPIL ratios of DAL-BR11 were either 1 or <1 for most tissues. The gamma camera images of mice using a pinhole collimator revealed tumor-localized radioactivity at both 3 days and 6 days post-injection. However at day 3, the mice had little remaining background body radioactivity in contrast to mice in other studies using different MABs. The tumor images were also more intense and distinct at day 3 (Figure 90) than at day 6.

FIGURES 85 TO 90:

DATA OBTAINED FROM INJECTING A MIXTURE OF ^{131}I -LABELED DAL-BR11 AND ^{125}I -LABELED DAL-B01 I.V. INTO NUDE MICE XENOGRAFTED WITH HTB-19 CELLS. FIGURE 90 IS A GAMMA CAMERA IMAGE AT 3 DAYS POST-INJECCION .

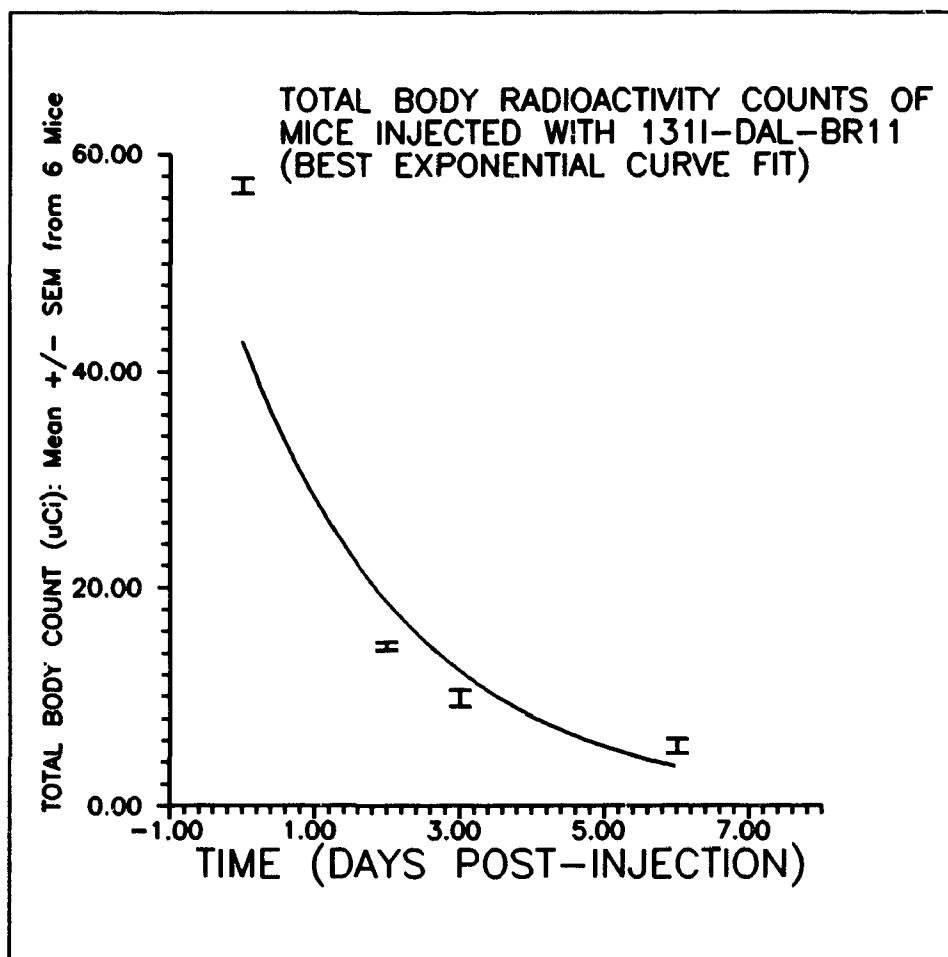


FIGURE 85

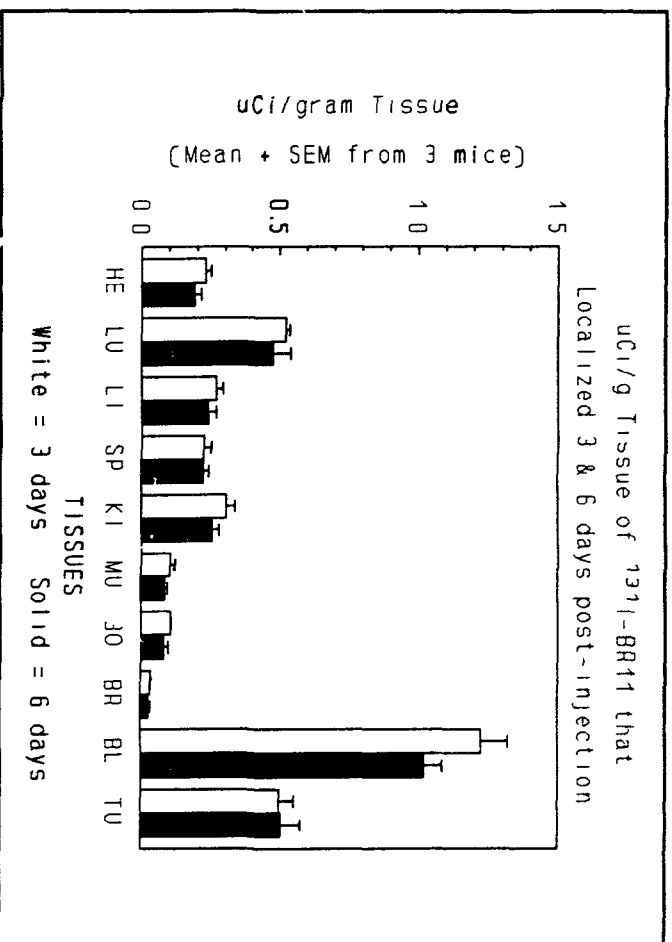


FIGURE 86

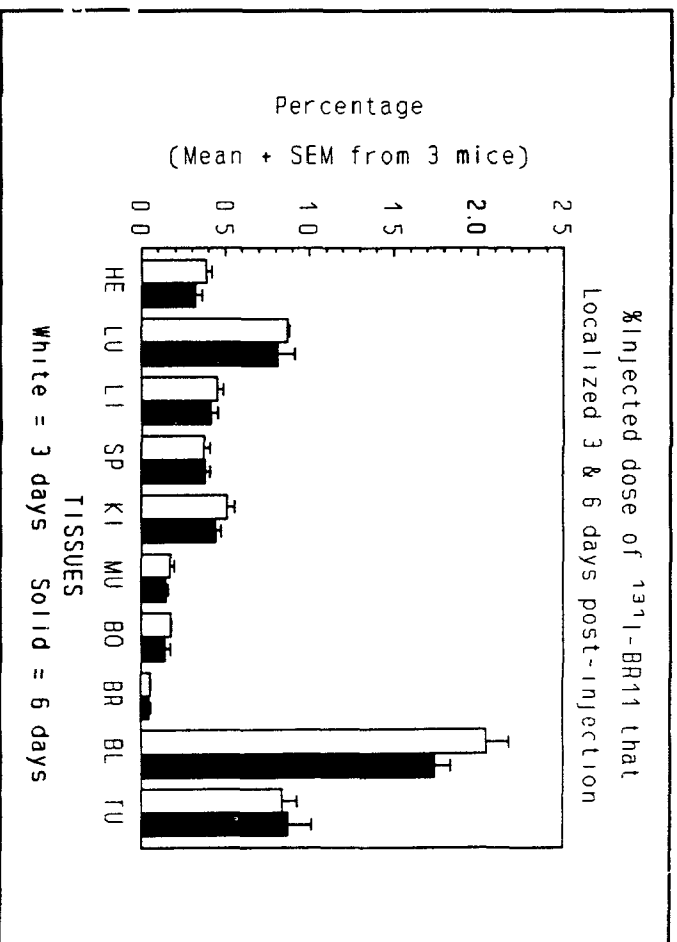


FIGURE 87

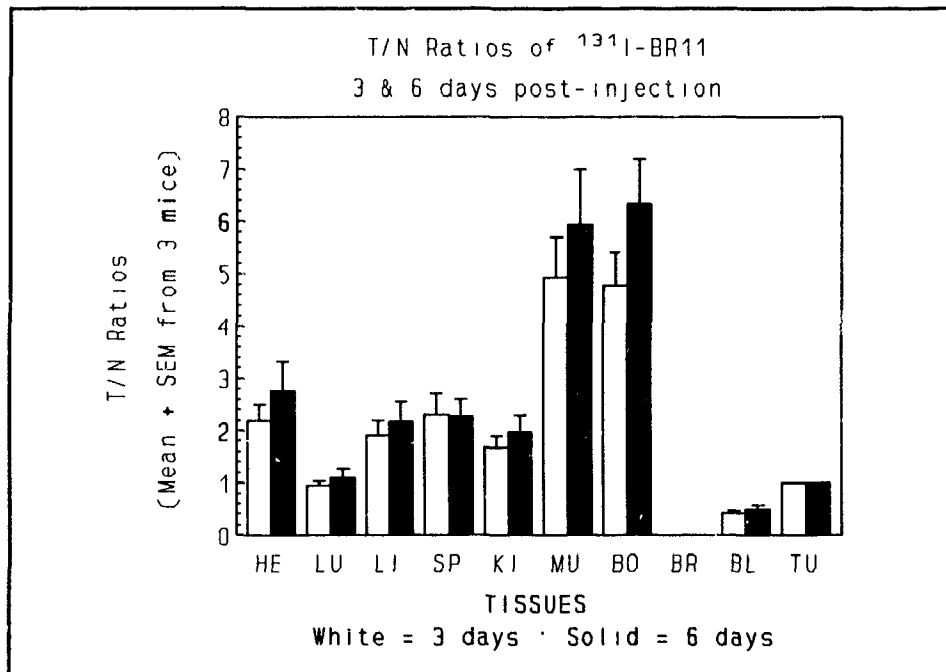


FIGURE 88

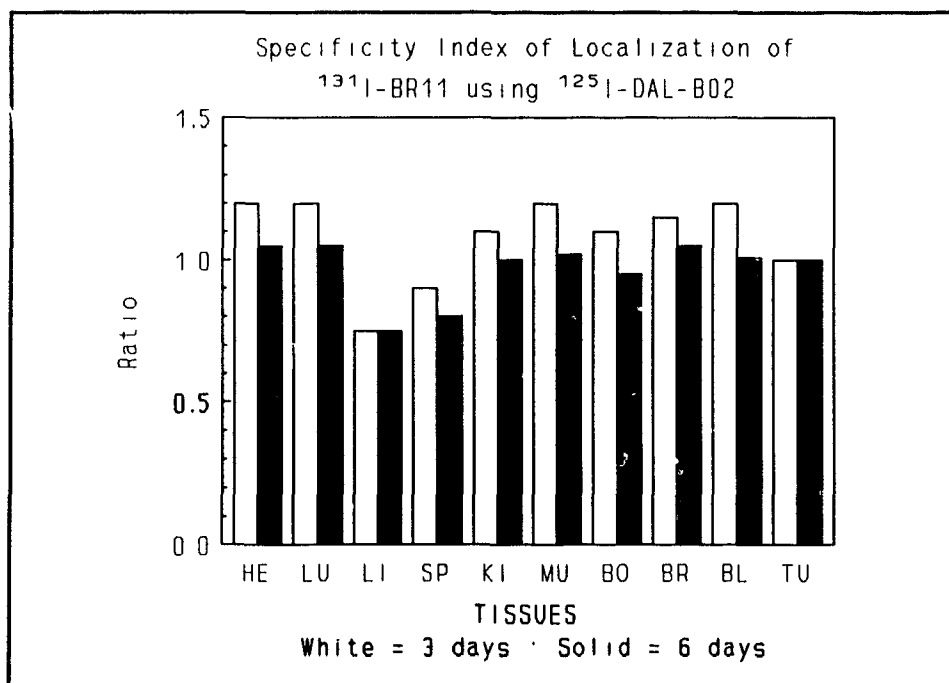


FIGURE 89



FIGURE 90

6. In vivo Localization of DAL-BR6 F(ab)₂ in HTB-19 Xenografts

The amounts of ¹³¹I-labeled DAL-BR6 F(ab)₂ and ¹²⁵I-labeled DAL-B02 F(ab)₂ that were injected into each mouse respectively were 13 uCi and 1 uCi. For both F(ab)₂ fragments, this corresponded to 6 ug of protein which was an equivalent molar amount of protein to that used previously in the experiment with the parent MAB, DAL-BR6. Figure 91 presents the clearance of radioactivity from these mice over time. The biological half-life of i.v. injected DAL-BR6 (Fab)₂ based on these data is 0.9 day. Figures 92, 93, 94 and 95 respectively show the amount of DAL-BR6 F(ab)₂ that localized in the tissues, the percentage of the injected dose of DAL-BR6 F(ab)₂ that localized in the tissues, the T/N ratios of DAL-BR6 F(ab)₂ for the tissues, and the SPIL ratios of DAL-BR6 F(ab)₂ for the tissues. The percentage of injected dose of DAL-BR6 F(ab)₂ that localized in tumor at day 2 and day 3 was about 0.6% which exceeded the levels in all other tissues including blood. The T/N ratios of DAL-BR6 F(ab)₂ for all tissues including blood were equal to or >5 and actually >10 for most tissues at day 3. These T/N ratios at day 3 were almost double the ratios at day 2 and were the highest attained by any MAB or F(ab)₂ fragment investigated in this study. The SPIL ratios of DAL-BR6 F(ab)₂ for all tissues were >1 and >5 for most tissues including blood. These SPIL ratios were like the T/N ratios in that they were the highest attained by any MAB or F(ab)₂ fragment investigated. The gamma camera images at both day 1 and day 2 clearly showed radioactivity localized in tumor xenografts. At day 2, there was virtually no background radioactivity (Figure 96).

FIGURES 91 TO 96:

DATA OBTAINED FROM INJECTING A MIXTURE OF ^{131}I -LABELED DAL-BR6 F(ab)_2 AND ^{125}I -LABELED DAL-B02 F(ab)_2 I.V. INTO NUDE MICE XENOGRAFTED WITH HTB-19 CELLS. FIGURE 96 IS A GAMMA CAMERA IMAGE AT 2 DAYS POST-INJECTION.

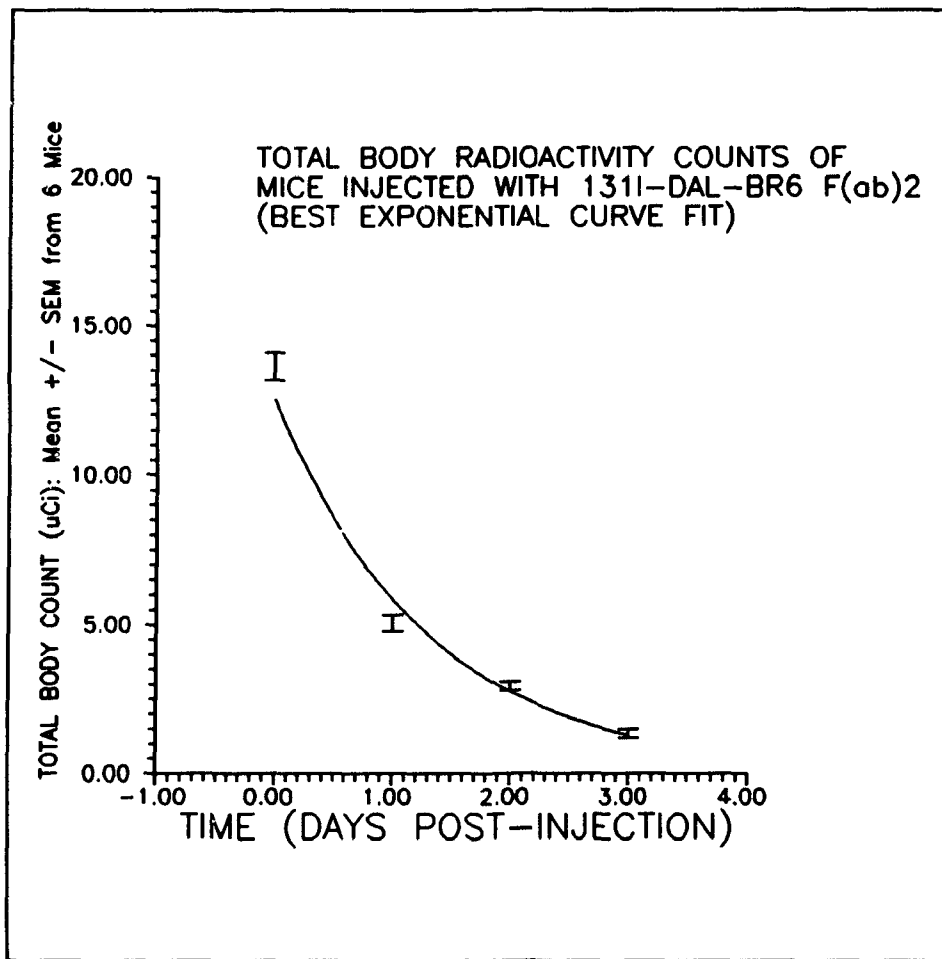


FIGURE 91

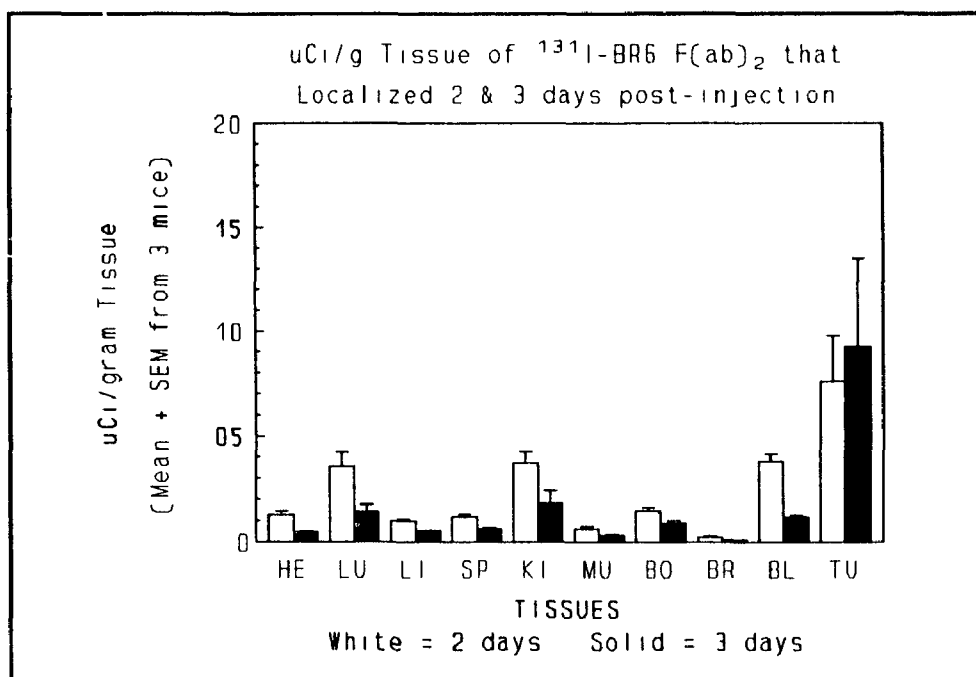


FIGURE 92

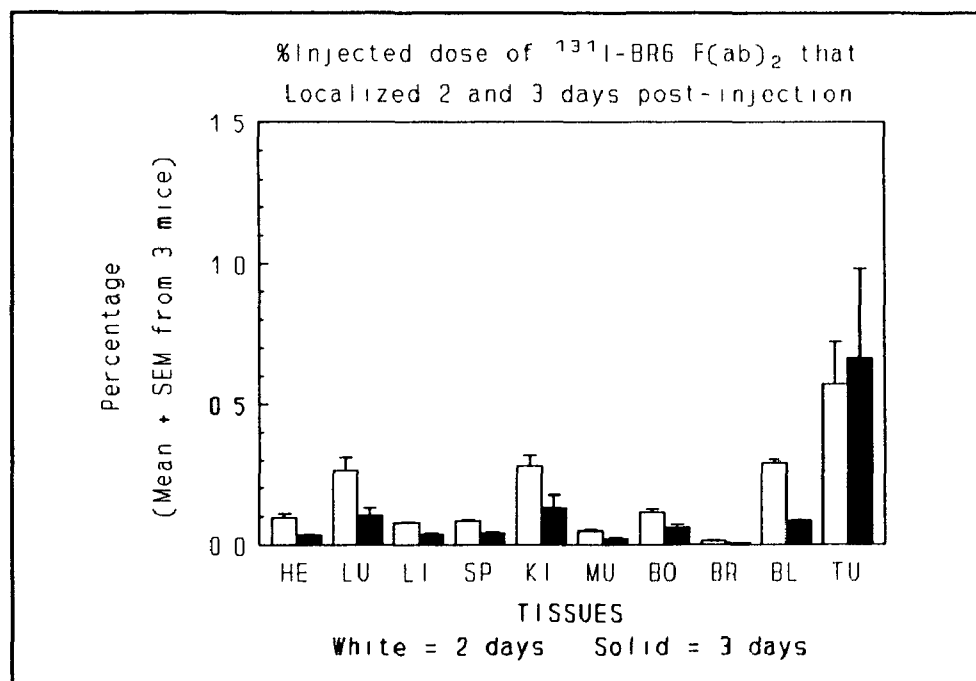


FIGURE 93

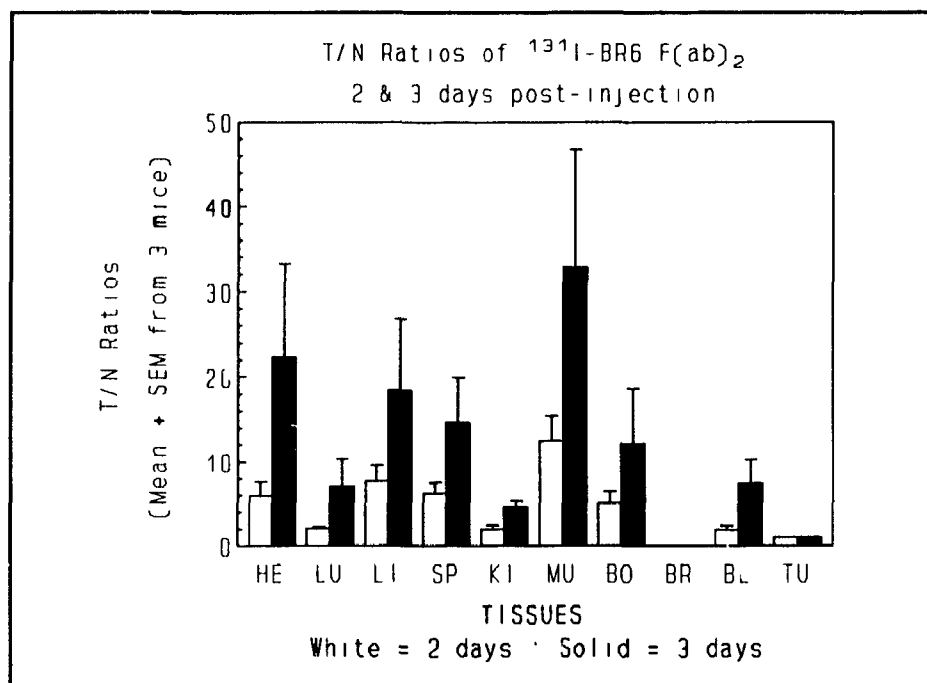


FIGURE 94

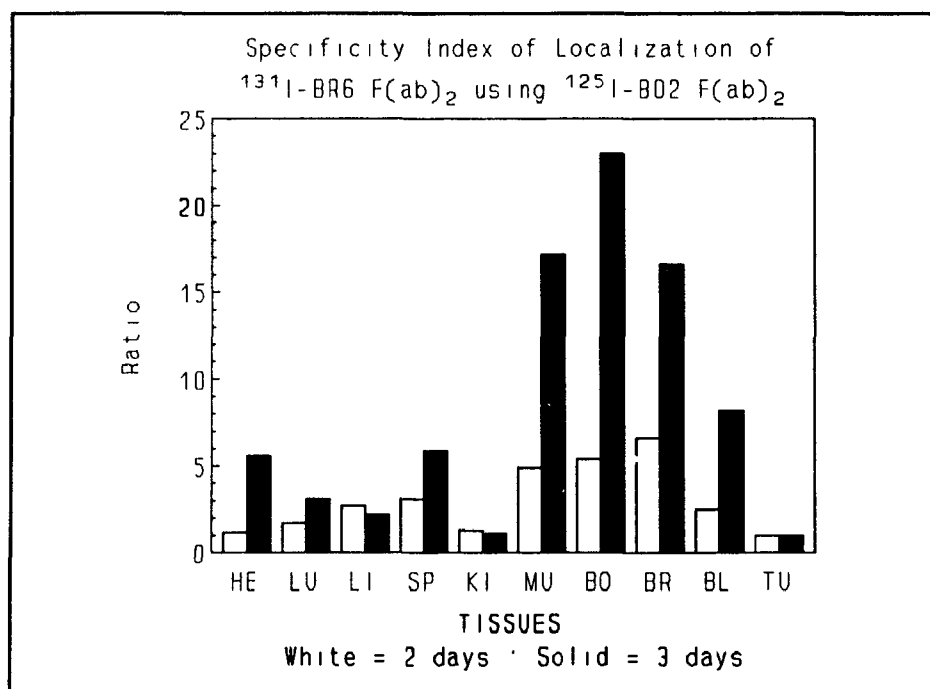


FIGURE 95

7. In vivo Localization of DAL-BR7 F(ab)₂ in HTB-19 Xenografts

Approximately 25 uCi of ¹³¹I-labeled DAL-BR7 F(ab)₂ and 2 uCi of ¹²⁵I-labeled DAL-B01 F(ab)₂ were injected i.v. into each mouse. The corresponding amount of protein of both F(ab)₂ fragments was 7.5 ug which, like the previous experiment with DAL-BR6 F(ab)₂, was an equimolar amount of protein to that used in the experiment with the parent MAB, DAL-BR7. Figure 97 presents the clearance of DAL-BR7 F(ab)₂ from the mice over time. The biological half-life of this radiolabeled F(ab)₂ fragment based on these data was 1.4 days. The amount of DAL-BR7 F(ab)₂ that localized in tissues and the percentage of the injected dose of this F(ab)₂ fragment that localized in each tissue are respectively presented in Figures 98 and 99. The percentage of the injected dose of DAL-BR7 F(ab)₂ that localized in tumor was about 3.5% both at day 1 and day 2 and was almost as much as attained in the experiment with MAB DAL-BR9. At day 2, this amount of DAL-BR7 F(ab)₂ that localized in the tumor exceeded the levels in all other tissues except blood. The T/N ratios and SPIL ratios of DAL-BR7 F(ab)₂ for the tissues are shown in Figures 100 and 101. The T/N ratios were near or >3 for all tissues except blood at day 2. These T/N ratios were about twice the T/N ratios observed at day 1. The SPIL ratios of DAL-BR7 F(ab)₂ for all tissues were >1 and near 2 for most tissues. Unfortunately, the mice in this experiment were scanned, like the mice in the experiment with DAL-BR6, with a gamma camera equipped with a wide field of view collimator which resulted in suboptimal images of the xenografted tumors.

FIGURES 97 TO 101:

DATA OBTAINED FROM INJECTING A MIXTURE OF ^{131}I -LABELED DAL-BR7
F(ab)₂ AND ^{125}I -LABELED DAL-B01 F(ab)₂ I.V. INTO NUDE MICE
XENOGRAFTED WITH HTB-19 CELLS.

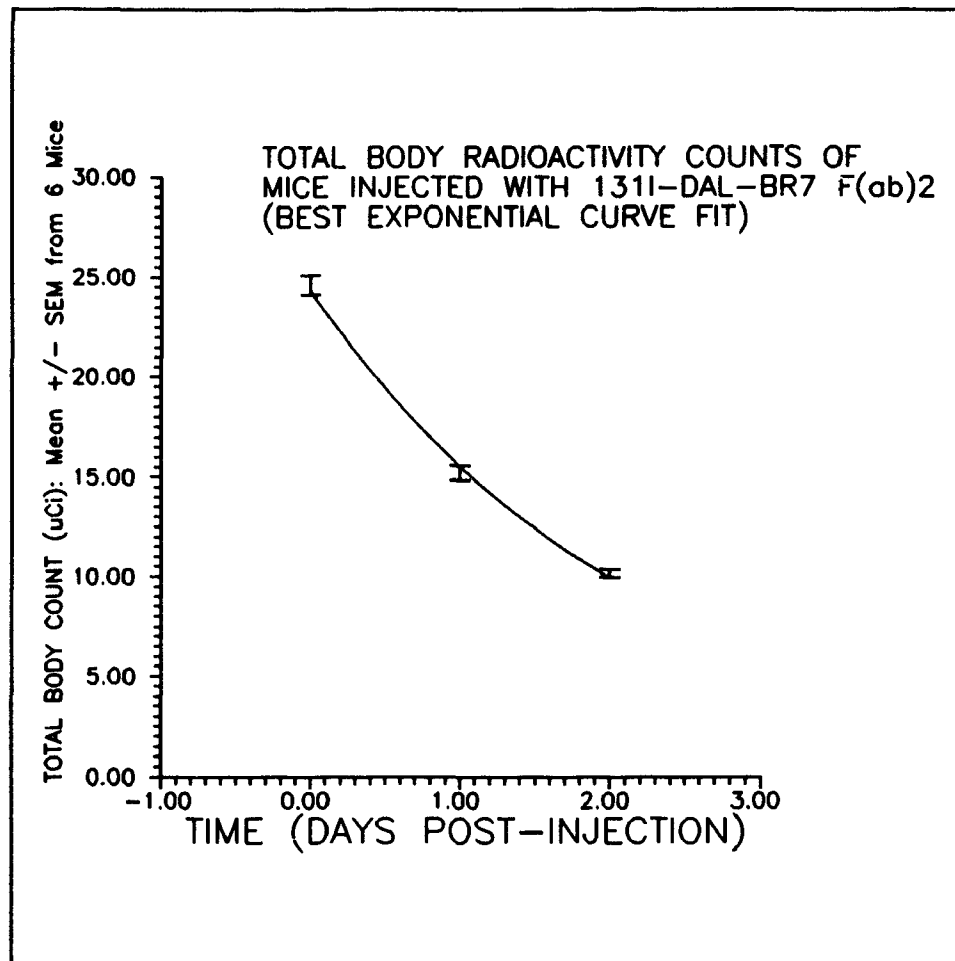


FIGURE 97

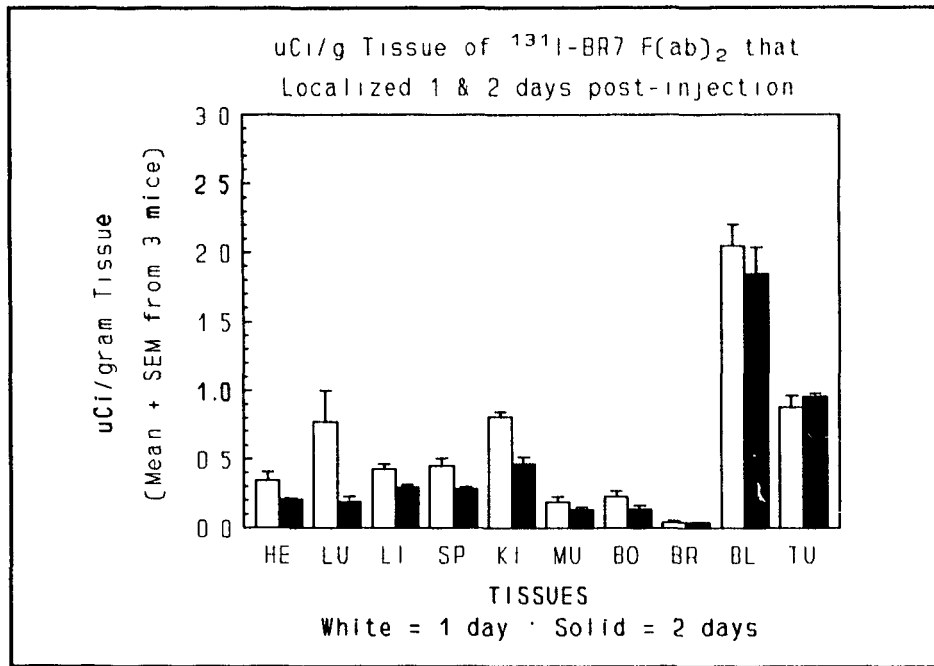


FIGURE 98

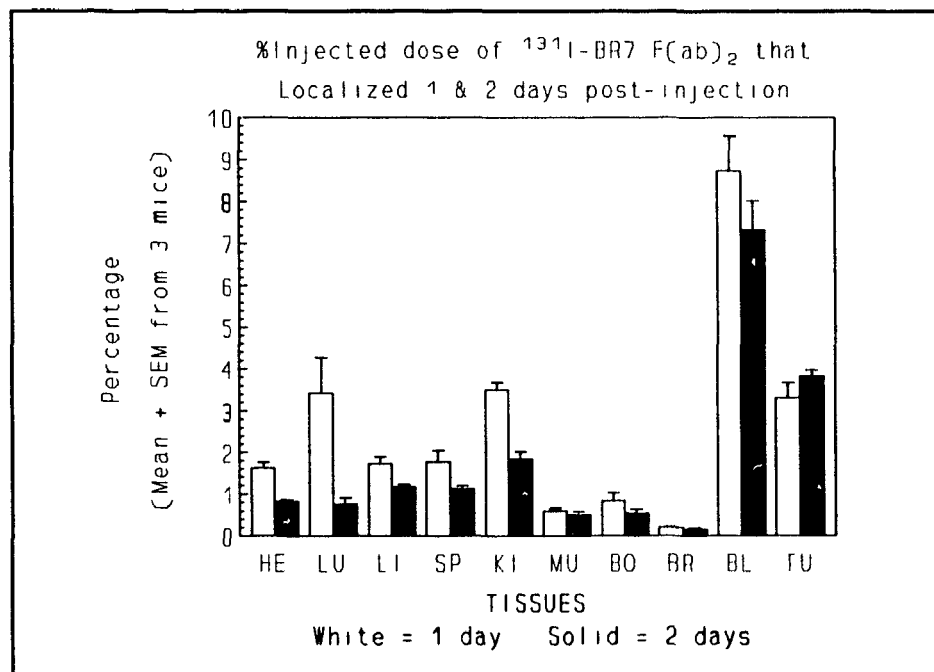


FIGURE 99

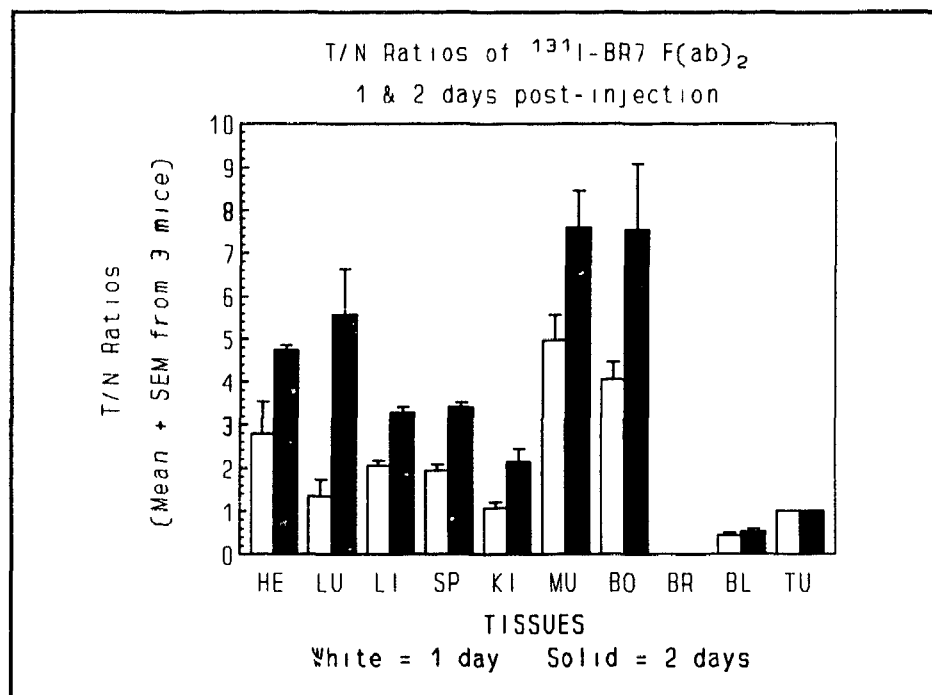


FIGURE 100

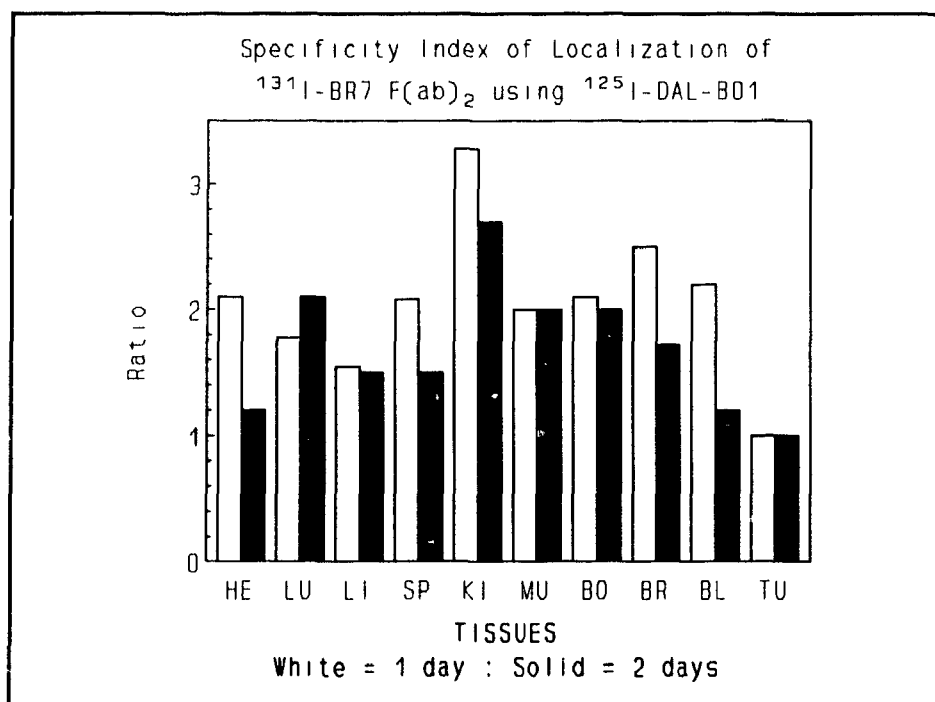


FIGURE 101

8. In vivo Localization of DAL-BR6 and DAL-BR7 in HTB-19 Xenografts

In this experiment, 28 ug of DAL-BR6 labeled with ^{125}I was mixed with an equivalent amount of DAL-BR7 labeled with ^{131}I and the mixture was injected i.v. into each mouse with HTB-19 xenografts. The corresponding amounts of radioactivity in the mixture were 4 uCi of ^{125}I -labeled DAL-BR6 and 40 uCi of ^{131}I -labeled DAL-BR7. Figures 102, 103 and 104 respectively present the amount of each MAB that localized in each tissue at day 6, the percentage of the injected dose of each MAB that localized to the same tissues at day 6, and the T/N ratios of the MABs for the tissues at day 6. It should be noted that Figure 102 presents the amount of MAB that localized in ug since presentation of the amount of radioactivity that localized in uCi (as was presented in all previous figures of the same type of data) would not adequately show the data for the ^{125}I -labeled MAB in the same figure which contains the data for the ^{131}I -labeled MAB. This is because the amount of ^{131}I -radioactivity injected was far in excess of the amount of ^{125}I -radioactivity injected. Also in Figure 104 depicting the T/N ratios, the ratio for bone is not presented since, like the ratio for brain (as was the case for all previous figures of this type), it far exceeded the scale in the figure. Used in combination, approximately equal amounts of DAL-BR6 and DAL-BR7 localized in the tumor. However, these tumor-localized amounts (about 2.5% of the injected dose of DAL-BR7 and 3.2% of the injected dose of DAL-BR6) far exceeded the amount localized in all tissues except blood and also interestingly exceeded the amount of each MAB that localized in the tumor at day 6 when the same MABs were injected separately in previous experiments. Furthermore, the T/N ratios of the

MABs when injected in combination were also generally higher for most tissues than when the MABs were injected separately in previous experiments.

9. In vivo Localization of DAL-BR7 and DAL-BR9 in HTB-19 Xenografts

Like the above experiment, 28 ug of ^{131}I -labeled DAL-BR7 was mixed with an equivalent amount of ^{125}I -labeled DAL-BR9 and the mixture injected i.v. into each mouse with HTB-19 xenografts. The corresponding amounts of radioactivity were again 40 uCi of the ^{131}I -labeled MAB and 4 uCi of the ^{125}I -labeled MAB. Figures 105, 106 and 107 respectively show the amount of each MAB that localized in each tissue at day 6 (again expressed as ug MAB/g tissue), the percentage of the injected dose of each MAB that localized in the same tissues at day 6, and the T/N ratios of each MAB for the tissues. The percentage of the injected dose of both MABs that localized in tumor exceeded the amounts that localized in other tissues and for DAL-BR7 this percentage exceeded the levels in blood as well. More of DAL-BR7 localized in tumor (about 4.5% of the injected dose) than DAL-BR9 (about 3%). Furthermore, the amount of DAL-BR7 that localized in tumor when injected as a mixture was about 3 times more than the amount of this MAB that localized in tumor when injected alone. In contrast, the % injected dose of DAL-BR9 that localized in tumor dropped from 4% when it was injected alone to 3% when it was injected as a mixture. A comparison of the results using DAL-BR7 in this experiment with the results using DAL-BR7 in the experiment described above (where DAL-BR6 instead of DAL-BR9 was the second MAB) shows that more DAL-BR7 localized in tumor when it was injected with DAL-BR9 than when it was injected with DAL-BR6.

FIGURES 102 TO 107:

DATA FROM EXPERIMENTS PERFORMED WITH MICE XENOGRAFTED WITH HTB-19 CELLS AND I.V. INJECTED WITH EQUIPROTEIN MIXTURES OF MABS. FIGURES 102 TO 104 SHOW DATA OBTAINED FROM INJECTING ^{131}I -DAL-BR7 MIXED WITH ^{125}I -DAL-BR6 WHILE FIGURES 105 TO 107 SHOW DATA OBTAINED FROM INJECTING ^{131}I -DAL-BR7 MIXED WITH ^{125}I -DAL-BR9. IN BOTH THESE EXPERIMENTS, THE MICE WERE SACRIFICED ON DAY 6 POST-INJECTION.

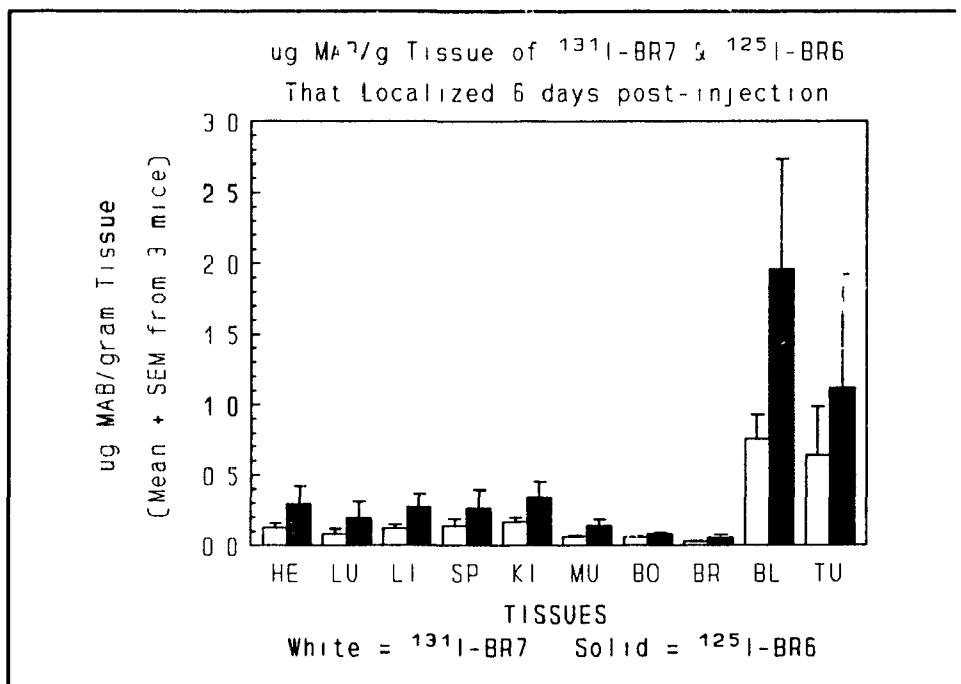


FIGURE 102

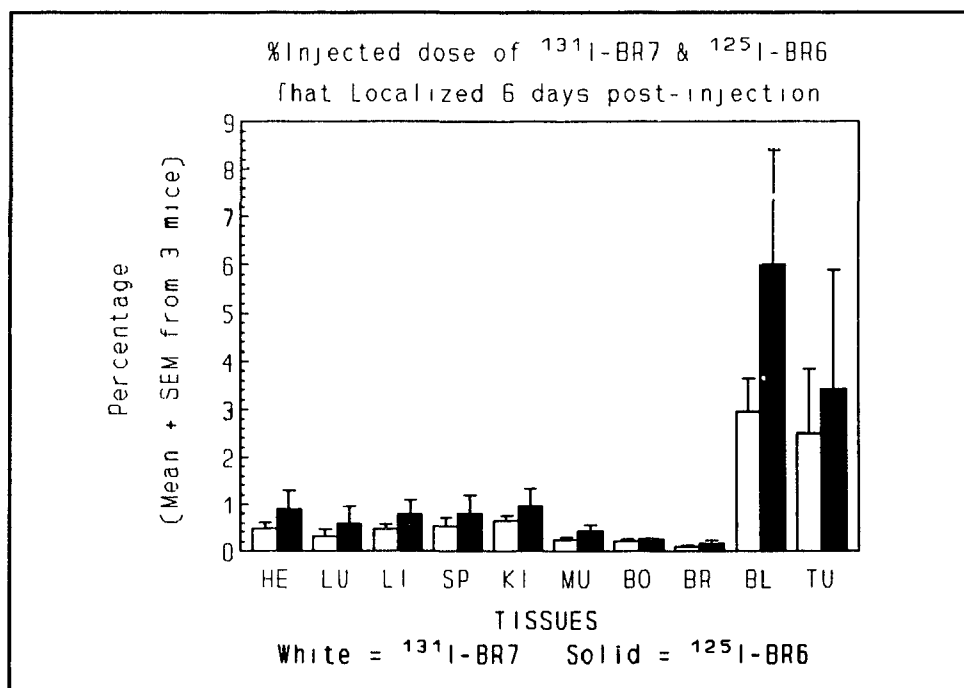


FIGURE 103

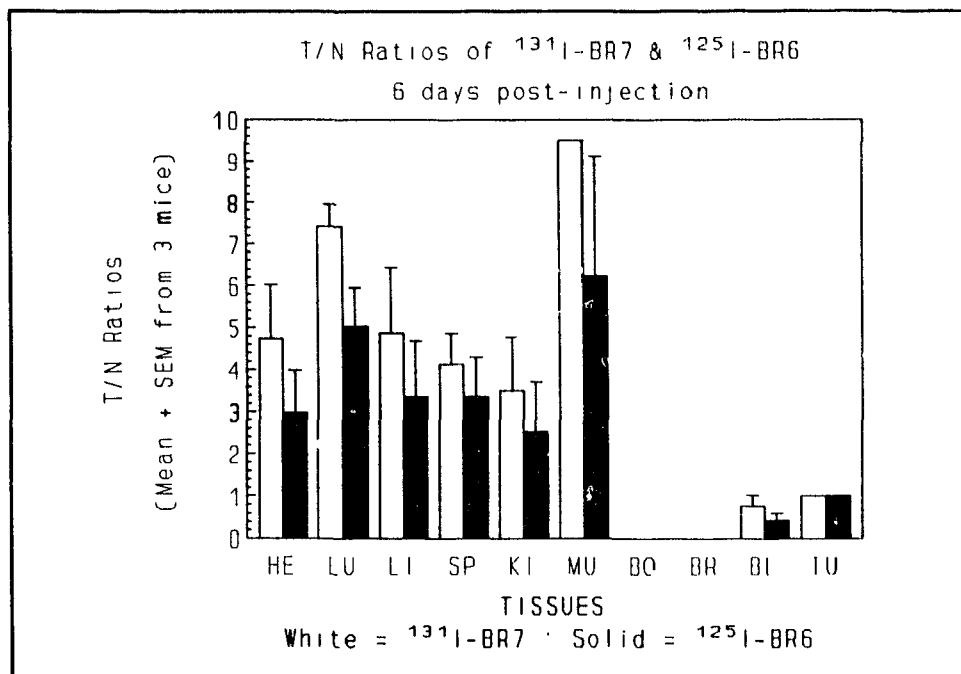


FIGURE 104

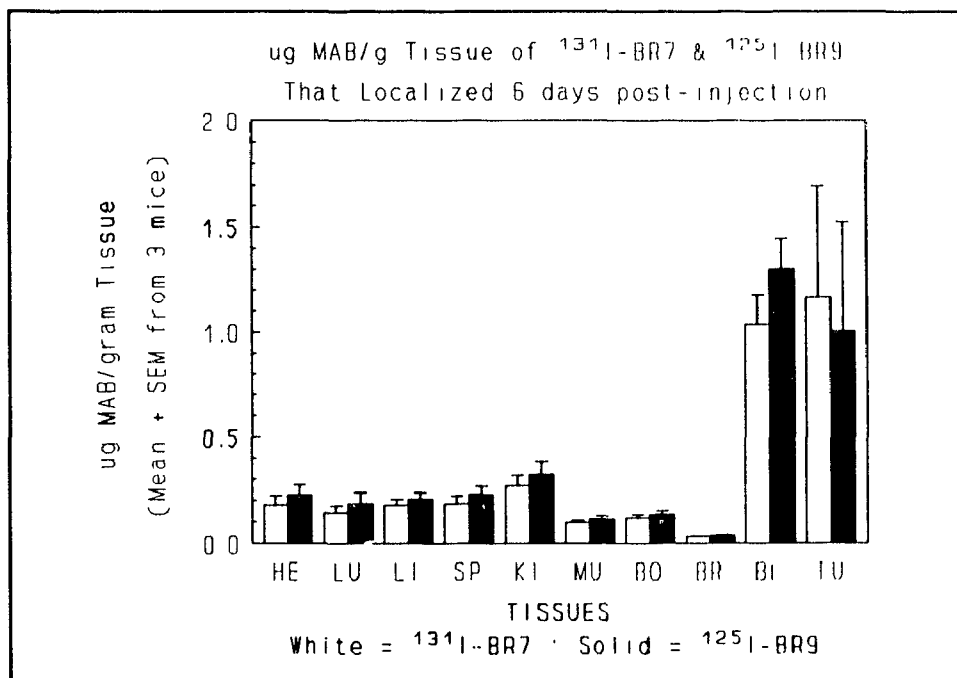


FIGURE 105

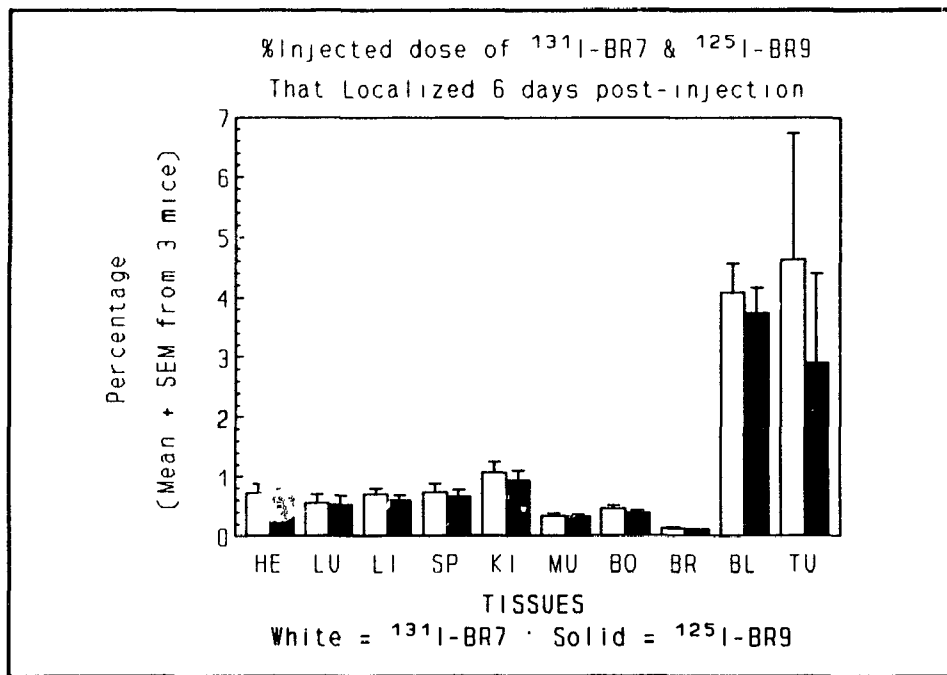


FIGURE 106

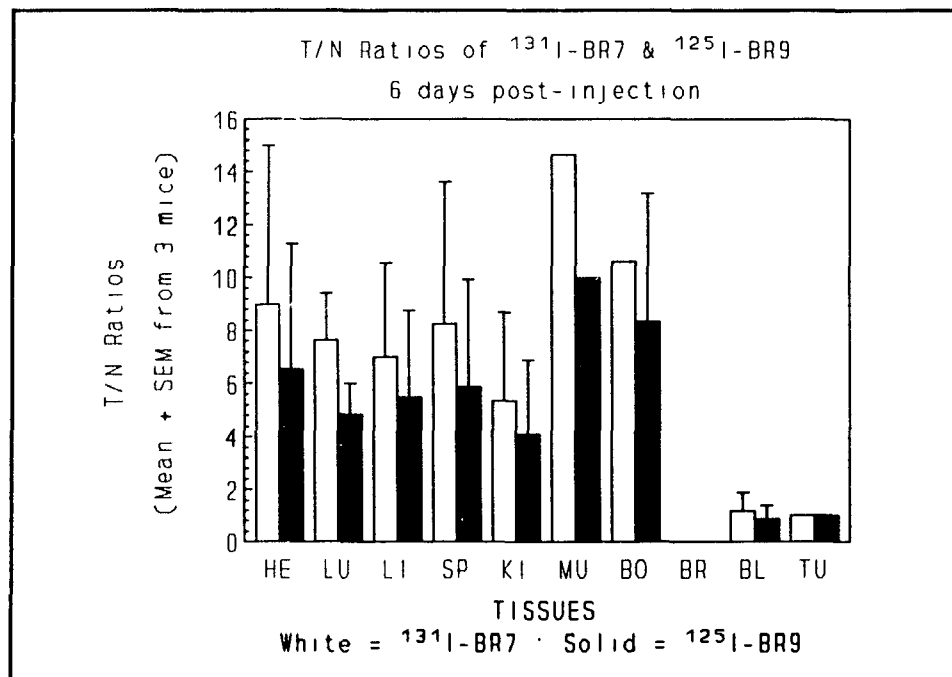


FIGURE 107

The T/N ratios of both DAL-BR7 and DAL-BR9 were also considerably higher for all tissues at day 6 when these MABs were injected together than when injected separately as described in previous experiments.

Distinct gamma camera images of tumors in the mice were obtained at day 6 in both these last two experiments that used mixtures of ^{131}I -labeled DAL-BR7 with ^{125}I -labeled DAL-BR6 or DAL-BR9. Representative gamma camera images of tumor-localized DAL-BR7 from these experiments are shown in Figures 108 and 109.

FIGURES 108 AND 109:

FIGURE 108. GAMMA CAMERA IMAGE AT DAY 6 OF A MOUSE BEARING A HTB-19 XENOGRAFT INJECTED WITH A MIXTURE OF ^{131}I -DAL-BR7 AND ^{125}I -DAL-BR6.

FIGURE 109. GAMMA CAMERA IMAGE AT DAY 6 OF A MOUSE BEARING A HTB-19 XENOGRAFT INJECTED WITH A MIXTURE OF ^{131}I -DAL-BR7 AND ^{125}I -DAL-BR9.



FIGURE 108

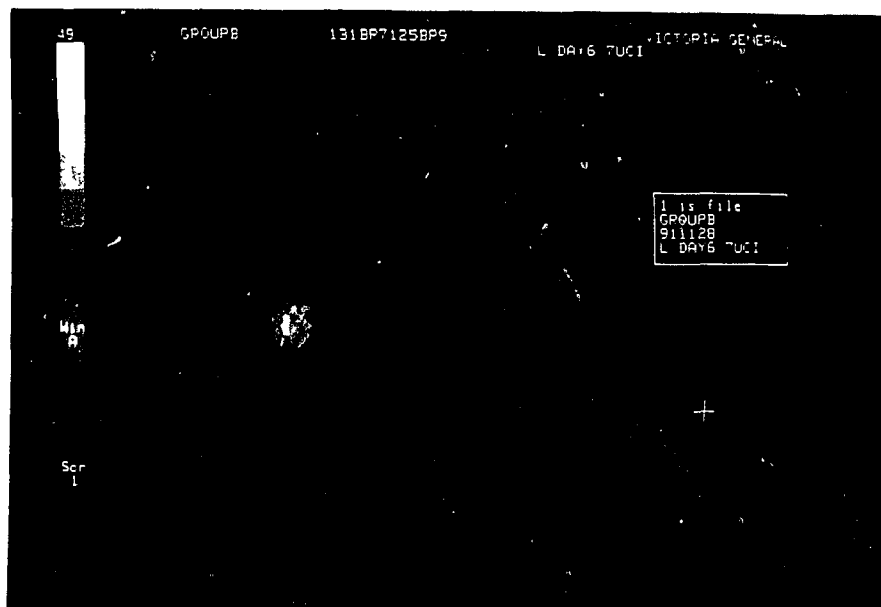


FIGURE 109

10. In vivo Localization of DAL-BR7 in Caki-1 Xenografts

Each Caki-1-xenografted mouse was injected i.v. with approximately 30 uCi of ¹³¹I-labeled DAL-BR7 and 2 uCi of ¹²⁵I-labeled DAL-B01. The corresponding amount of injected protein was 46 ug of each MAB. Figures 110 and 111 show respectively the amount of DAL-BR7 that localized in tissues and the percentage of the injected dose of DAL-BR7 that localized in the same tissues at 6 days post-injection. Approximately 1.3% of the injected dose of DAL-BR7 localized in tumor which exceeded all other tissues except blood. This percentage was comparable to the percentage of the injected dose of DAL-BR7 that localized at day 6 in HTB-19 cell xenografts as described earlier. Figures 112 and 113 respectively show the T/N ratios and the SPIL ratios of DAL-BR7 for the tissues. The T/N ratios were all >2 for all tissues except blood and were >6 for most tissues. The SPIL ratios were >1 and <3 for all tissues. These T/N and SPIL ratios were either comparable to or greater than the respective ratios described previously for DAL-BR7 in the HTB-19 xenograft model. Gamma camera images of mice xenografted with Caki-1 cells and injected with ¹³¹I-labeled DAL-BR7 will be presented and described in the next section where groups of mice were scanned at day 4 and day 6 post-injection.

FIGURES 110 TO 113:

DATA OBTAINED FROM MICE XENOGRAFTED WITH CAKI-1 CELLS
INJECTED I.V. WITH A MIXTURE ^{131}I -DAL-BR7 AND ^{125}I -DAL-B01 AND
SACRIFICED 6 DAYS POST-INJECTION.

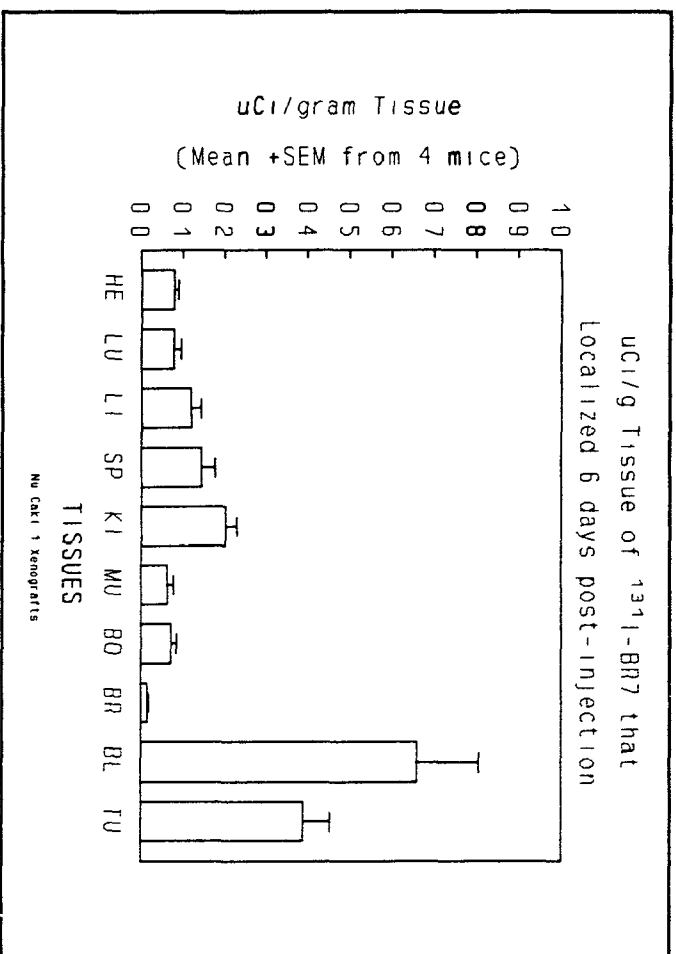


FIGURE 110

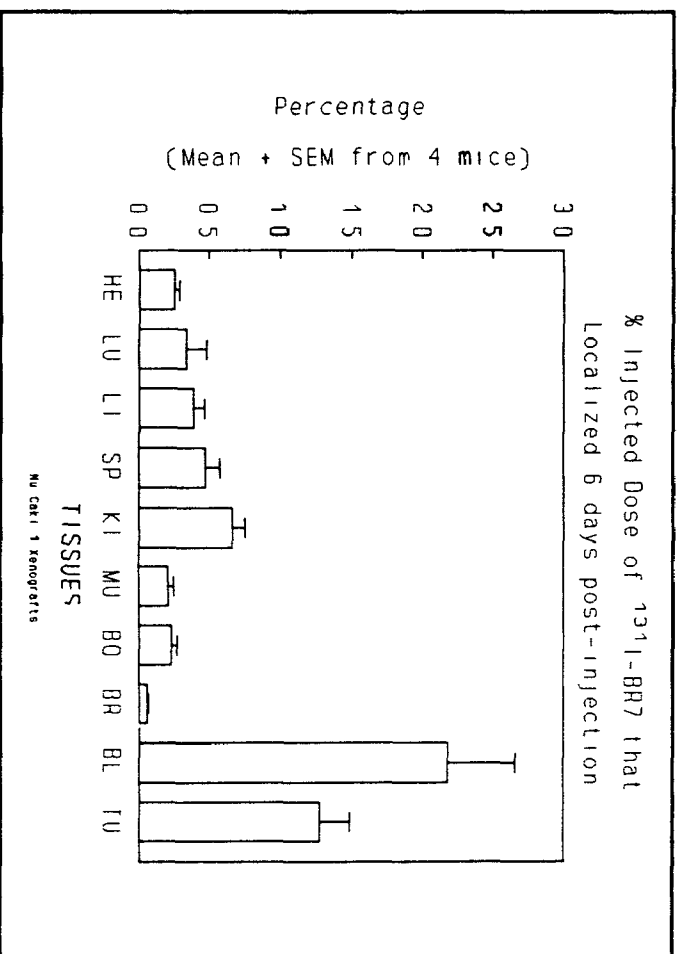


FIGURE 111

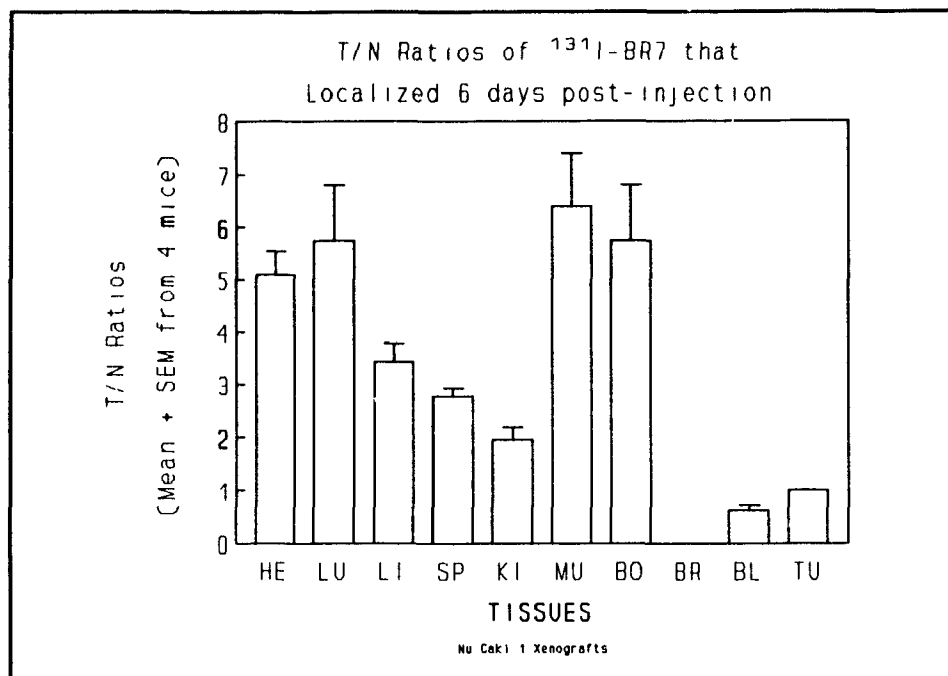


FIGURE 112

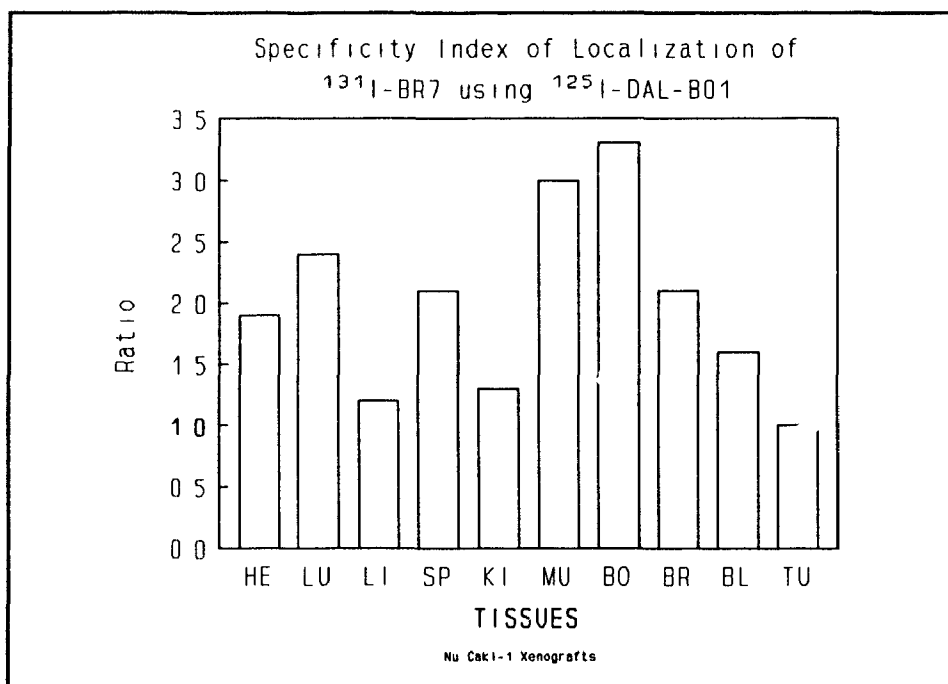


FIGURE 113

11. In vivo Localization of DAL-BR7 and K45 in Caki-1 Xenografts

In this experiment, mice bearing Caki-1 xenografts were segregated into four groups and were each injected i.v. either with a single radiolabeled MAB or with a mixture of radiolabeled MABs. Mice in the first group were injected with ^{131}I -labeled K45 alone while mice in the second group were injected with ^{131}I -labeled DAL-BR7 alone. The third group of mice was injected with a mixture containing ^{131}I -labeled K45 and ^{125}I -labeled DAL-BR7 while the fourth group of mice was injected with a mixture containing ^{131}I -labeled DAL-BR7 and ^{125}I -labeled K45. The amount of ^{131}I -radioactivity injected per mouse was approximately 50 μCi and the amount of ^{125}I -radioactivity injected per mouse was approximately 4 μCi . The corresponding protein amounts of the respective radiolabeled MABs injected per mouse were approximately 52 μg of ^{131}I -labeled K45, 57 μg of ^{131}I -labeled DAL-BR7, 52 μg of ^{125}I -labeled K45, and 47 μg of ^{125}I -labeled DAL-BR7.

Figures 114 and 115 respectively show the amount of the two MABs when injected alone that localized in tissues and the percentage of the injected dose of the two MABs that localized in the same tissues at day 6. Approximately 4.6% of the injected dose of K45 and 3.1% of the injected dose of DAL-BR7 localized in tumor. Both these amounts exceeded the amounts localized in all other tissues except blood. Figure 116 shows the T/N ratios of the two MABs for the tissues when each MAB was injected alone. Both MABs had T/N ratios >3 for all tissues except blood. Figures 117 and 118 respectively show gamma camera images of mice at day 4 that were injected with K45 or DAL-BR7 alone. In both images, the Caki-1 xenografts

are clearly visible but a considerable amount of background radioactivity still persisted. At day 6, gamma camera images of the same mice showed virtual loss of background radioactivity in case of K45 (Figure 119) and a marked decrease in the background radioactivity in the case of DAL-BR7 (Figure 120). For both K45 and DAL-BR7 though, the tumor xenografts were distinctly evident in the gamma camera images at day 6.

Figures 121 and 122 show the amount of each MAB (K45 and DAL-BR7) that localized in tissues when injected as mixtures. The corresponding percentage of the injected dose of each MAB in the mixtures that localized in the same tissues is presented in Figures 123 and 124. When a mixture of ^{131}I -labeled K45 and ^{125}I -labeled DAL-BR7 was injected, approximately 5.8% and 2.9% of K45 and DAL-BR7 respectively localized to tumor (Figure 123). These amounts exceeded the amounts localized to all tissues except blood. When a mixture of ^{131}I -labeled DAL-BR7 and ^{125}I -labeled K45 were injected, approximately 4.4% and 2.5% of DAL-BR7 and K45 localized to tumor (Figure 124). These amounts again exceeded the amounts localized to all other tissues except blood.

Figures 125 and 126 show the T/N ratios of the MABs (K45 and DAL-BR7) for the tissues when injected as mixtures. The T/N ratios of both MABs for almost all tissues except blood were >3 to 4. Gamma camera images at day 6 of mice injected with mixtures of the 2 MABs are shown in Figures 127 and 128. Very distinct images of tumor xenografts with little background radioactivity were obtained no matter which of the 2 MABs in the injected mixture was labeled with ^{131}I .

FIGURES 114 TO 128:

FIGURES 114 TO 116. DATA OBTAINED FROM MICE (XENOGRAFTED WITH CAKI-1 CELLS) INJECTED I.V. WITH EITHER ^{131}I -K45 ALONE OR ^{131}I -DAL-BR7 ALONE. THE MICE IN THESE EXPERIMENTS WERE ALL SACRIFICED 6 DAYS POST-INJECTION.

FIGURES 121 TO 126. DATA OBTAINED FROM MICE (XENOGRAFTED WITH CAKI-1 CELLS) INJECTED I.V. WITH EITHER A MIXTURE OF ^{131}I -K45 AND ^{125}I -DAL-BR7 OR A MIXTURE OF ^{131}I -DAL-BR7 AND ^{125}I -K45. THE MICE IN THESE EXPERIMENTS WERE ALL SACRIFICED 6 DAYS POST-INJECTION.

FIGURES 117 AND 118. GAMMA CAMERA IMAGES AT DAY 4 OF MICE INJECTED WITH ^{131}I -K45 OR ^{131}I -DAL-BR7 RESPECTIVELY.

FIGURES 119 AND 120. GAMMA CAMERA IMAGES AT DAY 6 OF THE SAME MICE RESPECTIVELY SHOWN IN FIGURES 117 AND 118.

FIGURES 127 AND 128. GAMMA CAMERA IMAGES AT DAY 6 OF MICE INJECTED RESPECTIVELY WITH (1) A MIXTURE OF ^{131}I -K45 AND ^{125}I -DAL-BR7 AND (2) A MIXTURE OF ^{131}I -DAL-BR7 AND ^{125}I -K45.

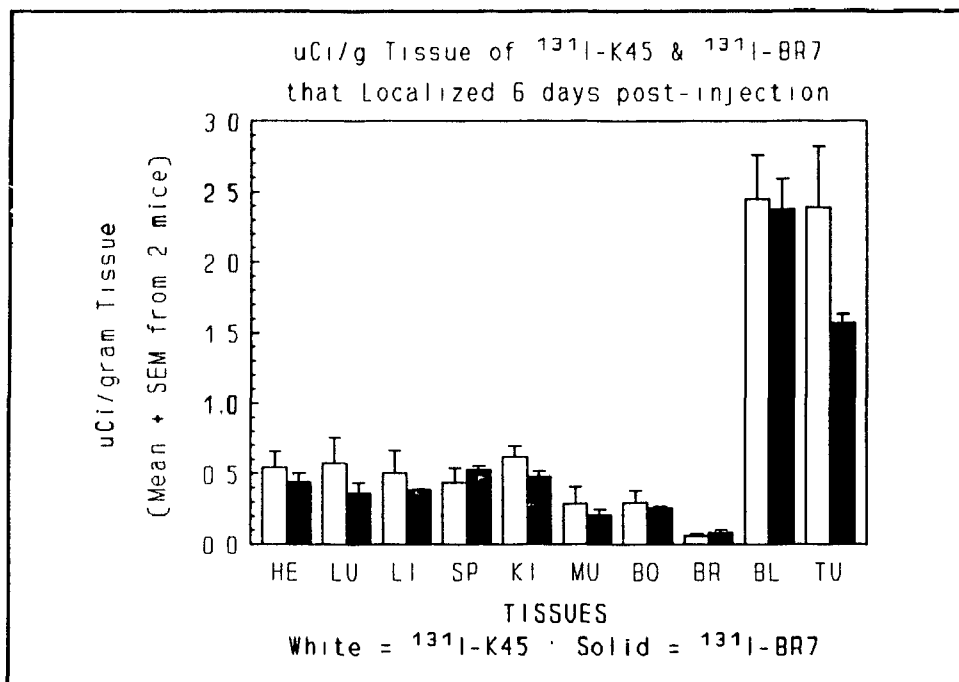


FIGURE 114

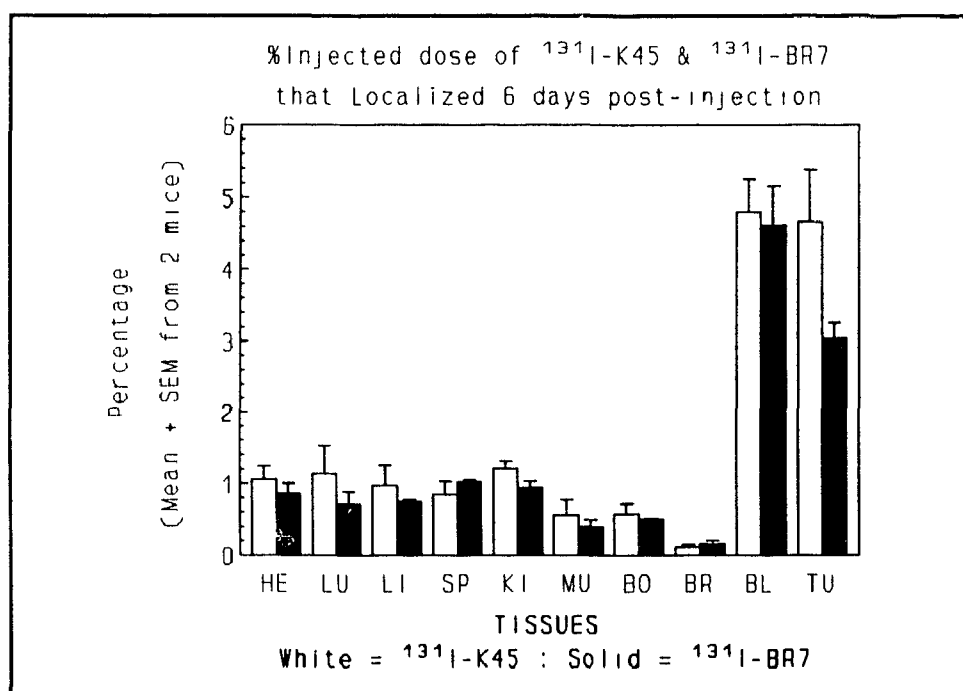


FIGURE 115

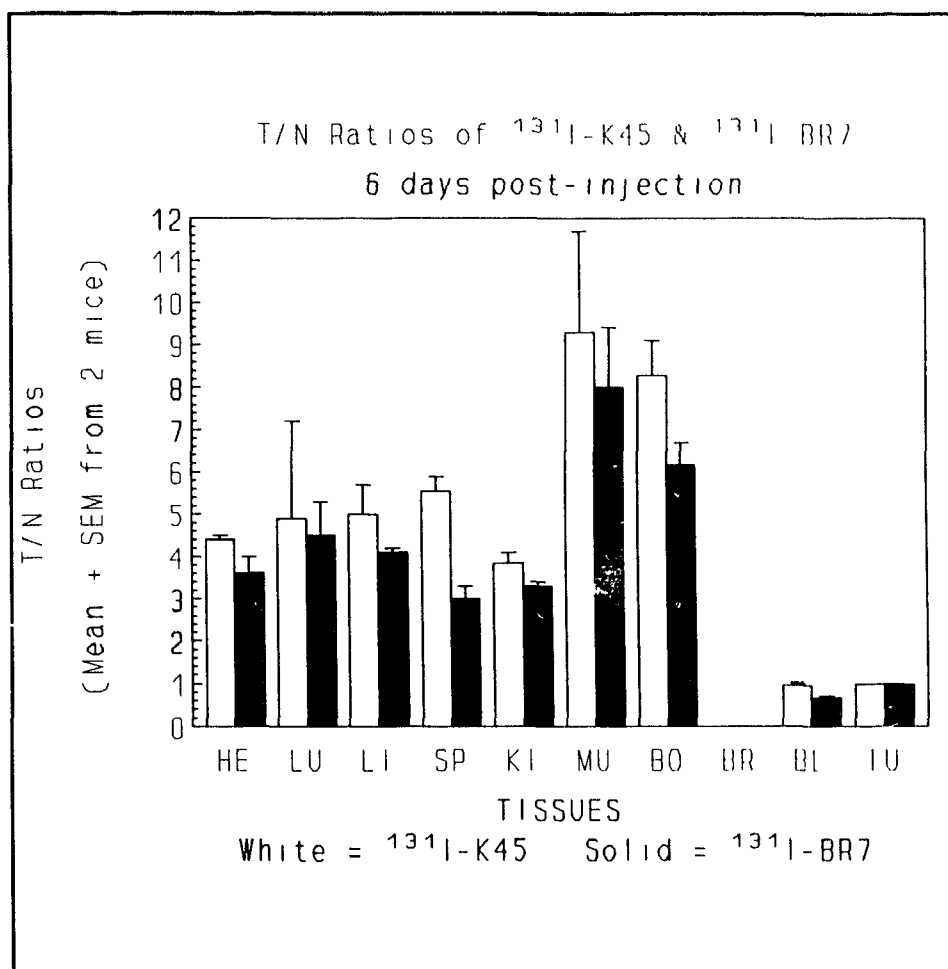


FIGURE 116



FIGURE 117

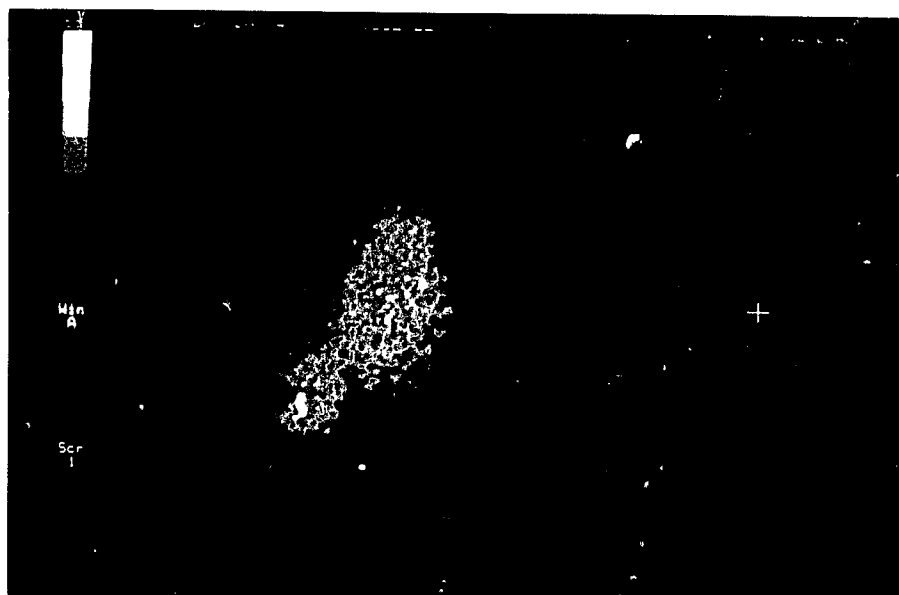


FIGURE 118

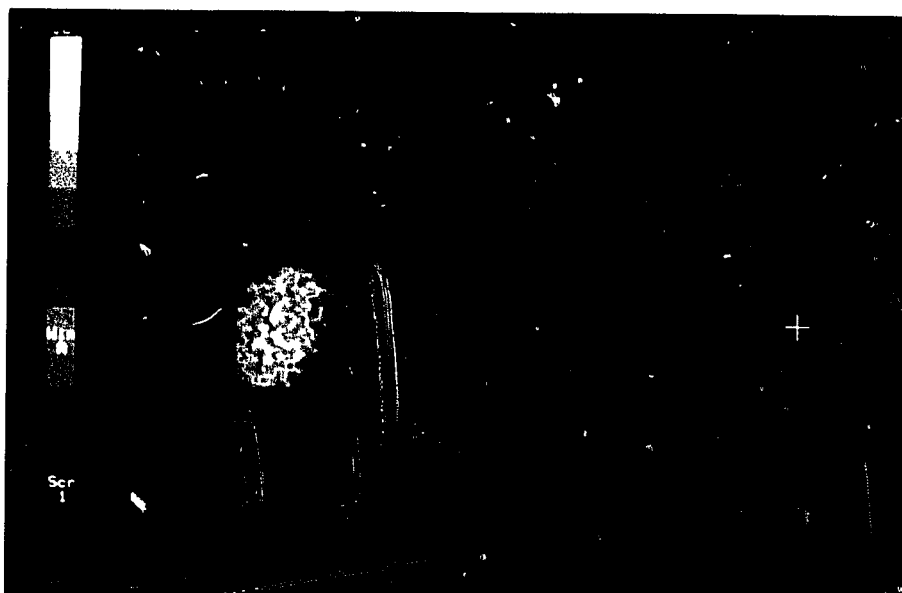


FIGURE 119

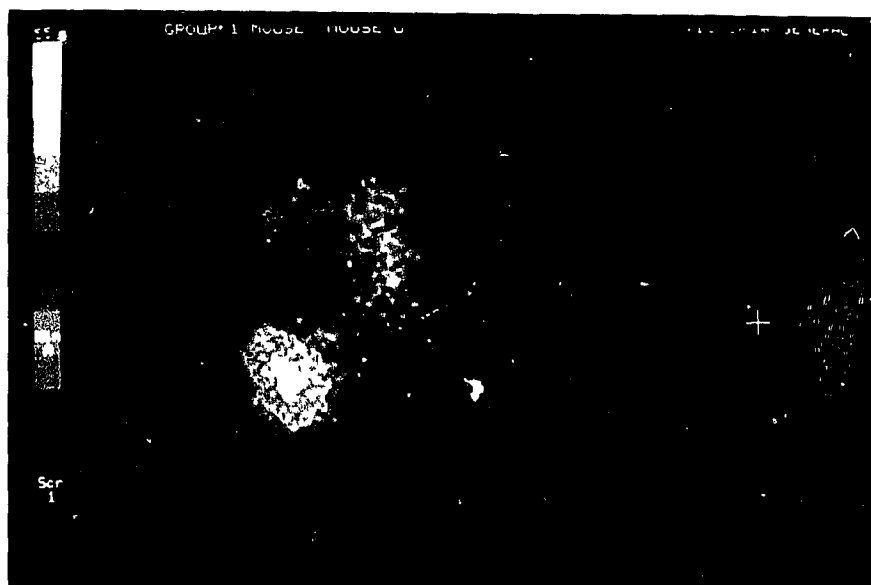


FIGURE 120

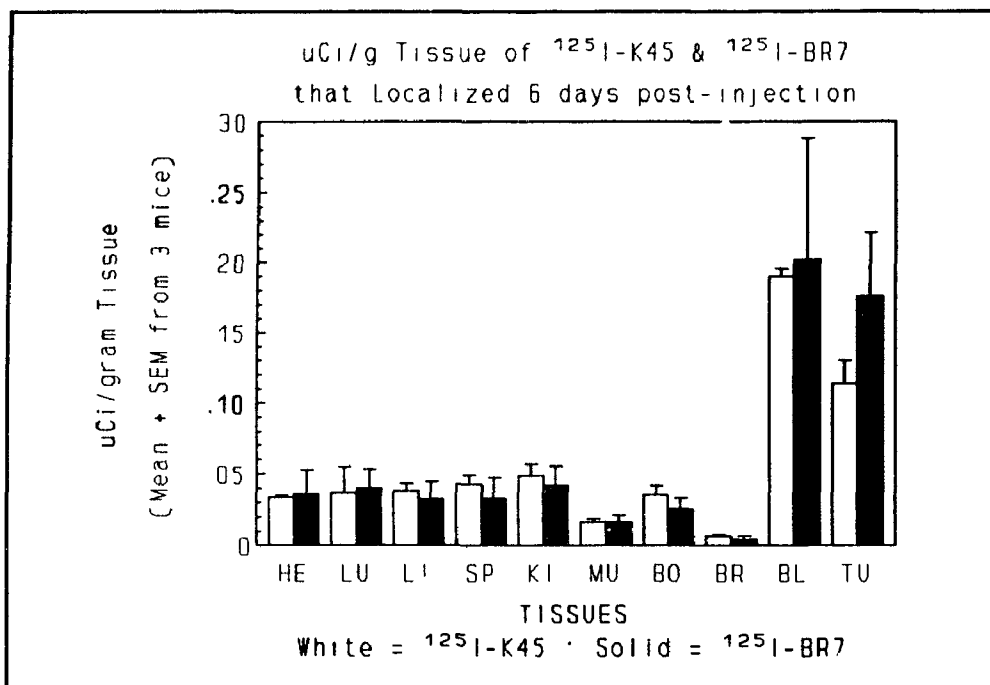


FIGURE 121

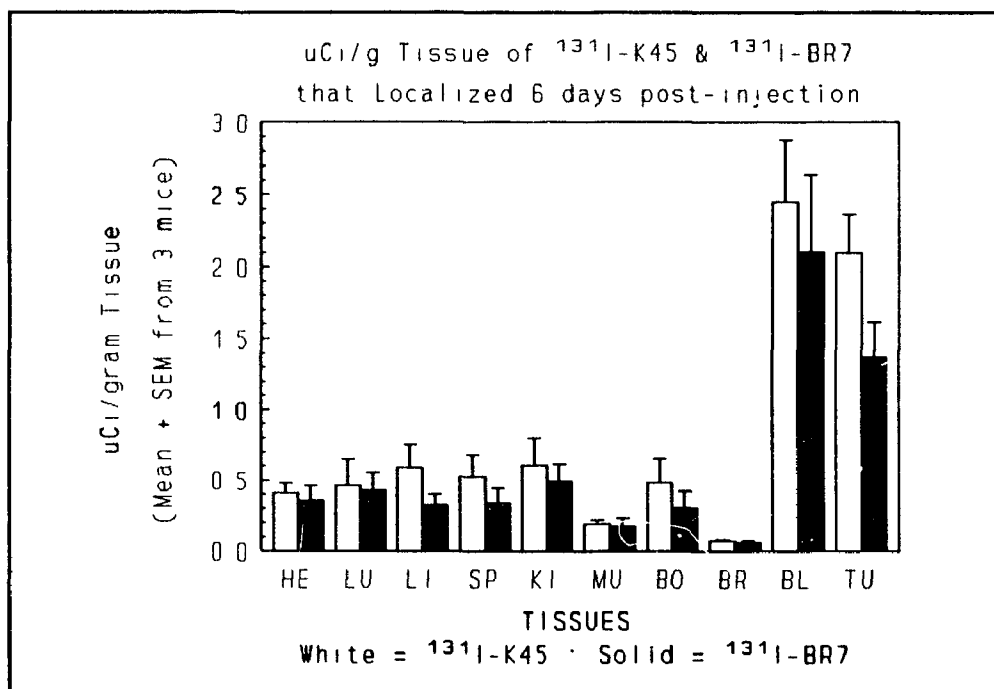


FIGURE 122

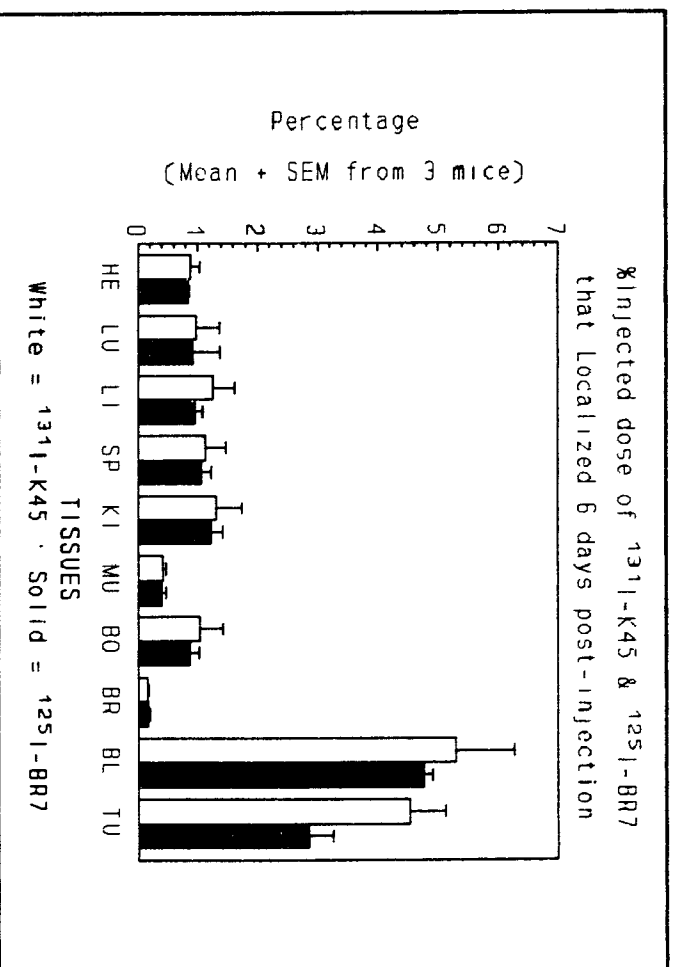


FIGURE 123

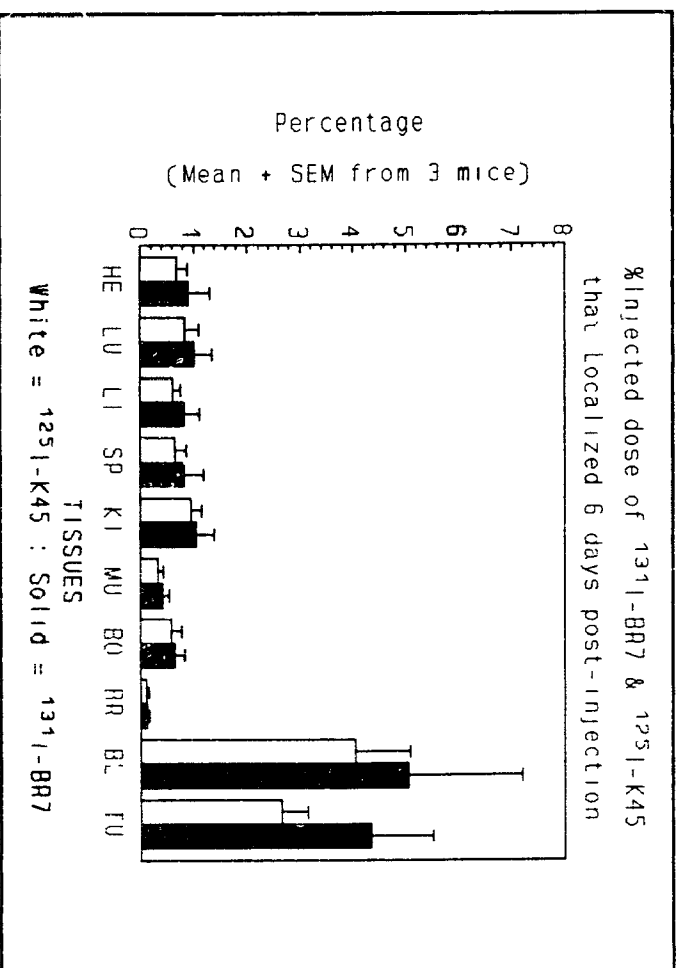


FIGURE 124

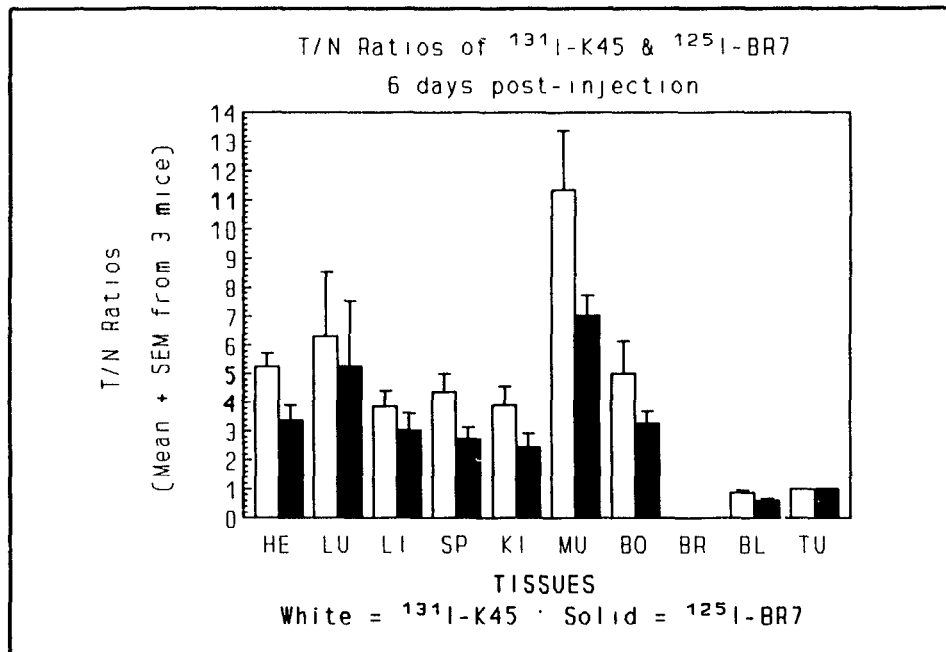


FIGURE 125

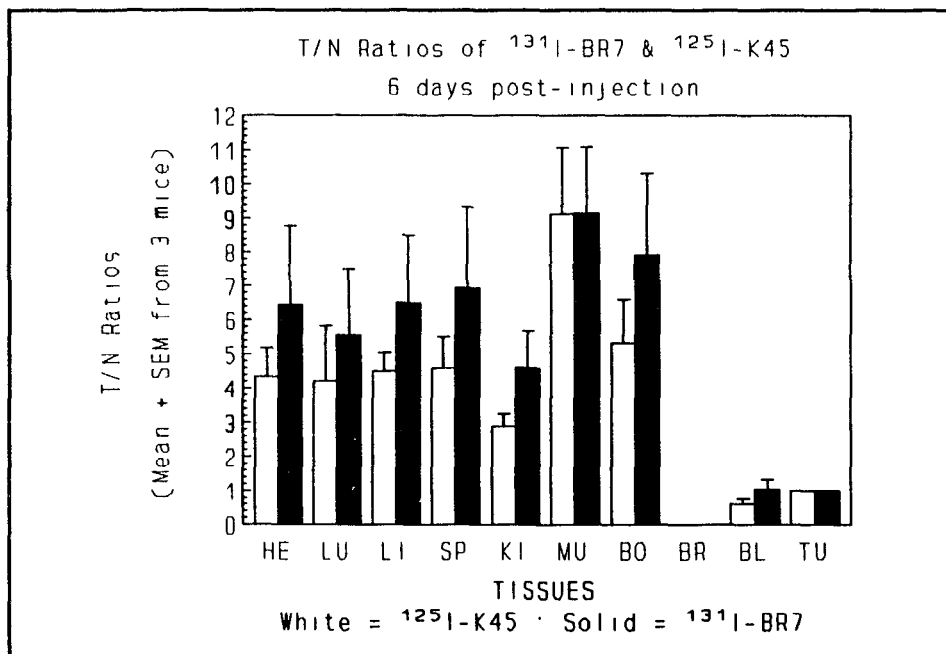


FIGURE 126

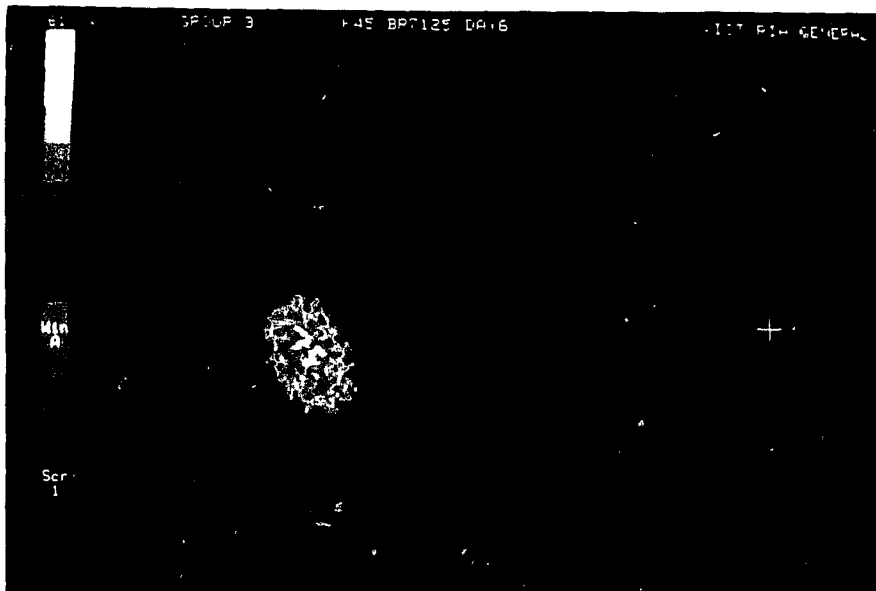


FIGURE 127

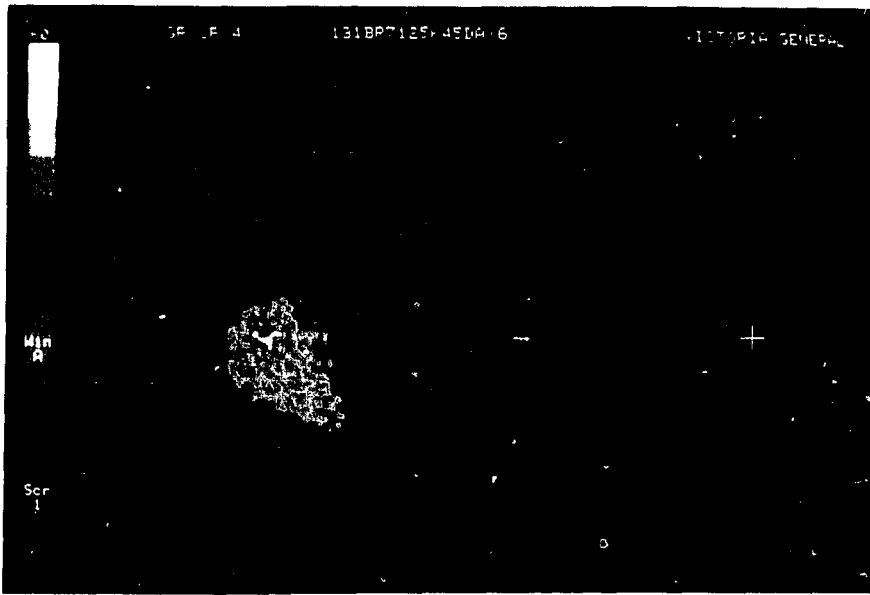


FIGURE 128

12. In vivo Localization of DAL-BR6 or DAL-BR7 in Melanoma Xenografts

Figures 129 to 135 present data from 2 experiments where either ^{125}I -labeled DAL-BR6 or a mixture of ^{131}I -labeled DAL-BR7 and ^{125}I -labeled DAL-B02 was injected i.v. into nude mice bearing M21 melanoma xenografts. In the first experiment, approximately 48 uCi, corresponding to 72 ug, of radiolabeled DAL-BR6 was injected into each mouse. In the second experiment, a mixture consisting of 50 uCi, corresponding to 10 ug, of radiolabeled DAL-BR7 and 2 uCi, corresponding to 9.5 ug, of radiolabeled DAL-B02 was injected into one mouse. Figures 129 and 130 respectively show the amount of DAL-BR6 and DAL-BR7 that localized in each tissue at day 3 and day 6 post injection. The corresponding percentages of the injected dose of each MAB that localized in the same tissues are respectively shown in Figures 131 and 132. Approximately 1% and 2% of the injected dose of DAL-BR6 localized in tumor respectively at day 3 and day 6. These amounts, however, were similar to the amount also localized in several major organs including lung, liver, spleen, and kidney at both day 3 and day 6. The percentages of DAL-BR7 that localized in tumor at day 3 and day 6 were respectively 1.8% and 0.9%. These amounts were respectively also similar to the amount localized to liver, spleen and kidney at both day 3 and day 6. Figures 133 and 134 respectively show the T/N ratios of DAL-BR6 and DAL-BR7 for the tissues. For DAL-BR6 at day 3, the T/N ratios for major organs such as lung, liver, spleen, and kidney were < 1 . At day 6, the T/N ratios were > 1 but < 2 . For DAL-BR7 on day 3, the T/N ratios for most major organs were near 1. At day 6, the T/N ratios for the same organs were < 1 .

FIGURES 129 TO 135:

DATA FROM EXPERIMENTS OF NUDE MICE XENOGRAFTED WITH M21 MELANOMA CELLS INJECTED I.V. WITH EITHER ^{125}I -DAL-BR6 OR A MIXTURE OF ^{131}I -DAL-BR7 AND ^{125}I -DAL-B02. THE MICE WERE SACRIFICED AT 3 AND 6 DAYS POST-INJECTION.

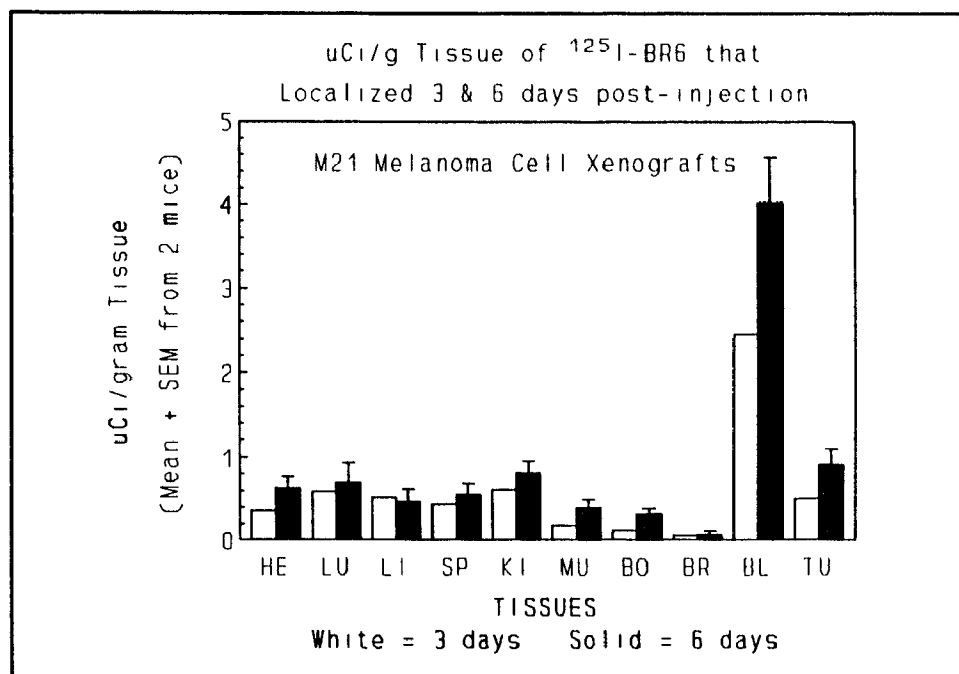


FIGURE 129

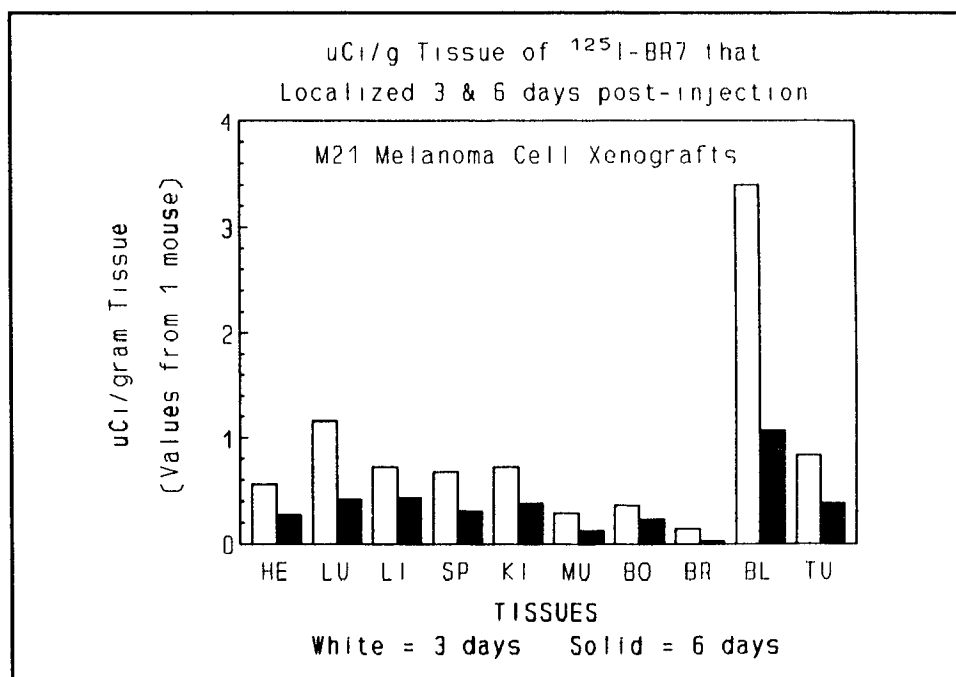


FIGURE 130

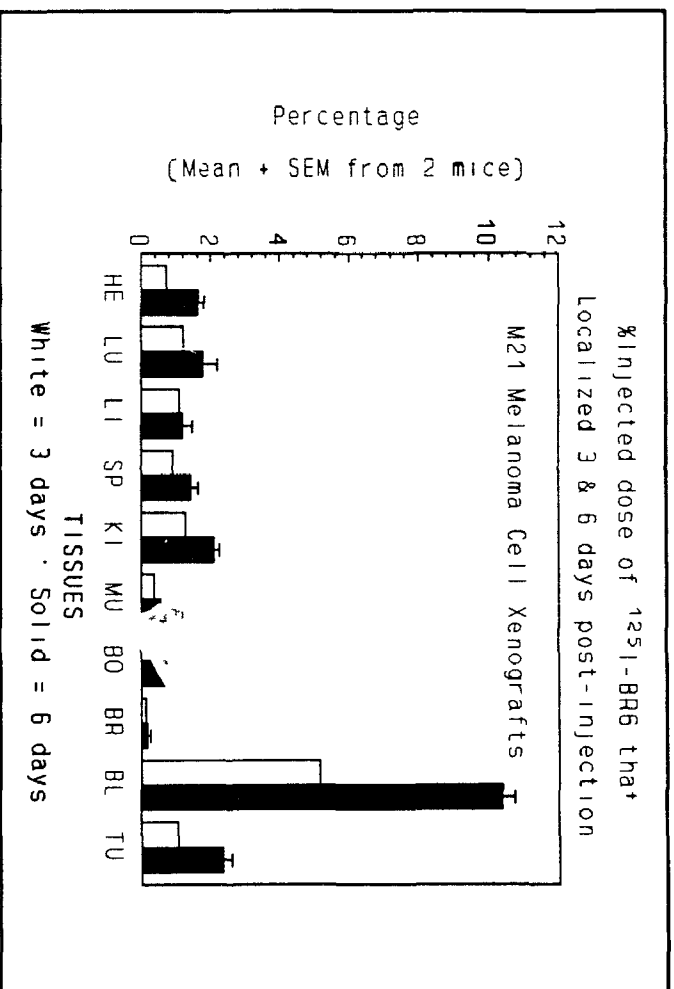


FIGURE 131

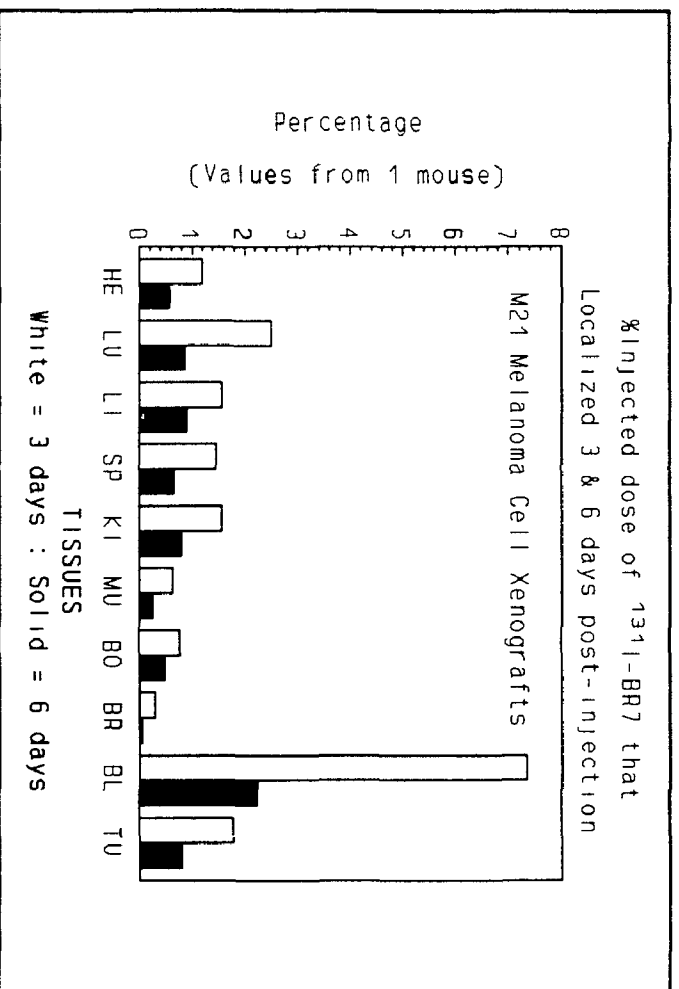


FIGURE 132

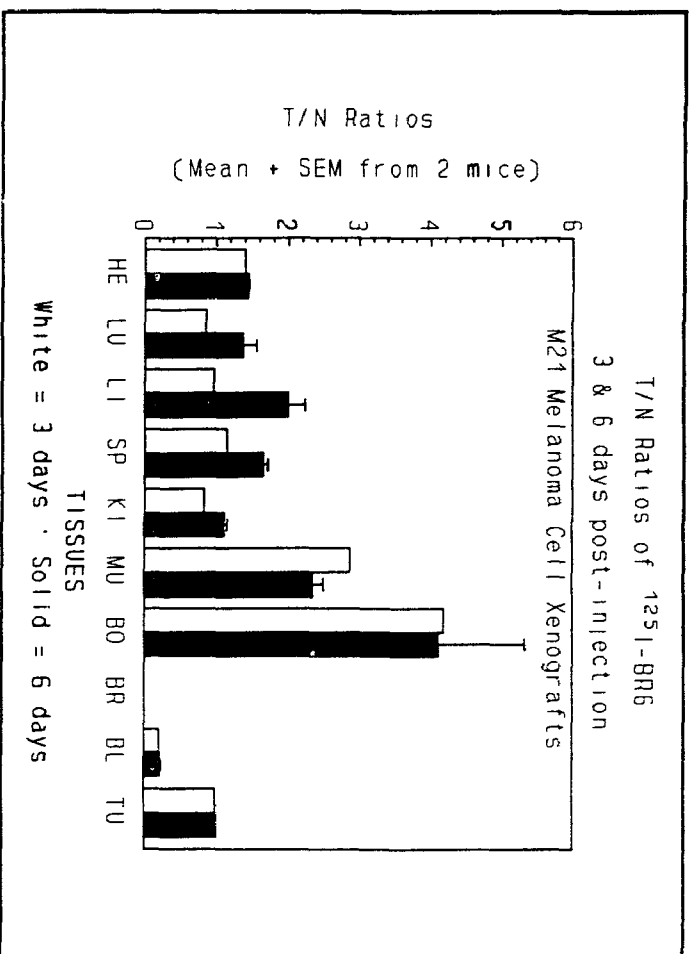


FIGURE 133

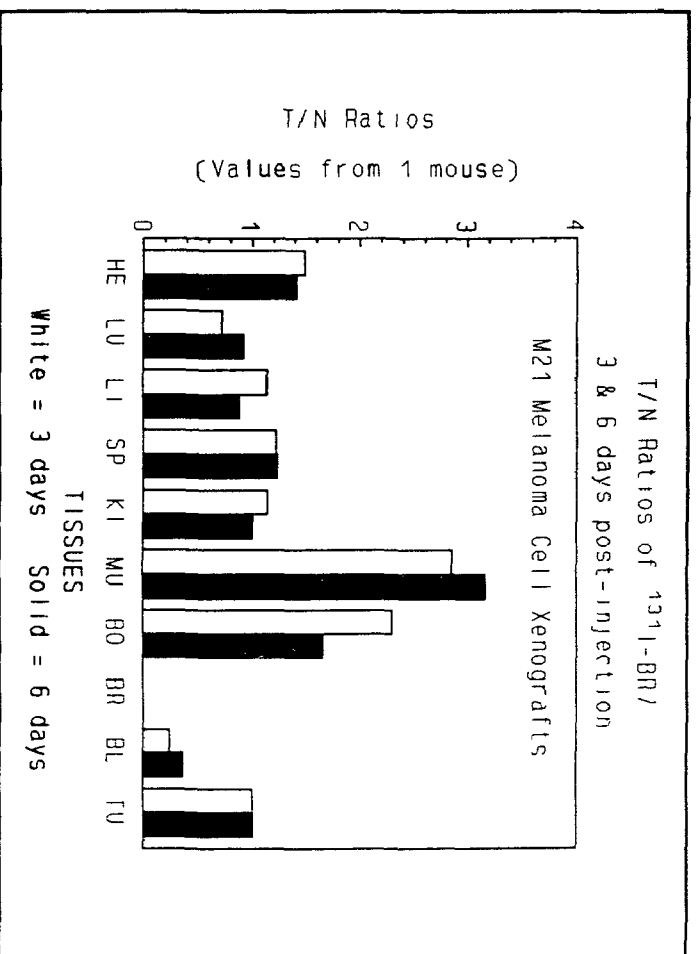


FIGURE 134

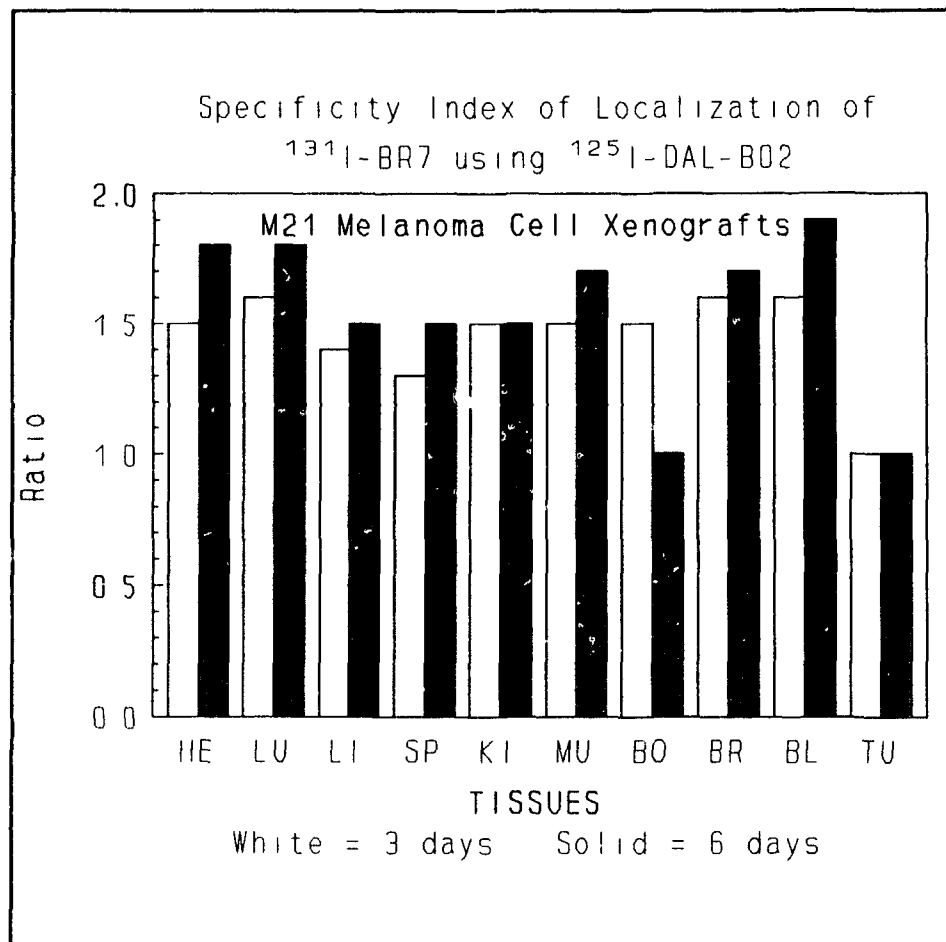


FIGURE 135

Figure 135 presents the SPIL ratios of DAL-BR7 for the tissues which were generally > 1 but < 1.8 at both day 3 and day 6.

13. In vivo Localization of DAL-BR6 Radiolabeled Using Either the PIB or Chloramine-T Method in HTB-19 Xenografts

These experiments evaluated the ability of two radiolabeled preparations of DAL-BR6, one prepared by the PIB method and the other prepared by the chloramine-T method, to localize in target xenografts. The nude mice with HTB-19 xenografts used in these experiments were not given Lugol's iodine in their drinking water prior to injecting the MABs intravenously. The reason for this was to assess the amount of radioactive iodine that localized in the thyroid gland of these animals when they were intravenously injected with the 2 different radiolabeled MAB preparations. Each mouse in one group was injected with approximately 10 uCi of ^{131}I -labeled DAL-BR6 (corresponding to 72 ug protein) prepared by the PIB method. Each mouse in a second group was injected with approximately 48 uCi of ^{125}I -labeled DAL-BR6 (also corresponding to 72 ug protein) prepared by the chloramine-T method. The IRF of ^{125}I -labeled DAL-BR6 using HTB-19 cells was 75% while the IRF of ^{131}I -labeled DAL-BR6 using the same cell line was only 12%. Despite the low IRF value of the labeled MAB prepared by the PIB method, it was decided to still determine the biodistribution of this agent in tumor-bearing nude mice. The amount of radioactivity that localized in the thyroid gland of these animals would reflect the degree of deiodination of this agent which occurs in vivo.

Figures 136 and 137 respectively show the amount of ^{131}I -labeled DAL-BR6 and ^{125}I -labeled DAL-BR6 that localized in each tissue at day 3 and day 6 post-injection. The corresponding percentage of the injected dose of each radiolabeled DAL-BR6 preparation that localized in the same tissues is presented in Figures 138 and 139. At day 3 and day 6, $<0.1\%$ of the injected dose of radiolabeled DAL-BR6 prepared by the PIB method localized in tumor. This amount that localized in tumor was far less than the 1% or greater amounts that localized in major organs such as liver, spleen and kidney. Also, this amount that localized in tumor at both days was far less than the 7.5% and 11% of the injected dose of radiolabeled DAL-BR6 prepared by the PIB method that localized in the thyroid glands of the mice respectively at day 3 and day 6. In contrast, approximately 4% of the injected dose of radiolabeled DAL-BR6 prepared by the chloramine-T method localized in tumor at both day 3 and day 6. This amount that localized in tumors was greater than the 1% or so that localized in most other tissues but far less than the 13% and 80% of the injected dose of radiolabeled DAL-BR6 prepared by the chloramine-T method that localized in the thyroid glands of these mice respectively at 3 and 6 days.

Figures 140 and 141 respectively present the T/N ratios of the 2 radiolabeled preparations of DAL-BR6 for the tissues. Radiolabeled DAL-BR6 prepared by the PIB method had T/N ratios much less <1 for major organs like liver, spleen and kidney as well as for neck at both day 3 and day 6. In contrast, radiolabeled DAL-BR6 prepared by the chloramine-T method was >2 for most tissues except blood and neck at day 6.

FIGURES 136 TO 141:

DATA OF EXPERIMENTS PERFORMED WITH NUDE MICE XENOGRAFTED WITH HTB-19 CELLS, INJECTED I.V. WITH RADIOLABELED DAL-BR6. THE MICE WERE NOT GIVEN LUGOL'S IODINE PRIOR TO THE INJECTIONS. DAL-BR6 WAS RADIOLABELED EITHER WITH ^{131}I USING THE PIB METHOD OR WITH ^{125}I USING THE CHLORAMINE-T METHOD. ONE GROUP OF MICE WAS INJECTED WITH THE PIB-METHOD PREPARATION WHILE ANOTHER GROUP OF MICE WAS INJECTED WITH THE CHLORAMINE-T-METHOD PREPARATION. MICE IN BOTH GROUPS WERE SACRIFICED EITHER ON DAY 3 OR DAY 6 POST-INJECTION. IN ADDITION TO ALL THE TISSUES THAT WERE EXCISED IN PREVIOUS EXPERIMENTS, THE NECK OF EACH MOUSE IN BOTH GROUPS WAS ALSO RESECTED, WEIGHED AND COUNTED FOR RADIOACTIVITY IN THESE EXPERIMENTS.

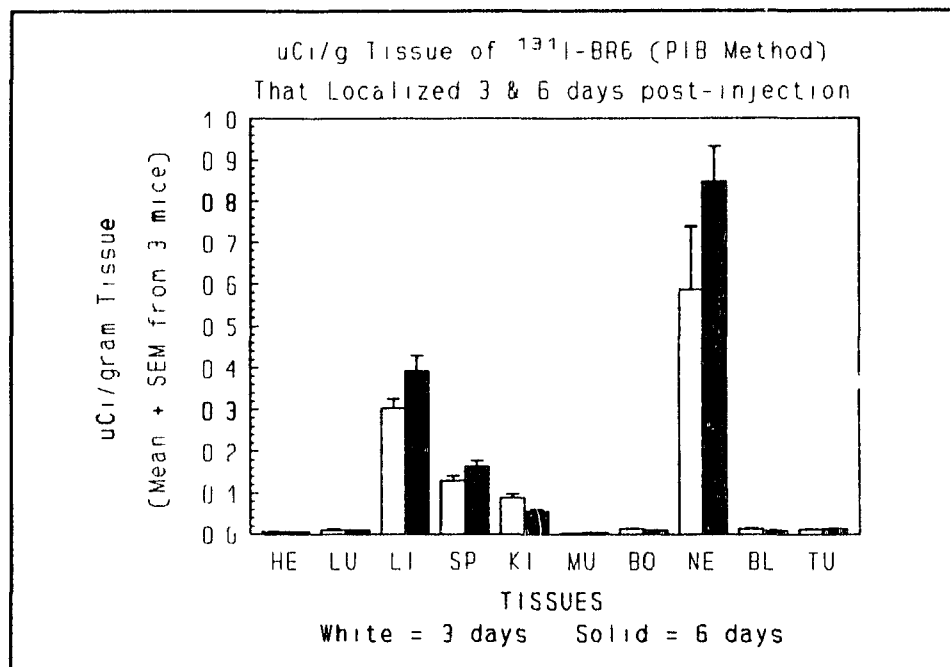


FIGURE 136

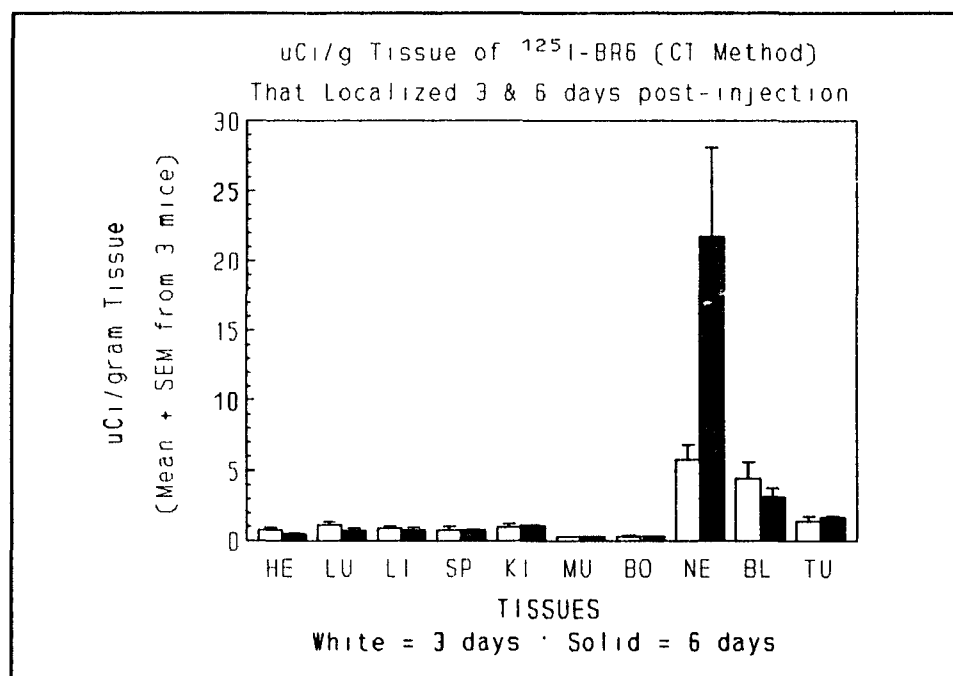


FIGURE 137

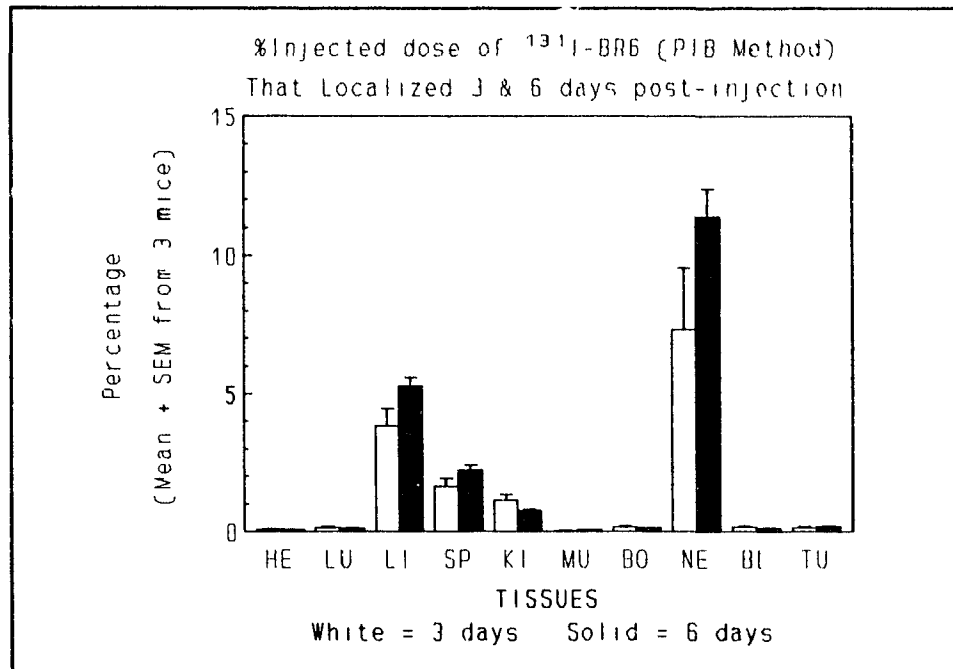


FIGURE 138

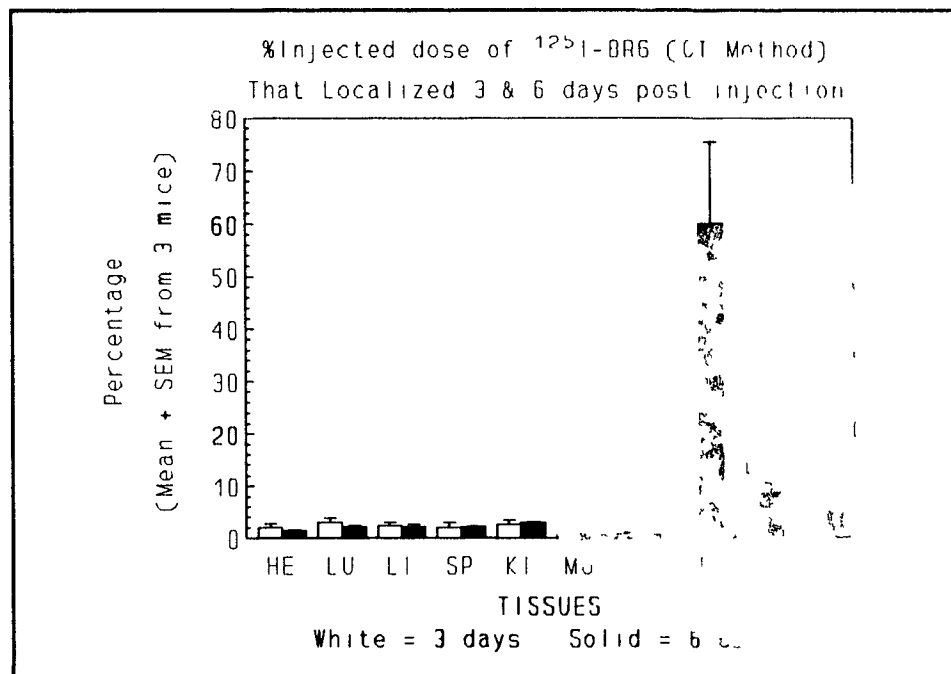


FIGURE 139

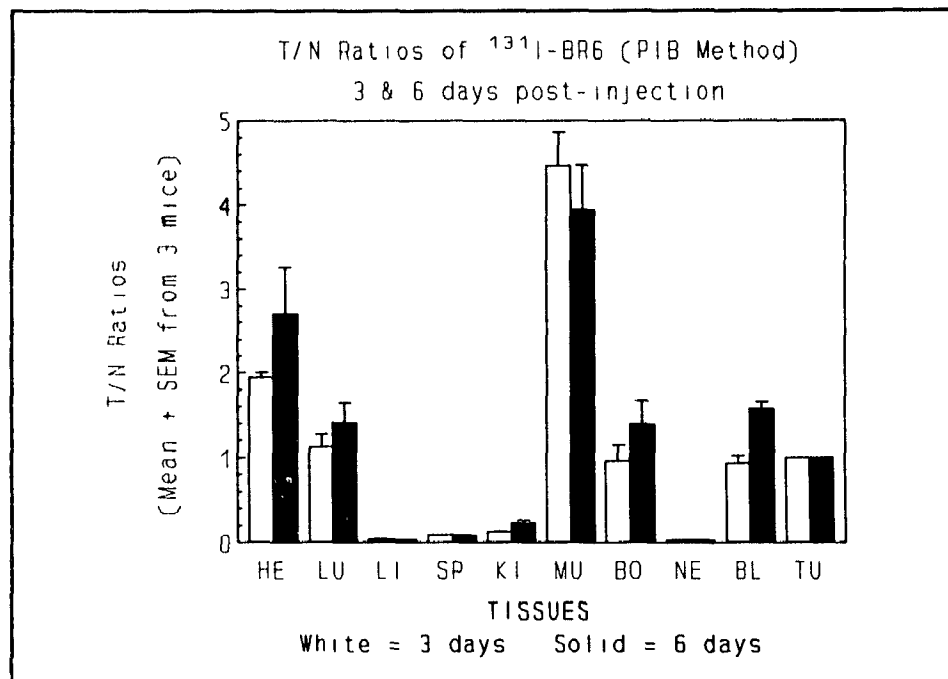


FIGURE 140

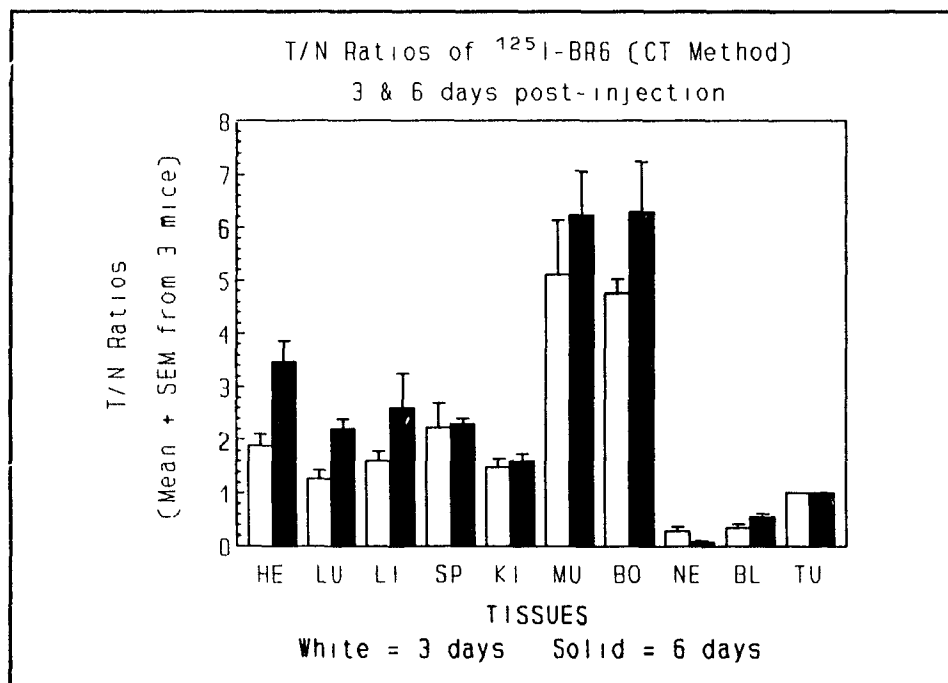


FIGURE 141

14. Autoradiography of Sections from HTB-19 Tumor Xenografts Excised From Mice 3 and 6 Days Post-intravenous Injection with Radiolabeled Anti-HMC MABs.

Autoradiography was done on 5 micron thick formaldehyde-vapor fixed, frozen sections of HTB-19 tumor xenografts that were removed from nude mice 3 and 6 days after they were intravenously injected with radiolabeled anti-HMC MABs. After developing and staining the sections with Hematoxylin-Eosin, light microscopy showed two patterns of deposition of silver grains on the sections which corresponded to the sites of radiolabeled MAB deposition. DAL-BR6 and DAL-BR7, the two MABs which were shown to react with a target cell-surface antigen, were localized along tumor cell surfaces and in vessels of the tumor xenografts. The results of an experiment with radiolabeled DAL-BR7 are shown in Figure 142. DAL-BR9 and DAL-BR11, two of the other 9 anti-HMC MABs which were shown to react with intracellularly as well as extracellularly located antigens, were localized more diffusely in sections of tumor xenografts and not confined in the tumor vasculature. The results of an experiment with radiolabeled DAL-BR11 are shown in Figure 143.

FIGURES 142 AND 143:

PHOTOGRAPHS OF AUTORADIOGRAPHS OF SECTIONS FROM HTB-19 TUMOR XENOGRAPHS REMOVED FROM NUDE MICE 3 DAYS AFTER INTRAVENOUS INJECTION WITH ^{131}I -DAL-BR7 (FIGURE 142) AND WITH ^{131}I -DAL-BR11 (FIGURE 143).

NOTE: IN FIGURE 142, THERE ARE GRAINS OF SILVER DECORATING THE TUMOR CELL SURFACES AND ALSO CONCENTRATED IN SMALL VASCULAR SPACES IN THE XENOGRAPHS. IN FIGURE 143, THERE ARE GRAINS OF SILVER DIFFUSELY COVERING TUMOR CELLS IN THE SECTION.

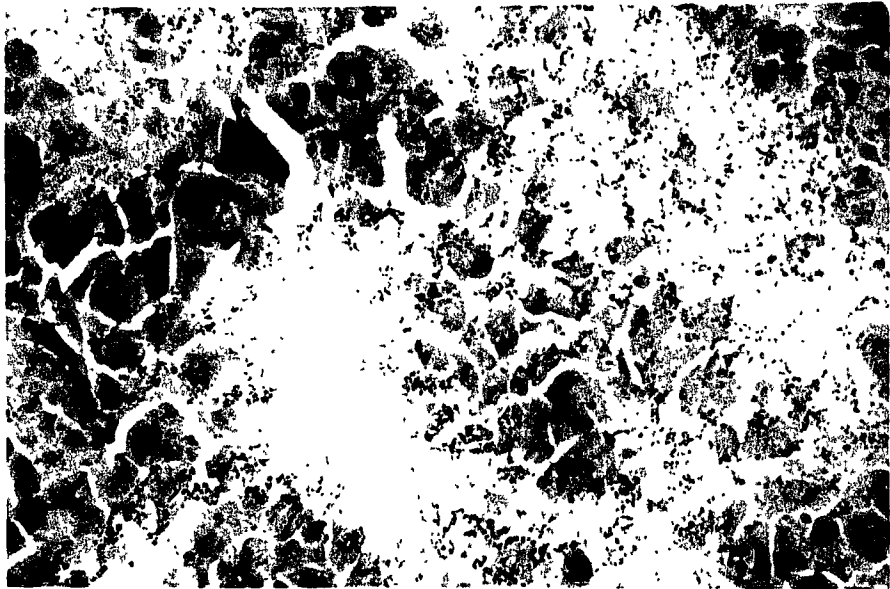


FIGURE 142

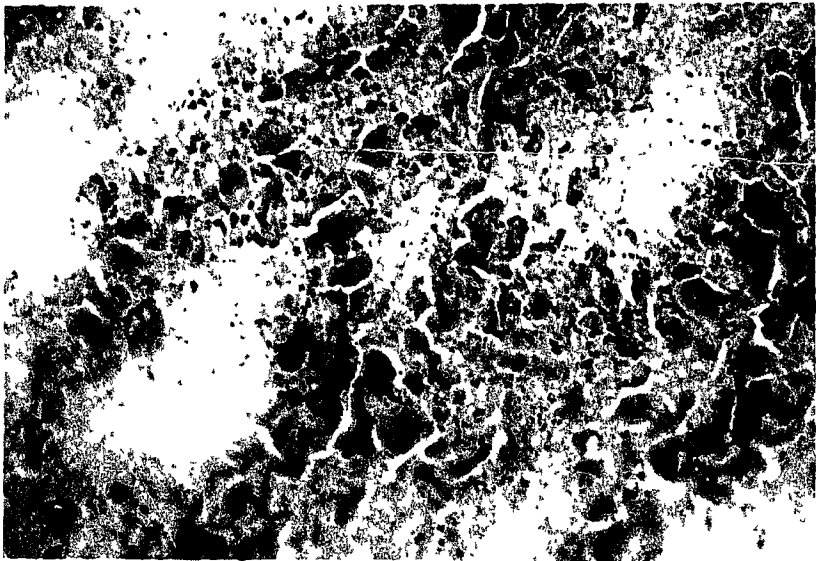


FIGURE 143

15. Summary of Radiolocalization Studies

The studies which evaluated the radiolocalization of each MAB or their F(ab)₂ fragments in the HTB-19 xenograft model demonstrated that these ¹³¹I-labeled agents did localize in tumors. In most cases, the amount of tumor-localized agent was sufficient to clearly detect the xenografts with gamma camera imaging. This was true irrespective of whether the MAB used was directed to a cell surface antigen, as was the case for both DAL-BR6 and DAL-BR7, or directed to cytosol and extracellular antigen(s), as was the case for DAL-BR5, DAL-BR9, and DAL-BR11. The clear gamma camera tumor images were partly due to the favorable T/N ratios observed in each experiment. However, the SPIL ratios in most experiments were just > 1 and < 2. The only experiment that demonstrated high SPIL ratios was the one using the F(ab)₂ fragment of DAL-BR6. As a result, this F(ab)₂ fragment demonstrated the most specific tumor localization of any agent tested.

The studies which evaluated the effect of injecting a combination of 2 radiolabeled MABs in the HTB-19 xenograft model demonstrated that the % injected dose of each MAB in the combination that localized in tumor was higher than that in experiments where each MAB was injected separately. A similar comparison showed that the T/N ratios were generally higher when each MAB was injected in combination than the T/N ratios when each MAB was injected alone. These findings were evident irrespective of whether the MABs were directed to the same antigen, as was the case for DAL-BR6 and DAL-BR7, or directed to different antigens, as was the case for DAL-BR7 and DAL-BR9.

The studies which evaluated the radiolocalization of DAL-BR7, when used alone or in combination with K45 in the Caki-1 xenograft model, demonstrated that in either case, DAL-BR7 did localize in these tumors and in amounts that clearly identified the tumors by gamma camera imaging. The T/N ratios and the SPIL ratios for DAL-BR7 were usually just higher than those in experiments using the HTB-19 xenograft model. These studies confirmed that DAL-BR7, which was known to react with both Caki-1 cells in vitro and frozen sections of Caki-1 xenografts, also localized in these tumors in vivo.

The studies which evaluated the radiolocalization of DAL-BR6 and DAL-BR7 in the melanoma xenograft model demonstrated that these 2 MABs, which were known to react with melanoma cells in vitro but not with frozen sections of melanoma xenografts, did not effectively localize in these tumors in vivo.

Finally, radiolabeling DAL-BR6 by the PIB method appeared to significantly decrease the immunoreactivity of this MAB to HMC cells. In addition, the biodistribution data of the MAB labeled by the PIB method showed a lower localization in the thyroid gland of the animals when compared to the data of this MAB labeled by the chloramine-T method. This finding is consistent with the possible decreased in vivo dehalogenation of ¹³¹I-labeled DAL-BR6 prepared by the PIB method. Similarly, the higher levels of radioactivity that localized in the thyroid gland of animals injected with ¹²⁵I-labeled DAL-BR6 prepared by the chloramine-T method is consistent with the dehalogenation known to occur in vivo with MABs radiolabeled by the chloramine-T method.

SUMMARY OF RESULTS

The 11 anti-HMC MABs, produced in Dr. Ghose's laboratory, could be purified from MAB-containing ascites fluid by either the Protein A or the caprylic acid method but the Protein A method yielded a more pure MAB preparation. However, despite the difference in purity of the preparations, MABs isolated by the caprylic acid method generally had comparable titers of MAB reactivity for target cells. This panel of 11 MABs consists of all murine IgG subclasses and all but 2 MABs have Kappa light chains. Furthermore, two of the MABs, DAL-BR6 and DAL-BR7, were able to induce caps on target cells after binding to their target antigen.

These MABs were shown to react with most, but not all, human carcinoma cell lines tested and with several fresh-frozen, unfixed breast cancer specimens. The reactivity with HMC specimens was heterogenous in terms of the number of specimens that reacted with each MAB, the percentage of tumor cells that reacted with each MAB, the staining intensity, and the site of tumor cells (i.e. cell surface or cytosol) that stained. There was limited or no reactivity to normal human tissues (including normal breast tissue), to non-epithelial tumor cell lines, and to a "normal" breast epithelial cell line, HTB-125. Several MABs did react with hyperplastic breast lesions and benign breast neoplasms but their reactivity with formalin fixed, paraffin embedded breast cancer specimens was reduced.

DAL-BR6 and DAL-BR7 were shown to react with a 47 KD cell surface antigen and to have overlapping epitopes. Of the other 9 MABs, DAL-BR2, 3, 9, and 11 immunoprecipitated a 73 KD antigen from target cells. The antigen(s) of all 11

MABs appear to be proteins but unlikely to be either of the common human or bovine milk proteins, CEA, or the vitronectin receptor which is expressed by HMC cells.

The MABs were shown to have on average, more than 10^6 binding sites per HMC cell and affinity constants between 10^7 and 10^8 M^{-1} . The IRF of DAL-BR6 and DAL-BR7, which react with the 47 KD antigen, was shown to be greater than 50% in most radiolabeled MAB preparations.

Radiolabeled preparations of DAL-BR6, DAL-BR7, K29, K45, and DAL-B02 could also be adsorbed onto gold particles. The immunogold studies demonstrated that MABs which bind to the surface of target cells get internalized.

While no MAB was directly cytotoxic to tumor cells, every MAB could agglutinate these cells and several MABs could inhibit their proliferation in vitro. Furthermore, the proliferation of HMC cells was specifically inhibited by exposure to the C13-ADM conjugate of MABs. The proliferation of MCF-7 cells was also selectively inhibited by exposure to the same agents. However, the sensitivity of HMC cells to either the CAA-ADM, C13-ADM, or MTX conjugate of MABs was usually much less than that to native drug.

The $F(ab)_2$ fragments of 4 MABs belonging to different murine subclasses were produced. However, only the pepsin digestion of the IgG_1 MAB resulted in high yield of its $F(ab)_2$ fragment.

Most radiolabeled MABs or their $F(ab)_2$ fragments localized in xenografted tumors and yielded distinct gamma camera tumor images. Of the agents evaluated, the $F(ab)_2$ fragment of DAL-BR6 had the most specific tumor localization.

DISCUSSION

Of the 2 standard purification methods investigated to isolate these MABs from ascites fluid, the Protein A affinity method was superior to the caprylic acid precipitation method in terms of the amount of MABs recovered as well as the ability of the method to yield an IgG preparation relatively free of contaminant proteins. However, in practice, the Protein A method is useful and efficient (in terms of the time and effort required) only when relatively small volumes of ascites fluid (5-10 ml or less) are being purified. This is because the Protein A columns progressively run slower with increasing volumes of ascites even when positive pressure is applied to the columns. The Protein A column flow is slower due to clogging by lipoproteins and other debris in the ascites fluid. These substances may be removed from the ascites fluid prior to Protein A purification by acetate buffer precipitation but this extra step prolongs the isolation procedure and lowers the IgG yield. Another drawback of the Protein A method is the possibility of denaturing the isolated MAB with the acidic elution buffer if the eluent is not promptly and adequately buffered. This buffering may also necessitate another dialysis step to equilibrate to PBS which may further dilute the isolate and may require reprecipitation of protein and further dialysis. All these manipulations defeat the purpose of an easy isolation procedure for MABs and decrease the yield of MABs. Furthermore, Protein A has a finite regeneration capacity and after the manufacturer's recommended number of runs, it is rather expensive to replace. For these reasons, particularly the fact that very limited volumes of ascites fluid could be handled efficiently by a Protein A column,

the rather inexpensive caprylic acid method, which could easily handle 50-100 ml of ascites fluid at a time, was used to produce the large quantities of MABs that were required for the bulk of the experiments.

It is interesting that the panel of anti-HMC MABs comprised the entire spectrum of murine IgG subclasses with 2 MABs possessing Lambda light chains and at least 2 other MABs reacting with overlapping antigenic determinants. The immunizing antigens in the HMC cells used in the production of the MABs must have been presented in a particularly immunogenic form. Our laboratory has described the production of MABs belonging to different murine subclasses directed to identical antigens before (Guha et al., 1990). Having MABs of different subclasses directed to different epitopes of the same target antigen may prove to be advantageous in the design of immunoassays to detect shed or secreted antigens in the serum or other body secretions from breast cancer patients. The rationale for this is that one MAB may be used to capture the antigen and another MAB of different subclass directed to a different epitope of the antigen may be used to detect the capture by using an appropriately tagged anti-subclass specific conjugate.

These MABs are referred to as anti-HMC in the thesis because they are produced by hybridomas formed with spleen cells from mice immunized with HMC cell lines. However, they really should be called anti-carcinoma MABs since they do react with a diverse array of human carcinoma cell lines including melanoma in vitro and in the case of RCC, also with xenografts. It is interesting that only 5 of 6 HMC cell lines were reactive to all 11 MABs. One of these positive reacting cell lines,

HTB-124, has a malignant phenotype in that it forms colonies in soft agar but it is not tumorigenic in nude mice unlike the other 4 positive reacting HMC cell lines. This cell line, also known as HBL-100, was derived from human milk cells of an apparently healthy woman and is diploid (Polanowski et al., 1976) but has an abnormal karyotype and is known to contain SV40 genetic information (Caron de Fromental et al., 1985). The one HMC line that was not reactive with the MABs, HTB-125, has a minimally malignant phenotype in that it can be propagated in vitro but not in soft agar or in nude mice and is considered a "normal" breast epithelium line by the ATCC. These results correlate well with the results of screening a panel of normal human tissues and surgical cancer specimens with the MABs. There was only very restricted reactivity of some of the MABs with mostly normal epithelial cells in a few organs but no reactivity with most normal tissues including breast epithelium. However, hyperplastic mammary duct epithelium, considered by pathologists as a preneoplastic condition (Elston, 1988), did show staining with 7 of our 11 MABs. Benign neoplastic breast lesions such as fibroadenoma also had ductal epithelial cells which were reactive with some MABs. Furthermore fresh frozen HMC, RCC, and some fresh melanoma biopsies reacted with a number of our MABs. These findings together with the results of screening cell lines indicate that the target antigen(s) for the MABs are detectable in carcinomas, in preneoplastic cells of benign breast conditions, and in cell lines with questionable or partial malignant phenotype such as HTB-124 but not in "normal" breast cell lines, such as HTB-125, or normal breast tissue. It is therefore possible that reactivity of cells with our MABs may be

an early sign of the neoplastic change. Further studies are needed to determine whether there are also correlations between the reactivity of lesions with our MABs and (1) the diagnosis of cancer and (2) the clinical course of patients with these lesions as was demonstrated with other anti-HMC MABs (Werner et al., 1991; Courtney et al., 1991; and Ceriani et al., 1992).

The finding that these MABs, which were produced against HMC, were also reactive with non-breast carcinomas including melanoma is not an unique occurrence (Ellis et al., 1984; Edwards et al., 1986; Pancino et al., 1989; Liao et al., 1990; Price et al., 1990; Larocca et al., 1991; and Pastan et al., 1991) and the reverse is not uncommon either (i.e. several MABs described earlier in the introduction to the thesis, which were produced against non-HMC carcinomas, were also reactive with HMC). Furthermore, anti-melanoma antibodies like HMB45 have been known to cross react with breast cancer as well as with normal breast tissue (Leong and Milios, 1989; and Bonetti et al., 1989). However, a more recent study has reported that these earlier findings of cross-reactivity may actually represent false-positive staining of these tissues with HMB45 as a result of excess background staining of sections due to improper technical use of this antibody (Bonetti et al., 1991). Several of the MABs did not react with sections of surgically excised cutaneous melanoma specimens and none reacted with sections of subcutaneous melanoma xenografts excised from nude mice. However, all the MABs reacted not only with melanoma cell lines but also with 100% of cells from surgically excised specimens as well as from xenografts that were grown in culture for 7-9 days. The expression of antigens by melanoma cells,

after growing in culture for several days, that are not expressed by the same type of cells growing in xenografts has been observed in Dr. Ghose's laboratory before and has been described by other authors as well (McCready et al., 1989). This occurrence may be attributed to the accelerated growth in the milieu of cell culture conditions that allow these melanoma cells to express a variety of antigens which are otherwise repressed when the same cells are grown in vivo as xenografts.

There was significant but variable reactivity of the MABs with unfixed, frozen sections of HMC surgical specimens and there was heterogeneous reactivity, as described earlier (page 262), of many MABs with tumor cells in a particular HMC specimen. This staining pattern of anti-HMC MABs with HMC specimens is not unusual and has been described before (Ellis et al., 1984). In addition, staining variability of anti-HMC MABs, such as those against human milk fat globules, with cells of the same morphology is neither an experimental artifact nor related to the mitotic cell cycle (Edwards, 1985). Compared to these results obtained with frozen sections, staining of sections from formalin fixed, paraffin embedded specimens with the MABs showed a marked reduction in the number of HMC specimens that were positive as well as the number of MABs that reacted with a given specimen. DAL-BR7 showed the most consistent staining with formalin fixed HMC specimens but also reacted, as did some other MABs, with benign breast lesions as well. As a consequence of these results, fresh-frozen, unfixed HMC specimens should probably be used in any future study that evaluates the immunohistological staining ability of a panel of our 11 MABs. One such study that may be considered in the future is to

investigate whether or not there is a relationship between the reactivity of HMC with the MABs and the clinical course of HMC patients.

The results from a number of investigations segregated the 11 MABs into 2 groups. The first group consisted of only 2 MABs, DAL-BR6 and DAL-BR7, which react with an identical cell surface Mr 47,000 dalton antigen while the second group consisted of the other 9 MABs which react with antigens present intracellularly and extracellularly. Four of these MABs in the second group immunoprecipitated an unlabeled high molecular weight antigen from the extracts of surface-labeled cells that under reducing SDS-PAGE conditions migrated at least partly to a band with an estimated Mr of 73,000 daltons. Unlike the other MABs, both DAL-BR6 and DAL-BR7 were able to induce caps on HMC cells and were shown by immunogold and electron microscopic studies to be endocytosed after binding to these cells (these studies will be discussed in more detail later).

Based on the results of enzyme digestion and heat treatment of target cells, the 47,000 dalton antigen recognized by DAL-BR6 and DAL-BR7 is likely to be a glycoprotein or glycolipid and sialic acid is not an integral part of the epitope for the two MABs. The apparent molecular weight of the target antigen for DAL-BR6 and DAL-BR7 is near the previously reported molecular weights of 2 cell-surface associated target antigens of 2 anti-HMC MABs that have been described by other authors (Edwards et al., 1986 and Larocca et al., 1991). However, as described below, there are both similarities and differences in a number of characteristics between the reactivity of DAL-BR6 and DAL-BR7 with their antigen and the

reactivity of each of the other 2 MABs with their respective antigens. The first antigen is the Mr 43,000 dalton cell-surface located glycoprotein defined by MAB 323/A3 which is secreted by a hybridoma produced from the spleen cells of a mouse immunized with MCF-7 (HTB-22) cells (Edwards et al., 1986). MAB 323/A3 has selectively localized in HMC xenografts in nude mice (Khaw et al., 1988) and the strong reactivity of cells in surgically excised breast tissue with this MAB against the 43,000 dalton antigen is highly indicative of carcinoma (Courtney et al., 1991). Like the antigen for DAL-BR6 and DAL-BR7, the 43,000 dalton antigen for 323/A3 is expressed on the same HMC lines as reported in this thesis but unlike the antigen for DAL-BR6 and DAL-BR7, which is also found on the HTB-124 (HBL-100) cell line, the 43,000 dalton antigen for 323/A3 is not. Like DAL-BR6 and DAL-BR7, 323/A3 did not react with most normal tissues including those of normal breast but 323/A3 reacted with normal colon and kidney epithelium but not with fallopian tube epithelium whereas the opposite pattern of reactivity with these tissues was observed with DAL-BR6 and DAL-BR7. Like DAL-BR6 and DAL-BR7, 323/A3 stained fibroadenomas and hyperplastic ductal epithelial cells but 323/A3 reacted with only 59% of formalin fixed, paraffin embedded HMC specimens whereas DAL-BR7 reacted with 88% of such specimens. Like DAL-BR6 and DAL-BR7, 323/A3 showed heterogenous staining of HMC specimens and of HMC cells in a specimen. Like DAL-BR6 and DAL-BR7, 323/A3 reacted with some non-HMC tumors but not with sarcomas. However, 7 of 9 formalin fixed, paraffin embedded colonic carcinoma specimens were reactive with 323/A3 whereas 0 of 4 similar specimens were reactive

with DAL-BR6 and DAL-BR7.

The second antigen is the Mr 46,000 dalton antigen component of the human milk fat globule protein which is an integral cell membrane protein whose cDNA has been cloned (Larocca et al., 1991) and which is recognized by MAB Mc³ and other MABs. This antigen is a glycosylated protein whose amino acid sequence does not code for a transmembrane domain but which is postulated to be anchored to the cell membrane either by an NH₂-terminal signal sequence or via other means such as an association with phospholipid or disulfide linkages with other membrane proteins. It also has sequence homology with the C1, C2 region of the light chain of the clotting factor VIII which is known to interact with phospholipid. Like the 47,000 dalton antigen of DAL-BR6 and DAL-BR7, this 46,000 dalton human milk fat protein antigen is expressed by several different carcinoma cell lines including HMC cell lines. MABs specific for this 46,000 antigen did not stain any formalin fixed, paraffin embedded normal breast tissues or non-breast tissues that were normal or malignant but did weakly stain the cytoplasm of tumor cells from some HMC specimens (Peterson et al., 1990). This is comparable to the staining pattern observed with DAL-BR6 using similar tissues except for its staining with some benign breast lesions. The staining pattern observed with DAL-BR7 using similar tissues, however, showed more reactivity with both malignant and benign breast tissues. It should also be noted that the 46,000 dalton antigen is found in the serum of breast cancer patients (Ceriani et al., 1982) indicating that this antigen either is secreted or shed by tumor cells into the blood stream or reaches the blood stream after tumor cell necrosis. Furthermore,

Mc8, which is another MAB that reacts with the 46,000 dalton antigen, has been shown to inhibit HMC xenografts grown in nude mice (Ceriani et al., 1987). In contrast, MABs DAL-BR6 and DAL-BR7 do not inhibit the proliferation of HMC cells in vitro.

The second group of 9 MABs react with an intracellularly and extracellularly located protein antigen that also does not need sialic acid to bind the MABs. Just recently, Dr. Luner has demonstrated that DAL-BR3 and DAL-BR5 have diminished reactivity with periodate oxidized cells indicating that part of their epitopes are carbohydrate in nature as well (personal communication). DAL-BR2, DAL-BR3, DAL-BR9, and DAL-BR11 also immunoprecipitated a 73,000 dalton protein band from extracts of HMC cells. Experiments in another laboratory that stripped the sugars from the large glycoprotein present in human milk fat globules yielded SDS-PAGE bands of Mr 68,000 and 72,000 daltons (Gendler et al., 1987) and considering the sensitivity of the deglycosylation and electrophoresis procedures, the Mr of the core protein antigen of human milk mucin is near the Mr of the immunoprecipitated antigen of these 4 MABs in our laboratory. However, milder deglycosylation methods used in recent studies have yielded an Mr of the core protein of the large glycoprotein in human milk fat globules closer to 200,000 daltons (Abe and Kufe, 1989). This correlates better with the cloned mRNA (to be described in greater detail later) of the core protein which is capable of coding for a protein between 170,000 to 230,000 daltons (Gendler et al., 1987; Siddiqui et al., 1988; and Gendler et al., 1988).

There are two other possible comparisons that can be made with the Mr 73,000

dalton antigen immunoprecipitated by the 4 MABs. The first comparison is with the Mr 76,000 dalton antigen immunoprecipitated by MAB 7B₁₀ which was produced against the HTB-133 (T47D) HMC cell line (Pancino et al., 1989) just as some of our MABs were. Like the 73,000 dalton antigen of our 4 MABs, this 76,000 dalton antigen is sensitive to trypsin but not to neuraminidase. Like our MABs, 7B₁₀ did not react with human milk fat globules but unlike our MABs, it did not react with HTB-124 (HBL-100) cells. Other differences from our results were that, using frozen sections, this 76,000 dalton antigen was recognized by 7B₁₀ in 50% of normal breast tissues as well as in a number of normal colon specimens, in apocrine ducts of skin, in ducts of the parotid gland, and in cells of luteal phase endometrium. Most of these normal tissues were not reactive with most of our MABs. Furthermore, 7B₁₀ reacted heterogeneously with HMC specimens like our MABs did but unlike our MABs, 7B₁₀ could detect the 76,000 dalton antigen in western blots of HMC extracts.

The second comparison is with the Mr 70,000 dalton human breast epithelial mucin-associated antigen that is a component glycoprotein of human milk fat globules (Larocca et al., 1990). MABs to this antigen have also been produced and characterized (Peterson et al., 1990). These MABs showed no staining with formalin fixed, paraffin embedded normal breast tissues, fibroadenomas or non-breast tissues, both normal and malignant. However, they only stained 2 of 48 HMC specimens. This is similar to the limited or no reactivity with similar tissues using our 4 MABs that immunoprecipitated the 73,000 dalton antigen. Furthermore, this 70,000 dalton protein is linked to the large glycoprotein of human milk fat globule by disulfide

bonds and also copurifies with the larger mucin complex (Duwe and Ceriani, 1989). HMC cell lines, including HTB-19 (BT20), HTB-22 (MCF-7), and HTB-133 (T47D), as well as other human cancer cell lines, including colonic, pancreatic, ovarian, and lung carcinoma cell lines, have been shown to contain high levels of mRNA coding for this 70,000 dalton antigen compared to the B-cell leukemia line, Raji, which does not contain high levels of this mRNA (Larocca et al., 1990). Two of these HMC cell lines containing the message for the synthesis of this 70,000 dalton protein were used to immunize mice for the production of our 11 anti-HMC MABs. However, the message for the synthesis of this protein is not restricted only to HMC cell lines. Considering the precision of the electrophoresis procedure and the polymorphism that can exist in the amount of carbohydrate that is attached to mucin glycoproteins (as will be discussed later), the 73,000 dalton Mr estimate of the antigen immunoprecipitated by DAL-2, DAL-BR3, DAL-BR9, and DAL-BR11 is indeed close to the 70,000 dalton protein just described. In addition, like the 70,000 dalton antigen which is known to be disulfide linked to the large human milk fat glycoprotein component, the 73,000 dalton antigen also appears to be disulfide linked to a larger protein. This was demonstrated by the observation that a 73,000 dalton protein band could be seen after SDS-PAGE only under reducing conditions where disulfide bonds are broken and by the observation that a large molecular weight protein stayed in the stacking gel during SDS-PAGE under non-reducing conditions where disulfide bonds remain intact. It is possible that the cell lines that were used to immunize the mice and which are known to synthesize this 70,000 dalton protein could have sensitized and stimulated murine

B-lymphocytes to this antigen resulting in the eventual production of / of our anti-HMC MABs. It should also be pointed out that the 70,000 dalton antigen like the previously discussed 46,000 dalton antigen is found in the serum of breast cancer patients (Ceriani et al., 1982) indicating again possible secretion or shedding of the antigen into the blood stream. This 70,000 antigen is present on the apical surface of normal breast epithelial cells and because of the disulfide linkages to human milk fat globule membranes, it has been postulated that this protein acts as a linker protein to hold the mucin complex together on the cell surface (Larocca et al., 1990). Furthermore, as will be discussed later when the results of the growth inhibition of HMC cells by some of our MABs are analyzed, one of the MABs specific for the 70,000 dalton antigen, McR2, has been reported to inhibit the growth of HMC xenografts in nude mice (Larocca et al., 1990; and Ceriani et al., 1987). The growth inhibitory effect on HMC xenografts by McR2 is similar to the growth inhibitory effect on HMC cells in vitro by 3 of the 4 MABs that immunoprecipitated the 73,000 dalton antigen. All these comparisons indicate that our 4 MABs that immunoprecipitated the 73,000 antigen may be specific for the same 70,000 dalton antigen that reacts with McR2 and other MABs. This 70,000 dalton mucin antigen is distinct from other breast-associated antigens in that there is no extended homology to the published amino acid sequence for any cloned structural mucin (Larocca et al., 1990). Also, there is only limited identity in the cDNA sequence that codes for this 70,000 dalton antigen with the cDNA sequence that codes for the MUC1 gene, whose structure and characteristics will be discussed later.

Assessing the reactivity of the MABs with known breast milk proteins and with the epithelial cancer marker CEA shows that only DAL-BR8 was reactive with human casein. However, casein is neither synthesized nor secreted by breast cancer cells and HMC specimens do not express this milk protein (Tjandra and McKenzie, 1988). Since DAL-BR8 is produced by a hybridoma constructed from the spleen cells of a mouse immunized with breast cancer cells (HTB-133 or T47D cells specifically) not known to express casein, it is unlikely that the antigen responsible for murine B-cell sensitization was human casein and therefore the target antigen for DAL-BR8 is unlikely to be casein. The possibilities may be that either the epitope of the antigen for DAL-BR8 is cross-reacting with the casein molecule or that the human casein product used in the ELISA assay to determine the reactivity of the MABs has small amounts of other contaminant breast proteins which might contain the epitope for DAL-BR8. Degradation peptide products resulting from the proteolytic action of plasmin in human milk have been known to contaminate otherwise immunologically homogenous preparations of human beta casein (Chtourou et al., 1985) and MABs to casein have been known to cross react with other human milk proteins such as alpha-lactalbumin, which has very little amino acid sequence homology with casein, indicating that the three-dimensional conformation of milk proteins, not the primary sequence, may be responsible for the cross-reactivity of MABs (Burchell et al., 1985). It should be noted that human caseins are heterogenous in their glycosylation and phosphorylation (Fiat et al., 1980; and Kunz and Lonnerdal, 1990) and this may account for the heterogeneity of its three-dimensional conformation.

As described in the introduction of this thesis, one of the targets for several anti-carcinoma MABs, including many that are called anti-HMC, is a group of high molecular weight glycoproteins or mucin molecules which are present either intracellularly, in the cell membrane, or extracellularly as secreted or shed products. These mucins have molecular weights of 250,000 to greater than 1 million daltons and are composed of 50-90% carbohydrate that is O-linked through N-acetylgalactosamine to serine and/or threonine of the core protein. At least 4 human genes designated MUC1 (on chromosome 1), MUC2 (on chromosome 11), MUC3 (on chromosome 7), and MUC4 (on chromosome 3) coding for these mucin molecules have been discovered and cloned (Porchet et al., 1991; Gross et al., 1992; and reviewed by Gendler et al., 1991; and Kim et al., 1991). The MUC1 gene, the first of the MUC genes to be cloned and whose complete cDNA is known (Gendler et al., 1988; Siddiqui et al.; Abe and Kufe, 1989; and Ligtenberg et al., 1990), codes for an identical core protein of the mucin produced in the breast, pancreas, and ovary but the mucin molecules from these sites are different due to the diversity of the attached carbohydrate. Of greater interest, there is altered glycosylation of this core peptide in carcinomas arising from these tissues. The core protein coded by the MUC1 gene as well as the other core proteins of mucins coded by the remaining human MUC genes have a consistent tandem repeat of amino acids. This amino acid sequence of the tandem repeat is different in each MUC gene product and as mentioned in the introduction of this thesis, the target of many anti-HMC MABs is a specific and often the most hydrophilic, sequence of this tandem repeat structure. The number of

tandem repeats in the core protein also varies in different individuals and this accounts for the observed polymorphism. Furthermore, since the tandem repeat structure acts like a skeleton for the linking of O-linked carbohydrate, the amount of attached carbohydrate also varies in mucin molecules causing a great diversity of the molecular weights of mucin. The MUC1 mucin therefore has been called by many names including polymorphic epithelial mucin (PEM), epithelial membrane antigen (EMA), and human milk fat globules (HMFG), the latter consisting of many glycoproteins derived from the MUC1 gene and with which many anti-HMC MABs react (Ceriani et al., 1992; and Ding et al., 1993).

In mice, the most immunogenic molecule of human milk fat globules and HMC cells appears to be the MUC1 mucin (Burchell and Taylor-Papadimitriou, 1989; and Ceriani et al., 1992). Therefore, it is not surprising that many MABs reported in the literature against breast cancer have specificity for MUC1 mucin epitopes. Since the production of our MABs involved immunizing mice with HMC cells, it is also possible that the target of some of our MABs may be this mucin molecule. The reason for the enhanced immunogenicity of human MUC1 mucin in mice, and hence an increased probability of producing MABs with MUC1 specificity, may be explained by comparing the murine MUC1 core protein sequence with its human counterpart and by examining the most common sequence of amino acids in the human core protein that comprises the epitope of many anti-HMC MABs. Such an evaluation reveals that the epitope of many anti-HMC MABs is PDTRP of the tandem repeat sequence of the human MUC1 core protein and that in the mouse, this sequence is replaced by

PATSA (Gendler et al., 1991). The inference is that the two charged amino acids, aspartic acid and arginine, which are present in the human MUC1 core protein but which are absent in its murine counterpart makes the human MUC1 protein very immunogenic in mice and accounts for the fact that many MABs are specific for this single epitope.

HTB-19 (BT20), HTB-22 (MCF-7), and HTB-133 (T47D) cells have been shown to possess mRNA for the core polypeptide of MUC1 mucin and the HTB-19 cell line expresses a sialomucin neoantigen which reacts with a MAB, DF3, that is specific for MUC1 (Gendler et al., 1987; Siddiqui et al., 1988; and Hull et al., 1989). Two of the cell lines mentioned above were used for immunizing mice in the production of our 11 MAB and since the MUC1 gene product is expressed by these cell lines, it is possible that the MUC1 antigen was the immunizing agent responsible for the generation of some of the MABs. Other results which support this hypothesis include those obtained from analyzing spent HMC culture medium for the presence of antigens that react with our MABs. Spent HMC culture medium was found not to contain any antigen that could react with any of our 11 MABs by ELISA. In contrast, Nonidet-P40 extracts of HMC cells were found by ELISA to contain highly immunoreactive antigen for all of our 11 MABs. The MUC1 protein is an integral transmembrane protein with an external domain, a transmembrane domain, and a cytoplasmic tail consisting of the carboxy terminal region (Jentoft, 1990; and Gendler et al., 1991). This mucin is not known to be secreted by most breast cancer cell lines and is not found in culture supernatants of these HMC cells (Gendler et al., 1991).

However a splicing event, that may be induced by hormonal signals in HMC cells, may occur to produce one or more different forms of MUC1 protein that are secretable (Williams et al., 1990). This alternative form of cDNA produced from splicing has not been identified in HMC cells like HPAF which produce and release large amounts of mucin in the spent culture media (Lan et al., 1990). The mechanism accounting for the presence of large quantities of mucin in human milk has yet to be definitively determined since it is not known whether this mucin is secreted by cells or whether this mucin arises in milk from the dissolution of the naturally unstable human milk globule membrane.

Furthermore, another HMC cell line, BT549, which is known to both express the MUC1 mucin on the cell surface and secrete large amounts of the MUC1 mucin into the cell culture medium, can be stimulated to express this mucin on the cell surface by fortifying the medium with insulin and hydrocortisone. Adding these supplements to the medium can increase the amount of mucin that is expressed by this cell line to levels 2-10 times more than the amount that is expressed by other cell lines such as HTB-22 (MCF-7), HTB-124 (HBL 100), and HTB-133 (T47D). However, in contrast to other cell lines like MCF-7 which do not secrete this mucin into the cell culture medium even with the addition of insulin and hydrocortisone, the BT549 cell line can secrete visible aggregates of the MUC1 mucin after growing in the supplemented medium (Williams et al., 1990). This secreted mucin in the medium was highly reactive with the anti-MUC1 MAB, MA5, in a slot blot assay that used the medium from freshly cultured BT549 cells. Still there is another study which

produced MABs by immunizing mice with either serum-free conditioned medium from MCF-7 cell cultures or extracts of MCF-7 cells (Kjeldsen et al., 1989). Every MAB produced in this study (8 generated from serum-free conditioned medium and 3 generated from cell extracts), reacted with components in the spent MCF-7 culture medium when tested by an ELISA that used wells coated with spent medium. Every MAB also stained MCF-7 cells by membrane immunofluorescence. The authors isolated a Mr 77,000 dalton "secreted" glycoprotein recognized by one MAB and a Mr 41,000 dalton "secreted" protein recognized by another MAB. The 41 KD protein is speculated to be homologous to cytokeratin or an enzymatically digested product of this molecule. It is possible that some of these components found in spent medium might have arisen from dead cells and may not be a product of cell secretion. It therefore appears that MABs which are specific for the MUC1 mucin do not usually react with any substance in the medium of HMC cell cultures and this lack of MAB reactivity to components in spent culture medium was also observed with our 11 anti-HMC MABs. It remains to be seen whether our 11 MABs can detect antigen in the serum or in body fluids, such as urine, of breast cancer patients as some of the anti-MUC1 MABs can. The pathogenetic mechanism which explains the presence of the MUC1 antigen in various body fluids of breast cancer patients is not yet elucidated and may not be related to the secretion of this antigen by tumor cells.

The location and function of the MUC1 mucin may also explain some of the results observed with our MABs. The membrane-bound MUC1 mucin, due to their O-linked sugar chains which are quite long and exist as semi-flexible rods, is expected

to extend its extracellular component far above the cell surface and protect the normal cell membrane from directly interacting with macromolecules or other cells (Jentoft, 1990). Cancer-associated mucins, on the other hand, often have altered or incomplete sugar chains (Hull et al., 1989; and Samuel et al., 1990) which may expose antigenic targets for MABs that are not accessible in normal cells or provide novel new epitopes for MABs to bind. The oligosaccharides of mucin molecules are known to serve as recognition signals for cells (Jentoft, 1990) and cell membrane-bound mucin participates in the maintenance of cell polarity possibly through interactions of its cytoplasmic domain with the microfilament cytoskeletal network (Parry et al., 1990). At high concentrations of MAB, the binding of some of our MABs to their HMC cellular antigens resulted in the detachment of cells from the culture wells and inhibited their proliferation. If the antigen of these MABs is the MUC1 mucin, then binding of MABs to this structure may alter the functions of cell membrane-bound mucin as described above and result in the observed findings. Other possibilities are that the MABs react with extracellular matrix components to which cultured HMC cells attach or with HMC cell receptors for these matrix components. HMC cell lines as exemplified by 734B cells appear not to synthesize extracellular matrix components such as type IV collagen, laminin, heparin, and chondroitin sulfate proteoglycans (Parry et al., 1990) but do express cell surface receptors for laminin (Terranova et al., 1983) and vitronectin as was demonstrated qualitatively in this thesis by showing HTB-19 and HTB-22 cells binding to these substrates. Vitronectin, which is present in the fetal calf serum used to make HMC cell culture medium, does form the

extracellular matrix component at the cell-substratum. HMC cells in culture do make contact with this component via their receptors and antibodies to the receptor can block attachment of HMC cells as well as promote detachment of HMC cells that have been in culture 24 hr prior to antibody addition (Parry et al., 1990). While similar observations of HMC cell detachment were made when high concentrations of some of our MABs were used in growth inhibition studies, none of our MABs were inhibited by anti-vitronectin receptor antibodies to bind to their antigens. This indicates that the target antigen for each of the 11 MABs is unlikely to be the vitronectin receptor.

To summarize the above, the similarities and differences between MABs and their target antigens reported in the literature and our panel of MABs and their target antigens have been discussed. To prove whether our MABs do in fact react with the 43,000 dalton antigen of MAB 323/A3 (Edwards et al., 1986) or with the 70,000 dalton antigen of MAB Mcr2 (Larocca et al., 1990) or with the MUC1 core protein or with the other possible antigens discussed above requires competition studies that compare the reactivity of our MABs with that of other well characterized MABs obtained from other authors and binding studies using our MABs with purified antigens such as the common 20 amino acid repeat sequence of the MUC1 mucin core protein. Since the cDNA of the MUC1 core protein and the cDNA of the 70,000 cell membrane-associated protein described by Larocca and colleagues (1990) are known, it may also be possible to synthesize these proteins here for these studies. There are now second generation anti-MUC1 MABs that have been produced by immunizing

mice with a peptide consisting of a sequence deduced from the MUC1 cDNA (Xing et al., 1992). It is hoped that in the future these MABs and antigens from other laboratories conducting breast cancer research can be obtained to conduct these studies or alternatively our MABs could be submitted for evaluation to international workshops on carcinoma-associated mucins such as the one held at San Francisco, USA (Taylor-Papadimitriou, 1991) or at Cambridge, UK, 1992.

To further characterize the MABs, it was possible to radioiodinate DAL-BR6 and DAL-BR7 with the chloramine-T method to a level of 3-5 ^{125}I atoms per 100 MAB molecules and obtain an immunoreactive fraction of most preparations greater than 50% and in some preparations as high as 97%. This is important when these radiolabeled MABs are used for imaging tumors in vivo. The affinity of binding constant as determined from a number of experiments was near 10^8 M^{-1} for DAL-BR7 and greater than 10^7 M^{-1} for DAL-BR6. The other 9 MABs also had an approximate affinity of binding constant of 10^7 M^{-1} and all 11 MABs had more than 1×10^6 binding sites per HMC cell. It has been stated that MABs with a million binding sites per tumor cell and affinity constants less than 10^8 M^{-1} will prove to be poor agents for radioimmunoimaging and drug targeting (Kennel et al., 1983) but as will be discussed later, most of our MABs did localize in tumor xenografts and in sufficient quantity to give distinct gamma camera tumor images. Also, as conjugates containing ADM in particular, most of our MABs also selectively inhibited the growth of tumor cells in vitro, albeit not as well as the free drug. Other authors have demonstrated the lack of correlation between binding of MABs to tumor cells in vitro and localization in

vivo (McCready et al., 1989).

Radiolabeled MABs were also used in experiments to map the epitopes recognized by DAL-BR6 and DAL-BR7. These experiments showed that DAL-BR7 could inhibit the binding of its radiolabeled counterpart to HMC cells by 80-95% whereas DAL-BR6 could only inhibit the binding of its radiolabeled counterpart by a maximum of 60%. However, DAL-BR7 could also just as effectively inhibit the binding of radiolabeled DAL-BR6 as could DAL-BR6. In contrast, although DAL-BR6 could inhibit the binding of radiolabeled DAL-BR7, it could not do it as effectively as could DAL-BR7 (i.e. DAL-BR6 could only achieve 70% of the binding inhibition observed with DAL-BR7). From these results it appears that the cell membrane-associated 47 KD protein, which is the target antigen for these 2 MABs, has overlapping epitopes for the 2 MABs and that the epitope of DAL-BR6 likely lies within a larger epitope for DAL-BR7.

Immunogold studies were also conducted to elucidate the conditions necessary to adsorb as many MAB molecules as possible onto gold particles and then to use these gold-labeled MABs in experiments that determined the fate of MABs that bind to the cell surface ultrastructurally. Prior labeling of these MABs with ¹²⁵I enabled the production of dual-labeled MABs and therefore also allowed us to monitor the radioactivity associated with the aliquots of cells taken for ultrastructural study. This radioactivity directly corresponded to the amount of cell-associated MAB in these specimens. The concentration variable isotherms at different pH conditions recommended in the literature for MABs were determined for our MABs only to

select the minimal amount of protein required to stabilize the gold particles at a particular pH. The pH at which more MAB molecules could be adsorbed onto gold was selected. The reason for this was that if more MABs could be adsorbed onto gold particles, there conceivably would be better binding of the reagent to target cells in the experiment. Since our MABs were radiolabeled, the process of adsorbing the MABs to gold particles could be monitored at every step. The centrifuged gold particle preparations that were produced not only had a specific number of gold particles as determined from the absorbance of the preparation but also had a specific number of MAB molecules adsorbed to each gold particle which could accurately be determined from the radioactivity of the preparation. The mere fact that radioactivity is associated with centrifuged pellets of gold particles testifies to the success of the adsorption procedure, the conditions of which were entirely based on the concentration variable isotherm data of each MAB. In addition, incubation of target cells with these dual-labeled MABs and subsequent monitoring of these cells both by determining the cell-associated radioactivity as well as by examining cell block sections ultrastructurally for gold particles demonstrated that there was specific binding of the dual-labeled MABs to target cells. These gold particles were also found in the cytosol after some time in a number of experiments indicating internalization of membrane-bound MAB by target cells.

The immunogold studies using DAL-BR6 and DAL-BR7 showed that these MABs were progressively internalized by HMC cells after they bound to the cell surface. Internalization of MABs may occur via different routes. They may be

endocytosed by endocytotic vesicles or taken in via non-coated plasma membrane invaginations or taken in via coated pits or coated vesicles, the latter two being similar to receptor-mediated endocytosis (Tilgen and Matzku, 1990). While some MABs after binding to their cell-surface located antigen may be rapidly internalized via coated pits, most MABs that are reactive with cell-surface antigens do not use this route to be internalized (Kyriakos et al., 1992). In fact, studies that determined the fate of antibodies bound to the surface of tumor cells *in vitro* have shown that antibody binding to the surface of viable cells is essentially an irreversible process and therefore the concept of affinity of the MAB for its antigen is not relevant (Kyriakos et al., 1992). This does not apply to a F(ab) fragment of an antibody since it can dissociate quickly after binding and hence bivalent attachment is necessary for this irreversible binding. Most MABs after binding to the cell surface are gradually internalized as a result of a normal turnover of cell-surface constituents via endocytosis not involving clathrin-coated pits or vesicles. It is also interesting to note that the ability to internalize proteins is often exhibited by tumor cell lines that are derived from tissues with protein secretory functions. Examples include HMC cells which can internalize cell-surface bound MAB (Della Torre et al., 1987) and a MAB that is specific for a component of the human milk fat globule membrane (Aboud-Pirak et al., 1988). The immunogold studies using DAL-BR6 and DAL-BR7 as well as those using K29 and K45 showed internalization of target cell-surface bound MAB by the more common route of cellular internalization of most reported MABs as described above (i.e non-coated plasma membrane invaginations). Once internalized,

virtually all the gold particles were within membrane bound vacuoles or disrupted organelles such as mitochondria. The cells which contained gold particles in disrupted mitochondria also contained nearby mitochondria and other cellular organelles that were intact indicating that these gold-containing cells were not dead. The most rapidly internalized cell-surface bound MAB was K29 and this was observed with both HTB-19 and Caki-1 cells. Cells from the experiments that used DAL-BR6, DAL-BR7, K29 and K45 all showed intracellular gold particles in various membrane-bound structures but only the gold particles associated with K29 localized in mitochondria.

The determination of the cell-associated radioactivity in specimens at 0 hr showed comparable amounts of DAL-BR6, DAL-BR7, and K29 bound to HMC cells and the electron microscopic examination of these same specimens supported this finding by showing no appreciable difference in the number of gold particles associated with HMC cells after incubation with any of these dual-labeled MABs. However, the cell-associated radioactivity in specimens at 0 hr indicated that a higher amount of K29 bound to Caki-1 cells than to HMC cells. The electron microscopic examination of these specimens also supported this finding by showing more gold particles associated with Caki-1 cells than with HMC cells after incubation with dual-labeled K29. These experiments demonstrated that the ability of DAL-BR6 or DAL-BR7 to bind to HMC cells is about the same but that the ability of K29 to bind to its natural target cell line exceeds the ability of K29 to bind to HMC cells. The findings may reflect the number of binding sites available for MABs on target cells recalling that DAL-BR6 and DAL-BR7 have about the same number of binding sites on the

HMC cell lines. There are about 1×10^6 binding sites for K29 per Caki-1 cell (Guha et al., 1991) and although the number of binding sites for K29 on HMC cells have not been determined, the results from these immunogold studies suggest that the number of available binding sites for dual-labeled K29 on HMC cells is less than those on Caki-1 cells.

Immunogold experiments also showed that dual-labeled K45 binds more to Caki-1 than to Caki-2 cells but that there was no significant binding of this agent to HMC cells which agrees with the known RCC restricted reactivity of K45 (Luner et al., 1986). An interesting finding was that after accounting for a higher specific activity of K45 compared to K29, there was comparable binding of these 2 MABs to Caki-1 cells at 0 hr as demonstrated by both cell-associated radioactivity determination and electron microscopic examination of these specimens. This finding was surprising since there is a 10 fold lower number of binding sites for K45 on this cell line compared to K29 (Guha et al., 1991). A possible explanation for this may be that relatively more K45 molecules and less K29 molecules could have initially bound to their respective available number of binding sites on Caki-1 cells as a result of the 100 fold higher affinity K45 has for its binding site compared to K29. An alternative explanation may be that steric factors may have hindered the binding of dual-labeled K29 to its antigen on target cells on the basis of the size of gold particles, especially if these antigens happen to be clustered.

Once bound to target cells, all the MABs showed some decline of bound radioactivity over time to generally stable levels except K45 and DAL-B02 with the

HMC cells where, in each case, there was no significant binding. Electron microscopic examination of sections of (1) HMC cells after incubating for 4 hr with dual-labeled DAL-BR6, DAL-BR7, or K29, of (2) Caki-1 cells after incubating for 4 hr with dual-labeled K29 or K45, and of (3) Caki-2 cells after incubating for 4 hr with dual-labeled K45 demonstrated gold particles intracellularly in various membrane bound bodies including lysosomes or their fusion product and organelles such as mitochondria. The significance of demonstrating that DAL-BR6 and DAL-BR7 as well as K29 and K45 are internalized by target cells, once binding of the MAB to cell-surface antigens occurs, is that drug-MAB conjugates may similarly be taken up by target cells. This satisfies one of the major goals for MAB-mediated drug targeting especially for the use of drugs that have intracellular targets.

Although each MAB could agglutinate viable HMC cells, none was cytotoxic to these cells in the presence of freshly obtained human AB serum as a source of complement. However, HMC cells exposed to MABs DAL-BR2, DAL-BR3, DAL-BR4, DAL-BR5, DAL-BR8, DAL-BR10 or DAL-BR11 either at concentrations of MAB greater than or equal to 100 ug/ml for a 6 hour pulse time period or at a concentration of MAB of 250 ug/ml for a continuous 7 day time period could inhibit the proliferation of these cells. Tumoricidal and tumor growth inhibitory effects of anti-HMC MABs on HMC xenografts in nude mice have been reported (Capone et al., 1983; and Ceriani et al., 1987) though the mechanism for these effects have not yet been defined. In one of these studies (Ceriani et al., 1987), MABs specific for the MUC1 core protein and those specific for the 46,000 dalton antigen (Larocca et

al., 1991) as well as the MAB reported by Larocca and colleagues (1990) to be specific for the 70,000 dalton antigen injected either alone or in combination as a "MAB cocktail" could inhibit the growth of HMC xenografts in nude mice. It remains to be seen whether our MABs that inhibit HMC cell proliferation in vitro can also inhibit HMC xenografts.

Subcutaneous inoculation of HMC cells (either HTB-19 or HTB-22 cells) with or without estradiol implants into nude mice that were either x-irradiated or not, did produce progressively growing tumors in about 60-70% of nude or SCID mice that were grafted with only the HTB-19 cell line. Regrafting tumor cells from growing xenografts into other mice did not increase the proportion of mice that produced tumors. Furthermore, in an attempt to produce HMC cell lines with possible greater in vivo growth as well as metastatic potential, transfection of the ras^H gene into HTB-19 and HTB-22 cells was attempted in Dr. Carole Waghorne's laboratory. The HTB-22 cell line has been transfected with ras^H gene before in another laboratory (Gelman et al., 1992) and these transfected cell lines while showing in vitro enhancement of invasive properties compared to the parental cell line, do not have increased metastatic properties in vivo. The results from Dr. Waghorne's experiment produced only HTB-22 transfectant cell lines and these cells did not grow well in nude mice. Difficulty in establishing and propagating breast cancers in culture and xenografts compared to other major tumor types is well known (Lewko et al., 1990) and while the reasons are not well understood, it may be related to the fact that breast tissue is composed of several different cell types and disruption of these critical cellular interactions in

culture or xenograft conditions could hamper the growth of HMC cells. Even when some HMC cell lines are xenografted into the mammary fat pad of the nude mouse there is only an increased, but not a 100%, take rate compared to subcutaneous xenografts (Price et al., 1990). While the metastatic potential of HMC xenografts also shows great variation (Thompson et al., 1992), the nude mouse can be used as an in vivo model to evaluate the capacity for HMC to invade and develop metastases especially when HMC cells in the xenograft are "tagged" with a marker like the lacZ gene (Brunner et al., 1993) which allows the detection of micrometastases. However, there are also in vitro assays to assess the invasion potential of HMC cells like the Boyden chamber invasion assay (Albini et al., 1987) or the new Matrigel-based assay (Bae et al., 1993). It will be interesting to see the effect that our panel of MABs, which can inhibit the proliferation of HMC cells in vitro, will have on the ability of HMC cells to grow, invade and metastasize either in vivo using models in nude mice or in vitro using the types of assays described above. It would be worthwhile to state that the effort to establish an in vivo HMC model in Dr. Ghose's laboratory was not in vain since all the mice that did develop tumors were utilized in radioimmunolocalization studies that evaluated a number of MABs or their F(ab)₂ fragments and the results of which will be discussed later.

Studies were also performed to evaluate the cell growth inhibitory effect of (1) two anti-cancer drugs (MTX and ADM); (2) MTX active ester conjugates of DAL-BR6 and DAL-BR7; (3) CAA-ADM and C13-ADM conjugates of DAL-BR6 and DAL-BR7; and (4) C13-ADM conjugates of DAL-BR8, DAL-BR9, and DAL-BR11.

The reasons for selecting DAL-BR6 and DAL-BR7 to prepare drug conjugates were that (1) they react with a cell membrane-associated antigen and, as discussed earlier, (2) they are internalized by target HMC cells after binding to their antigen and (3) they do not have a direct anti-proliferative effect on HMC cells. The reason for selecting MTX was that this drug binds to an intracellular target, dihydrofolate reductase, in order to inhibit the proliferation of cells. The reason for selecting ADM was that this drug not only has intracellular targets, topoisomerase II to name one, but also has cell surface effects to inhibit cell growth. The reason for selecting only the C13-ADM conjugate of MABs other than DAL-BR6 and DAL-BR7 to evaluate was that the experiments with the C13-ADM conjugate of DAL-BR6 or DAL-BR7 showed better tumor cell growth inhibition than with the CAA-ADM conjugate of each MAB. Finally, the reasons for selecting DAL-BR8, DAL-BR9, and DAL-BR11 from the panel of remaining MABs to make MAB-ADM conjugates were that (1) they had the highest titers of reactivity with HMC cells based on immunofluorescence and ELISA assays and (2) DAL-BR11 was one MAB that reacted with the 73,000 dalton antigen and could also inhibit the proliferation of HMC cells and (3) DAL-BR9 was one MAB that also immunoprecipitated the 73,000 dalton antigen but did not inhibit the proliferation of HMC cells and (4) DAL-BR8 was one MAB that did not immunoprecipitate an antigen but did inhibit the proliferation of HMC cells. The decisions for preparing MAB-drug conjugates were therefore based on the characteristics of the MABs that were determined in previous experiments.

Using native drug alone on both HMC cell lines, the IC_{50} for MTX was over

a 100 fold more than the IC_{50} for ADM. However, the two HMC cell lines tested did not show any difference in their sensitivity to ADM while the MCF-7 cell line was slightly more sensitive to MTX ($IC_{50} = 2.0$ ug/ml) than the HTB-19 cell line ($IC_{50} = 2.5$ ug/ml). The MTX-DAL-BR6 and MTX-DAL-BR7 conjugates had an identical IC_{50} on HTB-19 cells after a 6 hr pulse exposure that was about 2 times the IC_{50} of free drug. On MCF-7 cells, the IC_{50} of each MTX-MAB conjugate was less than what was observed with HTB-19 cells and the MTX-DAL-BR6 conjugate actually had an IC_{50} comparable to that of native drug. These findings correlate well with the results of the immunogold studies that used dual labeled MABs on the same 2 HMC cell lines. It was demonstrated that after 6 hours of incubation, the amount of cell-associated radioactivity was higher in MCF-7 cells than in HTB-19 cells with both DAL-BR6 and DAL-BR7. While these specimens from the immunogold studies at this 6 hr time interval were not examined with the electron microscope, earlier 4 hr specimens were examined and these demonstrated more intracellular than extracellular gold particles. Since the action of MTX is intracellular, it is conceivable that the lower IC_{50} of each MTX conjugate on MCF-7 cells may be due to better internalization of these conjugates by these cells than by the HTB-19 cells. An alternative explanation for the better growth inhibition of MCF-7 cells with each MAB-MTX conjugate may be that this cell line had a slightly lower IC_{50} for MTX (2.0 ug/ml) than the HTB-19 cell line did (2.5 ug/ml).

No such correlations could be made with either of the CAA-ADM or C13-ADM conjugate of DAL-BR6 and DAL-BR7. However, the CAA-ADM conjugates

of these 2 MABs had only slightly lower IC_{50} values on HMC cells (1.2 ug/ml to 3.0 ug/ml) than those observed with the MTX conjugates of the same MABs (1.9 ug/ml to 6.0 ug/ml). In contrast, the C13-ADM conjugates of these 2 MABs had significantly lower IC_{50} values (0.21 ug/ml to 0.30 ug/ml) on HMC cells than those observed with the MTX conjugates. Both the CAA-ADM and C13-ADM conjugates of the 2 MABs, nevertheless, had IC_{50} values on HMC cells that were well above those observed with free ADM ($IC_{50} = 0.015$ ug/ml). However, the C13-ADM conjugate of DAL-BR6 or DAL-BR7 appeared to be specifically cytotoxic to HMC cells since the IC_{50} of the C13-ADM conjugate of the nonspecific DAL-B01 on these cells was approximately 2-3 times more than that of either DAL-BR6-C13-ADM or DAL-BR7-C13-ADM .

A 6 hr pulse exposure of HMC cells to the C13-ADM conjugates of DAL-BR8, DAL-BR9, and DAL-BR11 also showed that these conjugates could inhibit the proliferation of these cells at generally comparable IC_{50} values as those observed using the conjugates of DAL-BR6 and DAL-BR7. Furthermore, with the exception of the growth inhibitory effect of the DAL-BR9 conjugate on HTB-19 cells, the IC_{50} values of all these MAB-C13-ADM conjugates were greater than twice the IC_{50} of the conjugate of the nonspecific DAL-B01. The observation that DAL-B01-C13-ADM could inhibit the growth of non-target HMC cells, though not as effectively as the conjugates of the anti-HMC MABs, possibly indicates that there was some cell surface action of ADM that contributed to the total growth inhibitory effect of the anti-HMC MAB conjugates. Another possibility that could account for the growth inhibitory

activity of the DAL-B01-C13-ADM conjugate on non-target HMC cells is the release of native ADM from the conjugate into the culture medium during the time these cells were exposed to the conjugate. This could occur from possible cell surface degradative action on the conjugate which was present in the cell culture medium and which could have interacted with cell surfaces. The released ADM could then directly inhibit the growth of these cells. The free drug would not have to be in too high a concentration in the medium to have a growth inhibitory effect on HMC cells since the IC_{50} of native ADM on HMC cells, as determined from another experiment, was only 0.015 ug/ml. Furthermore, there did not appear to be any clear cut correlation between the growth inhibitory activity of each MAB-ADM conjugate and the characteristics of the individual MABs with which conjugates were made.

There were similar findings in experiments with continuous exposure of HMC cells to the C13-ADM conjugates for 7 days except that lower concentrations of C13-ADM conjugates were needed to attain the same level of growth inhibition and that a non-target cell line, Caki-2, also showed some growth inhibition but not as much as observed with HMC cells. In contrast to the results of experiments that exposed cells to these agents for 6 hr, the MCF-7 cell line was more sensitive than other cell lines to continuous 7 day exposure. This finding concurs with the increased sensitivity of MCF-7 cells to MAB-MTX conjugates as discussed above. Additional findings in the experiments that evaluated a continuous 7 day exposure of cells to these C13-ADM conjugates include lack of specificity of these conjugates but selective growth inhibition of target cells, especially MCF-7 cells. This lack of specificity was

observed in experiments using ADM concentrations of each conjugate that exceeded the IC_{50} concentrations. Whether this lack of ADM conjugate specificity persists at concentrations below the IC_{50} , remains to be determined. However, even at these high ADM concentrations that were used, there still was selective inhibition of HMC cells.

The C13-ADM conjugates were more potent growth inhibitors than the CAA-ADM conjugates but none of these ADM conjugates inhibited the growth of cells as effectively as native ADM. The high potency of other C13-ADM conjugates has been described before (Greenfield et al., 1990) but unlike our C13-ADM conjugates, these were also more potent than native ADM. An ELISA assay of our C13-ADM conjugates demonstrated the titer of reactivity of these agents was either the same as or only 1-2 dilution factors less than that of native MAB. This finding also concurs with the retained immunoreactivity of the C13-ADM conjugates reported by Greenfield and colleagues (1990). In contrast, the growth inhibitory effect of CAA-ADM conjugates produced elsewhere has varied (Shen and Kyser, 1981; and reviewed by Ghose et al., 1983; and Ghose and Blair, 1987). The linkage used in this type of ADM conjugate is acid labile and therefore, cells which can internalize and route these conjugates into lysosomal compartments, can theoretically liberate free ADM from these conjugates (Ghose and Blair, 1987). The free ADM released in the cytoplasm could then exert growth inhibitory effects. However, if the conjugates remained intact after cell internalization, the CAA linkage to the amino sugar residue of the drug may impair the growth inhibitory activity of the agent. Furthermore, the

CAA-ADM conjugates produced from 2 of our MABs, DAL-BR6 and DAL-BR7, were shown by an ELISA assay to have diminished immunoreactivity when compared to that of native MAB or to that of each corresponding C13-ADM conjugate. The titer of reactivity of these CAA-ADM conjugates was 2-3 dilution factors less than that of the C13-ADM conjugates (or 4-6 dilution factors less than native MAB) and this reduced immunoreactivity may be the reason why there was less inhibition of target cell growth with these conjugates. It will be interesting to see if the CAA-ADM conjugate of MABs other than DAL-BR6 and DAL-BR7 also has reduced immunoreactivity to their respective antigen(s) or reduced growth inhibitory effect on target cells since the C13-ADM conjugates of these other MABs, for the most part, had similar growth inhibitory effects on target cells as did DAL-BR6 and DAL-BR7.

The optimal pepsin digestion conditions to prepare the F(ab)₂ fragments of 4 anti-HMC MABs that comprised all murine subclasses were also detailed in this thesis. Only DAL-BR6, an IgG₁ MAB could be digested with pepsin optimally and the resultant F(ab)₂ fragment could be recovered in quantities of high yield. The other 3 MABs belonging to other subclasses of IgG could be digested to their respective F(ab)₂ fragments but their yield was only 10-25%. This low yield of F(ab)₂ fragments of murine MABs other than those of the IgG₁ subclass after pepsin digestion has been recognized before and in particular, for the murine IgG_{2b} subclass. This subclass is particularly sensitive to proteases like pepsin (Demignot et al., 1989). While the amount of F(ab)₂ fragments purified from all 4 of these MABs was adequate to conduct the planned studies, a more suitable method of digestion using perhaps

another enzyme like ficin to obtain F(ab)₂ fragments of the MABs of subclasses other than IgG₁ is necessary. One type of study that requires large amounts of F(ab)₂ fragments and hence higher yields from enzymatic digestion of intact MABs is the preparation and evaluation of F(ab)₂-drug conjugates. Another study which also requires larger amounts of F(ab)₂ fragments is the evaluation of these fragments in breast cancer patients for both diagnostic and therapeutic purposes. Production of F(ab)₂ fragments of MABs belonging to subclasses other than IgG₁ for these types of investigations with pepsin digestion, as described in this thesis, is not economical since the yield of purified F(ab)₂ fragments with this digestion method is so low.

Radioimmunolocalization studies in tumor-xenografted nude mice were also presented. These studies used many of the 11 MABs in our panel and used the F(ab)₂ fragments of the 2 MABs which react with a HMC cell-surface 47,000 dalton antigen. The rationale for the selection of each MAB from our panel of 11 MABs that were used in these studies has been elaborated earlier in the thesis (page 172). All the MABs and the 2 F(ab)₂ fragments evaluated in these studies showed specific localization in tumor xenografts when compared to their localization in other tissues. Also, in most cases, very distinct gamma camera images of the xenografted tumors were obtained. Optimal imaging of the xenografted tumors with intravenously injected radiolabeled MABs was partly dependent on the type of collimator used with the gamma camera. Clear gamma camera images of tumors were obtained when a pinhole collimator was used in contrast to indistinct or blurred images of tumors that were observed due to diffuse body radioactivity when a wide field of view collimator

was used. This was quite evident when tumor-xenografted mice were injected with a MAB like DAL-BR7 and scanned with gamma cameras equipped with the 2 types of collimators. Also, imaging of mice injected with different MABs like DAL-BR6 and DAL-BR7 that had comparable T/N ratios of localization and absolute amounts of tumor localized radioactivity, yielded different qualities of tumor image due to the type of collimator used. Both these variables, the T/N ratio and absolute amount of tumor-localized radioactivity, are recognized as the determining factors in the sensitivity of gamma camera imaging (Bradwell et al., 1985).

In the studies using the HMC xenograft model, the biological half-lives of intravenously injected DAL-BR5 (IgG₁L), DAL-BR6 (IgG₁K), DAL-BR7 (IgG_{2b}K), and DAL-BR11 (IgG_{2a}K) all were between 1.6 to 2 days with DAL-BR7 having the longest half-life of 2 days followed by DAL-BR5 and DAL-BR11 both having half-lives of 1.8 days and by DAL-BR6 having a half-life of 1.6 days. In contrast, DAL-BR9 (IgG₃K) had a much longer half-life of 2.6 days. The rate of clearance of radiolabeled monoclonal antibodies from animals is influenced by the immunoglobulin subclass of the MAB used (Eccles et al., 1989) and by the strain of nude mice injected with the MABs (Sharkey et al., 1991). Also, the more denatured the radiolabeled MAB preparation is, the faster it is cleared. The importance of the rate of clearance of radiolabeled MABs as far as radioimmunoimaging is concerned lies in the selection of the optimal day post-injection to image patients with a gamma camera. It is desirable to use a radiolabeled MAB with a biological half-life of the radionuclide in humans that is as short as possible (hours to a few days) so that imaging of tumors

may be effectively done in a reasonable amount of time when the background body radioactivity has sufficiently cleared. However, the clearance rates of radiolabeled MABs in mice do not usually correlate well with the clearance rates of the same radiolabeled MABs in humans. This is exemplified by a pharmacokinetic study of an ^{111}In -labeled anti-HMC MAB which showed a 60-fold slower clearance of the radiolabeled MAB in mice than in breast cancer patients (Griffen et al., 1989) which indicates that prior to using radiolabeled murine MABs in patients, preliminary studies should be done to establish parameters such as the half-life of intravenously injected murine MABs. Recent advances may circumvent the variability observed with the clearance of different murine MAB subclasses since it is now possible to produce mouse-human chimeric antibodies consisting of different human IgG subclasses each with the specificity of a single mouse variable region as exemplified by the production of mouse-human chimeric F(ab)_2 fragments of the human IgG₁, IgG₂, and IgG₄ subclasses each with the same specificity for CEA (Buchegger et al., 1992).

Radiolabeled F(ab)_2 fragments of DAL-BR6 and DAL-BR7 were also evaluated in the HMC xenograft model. The biological half-lives of these two F(ab)_2 fragments were less than the half-lives of their parental MABs (0.3 days and 1.4 days respectively for the F(ab)_2 fragments of DAL-BR6 and DAL-BR7). This faster clearance of F(ab)_2 fragments as compared with the clearance of intact MABs has been described before by us (Guha et al., 1991) as well as by others (Goldenberg, 1988) and is postulated to be related to the smaller size of the F(ab)_2 fragments. A similar finding of rapid F(ab)_2 fragment clearance compared to the clearance of its parental

MAB was observed when radiolabeled preparations of an anti-HMC MAB and its F(ab)₂ fragment were studied in a HMC xenograft model in nude mice (Yemul et al., 1993). Both the T/N and SPIL ratios of localization of DAL-BR6 F(ab)₂ were the highest observed in all the radiolocalization studies conducted whereas these ratios of localization of DAL-BR7 F(ab)₂ were higher than those observed in radiolocalization studies using some MABs. However, only DAL-BR6 F(ab)₂ gave distinct gamma camera images of tumor. This was certainly due in part to the high ratios of localization observed but also due to the use of a pinhole collimator in this study. One of the reasons why DAL-BR7 F(ab)₂ did not give optimal gamma camera images of tumors may be that a wide field of view camera was used in this study since MABs with similar or lower ratios of localization did produce distinct gamma camera images when a pinhole collimator was used in those studies. It is interesting that although the % of injected dose of DAL-BR6 F(ab)₂ that localized in tumor at 2 and 3 days post-injection was only about 0.6%, there were very high T/N ratios of localization and tumors were clearly visualized on both days with very little background body radioactivity remaining on day 3. Furthermore, the high SPIL ratios for this agent indicate that of all the agents tested in the HTB-19 xenograft model, the F(ab)₂ fragment of DAL-BR6 was the most specifically tumor-localizing agent.

In contrast, the % of injected dose of DAL-BR7 F(ab)₂ that localized in tumor at 1 and 2 days post-injection was about 3%, which is much higher than the % of injected dose of DAL-BR6 F(ab)₂ that localized in tumor by day 2. However, the T/N ratios of localization for DAL-BR7 F(ab)₂ on day 2 were about 3, which is

comparable or better than the ratios observed in studies using other MABs as described above, but less than the ratios observed in the study using DAL-BR6 F(ab)₂. This may partially account for the obscured gamma camera tumor images observed in the study using DAL-BR7 F(ab)₂. Another reason that may have contributed to the suboptimal gamma camera images observed with DAL-BR7 F(ab)₂ compared to those observed with DAL-BR6 F(ab)₂ is that this F(ab)₂ fragment of DAL-BR7 did have a longer biological half-life than the F(ab)₂ fragment of DAL-BR6 which would account for the residual background body radioactivity obscuring the gamma camera images of the xenografts. Perhaps imaging mice with the gamma camera at 3 or more days post-injection with the F(ab)₂ of DAL-BR7 will yield better tumor images as a result of the clearance of background body radioactivity that is expected to occur over these longer times.

It is interesting that in these radioimmunolocalization studies using the panel of anti-HMC MABs we observed specific HMC tumor localization and gamma camera images of tumors irrespective of whether the MABs were directed to tumor cell-surface antigens or to antigens found inside and outside of tumor cells. Autoradiographs of sections from these xenografts demonstrated that the 2 MABs, DAL-BR6 and DAL-BR7 which are directed to the 47,000 dalton cell-surface antigen, were concentrated on the surface of tumor cells as well as in the tumor vasculature whereas the other MABs were diffusely distributed on tumor cells and not that concentrated in the tumor vasculature. While it is generally assumed that the optimal target for radioimmunolocalization, either for tumor detection or therapy, is a cell-

surface antigen, there are also internal antigens in breast cancer cells which are accessible to MABs (Dairkee and Hackett, 1988). Furthermore, DAL-BR6 and DAL-BR7 were shown to be internalized by HMC cells after they bound to their cell-surface antigen. This process may impact on the quality and diagnostic efficacy of tumor images, either negatively or positively, depending on a number of factors as now described. A complex inter-relation of a number of factors including choice of radioisotope, labeling technique, and biological events that occur after internalization determine the amount of retained or released radiolabel in tumor cells over time (Mariani et al., 1990) and impact on the quality of tumor images. The experiments that used DAL-BR6 and DAL-BR7 demonstrate that ^{131}I -labeling can be used to image tumors in nude mice. The tumor images obtained from the localization of ^{131}I -labeled MABs can be also be enhanced or optimized by technology such as Single-Photon Emission Computerized Tomography or SPECT, (Riggs et al., 1988) and more recently by technology that combines computerized tomography and SPECT, or CT-SPECT (Kramer and Noz, 1991; and Loats, 1993). The latter technique combines the precise anatomical localization of the high resolution CT images with the precise identification of functional abnormalities of the low resolution SPECT antibody images. The result is a remarkable decrease in the number of SPECT false positives as well as in the number of CT false negatives and an increase in the specificity of SPECT as well as an enhancement in the sensitivity of CT. Furthermore, SPECT can also assist in the planning of radioactive doses that must be given to patients to achieve diagnostic or therapeutic effects (Ljungberg and Strand, 1988).

In spite of the promise of using ^{131}I or other iodine isotopes labeled to MABs for radioimmunoimaging and radioimmunotherapy of tumors, there have been problems with the use of such radiolabels for these purposes. This is exemplified by ^{131}I which has a long 8 day half-life and whose beta decay accompanied by high energy gamma and x-rays with ranges from 80-740 keV causes an unacceptable amount of background radioactivity in many radioimmunoimaging studies. The beta decay of ^{131}I can have cytotoxic effects. Likewise, even though there may be a theoretical therapeutic effect of internalized MABs that are radiolabeled with ^{125}I which emits cascades of low energy electrons such as Auger or Coster-Kronig electrons that have radiobiological effects on DNA (Adelstein and Kassis, 1987), studies have not shown this to be the case (Aronsson et al., 1993). Another process which causes problems is the in vivo deiodination of MABs, which, not only decreases the amount of tumor-localized radioactivity but also concentrates the radioactive iodine in the thyroid gland of patients when there is inadequate blocking with administered iodine. There have been 2 approaches to solve these problems. The first is to select another radioisotope for radioimmunoimaging and to develop methods to conjugate the radioisotope to MABs; the second is to develop other methods to conjugate iodine isotopes to MABs so that they will be less susceptible to deiodination in vivo. Methods are now available to radiolabel MABs via metal chelates of the radioisotopes indium (^{111}In), bismuth (^{212}Bi), and yttrium (^{90}Y), which have favourable characteristics for medical imaging or therapy (Gansow, 1991) as well as technetium ($^{99\text{m}}\text{Tc}$) which is the common isotope used in many nuclear medicine

scans (Eckelman and Steigman, 1991). Methods are also available or being developed to conjugate MABs to the radioisotopes of rhenium (^{186}Re), lead (^{203}Pb), and copper (^{67}Cu) to name only a few (Breitz et al., 1992; Finn et al., 1991; Gansow, 1991; and Kozak et al., 1985). This diversity of available isotopes and methods to label MABs will allow the design and production of optimal radioimmunoimaging or radioimmunotherapy agents. In the case of HMC, MABs to the human milk fat globule have been labeled with $^{99\text{m}}\text{Tc}$ and radiation doses received by certain organs after the administration of the radiolabeled preparation were evaluated in primates (Calitz et al., 1993). The results of a number of clinical trials that evaluated the radioimmunotherapeutic potential of a number MABs labeled with a variety radioisotopes (including some of those described above) on both solid tumors and hematological malignancies have been reviewed (Langmuir, 1992). Radiosensitive tumors such as lymphomas have been responsive to radioimmunotherapy but solid tumors usually did not respond though no radioimmunotherapy studies of HMC were reported.

Traditional methods to iodinate MABs such as the chloramine-T, iodogen, or lactoperoxidase methods result in the labeling of predominantly tyrosine residues of MABs. The ortho-iodinated tyrosines produced with these traditional radioiodination methods have structures that mimic thyroid hormones and hence are susceptible to deiodinases which are present in a number of tissues (Enger and Burger, 1984). There are now several methods which use reagents that are all functionally similar to the Bolton-Hunter reagent (Bolton and Hunter, 1973) and that conjugate to lysine

residues (Khawli et al., 1991; Murray et al., 1991; Wilbur et al., 1991; Badger et al., 1990; and Vaidyanathan and Zalutsky, 1990). The iodinated product from these methods is a para-iodinated reagent which has a more stable carbon-iodine bond than the ortho-iodinated tyrosines obtained by the traditional methods and is not a substrate for the tissue deiodinases. This thesis described the in vivo radiolocalization of DAL-BR6 when it was labeled by one of these methods and reagents, PIB. The purpose of this study was to compare this PIB radiolabeled DAL-BR6 with a traditionally chloramine-T labeled DAL-BR6. There was a decrease in the amount of radioactivity that was localized in thyroid glands of mice injected with the PIB-labeled DAL-BR6 compared to the amount observed with the chloramine-T-labeled DAL-BR6 which indicates that there was likely less dehalogenation of the PIB-labeled MAB in vivo. However, the PIB-labeled DAL-BR6 had only an IRF of 12% and did not localize in xenografted tumors in this study indicating that PIB-labeling either alters the reactivity of DAL-BR6 with its antigen on tumor cells, probably as a result of lysine being part of the antigen binding site, or it denatures DAL-BR6, probably causing localization much more in organs such as liver, spleen, and kidney where excretion occurs. SPIL ratios were not determined in this experiment since a non-specific MAB labeled with a different iodine isotope was not injected along with either ¹³¹I-labeled DAL-BR6 or ¹²⁵I-labeled DAL-BR6. It will be interesting to see whether or not the labeling of other MABs in our panel (especially DAL-BR7 which reacts with the same antigen as DAL-BR6) using the PIB method will result in similar in vivo immunolocalization findings as observed in the experiment using PIB-labeled DAL-BR6.

A number of experiments also presented the data on the radiolocalization observed using pairs of anti-HMC MABs in the HMC xenograft model and using DAL-BR7 with or without K45 in the RCC xenograft model. It is well recognized that HMC, like many other tumors, consists of a heterogeneous cell population with variable expression of antigens that can be targeted. As such, many authors have suggested the use of MAB "cocktails" to target as many cells of the heterogeneous population found in tumors. This would conceivably allow either a definitive diagnosis to be established or allow comprehensive MAB-based immunotherapy to be administered. Therefore, using the HMC xenograft model, studies were conducted to evaluate the effect of injecting a pair of MABs that react with the same target antigen on tumor cells (DAL-BR6 and DAL-BR7) and of injecting a pair of MABs that react with different antigens on tumor cells (DAL-BR7 and DAL-BR9). Similarly, using the RCC xenograft model, studies were conducted to evaluate the effect of injecting DAL-BR7 and K45, which react with different antigens, either alone or in combination. Interestingly, although DAL-BR6 and DAL-BR7 partly share the same epitope on the 47,000 dalton cell-surface antigen, approximately equal amounts of each MAB localized in tumor when they were injected in combination and in amounts that exceeded that observed when injected individually. This type of enhanced binding of each MAB of a pair to tumor when injected together as opposed to when they are individually injected is not a unique occurrence since this observation as well as synergistic binding of MABs *in vitro* have been reported before (Saito et al., 1991). When DAL-BR9 was simultaneously injected with DAL-BR7,

even more DAL-BR7 bound than observed when DAL-BR6 was co-injected and about the same amount of DAL-BR9 bound as observed when it was injected alone. Also, distinct gamma camera images of tumor-localized DAL-BR7 in both these studies were observed. The implications of these results are that injecting "cocktails" of anti-HMC MABs which are directed to same or different antigens may be of value to enhance radioimmunoimaging of HMC tumors and perhaps also to enhance targeting of radionuclides or cytotoxic drugs to HMC tumors for therapy. Further studies are necessary to determine whether synergistic binding occurs with these MABs both in vitro and in vivo.

In the RCC xenograft model, DAL-BR7 when injected along with an irrelevant IgG localized in tumor in amounts comparable to or higher than that observed in the HMC xenograft model. The RCC xenografts were also clearly imaged with the gamma camera. In another study that was done using the melanoma xenograft model, DAL-BR7 as well as DAL-BR6 did not effectively localize in tumors. These results concur with the positive in vitro reactivity of the MABs with Caki-1 xenografts and the negative in vitro reactivity of the MABs with melanoma xenografts, as demonstrated by immunofluorescence assay. The implication of these results is that anti-HMC MABs can also potentially radioimmunoimage some different cancers like RCC but not others like melanoma. Further studies with other MABs in our panel using these and other xenograft models will identify other cancers besides HMC that may be radioimmunoimaged and that may be targeted for therapy with the anti-HMC MABs.

Injection of DAL-BR7 and K45 together into mice with RCC xenografts also showed a higher amount of each MAB that localized in tumor than when each MAB was injected along with an irrelevant MAB (the results of the radioimmunolocalization studies in the RCC xenograft model using K45 have previously been reported - Guha et al., 1991). There again appears to be enhanced tumor-localization of MABs when they are administered together as opposed to when they are administered alone. This observation appears to hold when the target antigens of the MABs are HMC related, as is the case for the target antigens of DAL-BR6, 7 and 9, or when the target antigens are clearly not related, as is the case for the target antigens of DAL-BR7 and K45. Further studies using other pairs of MABs from both the panel of 11 anti-HMC MABs and the panel of 3 anti-RCC MABs (Luner et al., 1986) will demonstrate whether this enhanced localization of MABs in tumor xenografts also occurs.

In conclusion, there is great potential to use these 11 anti-HMC MABs for the diagnosis and treatment of breast cancer or possibly other cancers like renal cell carcinoma. A good HMC xenograft model needs to be established in order to conduct studies that evaluate the potential of these MABs and MAB-drug conjugates to inhibit the growth of tumors in vivo. The results of tumor radioimmunolocalization are so promising that evaluation of these MABs in breast cancer patients is being planned by Ghose et al. To proceed with these clinical studies, it is necessary to produce and purify these anti-HMC MABs to standards established by the Food and Drug Administration of the USA and the Health Protection Branch of Canada. Although

there are many other experimental studies that can be done with these and other MABs that are available, one of the most urgent is the development of humanized versions of these MABs by genetic engineering. Once produced and characterized, these humanized MABs will more than likely find their way from the laboratory to the clinic at an accelerated pace. The results presented in this thesis have contributed to the knowledge of breast cancer and to the understanding of ways in which MABs may be used to diagnose and treat this disease. The results of future research will elucidate the full potential of these MABs in the fight against breast cancer.

ADDENDUM

An experiment was again performed to evaluate the direct cytotoxicity of the MABs using fresh human AB serum as a source of complement. Dr. S. Lee's laboratory at the Victoria General Hospital confirmed that the serum specimen used in this repeat experiment had complement activity up to a dilution of 1/32. For the experiment, HTB-19 cells were incubated at 37°C with each MAB at a concentration of 250 ug/ml in culture medium which contained human AB serum at a dilution of 1/10. Incubations in medium containing heat inactivated serum at the same dilution served as controls. Additional negative controls included incubations with the non-HMC specific MAB, DAL-B02, and with HTB-19 cells alone. The MABs studied in this experiment included DAL-BR3,4,5,6,7,8,9,10, and 11. Observations using the vital dye (trypan blue) exclusion test occurred after incubations for 0.5, 1, 2, 4, 6, 8 and 24 hours. None of the MABs tested demonstrated any complement-mediated cytotoxicity against HTB-19 cells at any time period. HTB-19 cells were, however, agglutinated by all the anti-HMC MABs but not by DAL-B02. The results of this repeat experiment are similar to the results of the experiment reported in the thesis that used a human AB serum specimen as source of complement but which did not have its complement activity confirmed.

REFERENCES

1. Aaltomaa S., Lipponen P., Eskelinen M., Kosma V.M., Marin S., Alhava E., and Syrjanen K. Prognostic Factors in Axillary Lymph Node-Negative (pN-) Breast Carcinomas. *Eur. J. Cancer* 27:1555-1559, 1991.
2. Abe M. and Kufe D. Sequence Analysis of the 5' flanking region of the DF3 Breast Carcinoma-Associated Antigen Gene. *Biochem. Biophys. Res. Commun.* 165:644-649, 1989.
3. Abe M. and Kufe D. Structural Analysis of the DF3 Human Breast Carcinoma-Associated Protein. *Cancer Research* 49:2834-2839, 1989.
4. Aboud-Pirak E., Sergent T., Otte-Slachmuylder C., Abarea J., Trouet A., and Shneider Y.J. Binding and Endocytosis of a Monoclonal Antibody to a High Molecular Weight Human Milk Fat Globule Membrane-Associated Antigen by Cultured MCF-7 Breast Carcinoma Cells. *Cancer Research* 48:3188-3196, 1988.
5. Adelstein S.J. and Kassis A.I. Radiobiological Implications of the Microscopic Distribution of Energy from Radionuclides. *Nucl. Med. Biol.* 14:165-169, 1987.
6. Albini A., Iwamoto Y., Kleinman H.K., Martin G.R., Aaronson S.A., Kozlowski J.M. and McEwan R.N. A Rapid In Vitro Assay for Quantitating the Invasive Potential of Tumor Cells. *Cancer Research* 47:3239-3245, 1987.
7. Aronsson E.F., Gretarsdottir J., Jacobsson L., Back T., Hertzman S., Lindegren S., Karlsson B., Lindholm L., Holmberg S., Hafstrom L., and Mattsson S. Therapy with ¹²⁵I-Labeled Internalized and Non-Internalized Monoclonal Antibodies in Nude Mice with Human Colon Carcinoma Xenografts. *Nucl. Med. Biol.* 20:133-

144, 1993.

8. Ashorn P., Kallioniemi O.P., Hietanen T., Ashorn R., and Krohn K. Elevated Serum HMFG Antigen Levels in Breast and Ovarian Cancer Patients Measured with a Sandwich ELISA. *Int. J. Cancer (Suppl.)* 2:28-33, 1988.
9. Baba M., Kobayashi T., Tamaki Y., Mishima H., Yagyu T., Morimoto H., Monden T., Shimano T., Tsuji Y., Murakami H., and Mori T. A Human Monoclonal Antibody Derived from Axillary Lymph Nodes of a Breast Cancer Patient Reactive to a Sulfated Glycolipid. *Hybridoma* 11:107-117, 1992.
10. Bacus S.S., Goldschmidt R., Chin D., Moran G., Weinberg D., and Bacus J.W. Biological Grading of Breast Cancer Using Antibodies to Proliferating Cells and Other Markers. *American J. Pathol.* 135:783-792, 1989.
11. Badger C.C., Wilbur D.S., Hadley S.W., Fritzberg A.R., and Bernstein I.D. Biodistribution of p-Iodobenzyl (PIB) Labeled Antibodies in a Murine Lymphoma Model. *Nucl. Med. Biol.* 17:381-387, 1990.
12. Bae S.N., Arand G., Azzam H., Pavasant P., Torri J., Frandsen T.L., and Thompson E.W. Molecular and Cellular Analysis of Basement Membrane Invasion by Human Breast Cancer Cells in Matrigel-Based In Vitro Assays. *Breast Cancer Research and Treatment* 24:241-255, 1993.
13. Bakir M.A., Eccles S.A., Babich J.W., Aftab N., Styles J.M., Dean C.J., and Ott R.J. c-erbB2 Protein Overexpression in Breast Cancer as a Target for PET Using Iodine-124-Labeled Monoclonal Antibodies. *J. Nucl. Med.* 33:2154-2160, 1992.
14. Ballow M., Levinson A.I., Gelfand E., and Schwartz S.A. Future Directions

- of Immunoglobulin Therapy: Foreword. *J. Clin. Immunol. Suppl.* 10:3-4, 1990.
15. Barbareschi M., Leonardi E., Mauri F.A., Serio G., and Palma P.D. p53 and c-erbB-2 Protein Expression in Breast Carcinomas: An Immunohistochemical Study Including Correlations with Receptor Status, Proliferation Markers, and Clinical Stage in Human Cancer. *American J. Clin. Pathol.* 98:408-418, 1992.
 16. Barsky S.H., Rao C.N., Hyams D., and Liotta L.A. Characterization of a Laminin Receptor from Human Breast Carcinoma Tissue. *Breast Cancer Res. Treat.* 4:181-188, 1984.
 17. Bartek J., Bartkova J., Vojtesek B., Staskova Z., Rejthar A., Kovarik J., and Lane D.P. Patterns of Expression of the p53 Tumour Suppressor in Human Breast Tissues and Tumours In Situ and In Vitro. *Int. J. Cancer* 46:839-844, 1990.
 18. Baschong W. and Wrigley N.G. Small Colloidal Gold Conjugated to Fab Fragments or to Immunoglobulin G as High-Resolution Labels for Electron Microscopy: A Technical Overview. *J. Electron Microscopy Technique* 14:313-123, 1990.
 19. Beesley J.E. Colloidal Gold: A New Perspective for Cytochemical Marking. *Royal Microscopical Society Microscopy Handbooks #17*, Oxford University Press, N.Y., pp. 1-59, 1989.
 20. Begent R.H.J. and Pedley R.B. Antibody Targeted Therapy in Cancer: Comparison of Murine and Clinical Studies. *Cancer Treatment Rev.* 17:373-378, 1990.
 21. Belanger D., Moore M., and Tannock I. How American Oncologists Treat

Breast Cancer: An Assessment of the Influence of Clinical Trials. *Journal of Clin. Oncol.* 9:7-16, 1991.

22. Benz C.C., Scott G.K., Sarup J.C., Johnson R.M., Tripathy D., Coronado E., Shepard H.M., and Osborne C.K. Estrogen-Dependent, Tamoxifen-Resistant Tumorigenic Growth of MCF-7 Cells Transfected with HER2/neu. *Breast Cancer Research and Treatment* 24:85-95, 1992.

23. Bergh J.C.S. Monoclonal Antibodies for Therapy of Human Malignant Tumors. *Eur. J. Surg. Suppl.* 561:59-64, 1991.

24. Bergmann J.F., Lumbrosa J.D., Manil L., Saccavini J.C., Rouger P., Assicot M., Mathieu A., Bellet D., and Bohuon C. Radiolabeled Monoclonal Antibodies Against Alpha-fetoprotein for In Vivo Localization of Human Hepatocellular Carcinoma by Immunotomoscintigraphy. *Eur. J. Nucl. Med.* 13:385-390, 1987.

25. Bertino J.R. Karnofsky Memorial Lecture: Ode to Methotrexate. *Journal of Clin. Oncol.* 11:5-14, 1993.

26. Bieglmayer C., Szepesi T., Neunteufel W., and Nowotny C. MCA, A Monoclonal-Antibody-Defined Breast-Tumor-Associated Antigen and its Relation to CA 15.3. *Tumor Biol.* 10:232-242, 1989.

27. Bieglmayer C., Szepesi T., Kopp B., Hoffman G., Petrik W., Guettuoche K., Grundler S., Gregorits M., and Strasser M. CA15.3, MCA, CAM26, CAM29 are Members of a Polymorphic Family of Mucin-Like Glycoproteins. *Tumor Biol.* 12:138-148, 1991.

28. Bolton A.E. and Hunter W.M. The Labeling of Proteins to a ¹²⁵I Containing

Acylating Agent. *Biochem. J.* 133:523-539, 1973.

29. Bonadonna G., Valagussa P., Brambilla C., Moliterni A., Zambetti M., and Ferrari L. Adjuvant and Neoadjuvant Treatment of Breast Cancer with Chemotherapy and/or Endocrine Therapy. *Seminars in Oncology* 18:515-524, 1991.

30. Bonetti F., Colombari R., Manfrin E., Zamboni G., Martignoni G., Mombello A., and Chilosi M. Breast Carcinoma Positive for Melanoma Marker (HMB-45): HMB-45 Immunoreactivity in Normal and Neoplastic Breast. *American J. Clin. Pathol.* 92:491-495, 1989.

31. Bonetti F., Pea M., Martignoni G., Mombello A., Colombari R., Zamboni G., Scarpa A., Piubello Q., Bacchi C.E., and Gown A.M. False-Positive Immunostaining of Normal Epithelia and Carcinomas with Ascites Fluid Preparations of Antimelanoma Monoclonal Antibody HMB45. *American J. Clin. Pathol.* 95:454-459, 1991.

32. Bradwell A.R., Fairweather D.S., Dykes P.W., Keeling A., Vaughn A., and Taylor J. Limiting Factors in the Localization of Tumours with Radiolabeled Antibodies. *Immunol. Today* 6:163-170, 1985.

33. Breitz H.B., Weiden P.L., Vanderheyden J.L., Appelbaum J.W., Bjorn M.J., Fer M.F., Wolf S.B., Ratliff B.A., Seiler C.A., Foisie D.C., Fisher D.R., Schroff R.W., Fritzberg A.R., and Abrams P.G. Clinical Experience with Rhenium-186-Labeled Monoclonal Antibodies for Radioimmunotherapy: Results of Phase I Trials. *J. Nucl. Med.* 33:1099-1112, 1992

34. Brouillet J.P., Theillet C., Maudelonde T., Defrenne A., Simony-Lafontaine J., Sertour J., Pujol H., Jeanteur P., and Rochefort H. Cathepsin D Assay in Primary

Breast Cancer and Lymph Nodes: Relationship with c-myc, c-erb-B-2, and int-2 Oncogene Amplification and Node Invasiveness. *Eur. J. Cancer* 26:437-441, 1990.

35. Brunner N., Boysen B., Romer J., and Spang-Thomsen M. The Nude Mouse as an In Vivo Model for Human Breast Cancer Invasion and Metastasis. *Breast Cancer Research and Treatment*. 24:257-264, 1993.

36. Buchegger F., Pelegri A., Hardman N., Heusser C., Lukas J., Dolci W., and Mach J.P. Different Behaviour of Mouse-Human Chimeric Antibody F(ab)₂ Fragments of IgG₁, IgG₂, and IgG₃ Sub-class In Vivo. *Int. J. Cancer* 50:416-422, 1992.

37. Burchell J., Bartek J., and Taylor-Papadimitriou J. Production and Characterization of Monoclonal Antibodies to Human Casein: A Monoclonal Antibody that Cross-React with Casein and Alpha-Lactalbumin. *Hybridoma* 4:341-350, 1985.

38. Burchell J. and Taylor-Papadimitriou J. Antibodies to Human Milk Fat Globule Molecules. *Cancer Invest.* 17:53-61, 1989.

39. Calitz M.M., Van Aswegen A., Van Der Merwe M.M.J., and Lotter M.G. Radiation Doses Obtained from ^{99m}Tc-labeled Human Milk Fat Globule Monoclonal Antibodies. *Nucl. Med. Biol.* 20:145-148, 1993.

40. Callahan R. and Campbell G. Mutations in Human Breast Cancer: An Overview. *J. Natl. Cancer Inst.* 81:1780-1786, 1989.

41. Capone P.M., Papsidero L.D., Croghan G.A., and Chu T.M. Experimental Tumoricidal Effects of Monoclonal Antibody Against Solid Breast Tumors. *Proc. Natl. Acad. Sci. USA* 80:7328-7332, 1983.

42. Carbone P.P. Adjuvant Therapy of Stage II Breast Cancer. *Cancer* 65:2148-

2154, 1990.

43. Caron de Fromental C., Nardeaux P.C., Soussi T., Laviaille C., Estrade S., Carloni G., Chandrasekaran K., and Cassingena R. Epithelial HBL-100 Cell Line Derived from Milk of an Apparently Healthy Woman Harbours SV40 Genetic Information. *Exp. Cell Res.* 160:83-94, 1985.
44. Ceriani R.L., Sasaki M., Sussman H., Wara W.M., and Blank E.W. Circulating Human Mammary Epithelial Antigens in Breast Cancer. *Proc. Natl. Acad. Sci. USA* 79:5420-5424, 1982.
45. Ceriani R.L., Blank E.W., and Peterson J.A. Experimental Immunotherapy of Human Breast Carcinomas Implanted in Nude Mice with a Mixture of Monoclonal Antibodies Against Human Milk Fat Globule Components. *Cancer Research* 47:532-540, 1987.
46. Ceriani R.L. and Blank E.W. Experimental Therapy of Human Breast Tumors with ¹³¹I-labeled Monoclonal Antibodies Prepared Against the Human Milk Fat Globule. *Cancer Research* 48:4664-4672, 1988.
47. Ceriani R.L., Peterson J.A., Blank E.W., and Lamport D.T.A. Epitope Expression on the Breast Epithelial Mucin. *Breast Cancer Res. and Treat.* 24:103-113, 1992.
48. Ceriani R.L., Chan C.M., Baratta F.S., Ozzello L., DeRosa C.M., and Habif D.V. Levels of Expression of Breast Epithelial Mucin Detected by Monoclonal Antibody BrE-3 in Breast-Cancer Prognosis. *Int. J. Cancer* 51:343-354, 1992.
49. Chtourou A., Brignon G., and Ribadeau-Dumas B. Quantification of Beta-

Casein in Human Milk. *J. Dairy Res.* 52:239-247, 1985.

50. Clarke R., Thompson E.W., Leonessa F., Lippman J., McGarvey M., Frandsen T.L. and Brunner N. Hormone Resistance, Invasiveness, and Metastatic Potential in Breast Cancer. *Breast Cancer Research and Treatment* 24:227-239, 1993.

51. Colcher D., Zalutsky M., Kaplan W., Kufe D., Austin F., and Schlom J. Radiolocalization of Human Mammary Tumors in Athymic Mice by a Monoclonal Antibody. *Cancer Research* 43:736-742, 1983.

52. Colcher D., Milenic D.E., Ferroni P., Roselli M., and Schlom J. In Vivo and In Vitro Clinical Applications of Monoclonal Antibodies Against TAG-72. *Nucl. Med. Biol.* 18:395-401, 1991.

53. Collier B.D. and Foley W.D. Current Imaging Strategies for Colorectal Cancer. *J. of Nucl. Med. Suppl.* 34:537-540, 1993.

54. Corcoran D. and Walker R.A. Ultrastructural Localization of Milk Fat Globule Membrane Antigens in Human Breast Carcinomas. *J. Pathology* 161:161-166, 1990.

55. Corcoran D., Jones J., and Walker R.A. In Vitro Modulation of Cellular Localization of Milk Fat Globule Membrane Antigens in Human Breast Carcinomas. *J. Pathology* 164:127-133, 1991.

56. Cote R.J., Rosen P.B., Lesser M.L., Old L.J., and Osbourne M.P. Prediction of Early Relapse in Patients with Operable Breast Cancer by Detection of Occult Bone Marrow Micrometastases. *J. Clin. Oncol.* 9:1749-1756, 1991.

57. Courtney S.P., Williams S., and Mansel R.E. Monoclonal Antibody 323/A3: A Marker for the Presence of Breast Carcinoma. *Cancer Letters* 57:115-119, 1991.

58. Cummings J., Willmott N., and Smyth J.F. The Molecular Pharmacology of Doxorubicin In Vivo. *Eur. J. Cancer* 27:532-535, 1991.
59. Czuppon A.B. Characterization of a New Tumor Associated Antigen from Mammary Carcinoma Cells by Monoclonal Antibodies. *Biochem. Int.* 15:359-372, 1987.
60. Dairkee S.H. and Hackett A.J. Internal Antigens Accessible in Breast Cancer: Implications for Tumor Targeting. *J. Natl. Cancer Inst.* 80:1216-1220, 1988.
61. Dalton W.S. Mechanisms of Drug Resistance in Breast Cancer. In: *Recent Advances in the Management of Lung and Breast Cancer (Proceedings of a Symposium Held Jan., 1990 in Tucson, AZ)*. *Seminars in Oncology* 17 (Suppl. 7):37-39, 1990.
62. Della Torre G., Canevari S., Orlandi R., and Colnaghi M.I. Internalization of a Monoclonal Antibody Against Human Breast Cancer by Immunoelectron Microscopy. *British J. Cancer* 55:357-360, 1987.
63. DeMey J. The Preparation and Use of Gold Probes. In: *Immunocytochemistry: Modern Methods and Applications*, 2nd Edition. Polak J.M. and Van Noorden S. (Editors), Wright, Bristol, pp. 115-144, 1986.
64. Demignot S., Garnett M.C., and Baldwin R.W. Mouse IgG_{2b} Monoclonal Antibody Fragmentation: Preparation and Purification of Fab, Fc, and Fab/c Fragments. *J. Immunol. Methods* 121:209-217, 1989.
65. Devine P.L., Bronwyn A.C., Birrell G.W., Layton G.T., Ward B.G., Alewood P.F., and McKenzie I.F.C. The Breast Tumor-Associated Epitope Defined

by Monoclonal Antibody 3E1.2 is an O-Linked Mucin Carbohydrate Containing N-Glycolylneuraminic Acid. *Cancer Research* 51:5826-5836, 1991.

66. Dillman R.O. Monoclonal Antibodies for Treating Cancer. *Ann. Intern. Med.* 11:592-603, 1989.

67. Ding L., Lalani E.L., Reddish M., Koganty R., Wong T., Samuel J., Yacyshyn M.B., Meikle A., Fung P.Y.S., Taylor-Papadimitriou J., Longenecker B.M. Immunogenicity of Synthetic Peptides Related to the Core Peptide Sequence Encoded by the Human MUC1 Mucin Gene: Effect of Immunization on the Growth of Murine Mammary Adenocarcinoma Cells Transfected with the Human MUC1 Gene. *Cancer Immunol. Immunother.* 36:9-17, 1993.

68. Diociaiuti M., Molinari A., Calcabrini A., and Arancia G. Electron Energy-Loss Spectroscopy Analysis of Adriamycin-Plasma Membrane Interaction. *Journal of Microscopy* 164 (Part 2):95-106, 1991.

69. Duda R.B., August C.Z., Rosen S.T. and Radosevich J.A. Monoclonal Antibody 44-3A6 as a Marker for Breast Carcinoma. *Tumor Biol.* 12:254-260, 1991.

70. Duwe A.K. and Ceriani R.L. Human Milk Fat Globule Membrane Derived Mucin is Disulfide-Linked Heteromer. *Biochem. Biophys. Res. Commun.* 165:1305-1311, 1989.

71. Eccles S.A., Purvies H.P., Styles J.M., Hobbs S.M., and Dean C.J. Pharmacokinetic Studies of Radiolabeled Rat Monoclonal Antibodies Recognizing Syngeneic Sarcoma Antigens: 1. Comparison of IgG Subclasses. *Cancer Immunol. Immunother.* 30:5-12, 1989.

72. Eckelman W.C. and Steigman J. Direct Labeling with ^{99m}Tc . Nucl. Med. Biol. 18:3-7, 1991.
73. Edwards P.A.W. Heterogenous Expression of Cell Surface Antigens in Normal Epithelia and Their Tumors, Revealed by Monoclonal Antibodies. British J. Cancer 51:149-160, 1985.
74. Edwards D.P., Grzyb K.T., Dressler L.G., Mansel R.E., Zava D.T., Sledge G.W. Jr., and McGuire W.L. Monoclonal Antibody Identification and Characterization of a Mr 43,000 Membrane Glycoprotein Associated with Human Breast Cancer. Cancer Research 46:1306-1317, 1986.
75. Ellis I.O., Robins R.A., Elston C.W., Blamey R.W., Ferry B., and Baldwin R.W. A Monoclonal Antibody, NCRC-11, Raised to Human Breast Cancer. I. Production and Immunohistological Characterization. Histopathology 8:501-506, 1984.
76. Elston C.W. Pathological Aspects of Breast Cancer Screening. Aust. N.Z. J. Surg. 58:355-363, 1988.
77. Engler D. and Burger A.G. The Deiodination of the Iodo-thyronines and of their Derivatives in Man. Endocrine Rev. 5:151-184, 1984.
78. Epenetos A.A. (Chairman). Advances in the Applications of Monoclonal Antibodies in Clinical Oncology. Proceedings of the 4th International Meeting Held in the Wolfson Institute, Royal Postgraduate School, Hammersmith Hospital, London, UK. 5-7 May, 1987. Int. J. Cancer Suppl. 2:1-133, 1988.
79. Eriksson E., Schimmelpenning H., Silfversward C. and Auer G. Immunoreactivity with Monoclonal Antibody A-80 and Nuclear DNA Content in

- Benign and Malignant Human Breast Disease. Human Pathol. 23:1366-1372, 1992.**
80. **Fanger M.W., Morganelli P.M., and Guyre P.M. Bispecific Antibodies. Critical Reviews in Immunology 12:101-124, 1992.**
81. **Fantyl V., Richards M.A., Smith R., Lammie G.A., Johnstone G., Allen D., Gregory W., Peters., Dickson C. and Barnes D.M. Gene Amplification on Chromosome Band 11q13 and Oestrogen Receptor Status in Breast Cancer. Eur. J. Cancer 46:423-429, 1990.**
82. **Fiat A.M., Jolles J., Aubert J.P., Loucheux-Lefebvre M.H. and Jolles P. Localization and Importance of the Sugar Part of Human Casein. Eur. J. Biochem. 111:333-339, 1980.**
83. **Finn R., Cheung N.K.V., Divgi C., St. Germain J., Graham M., Pentlow K., and Larson S.M. Technical Challenges Associated with Radiolabeling of Monoclonal Antibodies Utilizing Short-lived, Positron Emitting Radionuclides. Nucl. Med. Biol. 18:9-13, 1991.**
84. **Forrest A.P.M. The Surgeon and Breast Cancer 1987. Aust. N.Z. J. Surg. 58:3-12, 1988.**
85. **Galarndiuk S. Immunoscintigraphy in the Surgical Management of Colorectal Cancer. J. of Nucl. Med. Suppl. 34:541-544, 1993.**
86. **Galea M.H., Athanassiou E., Bell J., Dilks B., Robertson J.F.R., Elston C.W., Blamey R.W., and Ellis I.O. Occult regional Lymph Node Metastases from Breast Carcinoma: Immunohistological Detection with Antibodies CAM 5.2 and NCRC-11. J. Pathology 165:221-227, 1991.**

87. Gansow O.A. Newer Approaches to the Radiolabeling of Monoclonal Antibodies by Use of Metal Chelates. *Nucl. Med. Biol.* 18:369-381, 1991.
88. Garcia M., Capony F., Derocq D., Simon D., Pau B., and Rochefort H. Characterization of Monoclonal Antibodies to the Estrogen-Regulated Mr 52,000 Glycoprotein and their Use in MCF-7 Cells. *Cancer Research* 45:709-716, 1985.
89. Garcia M.B., Blankenstein M.A., van der Wall E., Nortier J.W.R., Schornagel J.H., and Thijssen J.H.H. Comparison of Breast Cancer Mucin (BCM) and CA 15-3 in Human Breast Cancer. *Breast Cancer Res. and Treat.* 17:69-76, 1990.
90. Garfinkel L. Current Trends in Breast Cancer. *CA - A Cancer J. for Clinicians* 43:4-5, 1993.
91. Gaudette L.A. and Makomaski Illing E.M. (Managing Editors). *Canadian Cancer Statistics 1992*. Statistics Canada (Health and Welfare Canada) and the Canadian Cancer Society.
92. Gelman E.P., Thompson E.W., and Sommers C.L. Invasive and Metastatic Properties of MCF-7 Cells and ras-Transfected MCF-7 Cell Lines. *Int. J. Cancer* 50:665-669, 1992.
93. Gendler S.J., Burchell J.M., Duhig T., Lamport D., White R., Parker M. and Taylor-Papadimitriou J. Cloning of Partial cDNA Encoding Differentiation and Tumor-Associated Mucin Glycoproteins Expressed by Human Mammary Epithelium. *Proc. Natl. Acad. USA* 84:6060-6064, 1987.
94. Gendler S.J., Taylor-Papadimitriou J., Duhig T., Rothbard J., and Burchell J. A Highly Immunogenic Region of a Human Polymorphic Epithelial Mucin

Expressed by Carcinomas is Made up of Tandem Repeats. *J. Biol. Chem.* 263:12820-12823, 1988.

95. Gendler S.J., Spicer A.P., Lalani E.N., Duhig T., Peat N., Burchell J., Pemberton L., Boshell M., and Taylor-Papadimitriou J. Structure and Biology of a Carcinoma-Associated Mucin, MUC1. *American Rev. Respir. Dis. Suppl.* 144:42-47, 1991.

96. Ghose T., Norvell S.T., Guclu A., Bodurtha A., Tai J., and MacDonald A.S. Immunochemotherapy of Malignant Melanoma with Chlorambucil-Bound Antimelanoma Globulins: Preliminary Results in Patients with Disseminated Disease. *J. Natl. Cancer Inst.* 58:845-852, 1977.

97. Ghose T., Blair A.H., and Kulkarni P.N. Preparation of Antibody-linked Cytotoxic Agents. *Methods Enzymol.* 93:280-333, 1983.

98. Ghose T. and Blair A.H. The Design of Cytotoxic-Agent-Antibody Conjugates. *CRC Critical Reviews in Therapeutic Drug Carrier Systems* 3:263-360, 1987.

99. Ghose T., Blair A.H., and vanRooyen C.E. Cancer of the Breast: Recent Advances in Immunological Treatment. *The Nova Scotia Medical Bulletin*, pp. 177-181, December 1987.

100. Ghose T., Blair A.H., and Uadia P.O. Synthesis and Testing of Antibody-Antifolate Conjugates for Drug Targeting. In: *Antibody-Mediated Delivery Systems*. Rodwell J.D. (Editor). Marcel Dekker, Inc., New York, pp. 81-122, 1988.

101. Ghose T., Singh M., Faulkner, G., Goundalkar A., and Mezei M. Antibody-Aided Liposomal Drug Delivery. In: *Liposomes as Drug Carriers*. Gregoriadis G.

(Editor). John Wiley and Sons Ltd., pp. 697-708, 1988.

102. Gion M., Mione R., Nascimben O., Valsecchi M., Gatti C., Leon A., and Bruscaignin G. The Tumour Associated Antigen CA15.3 in Primary Breast Cancer Evaluation of 667 Cases. *British J. Cancer* 63:809-813, 1991.

103. Goldenberg D.M. Current Status of Cancer Imaging with Radiolabeled Antibodies. *J. Cancer Res. Clin. Oncol.* 113:203-208, 1987.

104. Goldenberg D.M. Vistas in Immunopathology: Targeting of Cancer with Radiolabeled Antibodies: Prospects for Imaging and Therapy. *Arch. Pathol. Lab. Med.* 112:580-587, 1988.

105. Goldenberg D.M. Monoclonal Antibodies in Cancer Detection and Therapy. *The American J. of Medicine* 94:297-312, 1993.

106. Goldman I.D. The Characteristics of the Membrane Transport of Amethopterin and the Naturally Occurring Folates. *Ann. N.Y. Acad. Sci.* 180:400-422, 1971.

107. Goldman I.D. Membrane Transport Considerations in High-Dose Methotrexate Regimens with Leucovorin Rescue. *Cancer Treatment Reports.* 65(Sup.1):13-17, 1981.

108. Goldman I.D., Lichtenstein N.S., and Oliverio V.T. Carrier-Mediated Transport of the Folic Acid Analogue, Methotrexate, in the L1210 Leukemia Cell. *J. Biol. Chem.* 243:5007-5017, 1968.

109. Goodman G.E., Hellstrom I., Brodzinsky L., Nicaise C., Kulander B., Hummel D., and Hellstrom K.E. Phase I Trial of Murine Monoclonal Antibody L6 in Breast, Colon, Ovarian, and Lung Cancer. *J. Clin. Oncol.* 8:1083-1092, 1990.

110. Goodman G.E., Hellstrom I., Yelton D.E., Murray J.L., O'Hara S., Meaker E., Zeigler L., Palazollo P., Nicaise C., Usakewicz J., and Hellstrom K.E. Phase I Trial of Chimeric (Human-Mouse) Monoclonal Antibody L6 in Patients with Non-small-cell Lung, Colon, and Breast Cancer. *Cancer Immunol. Immunother.* 36:267-273, 1993.
111. Greenfield R.S., Kaneko T., Davies A., Edson M.A., Fitzgerald K.A., Olech L.J. Grattan J.A., Spitalny G.L., and Braslawsky G.R. Evaluation in vitro of Adriamycin Immunoconjugates Synthesized Using an Acid-Sensitive Hydrazone Linker. *Cancer Research* 50:6600-6607, 1990.
112. Greenwood F.C., Hunter W.M., and Glover J.S. The Preparation of ¹³¹I-Labeled Human Growth Hormone of High Specific Radioactivity. *Biochem. J.* 89:114-123, 1963.
113. Griffin T.W., Bokhari F., Collins J., Stoeche M., Bernier M., Gionet M., Seibecker D., Wertheimer M., Giroves E.S., Greenfield M., Houston L.L., Doherty P.W., and Wilson J. A Preliminary Pharmacokinetic Study of ¹¹¹In-labeled 260F9 Anti-(Breast Cancer) Antibody in Patients. *Cancer Immunol. Immunother.* 29:43-50, 1989.
114. Gross M.S., Guyonnet-Dupera^t V., Porchet N., Bernheim A., Aubert J.P., and Nguyen V.C. Mucin 4 (MUC4) Gene: Regional Assignment (3q29) and RPLP Analysis. *Annales de Genetique* 35:21-26, 1992.
115. Guclu A., Tai J., and Ghose T. Endocytosis of Chlorambucil-Bound Anti-Tumor Globulin Following "Capping" in EL4 Lymphoma Cells. *Immunological*

Communications 4:229-242, 1975.

116. Guha A.K., Singh M., and Ghose T. Application of Monoclonal Antibodies in the Diagnosis and Treatment of Cancer. *voxMEDAL (The Voice of the Medical Alumni of Dalhousie)* 15:13-16, 1988.

117. Guha A.K., Ghose T., Luner S.J., Cruz H.N., Uniyal S., Rajaraman R., Fernandez L.A., Lee S.S.H., and Lee, C.L.Y. Monoclonal Antibodies Against Epstein-Barr Virus Transformed B Lymphocytes from a CLL Patient. *Hybridoma* 9:119-132, 1990.

118. Guha A.K., Ghose T., Singh M., Aquino J., Blair A.H., Luner S.J., and Mammen M. Tumor Localization of Monoclonal Antibodies Against Human Renal Carcinoma in a Xenograft Model. *Cancer Letters* 61:35-43, 1991.

119. Habeeb A.F.S.A. and Francis R.D. Preparation of Human Immunoglobulin by Caprylic Acid Precipitation. *Preparative Biochem.* 14:1-17, 1984.

120. Hanna W.M., Kahn H.J., Zive S.E., Shackleton M., and Andrighetti L. Subcellular Localization of HMFG2 in Breast Carcinomas: An Immunohistochemical and Immunoelectron Microscopic Study. *Modern Pathology* 5:603-606, 1992.

121. Hartmann L.C., Marschke R.F. Jr., Schaid D.J., and Ingle J.N. Subspecialty Clinics: Oncology - Systemic Adjuvant Therapy in Women with Resected Node-Negative Breast Cancer. *Mayo Clin. Proc.* 66:805-813, 1991.

122. Hebert D.C., Burke R.E., and McGuire W.L. Casein and Alpha-lactalbumin Detection in Breast Cancer Cells by Immunocytochemistry. *Cancer Research* 38:2221-2223, 1978.

123. Hellman S. Dogma and Inquisition in Medicine: Breast Cancer as a Case Study. *Cancer* 71:2430-2433, 1993.
124. Henderson G.B. and Zevely E.M. Transport of Methotrexate in L1210 Cells: Effect of Ions on the Rate and Extent of Uptake. *Arch. Biochem. Biophys.* 200:149-155, 1980.
125. Henderson I.C. Basic Principles in the Use of Adjuvant Therapy. In: *Recent Advances in the Management of Lung and Breast Cancer (Proceedings of a Symposium Held Jan., 1990 in Tucson, AZ)*. *Seminars in Oncology* 17 (Suppl. 7):40-44, 1990.
126. Henderson I.C., Hayes D.F., Parker L.M., Love S., Garber J.E., Recht A., Breitmeyer J.B., Harris J.R., and Canellos G.P. Adjuvant Systemic Therapy for Patients with Node-Negative Tumors. *Cancer* 65:2132-2147, 1990.
127. Henry J.A., Hennessy C., Levett D.L., Lennard T.W.J., Westley B.R., and May F.E.B. int-2 Amplification in Breast Cancer: Association with Decreased Survival and Relationship to Amplification of c-erb-2 and c-myc. *Int. J. Cancer* 53:774-780, 1993.
128. Hilkens J., Kroezen V., Bonfrer J.M.G., De Jong-Bakker M., and Bruning P.F. MAM-6 Antigen, a New Serum Marker for Breast Cancer Monitoring. *Cancer Research* 46:2582-2587, 1986.
129. Hnatowich D.J., Gionet M., and Rusckowski M. Pharmacokinetics of ¹¹¹In-Labeled OC-125 Antibody in Cancer Patients Compared with the 19-9 Antibody. *Cancer Research* 47:6111-6117, 1987.

130. Hoagland M.H., Hafer L.J., and Demers L.M. CA-549 is not Diagnostically Useful as an Immunohistochemical Marker for Breast Carcinoma. *Arch. Pathol. Lab. Med.* 6:938-942, 1992.
131. Hoffman T., Kenimer J., Stein K.E. Regulatory Issues Surrounding Therapeutic Use of Monoclonal Antibodies: Points to Consider in the Manufacture of Injectable Products Intended for Human Use. In: Reisfeld R.A. and Sell S. (Editors) *Monoclonal Antibodies and Cancer Therapy, UCLA Symposia on Molecular and Cellular Biology, New Series. Vol 27*; Alan R. Liss, New York, pp 431-440, 1985.
132. Hubbard A.L. and Cohn Z. The Enzymatic Iodination of the Red Cell Membrane. *J. Cell Biol.* 55:390-405, 1972.
133. Hull S.R., Bright A., Carraway K.K., Abe M., Hayes D.F., and Kufe D.W. Oligosaccharide differences in the DF3 Sialomucin Antigen from Normal Human Milk and the BT-20 Human Breast Carcinoma Cell Line. *Cancer Communications* 1:261-267, 1989.
134. Hunter W.M. and Greenwood F.C. Preparation of Iodine-131 Labeled Human Growth Hormone of High Specific Activity. *Nature.* 194:495-496, 1962.
135. Hurlimann J. and van Meele G. Prognostic Value of Serum Proteins Synthesized by Breast Carcinoma Cells. *Am. J. Clin. Pathol.* 95:835-843, 1991.
136. Iacobelli S., Arno E., D'Orazio A., and Coletti G. Detection of Antigens Recognized by a Novel Monoclonal Antibody in Tissue and Serum from Patients with Breast Cancer. *Cancer Research* 46:3005-3010, 1986.
137. Ishida M., Major P., Ura Y., and Dion A.S. Related Glycoproteins from

- Normal Secretory and Malignant Breast Cells. *Tumor Biol.* 10:12-22, 1989.
138. Itzkowitz S.H., Bloom E.J., Kokal W.A., Modin G., and Hakomori S.I. Sialyl-Tn: A Novel Mucin Antigen Associated with Prognosis in Colorectal Cancer Patients. *Cancer* 66:1960-1966, 1990.
139. Jentoft N. Why are Proteins O-Glycosylated? *Trends Biochem. Sci.* 15:291-294, 1990.
140. Johnson V.G., Schlom J., Paterson A.J., Bennet J., Magnani J.L., and Colcher D. Analysis of a Human Tumor-Associated Glycoprotein (TAG-72) Identified by Monoclonal Antibody B72.3. *Cancer Research* 46:850-857, 1986.
141. Kalofonos H.P., Sackier J.M., Hatzistylianou M., Pervez S., Taylor-Papadimitriou J., Waxman J.H., Lavender J.P., Wood C., and Epenetos A.A. Kinetics, Quantitative Analysis and Radioimmunolocalization Using ¹¹¹In-HMFG1 Monoclonal Antibody in Patients with Breast Cancer. *Br. J. Cancer* 59:939-942, 1989.
142. Katoh Y., Nakata K., Kohno K., Shima M., Satoh A., Kusumoto Y., Ishii N., Kohji T., Shiku H., and Nagataki S. Immunoscintigraphy of Human Tumors Transplanted in Nude Mice with Radiolabeled Anti-ras p21 Monoclonal Antibodies. *J. Nucl. Med.* 31:1520-1526, 1990.
143. Kennedy M.J. and Abeloff M.D. Management of Locally Recurrent Breast Cancer. *Cancer* 71:2395-2409, 1993.
144. Kennel S.J., Foote L.J., Lankford P.K., Johnson M., Mitchell T., and Braslawsky G.R. Direct Binding of Radioiodinated Monoclonal Antibody to Tumor Cells: Significance of Antibody Purity and Affinity for Drug Targeting or Tumor

Imaging. *Hybridoma* 2:297-310, 1983.

145. Khaw B.A., Bailes J.S., Schneider S.L., Lancaster J., Powers J., Strauss H.W., Lasher J.C., and Mcguire W.L. Human Breast Tumor Imaging Using ¹¹¹In-labeled Monoclonal Antibody: Athymic Mouse Model. *Eur. J. Nucl. Med.* 14:362-366, 1988.

146. Khawli L.A., Chen F.M., Alauddin M.M., and Epstein A.L. Radioiodinated Monoclonal Antibody Conjugates: Synthesis and Comparative Evaluation. *Antibody, Immunoconjugates, and Radiopharmaceuticals* 4:163-182, 1991.

147. Kim Y.S., Gum Jr. J.R., Byrd J.C., and Toribara N.W. The Structure of Human Intestinal Apomucins. *American Rev. Respir. Dis. Suppl.* 144:10-14, 1991.

148. Kjeldsen T.B., Laursen I., Lykkesfeldt A., Briand P., and Zeuthen J. Monoclonal Antibodies Reactive with Components in Serum-Free Conditioned Medium from a Human Breast Cancer Cell Line (MCF-7). *Tumor Biol.* 10:190-201, 1989.

149. Kobayashi H., Toshihiko T., and Kawashima Y. Serum Sialyl Tn as an Independent Predictor of Poor Prognosis in Patients with Epithelial Ovarian Cancer. *Clin. Oncol.* 10:95, 1992

150. Koning J., Palmer P., Franks C.R., Mulder D.E., Speyer J.L., Green M.D., and Hellman K. Cardioxane-ICRF-187: Towards Anticancer Drug Specificity Through Selective Toxicity Reduction. *Cancer Treatment Reviews* 18:1-19, 1991.

151. Kozak R.W., Waldeman T., Atcher R.W., and Gansow O. Radionuclide Conjugated Monoclonal Antibodies: A Synthesis of Immunology, Inorganic

Chemistry, and Nuclear Science. *Trends Biotechnol.* 4:259-264, 1985.

152. Krag D.N. Clinical Utility of Immunoscintigraphy in Managing Ovarian Cancer. *J. of Nucl. Med. Suppl.* 34:545-548, 1993.

153. Kramer E.L., Sanger J.J., Walsh C., Kanamuller H., Unger M.W. and Halverson C. Contribution of SPECT to Imaging of Gastrointestinal Adenocarcinoma with ¹¹¹In-Labeled Anti-CEA Monoclonal Antibody. *American J. Radiol.* 151:697-703, 1988.

154. Kramer E.L. and Noz M.E. CT-SPECT Fusion for Analysis of Radiolabeled Antibodies: Applications in Gastrointestinal and Lung Carcinoma. *Nucl. Med. Biol.* 18:27-42, 1991.

155. Kueng W., Silber E., and Eppenberger U. Quantification of Cells Cultured on 96-Well Plates. *Anal. Biochem.* 182:16-19, 1989.

156. Kulkarni P.N., Blair A.H., and Ghose T. Covalent Binding of Methotrexate to Immunoglobulins and the Effect of Antibody-Linked Drug on Tumor Growth In Vivo. *Cancer Research* 41:2700-2706, 1981.

157. Kunz C. and Lønnerdal B. Human-Milk Proteins: Analysis of Casein and Casein Subunits by Anion-Exchange Chromatography, Gel Electrophoresis, and Specific Staining Methods. *American J. Clin. Nutr.* 51:37-46, 1990.

158. Kurtz J.M. Should Surgery Remain the Initial Treatment of "Operable" Breast Cancer? *Eur. J. Cancer* 27:1539-1542, 1991.

159. Kyriakos R.J., Shih L.B., Ong G.L., Patel K., Goldenberg D.M., and Mattes M.J. The Fate of Antibodies Bound to the Surface of Tumor Cells In Vitro. *Cancer*

Research 52:835-842, 1992.

160. Lan M.S., Batra S.K., Qi W.N., Metzgar R.S., and Hollingsworth M.A. Cloning and Sequencing of a Human Pancreatic Tumor Mucin cDNA. *J. Biol. Chem.* 265:15294-15299, 1990.

161. Langmuir V.K. Radioimmunotherapy: Clinical Results and Dosimetric Considerations. *Nucl. Med. Biol.* 19:213-225, 1992.

162. Larocca D., Peterson J.A., Walkup G., Urrea R., and Ceriani R.L. Cloning and Sequencing of a Complementary DNA Encoding a Mr 70,000 Human Breast Epithelial Mucin-Associated Antigen. *Cancer Research* 50:5925-5930, 1990.

163. Larocca D., Peterson J.A., Urrea R., Kuniyoshi J., Bistrain A.M., and Ceriani R.L. A Mr 46,000 Human Milk Fat Globule Protein that is Highly Expressed in Human Breast tumors Contains Factor VIII-like Domains. *Cancer Research* 51:4994-4998, 1991.

164. Larson S.M. Introduction: Second International Conference on Diagnosis and Therapy with Monoclonal Antibodies. *Nucl. Med. Biol.* 18:1-2, 1991.

165. Larson S.M. Radioimmunology: Imaging and Therapy. *Cancer* 67:1253-1260, 1991.

166. Layton G.T., Devine P.L., Warren J.A., Birrell G., Xing P.X., Ward B.G., and McKenzie I.F.C. Monoclonal Antibodies Reactive with the Breast Carcinoma-Associated Mucin Core Protein Repeat Sequence Peptide also Recognize the Ovarian Carcinoma-Associated Sebaceous Gland Antigen. *Tumor Biol.* 11:274-286, 1990.

167. Lee A.K., DeLellis R.A., Rosen R.P., Herbert-Stanton T., Tallberg K.,

Garcia C., and Wolfe H. Alpha-lactalbumin as an Histochemical Marker for Metastatic Breast Carcinomas. *Am. J. Surg. Pathol.* 8:93-100, 1984.

168. Lee C.L.Y., Uniyal S., Fernandez L.A., Lee S.H.S., and Ghose T. Growth and Spread in Nude Mice of Epstein-Barr Virus Transformed B-Cells from a Chronic Lymphocytic Leukemia Patient. *Cancer Research* 46:2497-2501, 1986.

169. Lefall L.D. Progress in Cancer. *The American J. Surg.* 161:272-278, 1991.

170. Leong A.S.-Y. and Milios J. An Assessment of a Melanoma Specific Antibody (HMB45) and Other Immunohistochemical Markers of Malignant Melanoma in Paraffin-Embedded Tissues. *Surg. Pathol.* 2:137-145, 1989.

171. Lewko W.M., Vaghmar R., Hubbard D., Moore M., He Y.J., Chang L., Hussein S., Wallwork K., Thurman G.B., and Oldham R.K. Cultured Cell Lines from Human Breast Cancer Biopsies and Xenografts. *Breast Cancer Research and Treatment* 17:121-129, 1990.

172. Liao S-K., Clarke B.J., Khosravi M., Kwong P.C., and Brickenden A. Human Melanoma-Specific Oncofetal Antigen Defined by a Mouse Monoclonal Antibody. *Int. J. Cancer* 30:573-580, 1982.

173. Liao S-K., Khosravi M.J., Brown J.P., and Kwong P.C. Difference in Cell Binding Patterns of Two Monoclonal Antibodies Recognizing Distinct Epitopes on a Human Melanoma-Associated Oncofetal Antigen. *Molecular Immunol.* 24:1-9, 1987.

174. Liao S-K., Flahart R.E., Kimbro B., Horton L., Oldham R.K., Hilgers J., van der Gaag R. Human Tumor and Normal Tissue Reactivity of the Anti-(Breast Cancer) Monoclonal Antibody BA-Br-3 and its Similarity to the Anti-(Epithelial Membrane

- Antigen) Monoclonal Antibody E29. *Cancer Immunol. Immunother.* 31:65-75, 1990.
175. Ligtenberg M.J.L., Vos H.L., Gennissen A.M.C., and Hilkens J. Episialin, a Carcinoma-Associated Mucin, is Generated by a Polymorphic Gene Encoding Splice Variants with Alternative Amino Termini. *J. Biol. Chem.* 265:5573-5578, 1990.
176. Liliemark J. Liposomes for Drug Targeting in Cancer Chemotherapy. *Eur. J. Surg. Suppl.* 561:49-52, 1991.
177. Lind P., Smola M.G., Lechner P., Ratschek M., Klima G., Koltringer P., Steindorfer P., and Eber G. The Immunoscintigraphic Use of Tc-99m-Labeled Monoclonal Anti-CEA Antibodies (BW 431/26) in Patients with Suspected Primary, Recurrent and Metastatic Breast Cancer. *Int. J. Cancer* 47:865-869, 1991.
178. Lindmo T. and Bunn Jr. P.A. Determination of the True Immunoreactive Fraction of Monoclonal Antibodies After Radiolabeling. In: *Methods in Enzymology, Immunochemical Techniques, Part 1, Hybridoma Technology and Monoclonal Antibodies.* Academic Press Inc., N.Y. 121:678-691, 1986.
179. Ljungberg M. and Strand S.E. Dose Planning with SPECT. *Int. J. Cancer Suppl.* 2:67-70, 1988.
180. Loats H. CT and SPECT Image Registration and Fusion for Spatial Localization of Metastatic Processes Using Radiolabeled Monoclonals. *J. Nucl. Med.* 34:562-566, 1993.
181. Lohmann D., Ruhri C., Schmitt M., Graeff F., and Hofler H. Accumulation of p53 Protein as an Indicator for p53 Gene Mutation in Breast Cancer: Occurrence of False-Positives and False-Negatives. *Diagnostic Molecular Pathology* 2:36-41,

1993.

182. Lowry O.H., Rosebrough N.J., Farr A.L., and Randall R.J. Protein Measurement with the Folin Phenol Reagent. *J. Biol. Chem.* 193:265-275, 1951.

183. Luner S.J., Ghose T., Chatterjee S., Cruz H.N., and Belitsky P. Monoclonal Antibodies to Kidney and Tumor-Associated Surface Antigens of Human Renal Cell Carcinoma. *Cancer Research* 46:5816-5820, 1986.

184. Mach J.P., Buchegger F., Fornni M., Ritschard J., Berche C., Lumbroso J.D., Schreyer M., Girardet C., Accola R.S., and Carrel S. Use of Radiolabeled Monoclonal Anti-Cea Antibodies for the Detection of Human Carcinomas by External Photoscanning and Tomoscintigraphy. *Immunol. Today* 2:239-249, 1981.

185. Mach J.P., Pellegrin A., and Buchegger F. Imaging and Therapy with Monoclonal Antibodies in Non-Hematopoietic Tumors. *Current Opinion in Immunology* 3:685-693, 1991.

186. MacLean G.C., Reddish M., Koganty R.R., Wong T., Gandhi S., Smolenski M., Samuel J., Nabholtz J.M., and Longenecker B.M. Immunization of Breast Cancer Patients Using a Synthetic Sialyl-Tn Glycoconjugate Plus Detox Adjuvant. *Cancer Immunol. Immunother.* 36:215-222, 1993.

187. MacPherson G.A. Analysis of Radiolabeled Binding Experiments. A Collection of Computer Programs for the IBM PC. *J. Pharmacological Methods* 14:213-228, 1985.

188. Manohar V. and Hoffman T. Monoclonal and Engineered Antibodies for Human Parenteral Clinical Use: Regulatory Considerations. *Trends in Biotechnology*

10:305-309, 1992.

189. Mansfield C.M., Krishnan L., Komarnicky L.T., Ayyangar M., and Kramer C.A. A Review of the Role of Radiation Therapy in the Treatment of Patients with Breast Cancer. *Seminars in Oncology* 18:525-535, 1991.

190. Mansi J.L., Easton D., Berger U., Gazet J.C., Ford H.T., Dearnaley D., and Coombes R.C. Bone Marrow Micrometastases in Primary Breast Cancer: Prognostic Significance After 6 Years' Follow-Up. *Eur. J. Cancer* 27:1552-1555, 1991.

191. Mariani G., Kassis A.I., and Adelstein S.J. Antibody Internalization by Tumor Cells: Implications for Tumor Diagnosis and Therapy. *J. Nuclear Medicine and Allied Sciences* 34:51-54, 1990.

192. Marshall E. Breast Cancer: Stalemate in the War on Cancer. *Science* 254:1719-1720, 1991.

193. Mazoujian G., Bodian C., Haagensen Jr. D.E., and Haagensen C.D. Expression of GCGFP-15 in Relationship to Pathologic and Clinical Factors. *Cancer* 63:2156-2161, 1989.

194. McCready D.R., Balch C.M., Fidler I.J., and Murray J.L. Lack of Comparability Between Binding of Monoclonal Antibodies to Melanoma Cells In Vitro and Localization In Vivo. *J. Natl. Cancer Inst.* 81:682-687, 1989.

195. McGuckin M.A., Wright R.G., McKenzie I.F.C., and Ward B.C. Demonstration of Two Ovarian Tumor-Associated Antigens in Primary and Metastatic Breast, Gastric, and Colonic Tumors. *American J. Clin. Path.* 94:137-141, 1990.

196. McGuire W.L. Breast Cancer Prognostic Factors: Evaluation Guidelines. .

Natl. Cancer Inst. 83:154-155, 1991.

197. McKinney M.M. and Parkinson A. A Simple, Non-Chromatographic Procedure to Purify Immunoglobulins from Serum and Ascites Fluid. *J. Immunol. Methods.* 96:271-278, 1987.

198. Miller B.A., Feuer E.J., and Hankey B.F. Recent Incidence Trends for Breast Cancer in Women and the Relevance of Early Detection: An Update. *CA - A Cancer J. for Clinicians* 43:27-41, 1993.

199. Mitra I. and MacRae K.D. A Meta-Analysis of Reported Correlations Between Prognostic Factors in Breast Cancer: Does Axillary Lymph Node Metastasis Represent Biology or Chronology? *Eur. J. Cancer* 27:1574-1583, 1991.

200. Moller E. (editor). Engineered Antibody Molecules. *Immunological Reviews* No. 130:1-212, 1992.

201. Muggia F.M. and Green M.D. New Anthracycline Antitumor Antibiotics. *Critical Reviews in Oncology/Hematology* 11:43-64, 1991.

202. Muller W.J. Expression of Activated Oncogenes in the Murine Mammary Gland: Transgenic Models for Human Breast Cancer. *Cancer and Metastasis Rev.* 10:217-227, 1991.

203. Murray J.L., Muzoo K., Wilmanns C., Mansfield P., Wilbur D.S., and Rosenblum M.G. Variables Influencing Tumor Uptake of Anti-Melanoma Monoclonal Antibodies Radioiodinated Using Para-Iodobenzoyl (PIB) Conjugate. *J. Nucl. Med.* 32:279-291, 1991.

204. Nakamura K., Kubo A., and Hashimoto S. Effects of Circulating Antigen on

Monoclonal Antibody Localization. *Hybridoma* 9:351-362, 1990.

205. Nolan O. and O'Kennedy R. Bifunctional Antibodies: Concept, Production and Applications. *Biochimica et Biophysica Acta* 1040:1-11, 1990.

206. O'Briant K.C., Shpall E.J., Houston L.L., Peters W.P., and Bast Jr. R.C. Elimination of Clonogenic Breast Cancer Cells from Human Bone Marrow. *Cancer* 68:1272-1278, 1991.

207. Ozzello L., DeRosa C.M., and Blank E.W. Potentiation of Antitumor Efficacy Resulting from the Combined Administration of Interferon-alpha and of an Anti-breast Epithelial Monoclonal Antibody in the Treatment of Breast Cancer Xenografts. In: *Breast Cancer Immunodiagnosis and Immunotherapy*. Ceriani R.L. (Editor), Plenum Press, New York, pp. 195-201, 1989.

208. Pancino G.F., Le Doussal V., Mortada M.H., Berthon P., Osinaga E., Calvo F., and Roseto A. Characterization and Distribution in Normal and Tumoral Human Tissues of Breast Cancer-Associated Antigen Defined by Monoclonal Antibody 7B10. *Cancer Research* 49:7078-7085, 1989.

209. Pancino G., Osinaga E., Charpin C., Mistro D., Barque J.Ph., and Roseto A. Purification and Characterization of a Breast-Cancer-Associated Glycoprotein not Expressed in Normal Breast and Identified by Monoclonal Antibody 83D4. *British J. Cancer* 63:390-398, 1991.

210. Pancino G., Mortada M.H., Charpin C., Osinaga E., De Cremoux P., Betaille B., Gobert M.G., Calvo F., and Roseto A. Two Monoclonal Antibodies Identify Antigens Preferentially Expressed on Normal Human Breast Cancer Cells. *Hybridoma*

10:241-253, 1991.

211. Parratt D., McKenzie H., Neilson K.H., and Cobb S.J. Radioimmunoassay of Antibody and its Clinical Applications. A Wiley-Interscience Publication, John Wiley and Sons, pp. 49-54, 1982.

212. Parry G., Beck J.C., Moss L., Bartley J., and Ojakian G.K. Determination of Apical Membrane Polarity in Mammary Epithelial Cell Cultures: The Role of Cell-Cell, Cell-Substratum, and Membrane-Cytoskeletal Interactions. *Exp. Cell Res.* 188:302-311, 1990.

213. Pastan I., Lovelace E.T., Gallo M.G., Rutherford A.V., Magnani J.L., and Willingham M.C. Characterization of Monoclonal Antibodies B1 and B3 that React with Mucinous Adenocarcinomas. *Cancer Research* 51:3781-3787, 1991.

214. Paul J. *Cell and Tissue Culture*. 5th Edition, Churchill Livingstone, Edinburgh, pp. 367-368, 1975.

215. Peltz G.A., Gallis B., and Peterlin M.B. Monoclonal Antibody Immunoprecipitation of Cell Membrane Glycoproteins. *Anal. Biochem.* 167:239-244, 1987.

216. Peterson J.A., Zava D.T., Duwe A.K., Blank E.W., Battifora H., and Ceriani R.L. Biochemical and Histological Characterization of Antigens Preferentially Expressed on the Surface and Cytoplasm of Breast Carcinoma Cells Identified by Monoclonal Antibodies Against the Human Milk Fat Globule. *Hybridoma* 9:221-235, 1990.

217. Peterson J.A., Larocca D., Walkup G., Amiya R., and Ceriani R.L.

Molecular Analysis of Epitope Heterogeneity of the Breast Mucin. In: Ceriani R.L. (Editor), *Breast Epithelial Antigens*. Plenum Press, New York, pp. 55-68, 1991.

218. Polanowski F.P., Gaffney E.V., and Burke R.E. HBL-100: Cell Line Established from Breast Milk. *In Vitro* 12:328-336, 1976.

219. Porchet N., Cong N.V., Dufosse J. et al. Molecular Cloning and Chromosomal Localization of a Novel Human Tracheobronchial Mucin cDNA Containing Repeated Sequences of 48 Base Pairs. *Biochem. Biophys. Res. Commun.* 175:414-422, 1991.

220. Prey M.U., Bedrossian C.W.M., and Masood S. The Value of Monoclonal Antibody B72.3 for the Diagnosis of Breast Carcinoma: Experience with the First Commercially Available Source. *Human Pathology* 22:598-602, 1991.

221. Price M.R. Breast-Cancer-Associated Antigens Defined by Monoclonal Antibodies. In: *Subcellular Biochemistry, Vol. 12: Immunological Aspects*. Chapter 1, Harris J.R. (Editor), Plenum Press, N.Y., pp. 1-30, 1988.

222. Price M.R. High Molecular Weight Epithelial Mucins as Markers in Breast Cancer. *Eur. J. Clin. Oncol.* 24:1799-1804, 1988.

223. Price M.R., Clarke A.J., Robertson F.R., O'Sullivan C., Baldwin R.W., and Blamey R.W. Detection of Polymorphic Epithelial Mucins in the Serum of Systemic Breast Cancer Patients Using the Monoclonal Antibody, NCRC-11. *Cancer Immunol. Immunother.* 31:269-272, 1990.

224. Price M.R., Pugh J.A., Hudecz F., Griffiths W., Jacobs E., Symonds I.M., Clarke A.J., Chan W.C., Baldwin R.W. C595 - A Monoclonal Antibody Against the

Protein Core of Human Urinary Epithelial Mucin Commonly Expressed in Breast Carcinomas. *British J. Cancer* 61:681-686, 1990.

225. Price J.E., Polyzos A., Zhang R.D., and Daniels L.M. Tumorigenicity and Metastasis of Human Breast Carcinoma Cell Lines in Nude Mice. *Cancer Research* 50:717-721, 1990.

226. Primus F.J. and Goldenberg D.M. Immunological Considerations in the Use of Goat Antibodies to Carcinoembryonic Antigen for Radioimmunodetection of Cancer. *Cancer Research* 40:2979-2983, 1980.

227. Rahman A., Panneerselvam M., Guirguis R., Castronova V., Sobel M.E., Abraham K., Daddona P.E., and Liotta L.A. Anti-Laminin Receptor Antibody Targeting of Liposomes with Encapsulated Doxorubicin to Human Breast Cancer Cells In Vitro. *J. Natl. Cancer Inst.* 81:1794-1800, 1989.

228. Reisfeld R.A. and Cheresch D.A. Human Tumor Antigens. *Adv. Immunol.* 40:323-327, 1987.

229. Riethmuller G. and Johnson J.P. Monoclonal Antibodies in the Detection and Therapy of Micrometastatic Epithelial Cancers. *Current Opinion in Immunology* 4:647-655, 1992.

230. Riggs S.J., Green A.J., Begent R.H.J., and Bagshawe K.D. Quantitation in ¹³¹I-Radioimmunotherapy Using SPECT. *Int. J. Cancer Suppl.* 2:95-98, 1988.

231. Saitoh S., Inoue T., Kawase I., Hara H., Tanio Y., Tachibana I., Hayashi S., Watanabe M., Matsunashi M., Osaki T., Masuno T., and Kishimoto S. Two Monoclonal Antibodies Against Small-Cell Lung Cancer Show Existence of Synergism

- in Binding. *Cancer Immunol. Immunother.* 33:165-170, 1991.
232. Samuel J., Noujaim A.A., Maclean G.D., Suresh M.R., and Longenecker B.B. Analysis of Human Tumor-Associated Thomsen-Friedenreich Antigen. *Cancer Research* 50:4801-4808, 1990.
233. Scambia G., Panici P.B., Ferrandia G., Battaglia F., Rossi S., Bellantone R., Crucitti F., and Mancuso S. Cathepsin D and Epidermal Growth Factor in Human Breast Cyst Fluid. *British J. Cancer* 64:965-967, 1991.
234. Scanlon E.F. Progress in the Treatment of Early Breast Cancer. *Cancer* 65:2110-2112, 1990.
235. Scanlon E.F. and Hutter R.V.P. Introduction: Summary of National Advisory Committee on Breast Cancer Control from a Workshop held in Naples, Florida (Sept., 1989). *Cancer* 65:2103-2104, 1990.
236. Scheinberg D.A. Current Applications of Monoclonal Antibodies for the Therapy of Hematopoietic Cancers. *Current Opinion in Immunology* 3:679-684, 1991.
237. Schlom J. Basic Principles and Applications of Monoclonal Antibodies in the Management of Carcinomas. The Richard and Hinda Rosenthal Foundation Award Lecture. *Cancer Research* 46:3225-3238, 1986.
238. Schlom J., Milenic D.E., Roselli M., Colcher D., Bird R., Johnson S., Hardman K.D., Guadagni F., and Greiner J.W. New Concepts in Monoclonal Antibody Based Radioimmunodiagnosis and Radioimmunotherapy of Carcinoma. *Nucl. Med. Biol.* 18:425-435, 1991.
239. Scholl S.M., Asselain B., Palangie T., Dorval T., Jouve M., Garcia-Giralt E.,

Vilcoq J., Durand J.C., and Pouillart P. Neoadjuvant Chemotherapy in Operable Breast Cancer. *Eur. J. Cancer* 27:1668-1671, 1991.

240. Serfani A.N. Introduction to Monoclonal Antibody-Based Imaging Agents in Nuclear Medicine. *J. of Nucl. Med. Suppl.* 34:531-532, 1993.

241. Sharkey R.M., Natale A., Goldenberg D.M., and Mattes M.J. Rapid Blood Clearance of Immunoglobulin G2a and Immunoglobulin G2b in Nude Mice. *Cancer Research* 51:3102-3107, 1991.

242. Shaw P., Buckman R., Law J., Baumal R., and Marks A. Reactivity of Tumor Cells in Malignant Effusions with a Panel of Monoclonal and Polyclonal Antibodies. *Tumor Biol.* 9:101-109, 1988.

243. Sheer D.G., Schlom J., and Cooper H.L. Purification and Composition of the Human Tumor-Associated Glycoprotein (TAG-72) Defined by Monoclonal Antibodies CC49 and B72.3. *Cancer Research* 48:6811-6818, 1988.

244. Shen W.C. and Ryser J.P. Cis-Aconityl Spacer Between Daunomycin and Macromolecular Carriers: A Model of pH-Sensitive Linkage Releasing Drug from a Lysosomotropic Conjugate. *Biochem. Biophys. Res. Commun.* 102:1048-1054, 1981.

245. Siddiqui J., Abe M., Hayes D., Shani E., Yunis E., and Kufe D. Isolation and Sequencing of a cDNA Coding for the Human DF3 Breast Carcinoma-Associated Antigen. *Proc. Natl. Acad. Sci. USA* 85:2320-2323, 1988.

246. Singh M., Kralovec J., Mezei M., and Ghose T. Inhibition of Human Renal Cancer by Methotrexate Linked to a Monoclonal Antibody. *J. Urol.* 141:428-431,

1989.

247. Sjogren H.A. Carriers in Cancer Treatment: Monoclonal Antibodies. *Eur. Surg. Suppl.* 561:53-57, 1991.

248. Skilton R.A., Earl H.M., Gore M.E., McIlhinney R.A.J., Gusterson B.A., Wilson P., Coombes R.C, and Neville A.M. Characterization of Monoclonal Antibodies Reactive with Normal Resting, Lactating, and Neoplastic Human Breast. *Tumor Biol.* 11:20-38, 1990.

249. Sommers C.L., Papageorge A., Wilding G., and Gelmann E.P. Growth Properties and Tumorigenesis of MCF-7 Cells Transfected with Isogenic Mutants of *ras^H*. *Cancer Research* 50:67-71, 1990.

250. Soomro S. and Shousha S. Monoclonal Antibody B72.3 Immunostaining of Breast Carcinoma. *Arch. Pathol. Lab. Med.* 116:32-35, 1992.

251. Stirling J.W. Immuno- and Affinity Probes for Electron Microscopy: A Review of Labeling and Preparation Techniques. *J. Histochem. Cytochem.* 38:145-157, 1990.

252. Swallow D.M., Gendler S., Griffiths B., Corney G., Taylor-Papadimitriou J., and Bramwell M. The Human Tumor-Associated Mucins are Coded by an Expressed Hypervariable Locus PUM. *Nature* 328:82-84, 1987.

253. Tandon A.K., Clark G.M., Chamness G.C., Chirgwin J.M., and McGuire W.L. Cathepsin D and Prognosis in Breast Cancer. *New Eng. J. Med.* 322:297-302, 1990.

254. Tavassoli M., Quirke P., Farzaneh F., Lock N.J., Mayne L.V., and Kirkham

N. c-erbB-2/c-erbA Co-Amplification Indicative of Lymph Node Metastasis, and c-myc Amplification of High Tumor Grade, in Human Breast Carcinoma. *British J. Cancer* 60:505-510, 1989.

255. Taylor-Papadimitriou J. Report on the First International Workshop on Carcinoma-Associated Mucins. *Int. J. Cancer* 49:1-5, 1991.

256. Terranova V.P., Rao C.N., Kalebic T., Margulies I.M., and Liotta L.A. Laminin Receptor on Human Breast Carcinoma Cells. *Proc. Natl. Acad. Sci. USA* 80:444-448, 1983.

257. Texter Jr. J.H. and Neal C. Current Applications of Immunoscintigraphy in Prostate Cancer. *J. of Nucl. Med. Suppl.* 34:549-553, 1993.

258. Thompson M.G. and Hickman J.A. Doxorubicin Interactions at the Membrane: Evidence for a Biphasic Modulation of Inositol Lipid Metabolism. *Eur. J. Cancer* 27:1263-1268, 1991.

259. Thompson A.M., Anderson T.J., Condie A., Prosser J., Chetty U., Carter D.C., Evans H.J., and Steel C.M. p53 Allele Losses, Mutations and Expression in Breast Cancer and Their Relationship to Clinico-Pathological Parameters. *Int. J. Cancer* 50:528-532, 1992.

260. Thompson E.W., Paik S., Brunner N., Sommers C.L., Zugmaier G., Clarke R., Shima T.B., Torri J., Donahue S., Lippman M.E., Martin G.R., and Dickson R.B. Association of Increased Basement Membrane Invasiveness with Absence of Estrogen Receptor and Expression of Vimentin in Human Breast Cancer Cell Lines. *J. Cell Physiol.* 150:534-544, 1992.

261. Tilgen W. and Matzku S. Pitfalls in the Clinical Application of Monoclonal Antibodies in Malignant Melanoma: Modulation by and Impaired Accessibility of Antigens to Monoclonal Antibodies. *Cancer Treatment Reviews* 17:357-371, 1990.
262. Tjandra J.J. and McKenzie I.F.C. Murine Monoclonal Antibodies in Breast Cancer: An Overview. *British J. Surg.* 75:1067-1077, 1988.
263. Tjandra J.J., Pietersz G.A., Smyth M.J., and McKenzie I.F.C. Role of Monoclonal Antibodies in the Therapy of Solid Tumors. *Aust. N.Z. J. Surg.* 58:843-849, 1988.
264. Tritton T.R. Cell Surface Actions of Adriamycin. *Pharmac. Ther.* 49:293-309, 1991.
265. Uadia P., Blair A.H., and Ghose T. Uptake of Methotrexate Linked to an Anti-EL4-Lymphoma Antibody by EL4 Cells. *Cancer Immunol. Immunother.* 16:127-129, 1983.
266. Vaidyanathan G. and Zalutsky M.R. Radioiodination of Antibodies Via N-Succinimidyl 2,4-Dimethoxy-3-(trialkylstannyl)benzoates. *Bioconj. Chem.* 1:387-393, 1990.
267. Van de Vijver M.J. and Nusse R. The Molecular Biology of Breast Cancer. *Biochimica et Biophysica Acta* 1072:33-50, 1991.
268. Verhoeyen M.E., Saunders J.A., Price M.R., Marugg J.D., Briggs S., Broderick E.L., Eida S.J., Mooren A.T.A., and Badley R.A. Construction of a Reshaped HMG1 Antibody and Comparison of its Fine Specificity with that of the Parent Mouse Antibody. *Immunology* 78:364-370, 1993.

269. Wagner Jr. H.N. and Conti P.S. Advances in Medical Imaging for Cancer. *Cancer* 67:1121-1128, 1991.
270. Walker R.A., Dearing S.J., Lane D.P., and Varley J.M. Expression of p53 Protein in Infiltrating and In-Situ Breast Carcinomas. *J. Pathol.* 165:203-211, 1991.
271. Weiner L.M., O'Dwyer J., and Kitson J. Phase I Evaluation of an Anti-breast Carcinoma Monoclonal Antibody 260F9-recombinant Ricin A Chain Immunoconjugate. *Cancer Research* 49:4062-4067, 1989.
272. Werner M., von Wasielewski R., Kausche F., and Georgi A. Immunohistochemical and Biochemical Characterization of the Mucin-Type Tumor Associated Antigen TAG-12 by the Monoclonal Antibody 7A9. *Path. Res. Pract.* 187:864-870, 1991.
273. Wilbur D.S., and Hadley S.W., Grant L.M., and Hylarides M.D. Radioiodinated Iodobenzoyl Conjugates of a Monoclonal Antibody Fab Fragment. In vitro Comparisons with Chloramine-T labeled Fab. *Bioconjugate Chem.* 2:111-116, 1991.
274. Williams C.J., Major P.P., and Dion A.S. Enhanced Expression and Secretion of an Epithelial Membrane Antigen (MA5) in a Human Mucinous Breast Tumor Line (BT549). *Tumor Biol.* 11:145-157, 1990.
275. Williams C.J., Wreschner D.H., Tanaka A., Tsarfaty I., Keydar I., and Dion A.S. Multiple Protein Forms of the Human Breast Tumor-Associated Epithelial Membrane Antigen (EMA) are Generated by Alternative Splicing and Induced by Hormonal Stimulation. *Biochem. Biophys. Res. Commun.* 170:1331-1338, 1990.

276. Wright A., Shin S.U., and Morrison S.L. Genetically Engineered Antibodies: Progress and Prospects. *Critical Reviews in Immunology* 12:125-168, 1992.
277. Wynford-Thomas D. p53 in Tumour Pathology: Can We Trust Immunocytochemistry. *J. Pathol.* 166:329-330, 1992.
278. Xing P.X., Prenzoska J., Quelch K., and McKenzie I.F. Second Generation Anti-MUC1 Peptide Monoclonal Antibodies. *Cancer Research* 52:2310-2317, 1992.
279. Yemul S., Leon J.A., Pozniakoff T., Esser P.D., and Estabrook A. Radioimmunoimaging of Human Breast Carcinoma Xenografts in Nude Mouse Model with ¹¹¹In-labeled New Monoclonal Antibody EBA-1 and F(ab)₂ Fragments. *Nucl. Med. Biol.* 20:325-335, 1993.
280. Yu Y.H., Crews J.R., Cooper K., Ramakrishnan S., Houston L.L., Leslie D.S., George S.L., Lidor Y., Boyer C.M., Ring D.B., and Bast Jr. R.C. Use of Immunotoxins in Combination to Inhibit Clonogenic Growth of Human Breast Carcinoma Cells. *Cancer Research* 50:3231-3238, 1990.
281. Zunino F. and Capranico G. DNA Topoisomerase II as the Primary Target of Anti-tumor Anthracyclines. *Anti-Cancer Drug Design* 1:1-12, 1992.